UNIVERSIDADE FEDERAL DO CEARÁ
CENTRO DE CIÊNCIAS AGRÁRIAS
DEPARTAMENTO DE FITOTECNIA
PROGRAMA DE PÓS-GRADUAÇÃO EM AGRONOMIA/FITOTECNIA

JESIMIEL DA SILVA VIANA

ANÁLISE FISIOLÓGICA E METABOLÔMICA DE PLANTAS DE ARROZ SOB CONDIÇÕES DE HIPÓXIA E SALINIDADE

FORTALEZA
2021

JESIMIEL DA SILVA VIANA

ANÁLISE FISIOLÓGICA E METABOLÔMICA DE PLANTAS DE ARROZ SOB CONDIÇÕES DE HIPÓXIA E SALINIDADE

Dissertação apresentada ao Programa de Pós-Graduação em Agronomia/Fitotecnia, da Universidade Federal do Ceará, como requisito parcial para obtenção do título de Mestre em Agronomia/Fitotecnia. Área de concentração: Fisiologia Vegetal.

Orientador: Prof. Dr. Enéas Gomes Filho.
Coorientador: Dr. Lineker de Sousa Lopes.

FORTALEZA

2021

Dados Internacionais de Catalogação na Publicação
Universidade Federal do Ceará
Biblioteca Universitária
Gerada automaticamente pelo módulo Catalog, mediante os dados fornecidos pelo(a) autor(a)

V667a Viana, Jesimiel da Silva.
Análise fisiológica e metabolômica de plantas de arroz sob condições de hipóxia e salinidade / Jesimiel da Silva Viana. – 2021.
145 f. : il. color.

Dissertação (mestrado) – Universidade Federal do Ceará, Centro de Ciências Agrárias, Programa de Pós-Graduação em Agronomia (Fitotecnia), Fortaleza, 2021.
Orientação: Prof. Dr. Enéas Gomes Filho.
Coorientação: Prof. Dr. Lineker de Sousa Lopes.

1. Crescimento e desenvolvimento. 2. Estresse abiótico. 3. Metaboloma. 4. Oryza sativa L.. 5. Tolerância à hipóxia. I. Título.

CDD 630

JESIMIEL DA SILVA VIANA

ANÁLISE FISIOLÓGICA E METABOLÔMICA DE PLANTAS DE ARROZ SOB CONDIÇÕES DE HIPÓXIA E SALINIDADE

Dissertação apresentada ao Programa de Pós-Graduação em Agronomia/Fitotecnia, da Universidade Federal do Ceará, como requisito parcial para obtenção do título de Mestre em Agronomia/Fitotecnia. Área de concentração: Fisiologia Vegetal.

Aprovada em: ___/___/_____.

BANCA EXAMINADORA

_____
Prof. Dr. Enéas Gomes Filho (Orientador)
Universidade Federal do Ceará (UFC)

_____
Dr. Lineker de Sousa Lopes (Coorientador)
Universidade Federal do Ceará (UFC)

_____
Profa. Dra. Maria Raquel Alcântara de Miranda
Universidade Federal do Ceará (UFC)

_____
Profa. Dra. Rosilene Oliveira Mesquita
Universidade Federal do Ceará (UFC)

Aos meus pais; e aos meus avós paternos (*In memorian*) e maternos.

... com amor!

AGRADECIMENTOS

À Deus, por toda sua infinita bondade e misericórdia para comigo, ajudando-me a ultrapassar os inúmeros percalços que tive ao longo dessa caminhada, mas com Ele tornou-se tudo mais leve.

Aos meus pais, Joel Gomes Viana e Francisca Esmerina da Silva, por serem meu alicerce e minha força desde sempre.

À minha sobrinha, Anna Laís Viana Bastos, por me dar o amor mais genuíno e puro que alguém possa ter, aliviando-me dos meus momentos de angústia e medo.

Ao Prof. Dr. Enéas Gomes Filho, pela indispensável e zelosa orientação, sem seus ensinamentos não seria possível chegar ao êxito dessa dissertação.

Ao meu coorientador, Dr. Lineker Sousa Lopes, por me apresentar o projeto básico dessa dissertação, auxiliando-me nas inúmeras tarefas essenciais à obtenção da mesma, ajudando indiscutivelmente em todo o processo. .

À UFC e ao programa de Pós-Graduação em Agronomia Fitotecnia - PPGAF, por todo o suporte estrutural, administrativo e intelectual, imprescindíveis a realização desta dissertação.

Ao coordenador do PPGAF, Prof. Dr. José Wagner Melo, pelos ensinamentos e orientações quanto às minhas obrigações e deveres como aluno do programa.

A todos os professores que tive a honra de adquirir conhecimento ao longo dessa jornada.

Ao Lucas Pacheco e ao Prof. Dr. Humberto de Carvalho por serem pessoas e profissionais extremamente solícitos, me ensinando e auxiliando em tudo sobre a análise de metabolômica, uma variável chave do estudo da presente dissertação.

Às professoras participantes da banca examinadora, Dra. Rosilene Mesquita e Dra. Maria Raquel Alcântara de Miranda, por suas valiosas colaborações e sugestões, e por terem contribuído efetivamente em muitas das análises imprescindíveis.

Ao Laboratório de análises de sementes e seus agregados, por terem me estimulando a ir além do que eu já sonhei, sem eles e seus valorosos ensinamentos não seria possível chegar até aqui.

Ao LABFIVE e seus participantes, por todo o conhecimento e aprofundamento sobre Fisiologia Vegetal, o que certamente servirá no meu engrandecimento profissional.

Aos meus professores do ensino fundamental e médio, que viram em mim potencial, fazendo acreditar que eu poderia tornar realidade os meus mais diversos sonhos, inclusive este, de cursar um mestrado.

Aos meus amigos e colegas que fiz no mestrado, em especial minha companheira de jornada acadêmica, Analya Roberta, que me agregou conhecimento, e acima de tudo, valores.

Aos meus amigos que fiz na graduação, Idayane Souza, Julia Queiros, Leonardo Quirino, Maria Fgenia Diógenes, Rubens Zimmermann e Sharon Gomes, por serem imutáveis em sua amizade, apreço e companheirismo.

Aos meus amigos de vida, José Wellington Ramos e Elielson Viana, por toda amizade compartilhada em anos.

E a todos que participaram, seja de forma direta ou indireta, o meu mais sincero e genuíno obrigado!

O presente trabalho foi realizado com apoio da Coordenação de Aperfeiçoamento de Pessoal de Nível Superior – Brasil (CAPES) – Código de Financiamento 001

"*Todo homem deve decidir se andará na luz do altruísmo criativo ou na escuridão do egoísmo destrutivo*"

Martin Luther King

RESUMO

A hipóxia e a salinidade são uns dos estresses abióticos mais prejudiciais ao crescimento e desenvolvimento das plantas, sendo muito comuns em solos sujeitos a alagamentos. Estes estresses trazem grande impacto na produtividade e disponibilidade de áreas de cultivo em todo o mundo. O cultivo do arroz tem grande importância econômica e social para o Brasil, atualmente o maior produtor de arroz fora do continente asiático, movimentando bilhões de dólares a cada ano. No Brasil, existem cultivares desenvolvidas para o cultivo em condições de sequeiro e sistema irrigado, porém a maior parte do arroz produzido no país se dá em cultivo irrigado, o qual está sujeito à hipóxia e à salinidade. Tendo em vista que a tolerância a esses estresses pode estar relacionada a modulações específicas no perfil metabólico, o objetivo do trabalho foi avaliar o desempenho das cultivares de arroz São Francisco (SF) e BRS Esmeralda (ES) aos estresses de salinidade e de hipóxia, e sua relação com as mudanças no perfil metabólico de folhas e raízes. Dois experimentos foram realizados em delineamento inteiramente casualizado, ambos com cinco repetições. O primeiro, em esquema fatorial 2 x 2 (duas cultivares x dois níveis de salinidade) para caracterizar os impactos da salinidade sobre os cultivares. O segundo, em esquema fatorial 2 x 3 (duas cultivares x três níveis de hipóxia) para avaliar os impactos da alteração dos níveis de hipóxia comuns em sistema irrigado. As plantas foram submetidas por 10 dias aos tratamentos de salinidade (0 e 80 mM NaCl) e de hipóxia: severa (109,4 μM de O_2), moderada (171,9 μM de O_2), e leve (234,4 μM de O_2). Após isso, as plantas foram coletadas aos 37 dias da semeadura e submetidas às avaliações de crescimento e desenvolvimento, pigmentos fotossintéticos, trocas gasosas, fluorescência da clorofila *a*, teores de íons inorgânicos, e análise do metaboloma de folhas e raízes. A salinidade promoveu redução nos parâmetros fisiológicos avaliados, porém, as cultivares não apresentaram tolerância diferencial à salinidade na fase de perfilhamento. Deste modo, foi possível observar apenas a diferenciação quanto ao padrão metabólico de folhas e raízes em resposta à salinidade e indicar alguns biomarcadores de estresse salino em plantas de arroz. Em condições salinas, 26 metabólitos foram diferencialmente expressos nas folhas e cinco nas raízes das duas cultivares, na maioria, aminoácidos e açúcares-chave, como frutose e ribose. No experimento com diferentes níveis de hipóxia, a maior limitação de oxigênio restringiu o crescimento e desenvolvimento. Ambas cultivares reduziram a assimilação de CO_2, e outros parâmetros de trocas gasosas sob hipóxia severa. Assim, o arroz, mesmo sendo uma espécie adaptada a condições de hipóxia, sofre com o seu agravamento, mas isto depende da cultivar. A cultivar SF apresentou maior plasticidade de resposta aos níveis de hipóxia, notando-se uma

clara diferença no perfil metabólico das raízes entre plantas sob hipóxia severa e moderada. Assim, esta cultivar foi capaz de mitigar os danos causados pela hipóxia severa, estimulando a glicólise e o ciclo do ácido cítrico em suas raízes.

Palavras-chave: crescimento e desenvolvimento; estresse abiótico; metaboloma; *Oryza sativa* L.; tolerância à hipóxia.

ABSTRACT

Hypoxia and salinity are some of the most harmful abiotic stresses for plant growth and development, being very commons in soils subject to flooding. These stresses have a significant impact on the productivity and availability of cultivated areas around the world. Rice cultivation has expressive economic and social importance for Brazil, currently the largest rice producer outside the Asian continent, moving billions of dollars each year. In Brazil, there are cultivars developed for cultivation under rainfed conditions and irrigated systems, but most of the rice produced in the country is in irrigated cultivation, subject to hypoxia and salinity. Considering that tolerance to these stresses may be related to specific modulations in the metabolic profile, the objective of this work was to evaluate the performance of rice cultivars São Francisco (SF) and BRS Esmeralda (ES) to salinity and hypoxia stresses and its relationship with changes in the metabolic profile of leaves and roots. Two experiments were carried out in a completely randomized design, both with five replications. The first to characterize the impacts of salinity on the cultivars was in a 2 x 2 factorial scheme (two cultivars x two salinity levels), and the second to evaluate the impacts of changing typical hypoxia levels in an irrigated system was in a 2 x 3 factorial scheme (two cultivars x three hypoxia levels). The rice plants were submitted for ten days to salinity (0 and 80 mM NaCl) and hypoxia treatments [severe (109.4 µM of O_2), moderate (171.9 µM of O_2), and slight (234.4 µM of O_2) hypoxia]. After that, the plants were collected 37 days after sowing and submitted to evaluations of growth and development, photosynthetic pigments, gas exchange, chlorophyll *a* fluorescence, inorganic ion content, and leaf and root metabolome analysis. Salinity promoted a reduction in the physiological parameters evaluated; however, the cultivars did not show differential tolerance to salinity in the tillering phase. Thus, it was only possible to observe the differentiation regarding the metabolic pattern of leaves and roots in response to salinity and indicate some biomarkers of salt stress in rice plants. Under saline conditions, 26 metabolites were differentially expressed in the leaves and five in the roots of the two cultivars, primarily amino acids and key sugars, such as fructose and ribose. In the experiment with different hypoxia levels, the highest oxygen limitation restricted growth and development. Both cultivars reduced CO_2 assimilation and other gas exchange parameters under severe hypoxia. Thus, despite the rice is a species adapted to hypoxia conditions suffers from its aggravation, according to the evaluated cultivar. SF Cultivar showed the best plasticity of response to hypoxia levels, noting a clear difference in the metabolic profile of roots between plants under severe and moderate hypoxia. Thus, this

cultivar mitigated the damage caused by severe hypoxia, stimulating glycolysis and the citric acid cycle in its roots.

Keywords: growth and development; abiotic stress; metabolome; *Oryza sativa* L.; hypoxia tolerance.

SUMÁRIO

1 INTRODUÇÃO GERAL

Em qualquer lugar onde as plantas cresçam estarão sujeitas às condições de estresses bióticos e/ou abióticos, os quais poderão limitar seu crescimento e desenvolvimento. Os estresses abióticos podem ser ocasionados por inúmeros fatores, como metais pesados (ABDELGAWAD *et al*., 2020), radiação ultravioleta (RYBUS-ZAJĄC; KUBIŚ, 2018), seca (KARTIKA *et al*., 2020), frio (TURK; ERDAL; DUMLUPINAR, 2019), altas temperaturas (JEONG *et al*., 2020), hipóxia do solo (XU *et al*., 2020), salinidade (CASTILLO-CAMPOHERMOSO *et al*., 2020), dentre outros.

Segundo estimativas da FAO (do inglês, Food and Agriculture Organization of the United Nations), aproximadamente 20% das áreas irrigadas do mundo encontram-se prejudicadas devido às elevadas concentrações de sais. Esse problema é alarmante, uma vez que cerca de 0,3 a 1,5 milhões de hectares de terras agricultáveis estão se tornando inutilizadas a cada ano (FAO, 2015). Além do mais, sabe-se que cerca de 60 a 80 milhões de hectares de terra são afetados, em certa medida, pelo encharcamento combinado ao estresse salino (FAO, 2011). Esses estresses ambientais exercem um impacto negativo sobre as culturas agrícolas no mundo, como por exemplo na produção de arroz (PANDEY *et al*., 2017).

O arroz é um exemplo de planta adaptada a solos alagados, apresentando aerênquimas que permitem a difusão de oxigênio até as raízes em condições de hipóxia. Entretanto, o transporte de oxigênio pode não ser muito efetivo devido ao alto custo metabólico para manter os estômatos abertos, às perdas de oxigênio para a rizosfera e ao aumento geral da demanda de oxigênio para o processo de respiração sob hipóxia, que ainda pode ser agravado quando associado a outro estresse abiótico, como a salinidade (LAMBERS *et al*., 2008).

No Brasil, existem cultivares de arroz desenvolvidas para o cultivo de sequeiro e em sistema irrigado. No sistema irrigado, podem ser utilizados métodos de irrigação que compreendem a inundação, a subirrigação ou a aspersão. No país, o método mais comum é o de irrigação por inundação contínua, que se caracteriza por ter todo o ciclo da cultura em solo alagado (STONE; SILVEIRA; MOREIRA, 2020) e que, segundo Magalhaes Junior, Gomes e Santos (2004), ocorre majoritariamente em planícies de rios, lagoas e lagunas que apresentam, dentre as suas características, a drenagem deficiente. Ainda segundo esses autores, tanto essas áreas de cultivo de arroz irrigado como as de sequeiro apresentam a salinidade como um fator limitante à produtividade. De acordo com Colmer, Munns e Flowers (2005), o melhor conhecimento da interação dos mecanismos de tolerância à hipóxia e à salinidade é

imprescindível para se conseguir novas cultivares com tolerância a esses estresses e, assim, sustentar a produção agrícola futura.

Nesta perspectiva, o entendimento dos mecanismos de tolerância a estresses ambientais desenvolvidos pelas plantas, mediante o estudo do metaboloma vegetal, se torna uma ferramenta importante. Isso porque o metabolismo das plantas, em função de perturbações induzidas pelos vários estresses, é estimulado à reconfiguração de sua própria rede metabólica, a fim de permitir tanto a manutenção da homeostase metabólica quanto a produção de compostos que melhorem a adaptação ao estresse (OBATA; FERNIE, 2012). Assim, o estudo da metabolômica vegetal permite se ter uma visão abrangente dos componentes cruciais da resposta metabólica das plantas aos estresses, e uma análise detalhada de cada um dos metabólitos modulados. Desta forma, o objetivo do presente trabalho foi avaliar se a tolerância do arroz aos estresses de salinidade e de hipóxia, está relacionada às modulações específicas no perfil metabólico das plantas de arroz (*Oryza sativa* L.).

2 REVISÃO DE LITERATURA

2.1 Cultura do arroz

2.1.1 Importância, histórico e características

Pertencente à família Poaceae, o arroz (*Oryza sativa* L.) é uma das culturas alimentares de maior importância na composição da dieta básica de grande parte da população mundial, sendo seu cultivo centrado em países do continente asiático, onde é fundamentalmente significativo na segurança alimentar (TRIPATHI *et al*., 2011). Além disso, a orizicultura é amplamente difundida em países da América Latina e do continente africano, onde melhora tanto os aspectos econômicos como os sociais (SANTOS; RABELO, 2008).

O arroz é uma monocotiledônea formada por raízes fasciculadas que atingem uma profundidade de até 50 cm, e que por serem longas e ramificadas promovem uma maior eficiência na absorção de água e nutrientes do solo; o caule, por sua vez, é formado por um colmo principal e por um conjunto de colmos secundários e terciários; as folhas, são constituídas pela lâmina, bainha, lígula e aurícula, sendo dispostas aos pares a cada nó do colmo (FONSECA *et al*., 2008). No estágio reprodutivo, o arroz emite inflorescências em seus perfilhos, denominadas panículas, que ao final do ciclo da cultura produzem frutos do tipo cariopses (HEINEMANN; PINHEIRO, 2019).

A espécie *Oryza sativa* L. foi introduzida no Brasil pela frota de Pedro Álvares Cabral e passou a assumir, tempo mais tarde, importância social, econômica e política (NUNES, 2016; PEREIRA,2002). No país, as lavouras de arroz podem ser encontradas sob diversos sistemas de produção, sendo os ecossistemas de várzea e de terras altas os principais ambientes de seu cultivo (SANTIAGO; BRESEGHELLO; FERREIRA, 2013). Fora do continente Asiático, o Brasil é o país de maior produção e consumo de arroz, possuindo um número significativo de indústrias de processamentos que agregam qualidade e tornam o cereal brasileiro destaque no comércio internacional (BRAZILIAN RICE, 2019). Embora as perspectivas para a safra 2020/2021 seja de uma queda de 0,8% em relação à safra anterior, a área plantada deverá ter um incremento de 1,4% (CONAB, 2021). Isto demonstra que a orizicultura é ainda uma prática agrícola essencial no desenvolvimento da nação, além de ser uma atividade econômica rentável, que serve de sustento, sobretudo, para agricultores de base familiar (CANTRELL, 2002).

2.1.2 Cultivares São Francisco e BRS Esmeralda

A cultivar São Francisco foi desenvolvida pelo Centro Internacional de Agricultura Tropical (CIAT), tendo sido introduzida no Brasil como a linhagem CNA 5544 pelo Centro Nacional de Pesquisa de Arroz e Feijão (CNPAF) da EMBRAPA - GO. No ano de 1996, seu cultivo foi indicado para os Estados de Alagoas, Sergipe e Pernambuco, sendo isto possível mediante estudos conduzidos em diferentes ambientes no baixo e médio São Francisco (EMBRAPA, 1996). Sua recomendação de cultivo é para sistemas produtivos de arroz irrigado por inundação nos ambientes de várzeas, podendo sua semeadura ocorrer de forma direta ou por transplantio de mudas. Um manejo adequado é crucial para o desenvolvimento vegetal e inclui um bom preparo do solo, o controle de ervas daninhas, o controle da lâmina de água de irrigação e um bom nível de fertilidade do solo (BARROS; UCHÓA; SANTOS, 2000).

A cultivar BRS Esmeralda foi desenvolvida para o plantio em terras altas (sistema de sequeiro), sendo indicada para cultivo nos estados de Goiás, Mato Grosso, Rondônia, Roraima, Pará, Tocantins, Maranhão, Piauí e Minas Gerais. Essa cultivar foi lançada pela Embrapa Arroz e Feijão, em 2012, a partir de um programa de melhoramento desenvolvido em 1997, que se iniciou com o cruzamento simples realizado entre a linhagem CNAX4909-68-MM2-PY2 e a cultivar BRS Primavera, com o objetivo principal de reunir em um único genótipo características de rusticidade e resistência a doenças, além de alta produtividade e qualidade de grãos (CASTRO *et al*., 2014). Dentre as características relevantes desta cultivar, destacam-se a alta produtividade e a qualidade dos grãos produzidos, sendo possível a obtenção de até 7.525 kg/ha nas áreas de plantio a que se destina (EMBRAPA ARROZ E FEIJÃO, 2013). É importante salientar que as plantas desta cultivar apresentam uma boa arquitetura, com colmos fortes e flexíveis e “stay green” (senescência tardia), que minimizam o potencial de acamamento, além de tolerância ao estresse hídrico (CASTRO *et al*., 2014).

2.2 Estresse salino

2.2.1 Aspectos gerais da salinidade

A salinidade em si é um grande problema global, presente em todos os continentes, que afeta mais de 100 países e que ocasiona a perda diária de 2000 ha de terra arável, impactando negativamente na produtividade e sustentabilidade agrícola (ZAMAN; SHAHID; HENG, 2018). A salinidade pode ser entendida como a elevada concentração de sais nas

camadas de solo mais próximas à superfície (LÄUCHLI; GRATTAN, 2014), as quais são favorecidas por condições de má drenagem e elevada evapotranspiração (RIBEIRO; RIBEIRO FILHO; JACOMINE, 2016). Tal fenômeno tende potencialmente a continuar e se intensificar em países menos desenvolvidos com clima áridos e semiáridos, que normalmente já possuem altas taxas de crescimento populacional e sofrem sérios problemas ambientais (SAFDAR *et al.*, 2019). Deste modo, a salinidade tem se tornando uma barreira iminente à segurança alimentar.

A salinização dos solos pode ocorrer de duas formas: primária e secundária. A salinização primária se desenvolve naturalmente, principalmente em áreas onde a evaporação é elevada e a precipitação é insuficiente para lixiviar os sais do perfil do solo (DPIRD, 2019), além da própria gênese do solo ser fator determinante; já a secundária, ou antropogênica, é induzida pela atividade humana, como as provocadas pelo desmatamento, irrigação com água salina e má drenagem, que alteram o equilíbrio hidrológico do ambiente (PARIHAR *et al*., 2014). Ambos os tipos criam condições desfavoráveis ao desenvolvimento e sobrevivência de muitas espécies vegetais. Estima-se que 20% da área total cultivada e 33% das terras agrícolas irrigadas são afetadas pela salinidade (SHRIVASTAVA; KUMAR, 2015).

2.2.2 Efeitos do estresse salino no crescimento, desenvolvimento e metabolismo vegetal

As condições de alta salinidade dos solos e da água de irrigação são um dos mais sérios desafios enfrentados pelas culturas agrícolas no mundo (XU; MOU, 2016). Isso porque tal estresse abiótico provoca um declínio no crescimento e produtividade das plantas (BATOOL; SHAHZAD; ILYAS, 2014), sendo esse decréscimo resultante da deficiência na absorção de água (efeito osmótico) ou da citotoxicidade relacionada à absorção excessiva de íons tóxicos (efeito iônico), além do próprio desequilíbrio nutricional (ISAYENKOV; MAATHUIS, 2019). O efeito osmótico é entendido como a primeira fase do estresse salino, na qual as plantas inicialmente são submetidas a um estresse hídrico (COLLADO *et al.*, 2019). Isto acontece porque os sais têm a capacidade de baixar o potencial osmótico da solução do solo, reduzindo o gradiente de potencial hídrico entre o solo e a planta, dificultando a absorção de água pelas raízes. O efeito iônico, por sua vez, é a segunda fase do estresse, sendo um pouco mais lenta que a primeira e que é caracterizada pelo acúmulo, em níveis tóxicos, de íons específicos como o sódio (Na^+) e o cloreto (Cl^-) dentro da célula (SHAVRUKOV, 2012). Além disso, a elevada concentração iônica associada com a inibição da absorção de elementos essenciais pode provocar um desbalanço nutricional, uma vez que existe certa competição entre os sais e os elementos essenciais por transportadores de membranas (SCHOSSLER *et al.*,

2012).

Dentre os órgãos que constituem um vegetal, a parte aérea demonstra ser a mais sensível ao estresse salino, principalmente na primeira fase caracterizada pelo estresse osmótico (MUNNS; TESTER, 2008). Isto porque a indisponibilidade de água e nutrientes, que são primordiais ao crescimento celular e manutenção da atividade metabólica, causa a formação de plantas com área foliar diminuta e ramificações atrofiadas (BATOOL, SHAHZAD, ILYAS, 2014). Associado a isto, a fotossíntese, processo essencial para a sobrevivência das plantas, também é um dos mais afetados pela salinidade (SANTOS *et al*., 2020). A salinidade, além de comprometer a absorção de água, também induz o fechamento estomático, o que consequentemente leva à diminuição do CO_2 fixado pela própria planta (DIAS *et al*., 2018). Assim, é esperado que plantas sensíveis ao estresse salino tenham grandes reduções em suas taxas fotossintéticas e condutância estomática, e como resultado apresentem menor crescimento e desenvolvimento.

É importante ressaltar, que a fotossíntese também pode ser limitada devido aos danos gerados pelo estresse salino sobre os pigmentos fotossintéticos, os cloroplastos, e à maquinaria fotossintética, principalmente sobre o Fotossistema II (PSII). Este é diretamente afetado pela salinidade, através da redução da disponibilidade de água para doação de elétrons e, consequentemente, comprometimento da cadeia transportadora de elétrons nos cloroplastos, resultando assim na diminuição da atividade fotossintética (OLIVEIRA *et al*., 2018). Também, é observado uma alteração na fluorescência da clorofila, cujo processo é essencial para a dissipação de radiação em excesso e retorno ao seu estado de baixa energia. Sendo a clorofila *a* o principal pigmento cuja fluorescência é comprometida devido a salinidade (CAMPOSTRINI, 2020).

Além das alterações nas estruturas das membranas (SOUSA *et al*., 2017), decaimento da atividade fotossintética e diminuição da abertura estomática (DIAS *et al*., 2018), tem-se observado a produção de espécies reativas de oxigênio (EROs), como uma reposta ao estresse salino (BARBOSA *et al*., 2014). Segundo Nxele, Klein e Ndimba (2017) as EROs incluem os radicais superóxido ($\bullet O_2^-$) e hidroxil ($\bullet OH$), além do peróxido de hidrogênio (H_2O_2) e do oxigênio singleto ($^1O_2$), que desempenham papel importante na inibição do crescimento e desenvolvimento das plantas se não forem cuidadosamente reguladas. Isto acontece porque a elevada concentração de EROs leva a danos oxidativos às membranas (peroxidação lipídica) e moléculas importantes como proteínas, RNA e DNA. Este processo é denominado como estresse oxidativo e pode até levar à destruição celular (MITTLER, 2002), mas pode ser evitado ou controlado pelo ajuste da atividade de algumas enzimas antioxidantes e ação de moléculas

antioxidantes não-enzimáticas (NUNES JUNIOR *et al*., 2017). Deste modo, o estresse salino induz uma série de mudanças nos vários processos fisiológicos e metabólicos nos vegetais, o que resulta em algum grau de redução no crescimento e desenvolvimento das plantas, cuja severidade dos danos é dependente da espécie, variedade e órgão vegetal (TAIZ; ZEIGER, 2017; SÁ *et al*., 2013).

2.3 Estresse por hipóxia

2.3.1 Aspectos gerais da hipóxia

Em algum momento do ciclo natural de vida dos vegetais é comum que existam períodos de deficiência de oxigênio em suas raízes, que a depender do tempo e da intensidade, podem resultar em morte (OLIVEIRA, 2020). Essa baixa disponibilidade de O_2 pode ser denominada de hipóxia, o que é referido ao oxigênio em uma pressão parcial menor que 3 kPa (BUCHANAN; GRUISSEM; JONES, 2015). A baixa oxigenação ou hipóxia está comumente associada a solos que se encontram inundados ou saturados por água, onde a difusão do oxigênio para os tecidos das raízes é reduzida (TAIZ; ZEIGER, 2017). O oxigênio proveniente dos espaços gasosos do solo é essencial para a respiração aeróbica e, assim, uma produção de energia mais eficiente para manutenção da atividade celular.

Dentre as características dos solos inundados, além das alterações do intercâmbio gasoso atmosfera-solo, existe também o aumento dos processos de redução química e, por conseguinte, alterações no pH e no potencial de óxido-redução, bem como alterações na dinâmica dos nutrientes (MORAES, 1973), o que pode interferir no aumento ou diminuição da disponibilidade de determinados elementos essenciais para a planta. Assim pode-se inferir que o oxigênio do solo também é fundamental para uma boa estruturação físico-química do solo, pois ele regula a atividade da microbiota do solo, que é crucial para a dinâmica de disponibilidade de nutrientes para os vegetais. Desse modo, o O_2 interfere diretamente ou indiretamente no desenvolvimento e crescimento das plantas.

2.3.2 Efeitos do estresse por hipóxia no crescimento, desenvolvimento e metabolismo vegetal

A princípio, o efeito gerado sobre o crescimento e desenvolvimento vegetal incide diretamente sobre o sistema radicular das plantas, uma vez que se trata do principal órgão que pode em algum momento ser submetido a um ambiente com quantidade insuficiente de oxigênio. Assim algumas espécies vegetais desenvolveram mecanismos que permitem a

passagem do oxigênio do ar atmosférico para a camada da rizosfera, como o desenvolvimento de aerênquimas nos colmos e raízes presentes em plantas de arroz sob hipóxia (SOCIEDADE SUL-BRASILEIRA DE ARROZ IRRIGADO, 2007). Os aerênquimas são espaços originados no córtex, que se formam pela morte celular programada e que têm a função de prover a difusão do ar (EVERT, 2013). Apesar disso, a baixa oxigenação pode ocasionar a diminuição do crescimento e do metabolismo do sistema radicular, devido à redução no fluxo de carboidratos transportados das folhas até as raízes (HENRIQUE *et al*., 2009).

Em algumas espécies, a hipóxia pode tornar as raízes incapazes de sustentar os processos fisiológicos que a parte aérea necessita (BRAGA, 2020). Além disso, o baixo teor de oxigênio pode levar a síntese de etileno que induz aumento no alongamento caulinar, na epinastia, na abscisão foliar, na senescência e na perda de clorofila (TAIZ; ZEIGER, 2017). As plantas, quando submetidas a ambientes de baixa disponibilidade de oxigênio, também são induzidas a realizar o metabolismo anaeróbico, denominada via metabólica fermentativa. Essa via se torna necessária, pois através dela ocorre a regeneração da coenzima da nicotinamida adenina dinucleotídio na forma reduzida (NADH) para assim dar continuação à glicólise, já que na condição de baixa disponibilidade de O_2 o ciclo de Krebs e a cadeia de transporte de elétrons não funcionam. Se essas duas vias metabólicas não ocorrem, o fornecimento da coenzima na forma oxidada (NAD^+) é bastante limitado, restringindo a reação da desidrogenase do gliceraldeído-3-fosfato, dependente de NAD^+ (TAIZ; ZEIGER, 2017).

As plantas podem se utilizar de duas vias fermentativas: a alcóolica e a láctica (Figura 1). A alcóolica é a via mais comum nas plantas e nela a enzima descarboxilase do piruvato catalisa a reação em que o piruvato é descarboxilado com liberação de CO_2 e formação de acetaldeído, o qual, em reação catalisada pela desidrogenase alcoólica (ADH), é reduzido na presença de NADH para formação de etanol e NAD^+, sendo este último utilizado novamente na glicólise (BUCHANAN; GRUISSEM; JONES, 2015). Já na fermentação láctica, o piruvato é convertido a lactato em uma reação com o NADH catalisada pela desidrogenase do lactato (LDH) regenerando NAD^+. Essa via fermentativa é precedida pela via alcóolica, com exceção durante a germinação de sementes, uma vez que o lactato, como produto da via, pode acidificar o citosol da célula vegetal comprometendo seu funcionamento (TAIZ; ZEIGER, 2017).

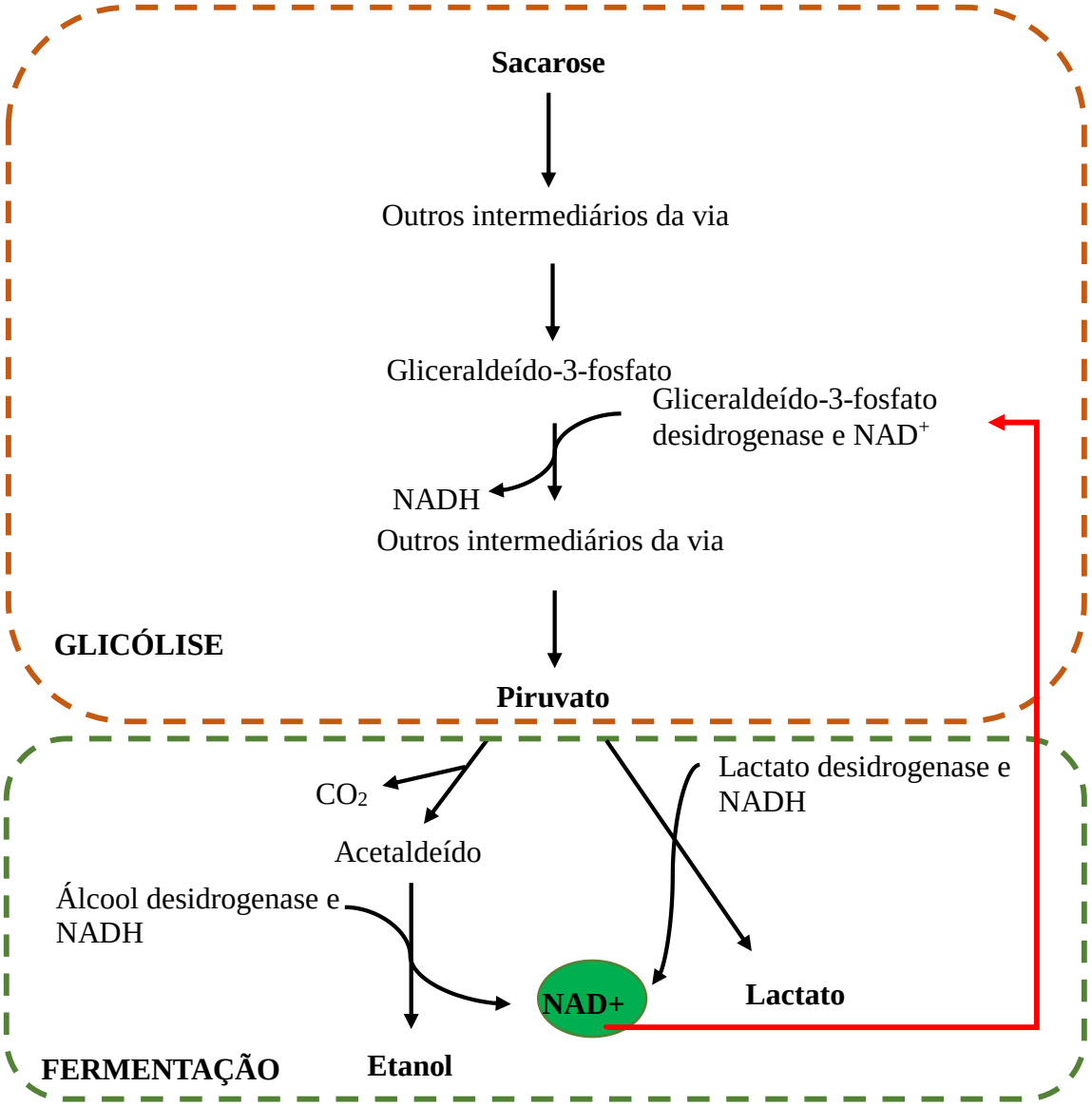

Figura 1 - Visão da glicólise e vias fermentativas.

Fonte: Adaptado de TAIZ; ZEIGER, 2017

2.4 Mecanismos de tolerância em plantas

O estresse em vegetais, quer seja devido a fatores abióticos e/ou bióticos, pode ser entendido como qualquer condição que sobreponha uma pressão restritiva à expressão total do potencial genético de crescimento, desenvolvimento e reprodutivo das plantas (KUSVURAN; KIRAN; ELLIALTIOGLU, 2016; TAIZ; ZEIGER, 2017). O estresse ambiental pode variar no tempo ou atingir diretamente apenas parte da planta, mas seu efeito prejudicial normalmente acomete todo metabolismo vegetal.

Dentre os fatores de estresses que mais influenciam os parâmetros de crescimento e desenvolvimento dos vegetais, os ambientais destacam-se como um dos principais

condicionadores limitantes (RHODES; NADOLSKA-ORCZYK, 2001), haja vista que afetam a distribuição espacial das plantas e diminuem a produtividade das culturas (ZHU, 2016). A ação conjunta ou isolada desses estresses, como metais pesados (SMEETS *et al.*, 2009), radiação ultravioleta (RYBUS-ZAJĄC; KUBIŚ, 2018), seca (SIMOVA-STOILOVA *et al.*, 2009), frio (LOUREIRO *et al.*, 2013), altas temperaturas (ZANDALINAS, *et al.*, 2017), hipóxia do solo (PEREIRA *et al.*, 2014) e salinidade (MIRANDA *et al.*, 2016), causam efeitos negativos na sobrevivência e desenvolvimento das plantas. Ressalte-se que, devido às constantes mudanças climáticas associadas à degradação do meio ambiente, tais fatores de estresse tornam-se uma grande ameaça à segurança alimentar mundial (HUANG; LEVINE; WANG, 2013).

É certo que as variações ambientais fora de seus limites normais têm consequências bioquímicas e fisiológicas negativas para as plantas, que por serem organismos vivos sésseis são incapazes de evitar o estresse abiótico pelo simples deslocamento (TAIZ; ZEIGER, 2017). Assim para superar os efeitos deletérios, os vegetais promovem mudanças em seu metabolismo de modo a manter seu crescimento, desenvolvimento e reprodução normais. Essas alterações metabólicas, em sua maioria, são de natureza reversível, ou seja, cessada a condição estressante as plantas voltam a sua condição normal, o que segundo Prisco e Gomes-Filho (2010) pode ser entendido por um período de aclimatação em que os vegetais respondem às variações periódicas do ambiente mediante mudança direta em sua morfologia e/ou fisiologia.

2.4.1 Aclimatação ao estresse salino

As plantas submetidas a condição de estresse salino se aclimatam, por exemplo, através dos processos de homeostases osmótica, iônica e bioquímica (PRISCO; GOMES-FILHO, 2010). É importante destacar que a homeostase se refere à capacidade do meio interno de se manter em equilíbrio quase constante com o ambiente externo, independentemente de suas oscilações (SANTOS, 2020); contudo, essa manutenção da homeostase é estritamente dependente do desempenho dos processos mencionados acima, os quais ajudam a distinguir as plantas em tolerantes e sensíveis ao estresse (PRISCO; GOMES-FILHO, 2010).

Na aclimatação ao estresse salino, a homeostase osmótica tem por finalidade o restabelecimento do gradiente de potencial hídrico entre a planta e o solo. Isto ocorre mediante a diminuição do potencial osmótico da planta que se dá pelo ácumulo de solutos orgânicos e inorgânicos (PRISCO; GOMES-FILHO, 2010; WILLADINO; CAMARA, 2010), diminuindo consequentemente o potencial hídrico da planta e favorecendo a absorção de água. Esse

ajustamento osmótico ocorre mediante mudanças nos principais processos fisiológicos da planta, que estimulam o acúmulo de íons como Na^+ e Cl^- no vacúolo (ALVES *et al*., 2015), além do acúmulo de solutos orgânicos compatíveis no citoplasma, como aminoácidos livres, açúcares solúveis, prolina e glicina-betaína, dentre outros (SILVA *et al*., 2015). Esses solutos protegem as estruturas celulares ao interagirem com componentes de membranas, complexos protéicos ou enzimas (ESTEVES; SUZUKI, 2008), o que contribui para a manutenção do crescimento vegetal (WILLADINO; CAMARA, 2010; PAN *et al*., 2016).

Outro meio empregado pelas plantas para se aclimatarem ao estresse salino é mediante a homeostase iônica, a qual envolve diversos processos, tais como: a exclusão de alguns íons do citosol, como o Na^+ e Cl^-; a restrição da entrada dos íons no citosol; a compartimentalização dos íons no vacúolo e/ou exportação dos íons do citosol para o meio apoplástico ou para o solo/substrato (COVA, 2016; WILLADINO; CAMARA, 2010). Embora exista uma preferência pelo efluxo de íons tóxicos do citosol para o apoplasto, estudos recentes mostram que outros íons, como o K^+, também possuem importância essencial para uma maior tolerância das plantas ao estresse salino. O efluxo de K^+ mediante canais de potássio, como o GORK (do inglês, Guard Cell Outward Rectifying K^+ channels), funciona como sinalizador ao estresse (WU *et al*., 2018), o qual estimula a regeneração da polarização da membrana, que é despolarizada inicialmente pelo estresse. Esse reajuste eletroquímico tem um custo metabólico menor quando comparado àquele realizado pela bomba de prótons H^+-ATPase (SHABALA, 2017). Portanto, inicialmente, as plantas mais tolerantes preferem utilizar o efluxo do K^+ para regulação eletroquímica da membrana, até que esse papel seja assumido por completo pela H^+-ATPase (CHEN *et al*., 2007; ALVAREZ-PIZARRO *et al*., 2009). Já, com a bomba de prótons H^+-ATPase atuando como responsável pela polarização eletroquímica da membrana, tem-se o estímulo da atividade do carreador de potássio de alta afinidade HAK (do inglês, High Affinity K^+ Transporter), o qual promove o retorno do K^+ ao citosol, funcionando assim como uma válvula de proteção ao estresse salino (SHABALA, 2017).

A homeostase bioquímica, outro mecanismo aclimatativo ao estresse, é um processo complexo, que envolve uma série de reações do metabolismo, seja pela síntese de novas enzimas, ou pelo aumento da atividade e/ou dimuição de outras (PRISCO; GOMES-FILHO, 2010). A exemplo disso, pode-se destacar o sistema de defesa antioxidante o qual é usado para sobrepujar os efeitos deletérios das EROs (EL-SHABRAWI *et al*., 2010). Este complexo sistema de defesa pode ser classificado como enzimático e não enzimático. Este último se deve à participação direta de composto antioxidantes, como o ascorbato (AsA), a glutationa (GSH), o β-caroteno e o α-tocoferol (BARBOSA *et al*., 2014), enquanto o enzimático

envolve a participação de enzimas, como a dismutase do superóxido (SOD), a catalase (CAT), a peroxidase da glutationa (GPX), a redutase da glutationa (GR) e a peroxidase do ascorbato (APX) (CAMARGO, 2013).

2.4.2 Aclimatação à hipóxia

Tratando-se do estresse por hipóxia ou anóxia, as plantas desenvolveram também alguns meios de contornar a deficiência de O_2 e a consequente redução da respiração aeróbica, bem como o indesejado acúmulo de CO_2, metano, etileno, gás sulfídrico (H_2S) e H^+ (PIRES; SOPRANO; CASSOL, 2002). Em algumas espécies de plantas, isso é conseguido pelo colapso mitocondrial, que leva a formação de estruturas denominadas de aerênquimas (NEILL *et al.* 2008; IGAMBERDIEV; HILL, 2008), como foi detalhado no tópico 2.3.2. O arroz é uma das principais culturas comerciais que apresentam essa adaptabilidade à baixa oxigenação, com um aerênquima do tipo lisígeno (RAJHI *et al*., 2010). Além do mais, tal cultura agrícola apresenta a capacidade de transferir o O_2 da atmosfera para as raízes, vindo de suas folhas e caule, o qual na rizosfera forma uma região de oxidação que abrevia os efeitos tóxicos gerados por elementos, como Fe^{2+} e Mn^{2+} (PIRES; SOPRANO; CASSOL, 2002). Também tem sido relatado a formação de barreiras radiais de perda de O_2 nas raízes, um mecanismo de mudança anatômica que pode conferir uma maior tolerância à baixa disponibilidade de oxigênio (LOPES *et al.* 2020). Ademais, assim como no estresse salino, o canal de potássio GORK tem uma importância relevante para uma maior tolerância das plantas a condições de hipóxia. Isto porque, ao contrário do estresse salino, a restrição da atividade desses canais permite uma resposta adaptativa eficiente da planta à hipóxia, como nas raízes de Arabidopsis mutante que apresentaram maior tolerância ao alagamento devido ao impedimento do efluxo de K^+ pela não expressão dos canais GORK (WANG *et al.*, 2017).

3 DIFFERENTIAL MODULATION OF METABOLITES INDUCED BY SALT STRESS IN RICE PLANTS

(Artigo a ser submetido)

Abstract

Salinity is one of the principal abiotic stresses that most impose limitations on the growth and development of crops, one of them is rice (*Oryza sativa* L.). Thus, the present study aimed to assess the metabolic profile pattern between two rice cultivars with contrasting tolerance to salt stress: São Francisco (SF) and BRS Esmeralda (ES). According to previous studies, the SF cultivar is more tolerant of salt stress than the ES cultivar. Therefore, physiological and biochemical parameters and untargeted metabolome were evaluated in these cultivars under salinity. The patterns of metabolic profiles of leaves and roots were detected using GCMS. Salinity caused a significant increase of toxic ions in the leaves, stems, and roots, negatively affecting plants' growth and photosynthesis parameters similarly in cultivars. Increases in Na^+ and Cl^- contents occurred at the detriment of K^+ contents. Both cultivars under salinity showed chlorophyll *total* content, effective quantum yield of PSII, electron transport rate, and PSII maximum efficiency reduced, as well as lower rates of CO_2 assimilation, stomatal conductance, and transpiration. While the carboxylation efficiency was not affected by salinity in the ES cultivar, in the SF cultivar it increased. The expected differential tolerance to salinity by the studied cultivars did not occur in the tillering phase. Nevertheless, the primary metabolites modulation by salt stress in rice plants and activation of the gamma-aminobutyric acid shunt in the SF leaves were evident. Besides, 26 metabolic were differentially expressed in leaves and five in roots by cultivars under salinity. Most of them were amino acids and key-sugars such as fructose and ribose. Thereby, there was differential modulation by salt in the metabolic profiles of leaves and roots between SF and ES rice cultivars.

Keywords: GABA; Metabolome; *Oryza sativa* L.; Salinity; Salt tolerance.

3.1 Introduction

Salt stress is one of the most damaging abiotic stresses to agriculture. Salinity occurs in approximately 1 billion hectares of land worldwide, affecting mainly the productivity

of crops (SHAHID; ZAMAN; HENG, 2018). Among these cultures, rice stands out (GUO *et al*., 2017; ARIF *et al*., 2020), a widespread Poaceae of significant socio-economic importance (SANTOS; RABELO, 2008; TRIPATHI *et al*., 2011).

The salinity damages are caused initially by osmotic stress, which hinders absorbing water and nutrients from the soil (SAFDAR et al., 2019), impacting plant growth and development (VAN ZELM; ZHANG; TESTERINK, 2020). In rice, for example, salinity significantly reduces plant height, leaf area, and dry mass accumulation (LEMES *et al.,* 2018). It is important to note that the high concentration of specific ions in the growth medium, such as Na^+ and Cl^-, generate toxic effects and nutritional imbalance (YANG; GUO, 2017). Although rice is a crop considered, among cereals, one of the most sensitive to salinity (MUNNS; TESTER, 2008), the severity of salt stress in the species depends on factors like the cultivar and phenological stage. According to Gadelha (2020), rice plants of the São Francisco cultivar were more tolerant of salt stress than the BRS Esmeralda cultivar. The tolerance of rice also depends on the phenological stage of the plants. Usually, germination, tillering, and maturity stages are considered low sensitivity to salt stress for the rice (SARKAR *et al*., 2019).

Plant responses to salinity are complex and multifaceted; they induce metabolic adjustments to ensure the best possible growth and development for plants under adverse environmental conditions (NEGRÃO; SCHMÖCKEL; TESTER, 2016; VAN ZELM; ZHANG; TESTERINK, 2020). In this perspective, an approach to the metabolomic study clarifies the modulation mechanisms developed by plants (ARIF *et al*., 2020). Metabolites are the end products of cellular functions and are essential for normal cellular function. They can be classified into primary or secondary, being the primary metabolites are related to plant growth, development, and reproduction (LLANES *et al*., 2018). Some amino acids can be mentioned among these metabolites, such as proline, glycine betaine, ethanolamine, and glutamate (HILDEBRANDT *et al*., 2015; NAM *et al*., 2015). Some other metabolites can also be used as markers of salt stress. The accumulation of some sugars, such as trehalose, raffinose, sucrose, and mannitol, are key indicators of salt tolerance in rice (CHANG *et al*., 2019). In contrast, the downregulation of shikimate, quinate, and malate may indicate sensitivity to salt stress (JORGE *et al*., 2017; ARAÚJO *et al*., 2021).

The present work aims to comparatively evaluate physiological responses to salt at tillering phase and the pattern of metabolic profile between two rice cultivars considered to be contrasting in salt tolerance at the pre-tillering stage. Thus, it is expected that the differential tolerance to salinity also occurs in the tillering phase and that the metabolic profile points to markers of tolerance to saline stress.

3.2 Material and methods

3.2.1 *Plant material, experimental conditions, and salinity treatments*

Two rice cultivars with differential salt tolerance, BRS Esmeralda (ES) and São Francisco (SF), were evaluated. ES cultivar was developed for cultivation in highlands, while the SF cultivar was intended for cultivation in an irrigated system. Also, the ES cultivar is considered less salt-tolerant than the SF cultivar (GADELHA, 2020). The SF and ES seeds were supplied from Instituto Agronômico de Pernambuco (IPA), Recife, PE, Brazil.

The experiment was carried out in a 2 x 2 factorial scheme, the first factor being two rice cultivars (ES and SF) and the second factor two salt conditions (0 and 80 mM NaCl). Is highlighted the definition of salinity levels was based on a study carried out by Lopes *et al.* (2020). Initially, the two rice cultivars were sown on germitest paper moistened with distilled water, in the proportion of 2.5 times the dry weight of the substrate. After sowing, the paper rolls containing the seeds were left in a BOD - type germination chamber at 30 °C, 90% relative humidity, and a photoperiod (12:12) for ten days, a period sufficient for the coleoptile would present an approximate size of 5 cm.

Soon after, the seedlings were transferred to bowls containing Clark nutrient solution (CLARK, 1975) modified, containing Fe - EDTA (0.076 mM). The nutrient solution was not oxygenated and presented approximately 171.9 μM dissolved oxygen, monitoring daily by an oximeter (HI 9146-10; Hanna instruments). Then the seedlings were placed on styrofoam supports fixed to the upper part of the bowls, the roots of the seedlings being completely submerged in the nutrient solution, for a period of 17 days for acclimatization, following the following schedule: five days under constant artificial light, five days under shade at 70% natural light, and seven days in full sun. At 27 days after sowing, the plants were transferred to 3,5 L plastic pots, where the salt treatments were applied for ten days. In the first salt-treatments application, the plants were submitted to saline treatment (80 mM NaCl) with the salt being applied in two doses daily of 40 mM to avoid osmotic shock (ARAÚJO *et al*., 2021). After that, 80 mM NaCl was applied to each solution change. Nutritional solutions were renewed every two days. In addition, the pH was monitored daily and corrected to 5.8 with KOH 20 mM. The experiment was conducted under greenhouse conditions: average air temperature of 32 °C, average air relative humidity of 70 %, and a 12-h photoperiod.

The collection of plant material for all the determinations described below was

carried out on the 37th day after the sowing, which corresponds to the beginning of tillering stage and ten days under salinity treatment.

3.2.2 Growth and development analysis

The lengths of shoots and roots were measured with a tape measure. The longest root of the plant was considered to measure the root length. After collecting leaves, stems, and roots, the dry mass determination was made in an oven with forced air circulation, at 80 ºC for 48 h, and then weighed.

3.2.3 Relative water content and relative humidity

For determining the relative water content (RWC), the plant material was collected at sunrise, which corresponds to the daytime period of greatest cell turgidity. The RWC was analyzed according to Barr and Weatherley (1962). The leaf samples consisted of ten leaf discs of 1 cm in diameter, taken from the first fully expanded leaf of the central tiller of the plant at the time of collection, while the roots samples were ten fragments of 1 cm from the median root part. The samples were weighed to obtain the fresh mass (FM), and immediately afterward, they were hydrated for three hours in distilled water under ambient light and temperature to get the turgid mass (TM) (ARNDT; IRAWAN; SANDERS, 2015). The samples were then dried in an oven at 65 ° C for 72 h to determine the dry mass (DM). To calculate the RWC, the formula was used: RWC (%) = [(FM-DM)/(TM-DM)] x 100. And to determine Relative humidity the formula used was: Relative humidity (%) = 100 - [(DM/FM) x 100].

3.2.4 Photosynthetic pigments contents

The levels of chlorophylls and carotenoids were determined using the method described by Wellburn (1994). At the time of collection, three leaf discs 1 cm in diameter were removed from the first fully expanded leaf of the rice plants and immersed in 2 ml of dimethyl sulfoxide solution saturated with $CaCO_3$ in test tubes protected from light for 48 h. Then, the tubes were incubated in a water bath at 65 °C for 30 min (BARNES *et al*., 1992). The concentrations of chlorophylls *a* (Chl *a*), *b* (Chl *b*) e *total* (Chl *total*) and carotenoids (CAR) were estimated using the following formulas: Chl *a* = $12.19A_{665} – 3.45A_{649}$, Chl *b* = $21.99A_{649} – 5.32A_{665}$, Chl *total* = $6.87A_{665} + 18.54A_{649}$; Car = $(1000A_{480} – 2.14$Clf *a* – 70.16Clf *b*)/220,

whereby A_i corresponded to the absorbance at wavelength i (665, 649 and 480 nm). After determining the pigment concentrations, their levels were expressed based on the dry mass. The dry mass was determined by drying the three leaf discs in a forced circulation oven at 65 °C for 72 h.

3.2.5 Gas exchange and chlorophyll a fluorescence

Gas exchange and chlorophyll *a* fluorescence measurements were performed in fully expanded leaves under constant CO_2 concentration and photosynthetic photon flux density (PPFD) of 400 µmol mol-1 CO_2 and 1,400 µmol photons m^{-2} s^{-1}, respectively. At harvesting, CO_2 assimilation (*A*), stomatal conductance (g_s), transpiration (*E*), and intercellular CO_2 concentration (*Ci*) were determined on the middle of the first fully expanded leaf from the apex using an infrared gas analyzer (IRGA, LI-6400XT, LI-COR, USA) coupled with artificial light. The instantaneous carboxylation efficiency (ICE) of ribulose-1,5-bisphosphate carboxylase/oxygenase (Rubisco) and instantaneous water use efficiency (WUEi) were estimated by the A/Ci and A/E ratios, respectively. Some chlorophyll *a* fluorescence parameters were also evaluated using a fluorometer (6400-40, LI-COR, USA) coupled to IRGA, as maximum (Fm') and variable (Fv') fluorescence in light-adapted leaves, steady-state fluorescence (F') in equilibrium state in the presence of light, and basal fluorescence (Fo') after excitation state of photosystem I. From these parameters were determined effective quantum yield of PSII [ΦPSII = (Fm' – F')/Fm'], photochemical quenching [qP = (Fm' – F')/(Fm' − Fo')], electron transport rate [ETR = (ΦPSII × PPFD absorbed × 0.5)], and PSII maximum efficiency (Fv'/Fm ').

3.2.6 Inorganic ions contents

To determine inorganic ions (Na^+, K^+, and Cl^-) contents, 20 mg of dry material from leaves, stems, and roots were homogenized separately with 2 mL of deionized water. The homogenates were kept in a water bath at 75 °C for one hour, shaking every 20 min. After that time, the samples were centrifuged at 3,000 x g for 10 min at room temperature (SARRUGE; HAAG, 1974). The Na^+ and K^+ contents were determined according to Malavolta, Vitti, and Oliveira (1989), with the aid of a flame photometer [Micronal, model B462 (São Paulo / SP, Brazil)] properly calibrated with 1 M NaCl and 1 M KCl solutions. The Cl^- content was determined according to a spectrophotometric mercury thiocyanate-iron method developed by

Gaines, Parker e Gascho (1984), with reading the absorbance at 460 nm, and using NaCl as standard.

3.2.7 Metabolomic analysis

The extraction and derivatization of the metabolites were performed according to Lisec *et al*. (2006). The extraction was carried out from fresh samples of leaves and roots soaked and macerated in liquid nitrogen. For this, 50 mg of the pulverized plant material were homogenized in 700 µL of an extracting solution (water: methanol: chloroform in the proportion 1: 2.5: 1, respectively), at -20 °C, for 30 min, in an environment with a temperature at 4 °C. In each sample, 30 µL of ribitol at 0.2 mg mL^{-1} was added as an internal standard. The samples were incubated in a dry bath (Thermomixer, Bioer) for 15 min at 70 °C with 350 rpm shaking. Then, the homogenate was centrifuged for 5 min at 12,000 x g. The collected supernatant was subjected to a split in 375 µL of pure chloroform and 750 µL of Milli-Q water. On that occasion, the mixture was homogenized in a vortex and centrifuged for 15 min at 2,200 x g, with the upper (polar) portion being collected. Subsequently, the polar phase of the partition was dried in SpeedVac overnight and stored at -80 ºC.

The metabolites in the dry polar fraction in SpeedVac were derivatized by adding 20 µL of methoxyamine hydrochloride solution (20 mg ml^{-1} of pyridine). The mixture was shaken in dry bath adjusted to 37 °C, for 2 h at 550 rpm, before adding 35 µL of N-methyl-N-trimethylsilyl-trifluoroacetamide (MSTFA). After MSTFA addition, the mixture was again stirred in dry bath adjusted to 37 °C, for 30 min at 550 rpm. The detection and relative quantification of the metabolites were done using a gas chromatograph-mass spectrometer (GCMS, model QP2010, Shimadzu, Tokyo, Japan). Then, 1 µL of the derivatized sample was injected into the capillary column RTX-5MS (30 m x 0.25 mm x 0.25 µm, ResteK, Bellefonte, USA), at a helium gas flow of 6,2 mL min^{-1}, injection in split mode, temperature, and interface of 230 °C, and ion source temperature of 250 °C. The chromatographic run was adjusted from a temperature of 80 °C for 2 min, followed by a heating ramp of 10 °C min^{-1} to 315 °C, with temperature maintenance for 8 min.

Each chromatography and mass spectrum were evaluated using Xcalibur™ 2.1 program (Thermo Fisher Scientific, Waltham, MA, USA) according to Roessner e*t al.* (2001). The compounds' identification was based on their retention times and mass spectrum fragmentation compared to standard mass spectra in the internal metabolite library and Golm metabolome database. Some unidentified metabolites were named as "unknown" and

enumerated in order of output in the chromatogram. The relative value of each metabolite was determined by the division of their respective peak areas by internal standard peak area (ribitol, Sigma–Aldrich) and, after, divided by the dry mass of the sample.

3.2.8 Experimental design and statistical analysis

The experiment was conducted in a completely randomized design under a 2 x 2 factorial scheme (two rice cultivars x two salinity levels) with five repetitions with two plants each. The ES and SF were the two rice cultivars, and the two salt conditions were established by nutrient solution added 0 and 80 mM NaCl. The physiological and biochemical data were submitted to a normality test (Shapiro-Wilk test) before the bidirectional analysis of variance (ANOVA). The Tukey test was applied to compare the means of the variables for a significant F-test at 5%. The software used for statistical analysis was GraphPad Prism 8.0. These data also were log-transformed and divided by the standard deviation of each variable (Autoscaling) for chemometrics analysis [PCA (Principal Component Analysis)] and correlation analysis [Pearson correlation ($p < 0.05$)] by MetabolAnalyst 5.0 (https://www.metaboanalyst.ca).

The relative abundance values of the metabolites were processed in MetabolAnalyst 5.0. The data were subjected to were cube root transformed and mean-centered and divided by the standard deviation of each variable (Autoscaling) before being subjected to one-way ANOVA and the Tukey test ($p < 0.05$). Besides, the transformed metabolomic data were submitted to the following multivariate analyzes: chemometric analysis [PLS-DA (Discriminant Analysis of Partial Least Squares)] and cluster analysis (hierarchical grouping). Hierarchical clustering was as a heatmap (Euclidean distance, Ward clustering algorithm).

3.3 Results

3.3.1 Growth and development

The saline conditions reduced the growth and development of the two rice cultivars (Figure 2). The accumulation of dry mass in leaves, stems, and roots was negatively affected (Figure 3a-c). The SF plants showed higher dry mass of the leaves and stem under non-saline conditions than ES plants, but no difference under salinity (Figure 3a, b). That way, the SF cultivar suffered a more significant loss than ES by salinity in the dry mass of leaves and stems, reducing 71% and 63%, respectively. While the root dry mass decayed 62% in both cultivars

(Figure 3c). Shoot and root lengths also decreased in the presence of NaCl (Figure 3d-e). However, only the ES cultivar maintained the length of its roots (Figure 3e). Thus, the shoot reduction was 34% in both cultivars, and the root length decrease by 16% in the SF cultivar.

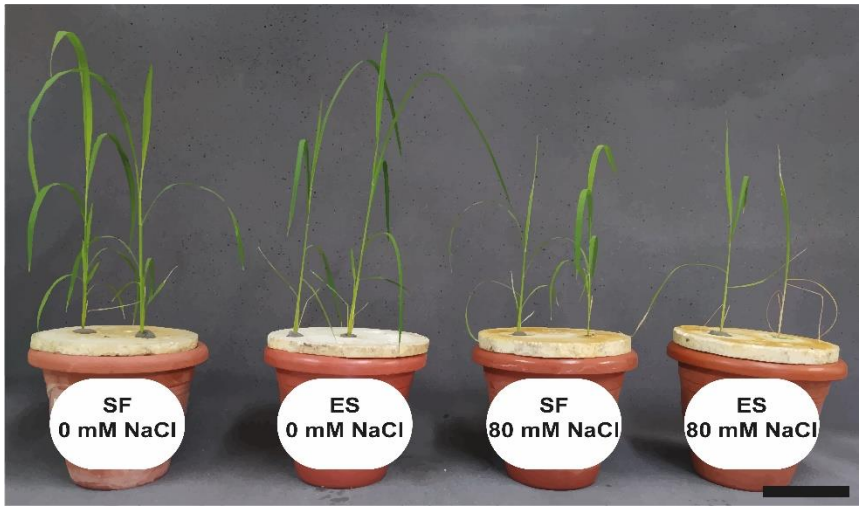

Figure 2 - Rice plants of the São Francisco (SF) and BRS Esmeralda (ES) cultivars under no-saline (0 mM NaCl) or saline (80 mM NaCl) conditions for ten days. *Scale bars*, 10 cm.

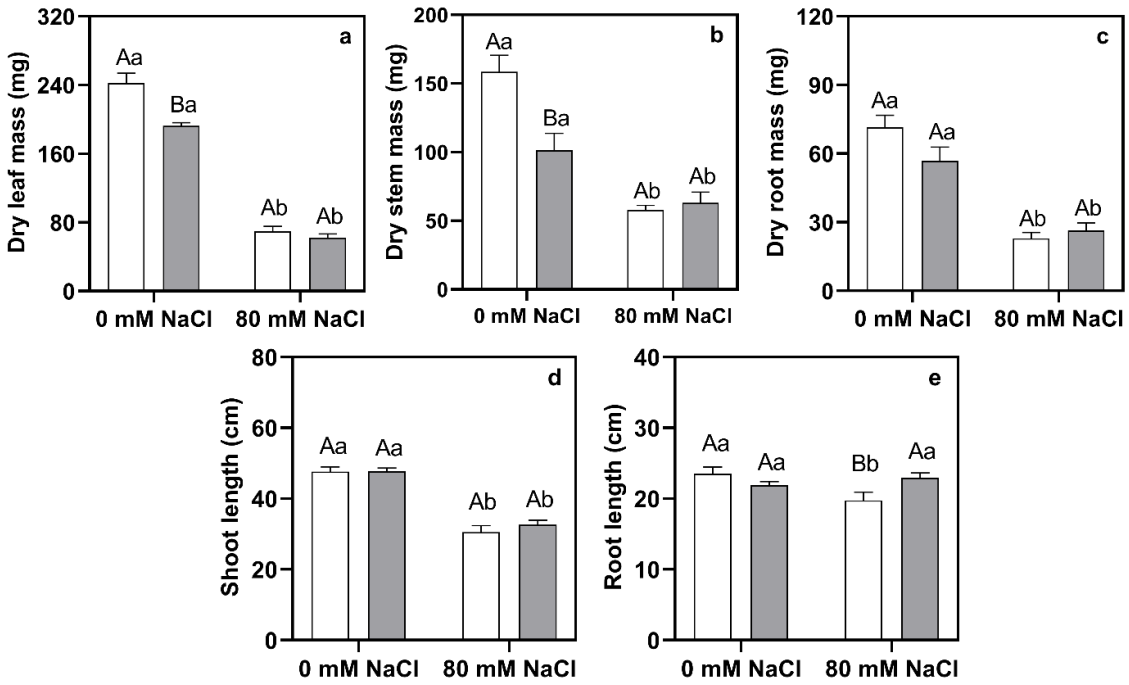

Figure 3 - Growth analysis of rice plants cv. São Francisco (SF, *white bars*) and BRS Esmeralda (ES, *grey bars*) under no-saline or saline (80 mM NaCl) conditions for ten days. Dry mass of leaves (**a**), stems (**b**), roots (**c**), and shoot (**d**) and root (**e**) length. For each variable, the capital letters and lowercase letters compare the cultivar and salinity treatments, respectively. All subfigures exhibit a significant interaction between treatments except **c** and **d**, according to F-test ($p < 0.05$). Bars represent means (n=5) + standard error.

The salinity did not affect the relative humidity of leaves and roots and RWC in the roots of both cultivars (Figure 4). However, there was a slight reduction on average of 8% in the RWC of the leaves of both cultivars (Figure 4b).

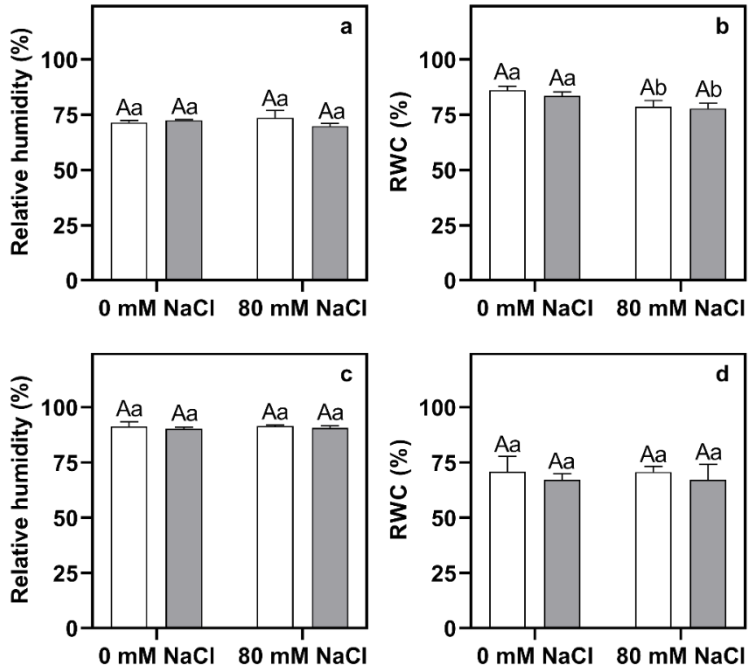

Figure 4 - Relative humidity and relative water content (RWC) of rice plants cv. São Francisco (SF, *white bars*) and BRS Esmeralda (ES, *grey bars*) under no-saline or saline (80 mM NaCl) conditions for ten days. Relative humidity of leaves (**a**) and roots (**c**), and RWC of leaves (**b**) and roots (**d**). For each variable, the capital letters and lowercase letters compare the cultivar and salinity treatments, respectively. Neither subfigures exhibit significant interaction between treatments, according to F-test ($p < 0.05$). Bars represent means (n=5) + standard error.

3.3.2 Photosynthetic pigments, gas exchange, and chlorophyll a fluorescence

The salinity did not affect Chl *a* and CAR contents (Figure 5a, d). In contrast, the content of Chl *b* presented a 42% reduction in ES plants cultivar under saline stress, while in the SF cultivar, it was not altered by salinity (Figure 5b). The Chl *total* contents decreased on average 15% with salt stress, regardless of the two rice cultivars (Figure 5c).

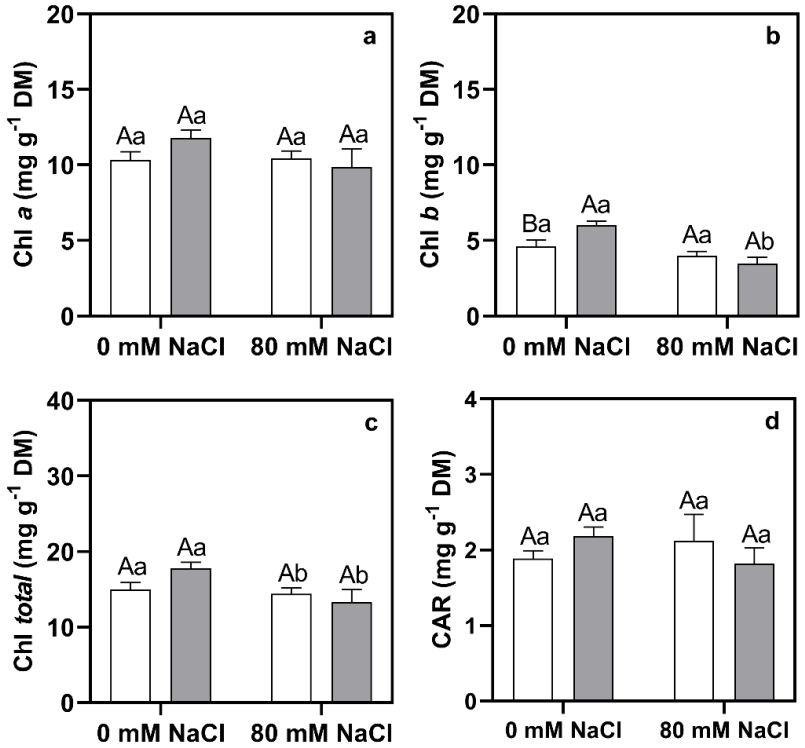

Figure 5 - Photosynthetic pigments contents of rice plants cv. São Francisco (SF, *white bars*) and BRS Esmeralda (ES, *grey bars*) under no-saline or saline (80 mM NaCl) conditions for ten days. Chlorophyll *a* (**a**, Chl *a*), *b* (**b**, Chl *b*), total (**c**, Chl *total*), and carotenoids (**d**, CAR). For each variable, the capital letters and lowercase letters compare the cultivar and salinity treatments, respectively. Only subfigure **b** exhibits a significant interaction between treatments, according to F-test ($p < 0.05$). Bars represent means (n=5) + standard error.

The *A*, g_s, *E* and ICE decreased on average by 43%, 54%, 38% and 39%, respectively, only with the presence of 80 mM NaCl and invariable to the cultivars (Figure 6a, b, d, e). However, ES cultivar presented a g_s 33% lower than SF cultivar regardless of saline condition (Figure 6b). *Ci* and WUEi were not affected by salt stress (Figure 6d, f). The fluorescence parameters of chlorophyll *a* were also reduced, except in qP (Figure 7). The salinity promoted the reduction of ΦPSII, ETR, and Fv'/Fm' on average by 20%; 19% e 11%, respectively (Figure 7a, c, d).

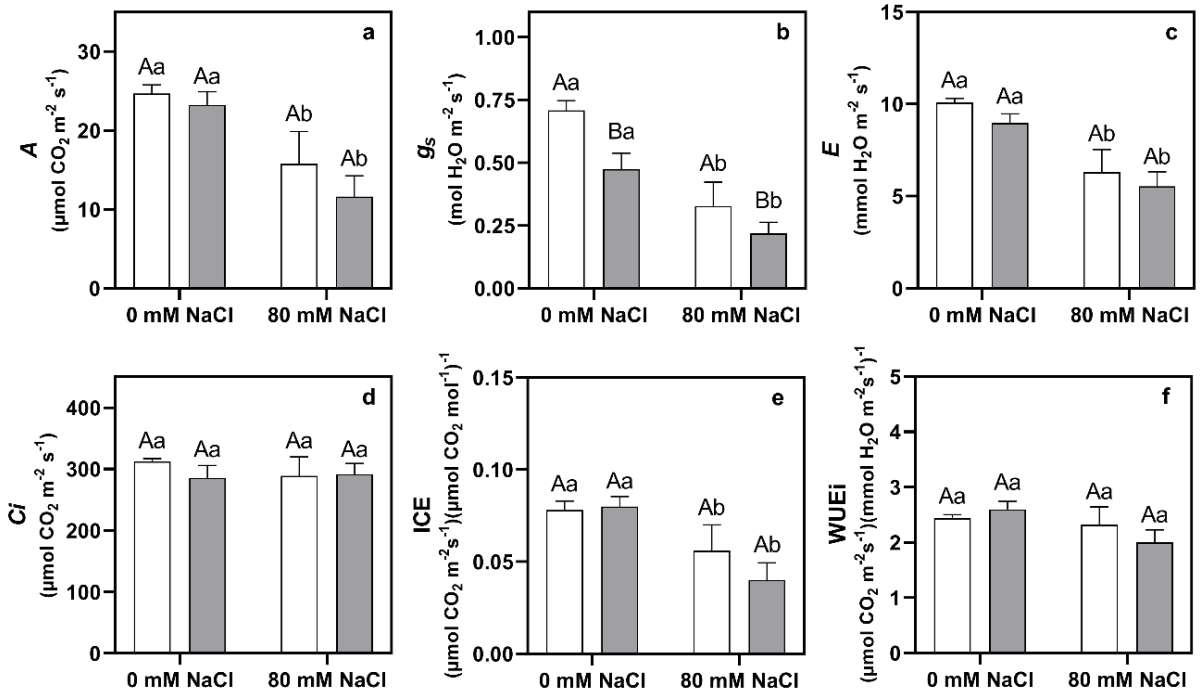

Figure 6 - Gas exchange of rice plants cv. São Francisco (SF, *white bars*) and BRS Esmeralda (ES, *grey bars*) under no-saline or saline (80 mM NaCl) conditions for ten days. CO_2 assimilation (**a**, *A*), stomatal conductance (**b**, g_s), transpiration (**c**, *E*), internal carbon concentration (**d**, *Ci*), instantaneous carboxylation efficiency (**e**, ICE), and instant water use efficiency (**f**, WUEi). For each variable, the capital letters and lowercase letters compare the cultivar and salinity treatments, respectively. Neither subfigures exhibit significant interaction between treatments, according to F-test ($p < 0.05$). Bars represent means (n=5) + standard error.

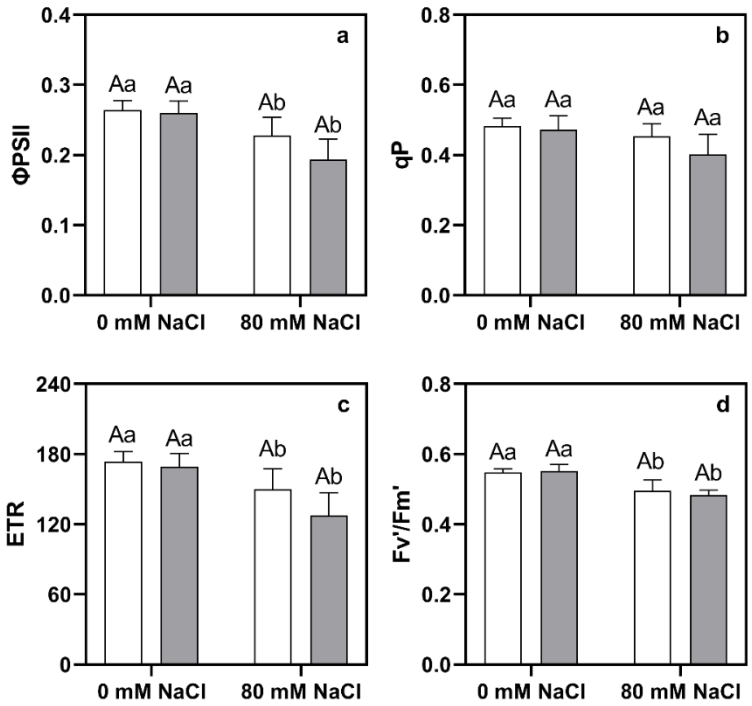

Figure 7 - Chlorophyll *a* fluorescence of rice plants cv. São Francisco (SF, *white bars*) and BRS Esmeralda (ES, *grey bars*) under no-saline or saline (80 mM NaCl) conditions for ten days. Effective quantum yield of PSII (**a**, ΦPSII), photochemical quenching (**b**, qP), electron transport rate (**c**, ETR), and PSII maximum efficiency (**d**, Fv'/Fm'). For each variable, the capital letters and lowercase letters compare the cultivar and salinity treatments, respectively. Only subfigure **b** exhibits a significant interaction between treatments, according to F-test ($p < 0.05$). Bars represent means (n=5) + standard error.

3.3.3 Inorganic ions contents

The accumulation and distribution of ions Na^+, Cl^- e K^+ promoted by salinity dependent on the cultivar (Figure 8). The salinity induced a significant increase in Na^+ content in leaves, stems, and roots on average of 973%, 662%, and 359%, respectively, in both cultivars (Figure 8a-c). There were no differences in the Na^+ content in the leaves and roots between the cultivars in both saline conditions.

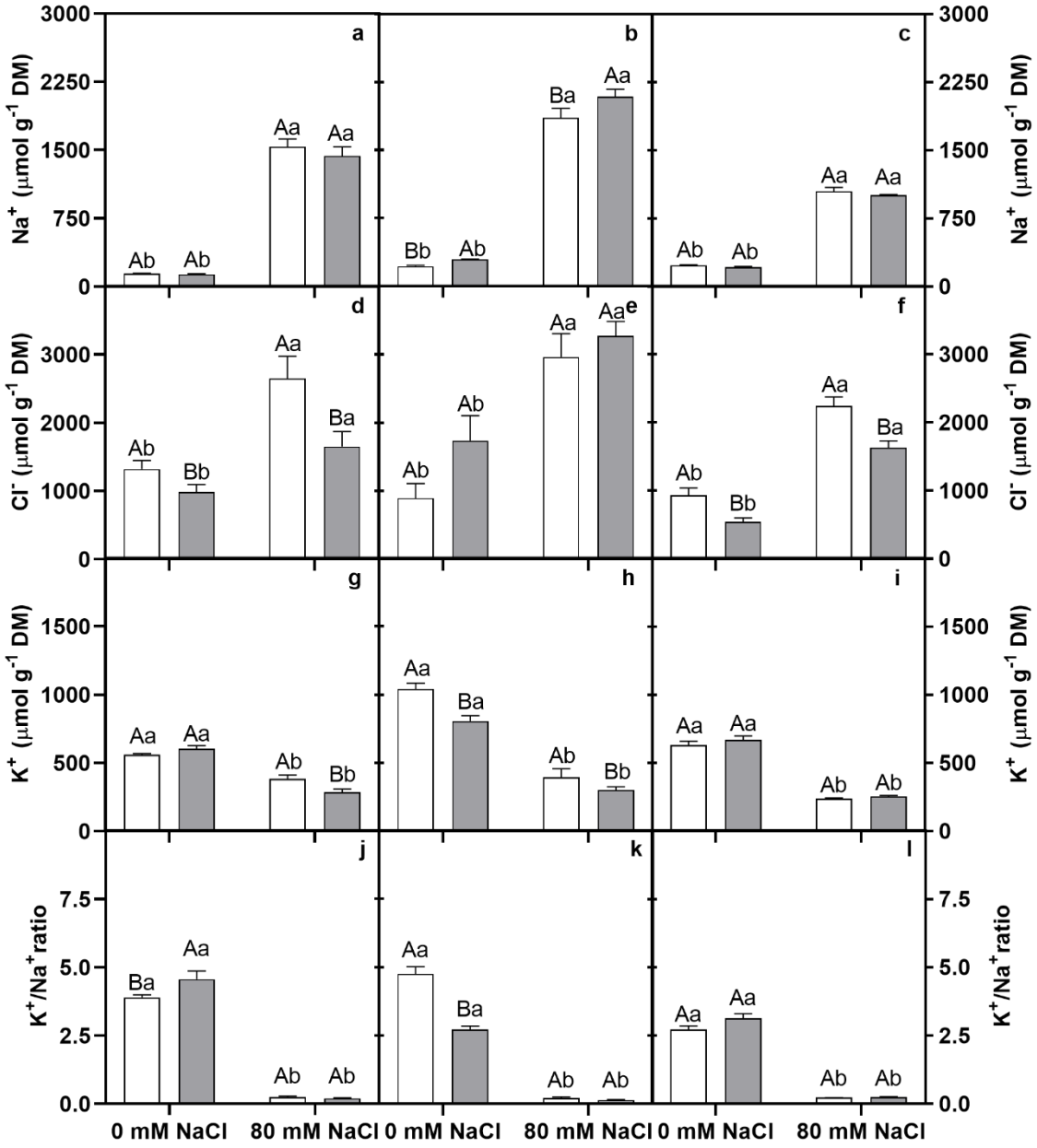

Figure 8 - Inorganic ions of rice plants cv. São Francisco (*white bars*) and BRS Esmeralda (*grey bars*) under no-saline or saline (80 mM NaCl) conditions for ten days. Na^+ content in leaves (**a**), stems (**b**), and roots (**c**); Cl^- content in leaves (**d**), stems (**e**), and roots (**f**); and K^+ content in leaves (**g**), stems (**h**), and roots (**i**)); and K^+/ Na^+ ratio in leaves (**j**), stems (**k**), and roots (**l**). For each variable, the capital letters and lowercase letters compare the cultivar and salinity treatments, respectively. Only subfigure **g** exhibits a significant interaction between treatments, according to *F*-test ($p < 0.05$). Bars represent means (n=5) + standard error.

Salinity also promoted an increase on average of 84%, 160%, and 170% in the Cl^- content in leaves, stems, and roots both cultivars, respectively (Figure 8 d-f). The Cl^- contents were 31% and 35% lower in leaves and roots, respectively, in ES cultivar than SF cultivar regardless of saline condition (Figure 8d, f). Also, there was no significant difference between cultivars in the accumulation of Cl^- in the stems (Figure 8e).

The K^+ contents were reduced by the salinity in both cultivars (Figure 8g-i). However, there was a significant interaction between salinity and cultivars in leaves (Figure 8g). So that salinity reduced the K^+ content in SF cultivar by 31%, while in ES cultivar, the reduction was 52%. On the other hand, ES plants presented 23% fewer K^+ in stems than SF plants regardless of salinity (Figure 8h). Also, the salinity promoted a reduction on average of 62% in the K^+ content in the stems of both cultivars. In the roots, the decrease avarage in the K^+ content was 62% in both cultivars (Figure 8i). The stem was the plant organ that most accumulated Na^+ and Cl^- under saline conditions, with mean values of 1973.53 μmol of Na^+ g^{-1} DM and 3119.95 μmol of Cl^- g^{-1} DM. Followed by leaves and roots, with mean values of 1486 μmol of Na^+ g^{-1} DM and 2149 μmol of Cl^- g^{-1} DM, and 1027 μmol of Na^+ g^{-1} DM and 1938 μmol of Cl^- g^{-1} DM, respectively. In addition, stems and roots showed the most significant reductions in the K^+ content, provoked by salinity.

The K^+/Na^+ ratio of plant organs, except for roots, showed a significant interaction between salinity and cultivar (Figure 8j-l). In leaves, the K^+/Na^+ ratio in a non-salt environment was 17% higher in ES than in SF (Figure 8j). In the stems, this value was 75% higher in the SF than in the ES (Figure 8k). Considering the saline environment, both in the leaves and in the stems, this proportion was indifferent to the cultivar. Furthermore, it was possible to observe only a reduction in the K^+/Na^+ ratio with salinity. In leaves, cultivar ES was the most affected, decreasing 95% of K^+/Na^+ values (Figure 8j), while in the stems, both SF and ES reduced 95% of their values with salinity (Figure 8k). In roots, the most notable effect was due only to salinity, who's K^+/Na^+ ratio values were reduced on average by 92% (Figure 8l).

3.3.4 PCA of physiological and biochemical data

The first two principal components were sufficient to explain 63% of the total variation considering all the physiological and biochemical data obtained of rice plants of ES cultivar growing under non-salt conditions (ES-C) and salt stress conditions (ES-S), and SF cultivar growing under non-salt conditions (SF-C) and salt stress conditions (SF-S) (Figure 9a). With them, it was noticeable the clear separation between the groups of plants of both cultivars

under absence (ES-C and SF-C) and presence (ES-S and SF-S) of salinity. However, it was not possible to differentiate the cultivars SF and ES in the two environmental conditions evaluated. With the loading plot and biplot, it was possible to observe the disposition of the variation of the physiological and biochemical parameters (Figure 9b, c). The first principal component (PC 1) was positively influenced by 7 out of 32 evaluated parameters, while it was indifferent to one and negatively influenced by 24 parameters. The second principal component (PC 2) was positively influenced by 12 parameters, while it was indifferent to one and negatively influenced by 19 parameters. Furthermore, PC 1 explained the separation between stressed and non-stressed plants (Figure 9c). The Na^+ e Cl^- contents were the parameters that most increased under salinity and together with the parameters that most reduced under salinity: shoot length, leaf dry mass, root dry mass, A, g_s, E, ICE, K^+ content, were the parameters pointed out by the loading plot that most contributed to the separation of the ES-C and SF-C group of the ES-S e SF-S group (Figure 9b). The PC 2 did not contribute sufficiently to a clear separation of the four groups (Figure 9a).

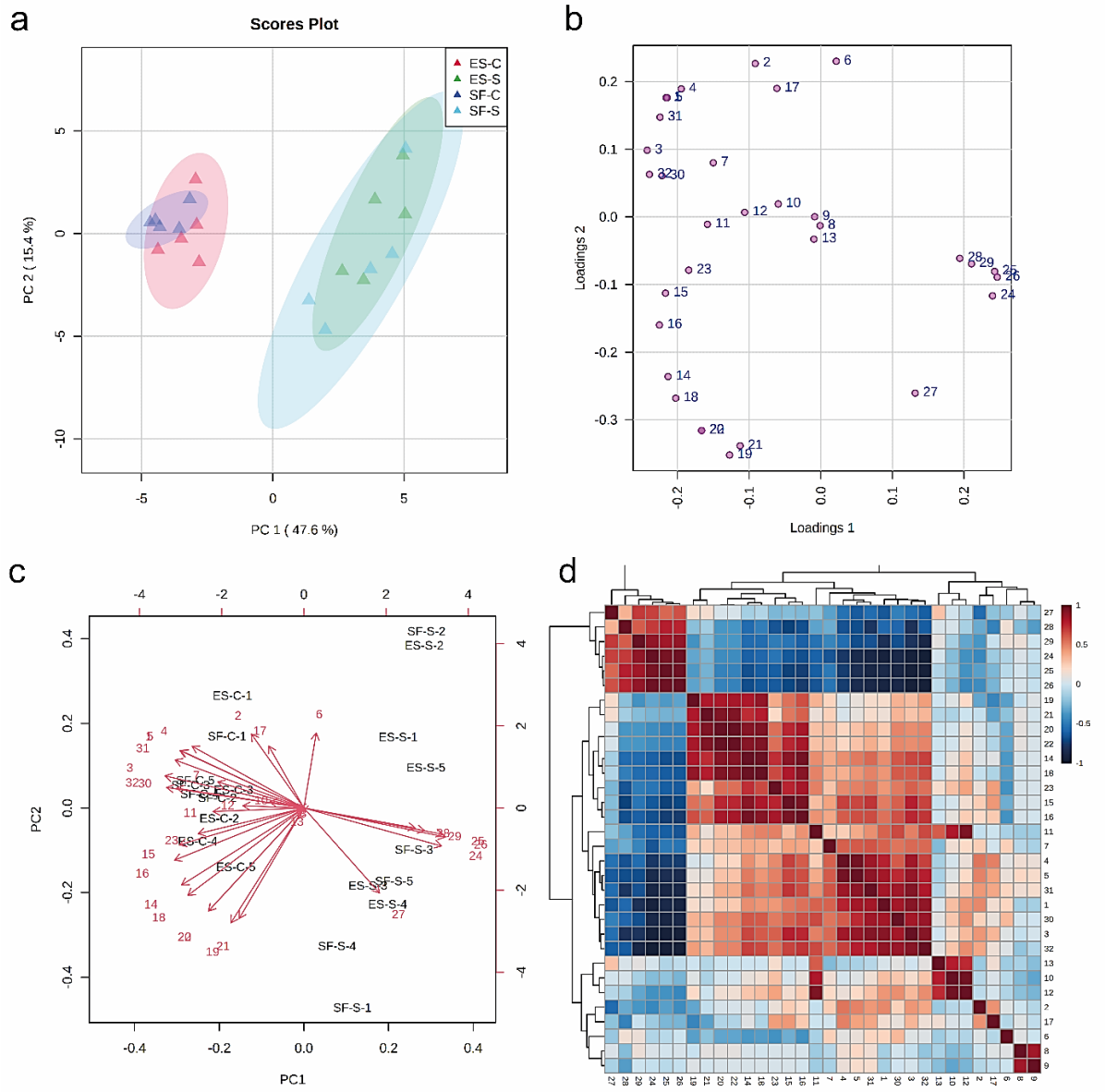

Figure 9 - Principal component analysis (PCA) of physiological and biochemical parameters of rice cv. BRS Esmeralda growing under non-salt conditions (ES-C) and salt stress conditions (ES-S) and cv. São Francisco growing under non-salt conditions (SF-C) and salt stress conditions (SF-S) for ten days. Scores plot (**a**), loading plot (**b**), and biplot (**c**) of the first and second components (PC 1 and PC 2), indicating the clustering of samples into four groups. The correlation heatmaps (**d**) shows the Pearson correlation level of the analyzed parameters. For more details, see Apêndice A. Paraments list: **1** - Shoot length, **2** - Root length, **3** - Leaf dry mass, **4** - Stem dry mass, **5** - Root dry mass, **6** - Leaf relative humidity, **7** - Relative water content of leaf, **8** - Root relative humidity, **9** - Relative water content of root, **10** - Chlorophyll *a*, **11** - Chlorophyll *b*, **12** - Chlorophyll *total*, **13** - Carotenoids, **14** - CO_2 assimilation, **15** - Stomatal conductance, **16** - Transpiration, **17** - Intercellular CO_2 concentration, **18** - Carboxylation efficiency of Rubisco, **19** - Instantaneous water use efficiency, **20** - Effective quantum yield of PSII, **21** - Photochemical quenching, **22** - Electron transport rate, **23** - PSII maximum efficiency, **24** - Na^+ leaf, **25** - Na^+ stem, **26** - Na^+ root, **27** - Cl^- leaf, **28** - Cl^- stem, **29** - Cl^- root, **30** - K^+ leaf, **31** - K^+ stem, **32** - K^+ root. All data were divided by the standard deviation of each variable (Autoscaling) for chemometrics analysis (PCA) and Pearson r-test by MetabolAnalyst 5.0.

As for the correlation of parameters, the group of variables: Na^+ content in leaves, stems and roots and Cl^- content in roots showed a strong positive correlation ($r > 0.7$, $p < 0.05$) with each other (Figure 9d; Apêndice A). The same is true for the group of variables formed by shoot length, leaf dry mass, root dry mass, K^+ contents in leaves, stems and roots. However, when considering the parameters of these same groups, there was a strong negative correlation ($r < -0.7$, $p < 0.05$) between them. It is also important to note that the set of variables formed

by the variables Na^+ stem and Na^+ root was also negatively correlated ($r < -0.7$, $p < 0.05$) to the variables g_s e E.

3.3.5 Leaf metabolomic profiling

The scores plot showed that the first two components accounted for 61% of the total variability (83% - data not shown) in leaves, according to the partial least squares-discriminant analysis (PLS-DA) model with the five principal components (Figure 10a). Based on the pattern of leaf metabolic profile of the four groups (ES-C, ES-S, SF-C, and SF-S) and PLS-DA analysis, it was possible to observe an overlap of the ES-S and SF-C groups, as well as the distinction between these two groups and the ES-C and SF-S groups, also distinct from each other. Loading plots generated show the variation of individual metabolites (Figure 10b). The PC 1 was positively affected by 94 metabolites and negatively affected by eight metabolites, while PC 2 was positively affected by 11 metabolites and negatively by 91 metabolites. Besides, a cross-validation and permutation test ($p < 0.05$) allowed us to use PLS-DA instead of PCA analysis (Figure 10c), being this more efficient to discriminate against the groups.

In the rice leaves, 102 metabolic compounds were detected (Figura 10; Apêndice B). Among these, 69 were identified: 24 sugars and their derivatives, 20 amino acids and their derivatives, 17 organic acids, two phenolic precursors, two nitrogen compounds, one flavonoid, one nucleotide, one polyamine, and one inorganic acid. Considering the totality of the metabolites found, the metabolites with the highest relative abundances were sucrose, phosphoric acid, glutamic acid, shikimic acid, and quinic acid. Meanwhile, the metabolites unknown 1, 2-aminoisobutyric acid, xylitol, unknown 31 e pyroglutamic had the lowest relative abundances. However, the variable importance in projection (VIP) scores graph displayed the most important metabolites for differentiating the treatments by the abundance of metabolites in each treatment (Figure 10d). VIP plot showed 34 metabolites of more than 1.2 VIP scores, in descending order of VIP score they are: glucopyranoside, lysine, ornithine, 2-aminoisobutyric acid, glutamine, cysteine, alanine, proline, asparagine, glutamic acid, unknown 24, tyrosine, serine, xylitol, unknown 13, unknown 15, fructose, sorbose, ribose, galactose, putrescine, gulonic acid, galactinol, unknown 1, threonine, isoleucine, phenylalanine, unknown 9, mannose, 2-oxobutyric acid, guanidine, leucine, succinic acid, and maltotriose.

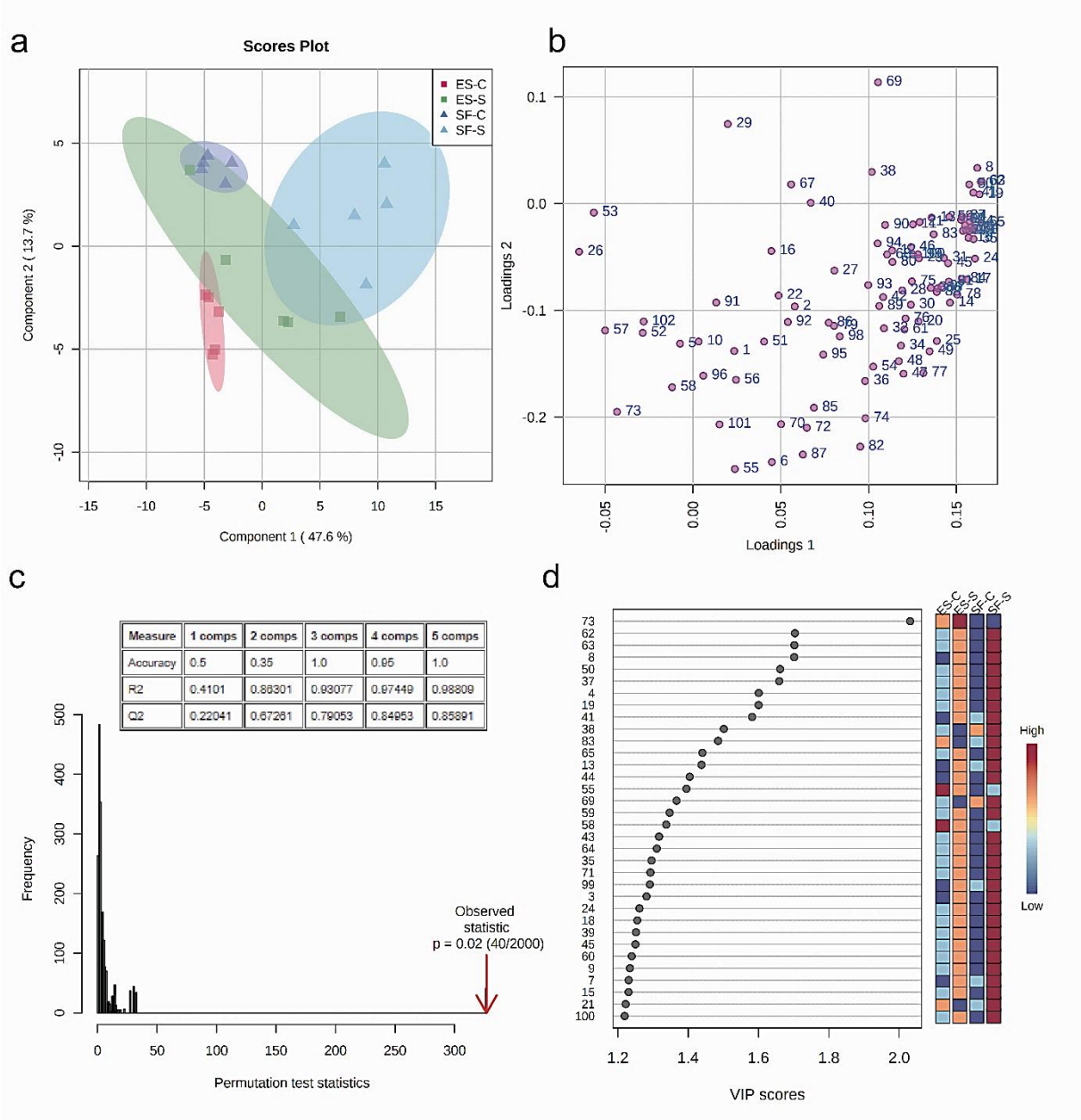

Figure 10 - Partial least squares - discriminant analysis (PLS-DA) of metabolic profiles in leaves of rice cv. BRS Esmeralda growing under non-salt conditions (ES-C) and salt stress conditions (ES-S) and cv. São Francisco growing under non-salt conditions (SF-C) and salt stress conditions (SF-S) for ten days. Scores plot (**a**), loading plot (**b**), and PLS-DA cross-validation and permutation test (**c**) of the first and second components indicating the clustering of samples into four groups. VIP scores plot of metabolites (**d**) shows metabolites for displaying a VIP score of greater than 1.2. Red or blue squares on the right indicate the high and low abundance of the corresponding metabolite in each treatment, respectively. VIP score was based on the first component of the PLS-DA model. Metabolites class: **Amino acid** – Alanine (4), Valine (11), Serine (13), Leucine (15), Isoleucine (18), Proline (19), Glycine (20), Threonine (24), Aspartic acid (28), Hydroxyproline (29), Cysteine (37), Glutamic acid (38), Phenylalanine (39), Asparagine (41), Glutamine (50), Lysine (62), Ornithine (63), Tyrosine (65), Cystine (78); **Amino acid derived** - Pyroglutamic acid (30); **Flavonoid** – Quercetin (102); **Inorganic acid** - Phosphoric acid (16); **Nitrogenous compounds** – Guanidine (7), Urea (12); **Nucleotide** - Adenosine-5-monophosphate (101); **Organic acid** - Pyruvic acid (1), Lactic acid (2), Oxalic acid (5), 2-aminoisobutyric acid (8), 2-oxobutyric acid (9), Malonic acid (10), Succinic acid (21), Glyceric acid (22), Fumaric acid (23), Malic acid (26), Erythronic acid (33), Lyxose (34), 2-aminoadipic acid (46), Citric acid (53), Glucaric acid (67), Gulonic acid (71), Glucuronic acid (76); **Phenolic precursor** - Shikimic acid (52), Quinic acid (57); **Polyamine** – Putrescine (35); **Sugar** – Lyxose (27), Xylulose (31), Erythrose (36), Ribose (43), Allose (56), Sorbose (58), Fructose (59), Mannose (60), Glucose (61), Galactose (64), Cellobiose (91), Sucrose (93), Trehalose (95), Raffinose (97), Fructose-1,6-diphosphate (98), Maltotriose (100); **Sugar alcohol** – Xylitol (44), Arabitol (48), Glycerol-2-phosphate (49), Mannitol (66), Inositol (74), Galactinol (99), **Sugar derived** – Mannopyranoside (42), Glucopyranoside (73); **Unidentified Metabolites** - Unknown 1 (3), Unknown 2 (6), Unknown 3 (14), Unknown 4 (17), Unknown 5 (25), Unknown 7 (32), Unknown 8 (40), Unknown 9 (45), Unknown 10 (47), Unknown 11 (51), Unknown 12 (54), Unknown 13 (55), Unknown 14 (68), Unknown 15 (69), Unknown 16 (70), Unknown 17 (72), Unknown 18 (75), Unknown 19 (77), Unknown 20 (79), Unknown 21 (80), Unknown 22 (81), Unknown 23 (82), Unknown 24 (83), Unknown 25 (84), Unknown 26 (85), Unknown 27 (86), Unknown 28 (87), Unknown 29 (88), Unknown 30 (89), Unknown 31 (90), Unknown 32 (92), Unknown 33 (94), Unknown 34 (96). All data were cube root transformed and divided by the standard deviation of each variable (Autoscaling) for chemometrics analysis (PLS-DA) by MetabolAnalyst 5.0.

Seventy-nine metabolites were differentially expressed in the rice leaves considering the four groups analyzed (Figure 11; Apêndice B). Salinity upregulated 26 metabolites in both cultivars, these being: unknown 1, guanidine, 2-aminobutyric acid, valine, unknown 3, leucine, isoleucine, proline, threonine, pyroglutamic acid, xylulose, putrescine, phenylalanine, asparagine, methyl α-D-mannopyranoside, xylitol, 2-aminoadipic acid, glutamine, fructose, glucose, galactose, tyrosine, unknown 14, cystine, unknown 21, and unknown 22. Salinity upregulated 37 metabolites only in the SF cultivar, these being: alanine, 2-oxobutyric acid, urea, unknown 4, glycine, fumaric acid, unknown 5, aspartic acid, erythronic acid, erythrose, cysteine, glutamic acid, ribose, unknown 9, unknown 10, arabitol, glycerol-2-phosphate, mannose, lysine, ornithine, mannitol, inositol, gulonic acid, unknown 18, glucuronic acid, unknown 19, unknown 23, unknown 24, unknown 25, unknown 29, unknown 30, sucrose, trehalose, fructose-1,6-diphosphate, galactinol, maltotriose, and adenosine-5-monophosphate. In contrast, upregulated three metabolites (phosphoric acid, glucopyranoside, unknown 31) and downregulated seven metabolites (malonic acid, malic acid, citric acid, unknown 23, cellobiose, trehalose, and unknown 34) only in ES cultivar. Thus, two metabolites (phosphoric acid and glucopyranoside) showed fewer relative abundance in SF cultivar than in ES, and 24 metabolites showed higher relative abundance in SF cultivar than in ES, being these: alanine, isobutyric acid, urea, proline, fumaric acid, aspartic acid, cysteine, glutamic acid, asparagine, ribose, unknown 9, glutamine, fructose, lysine, ornithine, tyrosine, mannitol, unknown 18, glucuronic acid, unknown 19, unknown 23, unknown 30, sucrose, and trehalose.

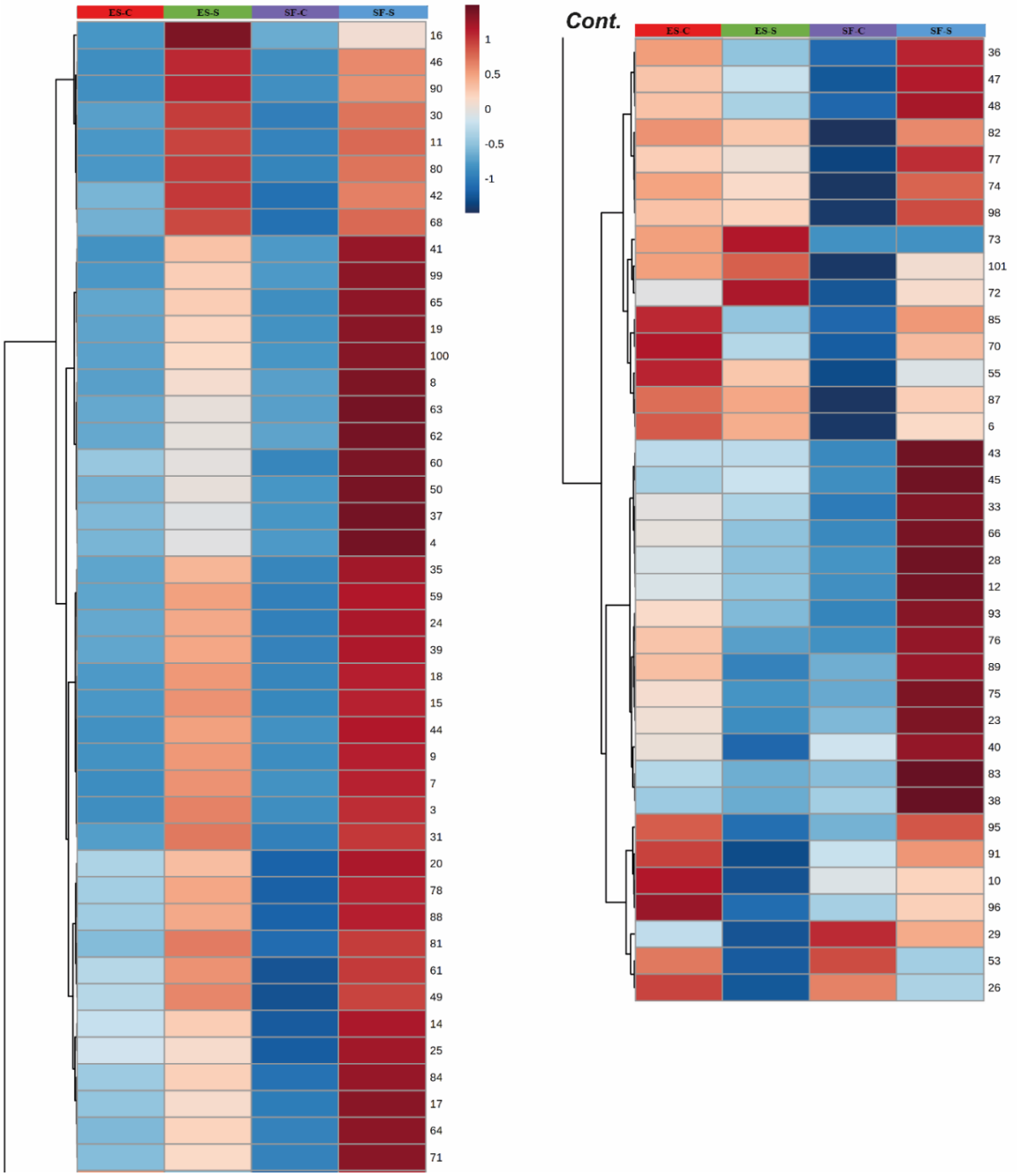

Figure 11 - Heatmap of normalized values of metabolites in leaves of rice cv. BRS Esmeralda growing under non-salt conditions (ES-C) and salt stress conditions (ES-S) and cv. São Francisco growing under non-salt conditions (SF-C) and salt stress conditions (SF-S) for ten days. The heatmap shows a high (red scale) or low (blue scale) relative amount of each metabolite. Significant metabolites list ($p < 0.05$) grouped according to metabolites class: **Amino acid** – Alanine (4), Valine (11), Serine (13), Leucine (15), Isoleucine (18), Proline (19), Glycine (20), Threonine (24), Aspartic acid (28), Hydroxyproline (29), Cysteine (37), Glutamic acid (38), Phenylalanine (39), Asparagine (41), Glutamine (50), Lysine (62), Ornithine (63), Tyrosine (65), Cystine (78); **Amino acid derived** - Pyroglutamic acid (30); **Flavonoid** – Quercetin (102); **Inorganic acid** - Phosphoric acid (16); **Nitrogenous compounds** – Guanidine (7), Urea (12); **Nucleotide** - Adenosine-5-monophosphate (101); **Organic acid** - Pyruvic acid (1), Lactic acid (2), Oxalic acid (5), 2-aminoisobutyric acid (8), 2-oxobutyric acid (9), Malonic acid (10), Succinic acid (21), Glyceric acid (22), Fumaric acid (23), Malic acid (26), Erythronic acid (33), Lyxose (34), 2-aminoadipic acid (46), Citric acid (53), Glucaric acid (67), Gulonic acid (71), Glucuronic acid (76); **Phenolic precursor** - Shikimic acid (52), Quinic acid (57); **Polyamine** – Putrescine (35); **Sugar** – Lyxose (27), Xylulose (31), Erythrose (36), Ribose (43), Allose (56), Sorbose (58), Fructose (59), Mannose (60), Glucose (61), Galactose (64), Cellobiose (91), Sucrose (93), Trehalose (95), Raffinose (97), Fructose-1,6-diphosphate (98), Maltotriose (100); **Sugar alcohol** – Xylitol (44), Arabitol (48), Glycerol-2-phosphate (49), Mannitol (66), Inositol (74), Galactinol (99), **Sugar derived** – Mannopyranoside (42), Glucopyranoside (73); **Unidentified Metabolites** - Unknown 1 (3), Unknown 2 (6), Unknown 3 (14), Unknown 4 (17), Unknown 5 (25), Unknown 7 (32), Unknown 8 (40), Unknown 9 (45), Unknown 10 (47), Unknown 11 (51), Unknown 12 (54), Unknown 13 (55), Unknown 14 (68), Unknown 15 (69), Unknown 16 (70), Unknown 17 (72), Unknown 18 (75), Unknown 19 (77), Unknown 20 (79), Unknown 21 (80), Unknown 22 (81), Unknown 23 (82), Unknown 24 (83), Unknown 25 (84), Unknown 26 (85), Unknown 27 (86), Unknown 28 (87), Unknown 29 (88), Unknown 30 (89), Unknown 31 (90), Unknown 32 (92), Unknown 33 (94), Unknown 34 (96). Each square represents the mean of five biological replicates, and the statistical difference was obtained according to *F*-test ($p < 0.05$) and Tukey test ($p < 0.05$). For more details, see Apêndice B.

3.3.6 Root metabolomic profiling

The scores plot showed that the first two components accounted for 49% of the total variability (78% - data not shown) in roots, according to the PLS-DA model with the five principal components (Figure 12a). Loading plots generated show the variation of individual metabolites (Figure 12b). Besides, a cross-validation and permutation test ($p < 0.01$) allowed us to use PLS-DA instead of PCA analysis (Figure 12c). In the roots, 64 metabolites were detected (Apêndice C). Of these, 54 were identified: 20 sugars and their derivatives, 17 amino acids and their derivatives, 11 organic acids, two phenolic precursors, two nitrogen compounds, a polyamide, and an inorganic acid. From the root metabolic profile of the four groups (ES-C, ES-S, SF-C, and SF-S) and PLS-DA analysis, it was possible to observe the overlap of the ES-C and ES-S groups, as well as the distinction between these two groups and the groups SF-C and SF-S, also distinct from each other (Figure 12a). PC 1 was positively affected by 15 metabolites and negatively affected by 47 metabolites (Figure 12b), while PC 2 was positively affected by 57 metabolites and negatively by seven metabolites. VIP plot showed 22 metabolites of more than 1.0 VIP scores (Figure 12d), in descending order of VIP score they are: arabitol, glyceric acid, glucopyranoside, unknown 32, 2-oxoglutaric acid, sorbose, glycerol-2-phosphate, ornithine, lyxose, fructose-1,6-diphosphate, unknown 13, fructose, glucose, galactinol, erythrose, lysine, mannose, inositol, raffinose, isoleucine, ribose, leucine.

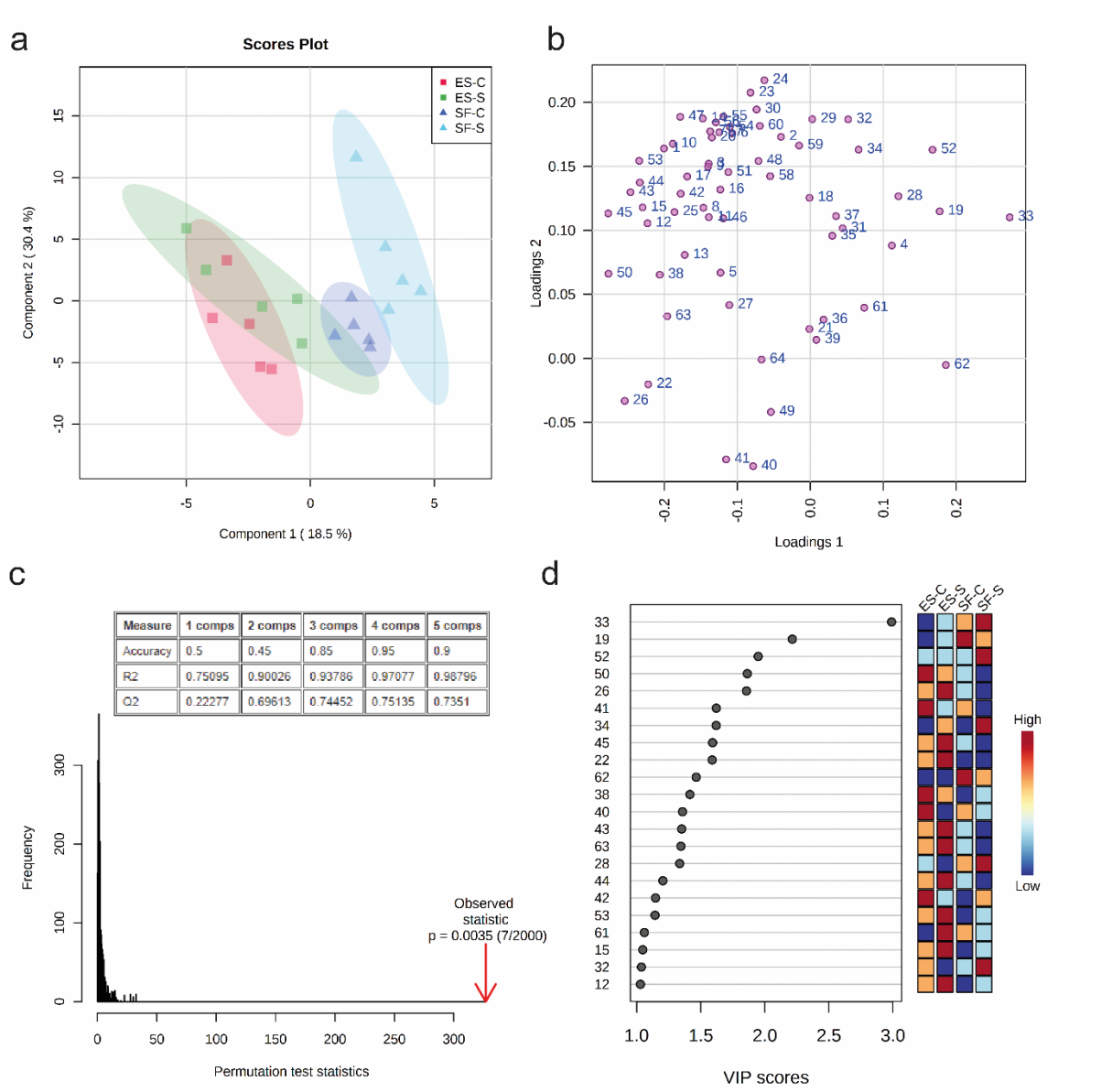

Figure 12 - Partial least squares - discriminant analysis (PLS-DA) of metabolic profiles in roots of rice cv. BRS Esmeralda growing under non-salt conditions (ES-C) and salt stress conditions (ES-S) and cv. São Francisco growing under non-salt conditions (SF-C) and salt stress conditions (SF-S) for ten days. Scores plot (**a**), loading plot (**b**), and PLS-DA cross-validation and permutation test (**c**) of the first and second components indicating the clustering of samples into four groups. VIP scores plot of metabolites (**d**) shows metabolites for displaying a VIP score of greater than 1.0. Red or blue squares on the right indicate the high and low abundance of the corresponding metabolite in each treatment, respectively. VIP score was based on the first component of the PLS-DA model. Metabolites class: **Amino acid** – Alanine (3), Valine (8), Serine (10), Leucine (12), Isoleucine (15), Proline (16), Glycine (17), Threonine (20), Aspartic acid (23), Hydroxyproline (24), Glutamic acid (29), Phenylalanine (30), Asparagine (31), Glutamine (35), Lysine (44), Ornithine (45), Tyrosine (47); **Inorganic acid** - Phosphoric acid (13); **Nitrogenous compounds** – Guanidine (6), Urea (9); **Organic acid** - Pyruvic acid (1), Lactic acid (2), Oxalic acid (4), Malonic acid (7), Succinic acid (18), Glyceric acid (19), Malic acid (21), 2-Oxoglutaric acid (26), Citric acid (37), Glucaric acid (49), Gulonic acid (49), Glucuronic acid (51); **Phenolic precursor** - Shikimic acid (36), Quinic acid (39); **Polyamine** – Putrescine (27); **Sugar** – Lyxose (22), Xylulose (25), Erythrose (28), Ribose (32), Fructose (40), Sorbose (41), Mannose (42), Glucose (43), Galactose (46), Sucrose (58), Trehalose (60), Raffinose (61), Fructose-1,6-diphosphate (62), Maltotriose (64); **Sugar alcohol** – Arabitol (33), Glycerol-2-phosphate (34), Mannitol (48), Inositol (53), Galactinol (63), **Sugar derived** – Glucopyranoside (52); **Unidentified Metabolites** - Unknown 2 (5), Unknown 3 (11), Unknown 4 (14), Unknown 13 (38), Unknown 32 (50), Unknown 20 (54), Unknown 21 (55), Unknown 26 (56), Unknown 27 (57), Unknown 33 (59). All data were cube root transformed and divided by the standard deviation of each variable (Autoscaling) for chemometrics analysis (PLS-DA) by MetabolAnalyst 5.0.

Fifteen metabolites were differentially expressed in the rice roots considering the four groups analyzed (Figure 13; Apêndice C). Salinity upregulated only glycerol-2-phosphate and downregulated four metabolites (fructose, sorbose, malic acid, and quinic acid) in both

cultivars. Salinity upregulated two metabolites (unknown 2 and glucopyranoside) and downregulated 2-oxoglutaric acid in the SF cultivar. In contrast, salinity upregulated five metabolites (proline, 2-oxoglutaric acid, putrescine, arabitol, and maltotriose) and downregulated shikimic acid only in ES cultivar. Thus, three metabolites (2-oxoglutaric acid, putrescine, and galactinol) showed fewer relative abundance in SF roots than in ES, and two metabolites (arabitol and glucopyranoside) showed higher relative abundance in SF cultivar than in ES.

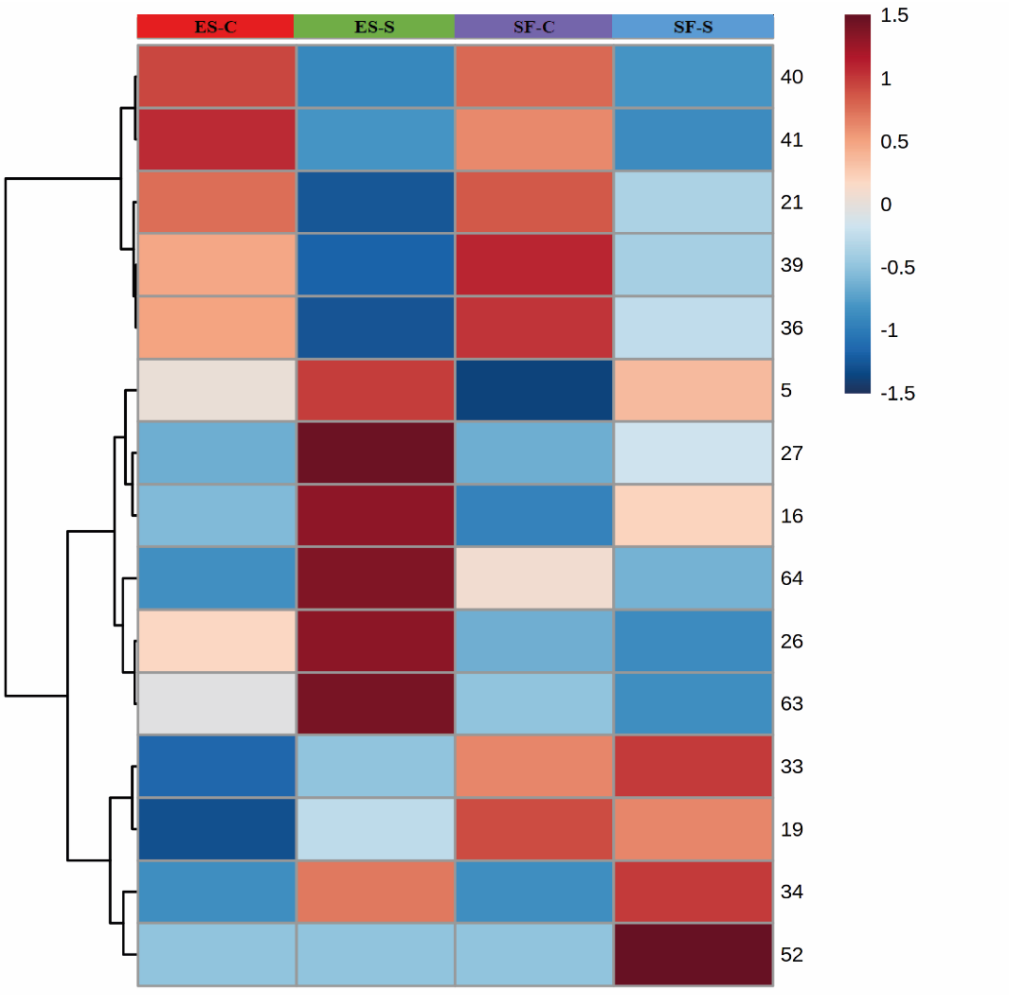

Figure 13 - Heatmap of normalized values of metabolites in roots of rice cv. BRS Esmeralda growing under non-salt conditions (ES-C) and salt stress conditions (ES-S) and cv. São Francisco growing under non-salt conditions (SF-C) and salt stress conditions (SF-S) for ten days. The heatmap shows a high (red scale) or low (blue scale) relative amount of each metabolite. Significant metabolites list ($p < 0.05$) grouped according to metabolites class: **Amino acid** – Alanine (3), Valine (8), Serine (10), Leucine (12), Isoleucine (15), Proline (16), Glycine (17), Threonine (20), Aspartic acid (23), Hydroxyproline (24), Glutamic acid (29), Phenylalanine (30), Asparagine (31), Glutamine (35), Lysine (44), Ornithine (45), Tyrosine (47); **Inorganic acid** - Phosphoric acid (13); **Nitrogenous compounds** – Guanidine (6), Urea (9); **Organic acid** - Pyruvic acid (1), Lactic acid (2), Oxalic acid (4), Malonic acid (7), Succinic acid (18), Glyceric acid (19), Malic acid (21), 2-Oxoglutaric acid (26), Citric acid (37), Glucaric acid (49), Gulonic acid (49), Glucuronic acid (51); **Phenolic precursor** - Shikimic acid (36), Quinic acid (39); **Polyamine** – Putrescine (27); **Sugar** – Lyxose (22), Xylulose (25), Erythrose (28), Ribose (32), Fructose (40), Sorbose (41), Mannose (42), Glucose (43), Galactose (46), Sucrose (58), Trehalose (60), Raffinose (61), Fructose-1,6-diphosphate (62), Maltotriose (64); **Sugar alcohol** – Arabitol (33), Glycerol-2-phosphate (34), Mannitol (48), Inositol (53), Galactinol (63), **Sugar derived** – Glucopyranoside (52); **Unidentified Metabolites** - Unknown 2 (5), Unknown 3 (11), Unknown 4 (14), Unknown 13 (38), Unknown 32 (50), Unknown 20 (54), Unknown 21 (55), Unknown 26 (56), Unknown 27 (57), Unknown 33 (59). Each square represents the mean of five biological replicates, and the statistical difference was obtained according to *F*-test ($p < 0.05$) and Tukey test ($p < 0.05$). For more details, see Apêndice C.

3.4 Discussion

3.4.1 Physiological performance of cultivars São Francisco and BRS Esmeralda under salinity

Plants submitted to saline environments exhibit inhibition of growth and development (RAO *et al*., 2019). In this way, salinity significantly reduced the dry mass content and the length of the shoot and roots in both rice cultivars, SF and ES (Figures 2, 3). Although the cultivars studied here are considered distinct in salt tolerance during the seedling establishment phase (GADELHA, 2020), between 7 and 19 days after sowing, the differential tolerance was not confirmed in older rice plants evaluated at 37 days after sowing under similar salt stress levels. Here is because it was not possible to discriminate a cultivar more tolerant to saline stress considering all the physiological and biochemical results by PCA together (Figure 9a). Thus, the tolerance or susceptibility to salt stress is significantly altered by the phenological stage in the rice culture (SARKAR *et al*., 2019). In addition, it is noteworthy that the plants evaluated by Gadelha (2020) were growing with 234.4 μM dissolved oxygen dissolved in the nutrient solution, while here the rice plants were with 171.9 μM. This increase in hypoxia imposed on plants can alter the growth pattern in plants under salinity (LOPES *et al*., 2020).

In part, the damage caused by salinity is due to osmotic stress, which leads to a limitation in water absorption by plants, compromising cell expansion essential to the growth of tissues and organs (JOUYBAN, 2012). Furthermore, due to the restrictions on water availability, the water status of the plants may be compromised, as observed in the slight reduction in leaf RWC of both rice cultivars (Figure 4b). Another responsible for the prejudices in growth and development under salinity is the excess of absorbed ions, which causes ionic stress (Figure 4b). There were substantial increases in Na^+ and Cl^- contents in both rice cultivars under salinity (Figure 8). Thus, they contributed high to the separation of the groups of stressed plants (SF-S and ES-S) from the other groups of non-stressed plants (SF-C and ES-C) (Figure 9a-c). The excessive accumulation of ions, mainly Na^+, triggers a series of limitations to plants (PASSAMANI *et al*., 2017). The cultivars SF and ES had smaller g_s under salinity due to the significant increase in Na^+, mainly in the stem and roots, since this variable showed a strong negative correlation with g_s (Figure 9d; Apêndice A). In addition, the generalized accumulation of Na^+ in rice plants was negatively correlated ($r < -0.7$) with all growth parameters except root length (Figure 9d; Apênice A).

The Na^+ and Cl^- have toxic effects on plant cells when accumulated (SHAHID *et al*., 2020). Therefore, the increase in Cl^- contents in the stem and roots also contributed to salinity's negative impact on plant growth and development (Figures 8, 9d; Apênice A). The accumulation of Cl^- in the stem presented a high negative correlation with g_s and leaf dry mass, and the Cl^- content in the roots also showed a strong negative correlation with the shoot length. It is essential to note that although Cl^- is a micronutrient, its accumulation at high levels can undoubtedly lead to cell death or even limit vital processes to plants, such as photosynthesis (MUNNS; GILLIHAM, 2015; QIU *et al*., 2016). However, Cl^- content in the leaves did not have any strong correlation with the growth parameters, so the higher Cl^- content accumulated in the leaves of SF cultivar, concerning ES cultivar, did not impose additional prejudices on cultivating SF cultivar (Figure 8; Apêndice A).

It is important to note also that the high levels of high contents of Na^+ and Cl^- promoted a reduction in K^+ throughout the plant (Figure 8g-i). This excess of Na^+ and Cl^-, found in saline environments, has a strong inhibitory effect on K^+ absorption (PASSRICHA *et al*., 2020), and this corroborates the high negative correlation shown by these variables (Figure 9d, Apêndice A). Although in some cases, the reduction of K^+ can be beneficial, as long as it occurs transiently (SHABALA, 2017). The unavailability of this chemical element for a long period of time can harm plants. This is because potassium is vital in plant growth and development, acting as a regulator of osmotic pressure, reducing plant lodging and improving grain quality (BARKER; PILBEAM, 2015). Therefore, K^+ accumulation was positively correlated with shoot length and leaf and root dry mass (Figure 9d, Apêndice A). Furthermore, it is important to highlight that between Na^+ and Cl^-, Na^+ has the most significant and inhibitory effects on K^+ (KUMAR; KHARE, 2016). This is denoted by the K^+/Na^+ ratio observed in the present study, whose values were reduced due to salinity, highlighting that in the presence of Na^+ at high levels, there is low accumulation of K^+ contents in leaves, stems and roots. (Figure 8j-1).

The photosynthetic pigments in plants under salt stress are degraded due to the strong stimulus to the production of free radicals by ionic excess, which can also promote other disorders in chloroplasts (KHUNPON *et al*., 2017; ARAÚJO *et al*., 2021). The Chl *total* content decreased slightly in leaves of plants stressed with salt (Figure 5b, c). However, there was an expressive reduction in Chl *b* only in the ES cultivar. Chl *b* acts as an accessory pigment, and as such, assists in capturing light energy leading to the centers of photochemical reactions carried out by a Chl *a* (STREIT *et al*., 2005). Moreover, under conditions of saline stress, the maintenance, to a certain degree, of the capture of light energy is essential to the maintenance of photosynthesis (PESSARAKLI *et al*., 2016).

Photosynthesis is also dependent on other factors, such as water and CO_2 availability. As previously reported, the first phase of salt stress is characterized by limited water absorption by the roots. In this situation, the plant enters a signaling phase. This alert results from the synthesis of abscisic acid (ABA), which takes the information to specific cells that amplify the signal and generate a response; one of these initial responses is stomatal closure (RYU; CHO, 2015). Hence, the reduction of gs in both cultivars under salt stress was notorious, as well as the reduction of water loss due to lower transpiration values (Figure 6b, c). However, despite limiting water loss under osmotic stress, there was a drastic commitment of CO_2 and ICE uptake (Figure 6a, e). The cultivars did not differ in their gas exchange behavior, except for greater g_s in the SF cultivar, without causing any improvement in *A* or *E*. Besides, both rice cultivars adjusted to maintain their WUEi. It is noteworthy that the higher g_s in cultivar SF under salinity was due to a more significant accumulation of K^+ in leaves than in cultivar ES under the same conditions (Figure 8g), since K^+ in leaves has a positive correlation with g_s (Figure 9d; Apêndice A), in addition to its close relationship with the turgor of guard cells and consequent stomatal opening (PANDEY; MAHIWAL, 2020).

Saline environments also influence the fluorescence parameters of chlorophyll a. The ΦPSII, ETR, and Fv'/Fm' were limited in stressed plants of both cultivars (Figure 7a, c, d), characterizing a low photochemical efficiency. In this situation, the flow of electrons is lower in the thylakoid membranes, contributing to the lower availability of ATP and NADPH necessary for carbon metabolism (FERREIRA *et al*., 2018). This explains the reduction in *A* under salinity, despite maintenance in qP and *Ci* (Figures 6d, 7a, b). Similar results were found by YIN *et al*. (2021) in ginger seedlings under saline stress, which presented meaningful decreases in ΦPSII and Fv'/Fm'.

3.4.2 Adjustment in the metabolic profile against the salinity impacts is dependent on the cultivar

In the present study, 102 metabolites were detected in the leaves and 64 in the roots, whose modulation patterns were distinguished given the salt stress and the cultivar (Apêndice B, C). Acclimation and adaptive processes are complex and multifaceted (NEGRÃO; SCHMÖCKEL; TESTER, 2016). Saline stress alone induces a series of disorders that limit plant growth and development. So, to bypass the limitations imposed by the saline environment, plants modulate their morphological, physiological, and biochemical characteristics (PRISCO; GOMES-FILHO, 2010). This perception of adversities of the environment is due to the

synthesis of some plant hormones, such as ABA. The ABA functions as a stress hormone, whose conjugated form to a sugar derivative, glucopyranoside, accumulates in plant tissues during saline stress (HARRIS; DUGGER, 1986). In agreement, the high upregulation of glucopyranoside was evident in ES leaves and SF roots from plants under salt stress (Figures 11, 13; Apêndice B, C).

Since there is difficulty absorbing water by roots under salt stress, one of the main strategies is the accumulation of osmoregulators. Soluble sugars, such as glucose and fructose, in addition to energy sources, are osmoregulators (SINGH *et al*., 2015). Fructose was accumulated distinctly between the evaluated organs, being strongly upregulated by salinity in the leaves and downregulated in the roots of both cultivars (Figures 11, 13; Apêndice B, C). Also, galactose, a precursor to fructose, was upregulated in the leaves of rice cultivars (Figure 11; Apêndice B) (MELLO, 1998). The fructose possibly upregulation mitigates salinity damages since it acts to eliminate reactive oxygen species (ROS) in addition to being an osmoregulator (KEUNEN *et al*., 2013). The same happened with galactinol (NISHIZAWA; YABUTA; SHIGEOKA, 2008), a sugar alcohol found in the leaves and roots, and that was upregulated by salinity only in the SF leaves (Figures 11, 13; Apêndice B, C). This additional protection against ROS may have contributed to the maintenance of Chl *b* in the SF cultivar under salt stress (Figure 5b). In addition, was observated upregulated arabitol in leaves of cv. SF and in root of cv. ES (Apêndice B). This sugar alcohol although does not have a common occurrence in agricultural plants, in rice the same is not true, as its presence was identified in the present study, which may act as an osmoprotector of proteins (KHAN; KANWAL; NAZIR, 2015).

It is noteworthy that other sugars were also modulated. In leaves, in addition to galactose, xylitol was upregulated in both cultivars due to salt stress (Figure 11; Apêndice B). Xylitol in many microorganisms can be converted to other precursors that enter the pentose phosphate pathway (ZHAO *et al*. 2020). In rice plants, the same seems to be true, since by-products of this pathway were also upregulated, such as ribose, but this was only observed in leaves of cv. SF (STINCONE *et al*., 2014). This sugar is essential for the biosynthesis of nucleotides and nucleic acids (BANFALVI *et al*., 2021). Unlike leaves, the pentose pathway is not significantly stimulated in roots under salinity, specifically in cv. SF. This is because was observed downregulation of shikimic acid and quinic acid, which are phenolic precursors originating from the shikimic acid pathway, and which in turn is dependent on the pentose phosphate pathway, as has been observed (TAIZ; ZEIGER, 2017; SANTOS-SÁNCHEZ *et al*.; 2019). This result corroborates that of Li *et al*. (2021), who emphasizes that the reduction of

shikimic acid and quinic acid in roots can lead to negative effects on plant root development. As also evidenced in this research.

In addition to sugars, amino acids also were considerably modulated. However, the changes by salinity were more notable in the leaves (Figure 11; Apêndice B). All amino acids identified in the leaves were upregulated by salinity except for serine and hydroxyproline. Among these, leucine, isoleucine, proline, threonine, cystine, phenylalanine, glutamine, tyrosine, and asparagine can be highlighted in both cultivars. The proline, asparagine, and glutamine had the high VIP values (Figure 10d). The proline is a relevant osmoprotectant, antioxidant system inducer, besides helping in the redistribution of nitrogen and the control of tiny energy sources (ZHANG; BECKER, 2015, RADY *et al*., 2019). Asparagine, in turn, acts indirectly on proline metabolism, as does glutamine (FREITAS *et al*., 2019). However, glutamine can also act as a signal to the activation of antiports linked to Na^+ exclusion (MIRANDA *et al*., 2017). Other amino acids such as alanine, lysine, and ornithine were upregulated only in the SF cultivar. Such metabolites play several roles as a raw material for protein biosynthesis and other pathways, signaling, and providing energy in catabolic pathways (HILDEBRANDT *et al*., 2015). Not only have amino acids been significantly modulated, but some of their derivatives as well. Pyroglutamic acid, for example, was upregulated in the leaves of both cultivars. It is an essential metabolite for the glutathione cycle and a precursor to gamma-aminobutyric acid (GABA) (JIMÉNEZ-ARIAS *et al*., 2019; LI *et al*, 2020).

Rice plants also accumulated nitrogen compounds in their leaves with exposure to salinity (Figure 11; Apêndice B). The urea being upregulated only in the SF cultivar and guanidine in both cultivars. The accumulation of urea and guanidine can limit plant growth and development since these metabolites also act as protein denaturants bring structural and functional alterations, thereby affecting the normal functioning of crucial proteins (SIDDIQUI; BANO 2018). However, urea is a precursor to glutamate, an essential amino acid in the synthesis of chlorophyll (BREDEMEIER; MUNDSTOCK, 2000). Also, a polyamine was identified, putrescine, showed upregulation in the leaves of the two rice cultivars and the ES roots (Figure 13; Apêndice C). Putrescine is the main product of the polyamine's pathway, which also includes spermidine and spermine (CHEN *et al*., 2019). One of the main benefits of polyamines includes regulating the structures and functionalities of the photosynthetic apparatus, which can alleviate the oxidative and ionic damage caused by salt stress and contribute to the osmotic adjustment (SHU *et al*., 2015; EBEED; HASSAN; ALJARANI, 2017). However, instead of spermidine and spermine, the increase in putrescine has been pointed out as a sensitivity indicator to saline stress in sorghum plants (OLIVEIRA; LOPES;

GOMES-FILHO, 2020).

Organic acids were another group of metabolites that varied due to salinity according to the cultivars analyzed. In the leaves, 2-oxobutyric acid was modulated upregulated in both cultivars (Figure 11; Apêndice B). Gulonic acid, a by-product of the Krebs cycle and intermediate in synthesizing some amino acids, was upregulated only in the SF cultivar (Figure 11; Apêndice B). The same occurred for the metabolites 2-aminoisobutyric acid and glutamic acid, which are precursors of GABA (KINNERSLEY; TURANO, 2010). Thus, the upregulation of 2-aminoisobutyric acid and glutamic acid is possibly associated with the activation of an alternative mitochondrial breathing pathway, termed as GABA shunt, in response to inhibition of the pyruvate dehydrogenase and 2-oxoglutarate dehydrogenase enzymes, which are highly sensitive to salt stress, in order to provide an alternative carbon skeleton in the Krebs cycle (CHE-OTHMAN *et al.*, 2019). According to these authors, the increased activity of the GABA shunt is accompanied by increases in some amino acids, such as proline, asparagine, lysine, and ornithine. These amino acids also had higher relative abundances and high VIP scores in the SF leaves under salinity (Figures 10d, 11; Apêndice B). In this way, it can be conjectured that one of the modulatory mechanisms to the salt stress developed by the SF cultivar is the shunt GABA.

On the other hand, there were strong indications that 2-oxoglutaric acid, an organic acid intermediate in the Krebs cycle, acts in other processes in the roots, considering an upregulation in ES roots and downregulation in SF roots (Figure 13; Apêndice C). The 2-oxoglutarate also acts as a cofactor in numerous enzymes involved in the metabolism of amino acids, glucosinolates, flavonoids, alkaloids, and gibberellins (ARAÚJO *et al.* 2014). Another tricarboxylic cycle intermediate modulated was citric acid, downregulated only on the ES leaves (Apêndice B). Citric acid is an essential metabolite in the mitigation of salt stress. It helps increase the activity of certain antioxidant enzymes, which are responsible for eliminating reactive oxygen species (SUN; HONG, 2010).

3.5 Conclusion

The differential tolerance to salinity of rice cultivars SF and ES in phenological stages of pre-tillering did not occur in the tillering stage. However, SF and ES cultivars showed distinctly metabolic profiles under no-salt conditions that become more distinct in the face of saline stress. Comparing cultivars under saline conditions, 26 metabolites were differentially expressed in leaves and five in roots. The majority of them were amino acids and key-sugars

such as fructose and ribose. Only the SF cultivar activated the GABA shunt in leaves as a means of defense against salt stress. Among the salinity-adjusted metabolites in rice plants, glucopyranoside, lysine, ornithine, 2-aminoisobutyric, glutamine, arabitol, glyceric acid, and 2-oxoglutaric acid stand out by high potential as salt stress biomarker in rice plants.

4 IMPACT OF THE HYPOXIA LEVEL ON GROWTH AND METABOLITES MODULATION IN RICE CULTIVARS WITH DIFFERENT CULTIVATION RECOMMENDATIONS

(Artigo a ser submetido)

Abstract

Rice is an agricultural crop that is significantly important in the economy and the staple diet of most human beings. Although it is an adaptable species to flooded soil conditions, some cultivars respond distinctly to limited oxygenation levels in the environment. Thus, the present study evaluated two rice cultivars' growth patterns and metabolic profiles under different hypoxia levels. Hence, the São Francisco (SF) and BRS Esmeralda (ES) cultivars were subjected to three hypoxia levels (severe, moderate, and slight hypoxia). Considering all physiological and biochemical data, cultivar SF showed more remarkable plasticity of response to hypoxia levels, making explicit a performance separation between plants under severe and moderate hypoxia. Nevertheless, the dry mass of leaves and stems and root length in both cultivars were higher under slight hypoxia than severe hypoxia. Also, the severe hypoxia reduced CO_2 assimilation, stomatal conductance, transpiration, and instantaneous carboxylation efficiency concerning moderate or slight hypoxia. Photosynthetic pigments have a strong positive correlation with each other, and they have been reduced by severe hypoxia concerning slight hypoxia, just like electron transport rate and PSII maximum efficiency, in both cultivars. The accumulation profile of Na^+, Cl^- and K^+ ions varied according to hypoxia level and cultivar. Thirty-nine metabolites in leaves and forty in roots were distinctly modulated by hypoxia levels or rice cultivars. Severe hypoxia generated losses in both rice cultivars. Still, the SF cultivar mitigated damages from oxygen restriction by stimulating glycolysis and the citric acid cycle in its roots, thus confirming its adaptability to flooded environments.

Keywords: Hypoxia stress; Hypoxia tolerance; Metabolome; *Oryza sativa* L.; Soil flooding

4.1 Introduction

The *Poaceae* family comprises the most economically important crops globally, includes rice (*Oryza sativa* L.) (HANAFIAH *et al*., 2020), a staple and energy food for almost half of the world's population (ZHANG *et al*., 2017). Although rice is a species easily adaptable

to flooding conditions (HOLZSCHUH; BOHNEN; ANGHINONI, 2010), this does not prevent certain varieties from being negatively impacted by the low availability of oxygen since there are differences in tolerance level to hypoxia stress (MARIANI; FERRANTE, 2017).

Several agricultural lands are flooded due to elevated precipitation incidences (SHABALA *et al*., 2014). Soil flooding is one of the abiotic stresses that most limit plants' normal growth and development (DUHAN *et al*., 2018). Waterlogging promotes O_2 restriction (hypoxia), once O_2 has low solubility in water, about 280 μmol L^{-1} (BARRETT-LENNARD, 2003). Hypoxia damages are because oxygen availability deficit in the rhizosphere leads to gas exchange restriction and photosynthesis reduction (TAVARES, 2018; LAMERS; MEER; TESTERINK, 2020). Oxygen is the essential chemical element in energy production, the absence of which limits the cellular respiration process, thus compromising all ATP-dependent metabolic reactions (TAIZ; ZEIGER, 2017). Through this, plants seek to modulate their metabolism to ensure energy production and consumption (PEDERSEN; PERATA; VOESENEK, 2017).

The rice under hypoxic conditions expresses morphological changes adaptive to root oxygen restriction, such as the development of aerenchyma and barriers in the basal root zone, allowing oxygen transport and radial O_2 loss limiting, respectively. (COLMER, 2003; LOPES *et al*., 2020). However, severe oxygen restriction can still promote reduced growth and development of rice plants (LOPES *et al*., 2020). Thus, there is a need for a better understanding of the tolerance of rice plants to the fine adjustment of hypoxia levels and the modulation of primary metabolites to different hypoxia conditions. So, understanding the metabolic pattern produced allows elucidating how plants adjust to stressful abiotic conditions such as hypoxia. The secondary metabolites are strongly linked to plant defense, while the primary metabolites are related to survival and play a crucial role in photosynthesis, respiration, and nutrient assimilation (ERB; KLIEBENSTEIN, 2020). Secondary metabolites are terpenoids, phenolic compounds, alkaloids, and sulfur-containing compounds (LOBO; HOUNSOME; HOUNSOME, 2018), while the main primary metabolites are carbohydrates, amino acids, and organic acids and their derivatives (JORGE *et al*., 2017).

Thus, the present study evaluates the growth and metabolic profile pattern between two rice cultivars under different hypoxia levels. It used one cultivar recommended for farming in upland areas, where it is not common to have hypoxia conditions, and another cultivar for cultivation in flooded soil (hypoxic conditions). Thus, it is expected to obtain a differential tolerance to severe hypoxia and identify metabolic markers to hypoxia stress.

4.2 Material and methods

4.2.1 Plant material, experimental conditions, and hypoxia treatments

Two varieties of rice were evaluated, BRS Esmeralda (ES) and São Francisco (SF). The SF cultivar is indicated for cultivation in an irrigated system, producing 8% more than other commercial cultivars on flooded cultivation (EMBRAPA, 2013). On the other hand, the ES cultivar exhibits drought tolerance and has high productivity in rainfed cultivation (CASTRO *et al*., 2014, PERES *et al*., 2018). The SF and ES seeds were supplied from Instituto Agronômico de Pernambuco (IPA), Recife, PE, Brazil.

The experiment was carried out in a 2 x 3 factorial scheme, the first factor being two rice cultivars (ES and SF cultivars) and the second factor three hypoxia levels (severe, moderate, and slight hypoxia). Initially, the two rice cultivars were sown on germitest paper moistened with distilled water, in the proportion of 2.5 times the dry weight of the substrate. After sowing, the paper rolls containing the seeds were left in a BOD-type germination chamber at 30 °C, 90% relative humidity, and a photoperiod (12:12) for ten days, a period sufficient for the coleoptile would present an approximate size of 5 cm.

Soon after, the seedlings were transferred to bowls containing Clark nutrient solution (Clark, 1975) modified, containing Fe - EDTA (0.076 mM). Then the seedlings were placed on styrofoam supports fixed to the upper part of the bowls, the roots of the seedlings being completely submerged in the nutrient solution, for a period of 17 days for acclimatization, following the following schedule: five days under constant artificial light, five days under shade at 70% natural light, and seven days in full sun. At 27 days after sowing, the plants were then transferred to 3.5 L plastic pots, where the hypoxia treatments were applied for ten days. The experiment was conducted under greenhouse conditions: average air temperature of 32 °C, average air relative humidity of 70 %, and a 12-h photoperiod.

Hypoxia treatments were established according to Lopes *et al*. (2020) so that severe hypoxia [dissolved oxygen (DO) < 3.5 ppm ~ 109.4 µM O_2)] were established with daily application of 0.4 mL of sodium metabisulfite ($Na_2S_2O_5$ at 1 M) per liter of the nutrient solution. Moreover, moderate hypoxia (DO = ± 5.5 ppm ~ 171.9 µM O_2) represents the natural oxygenation condition of the nutrient solution at sea level, and slight hypoxia (DO = ± 7.5 ppm ~ 234.4 µM O_2) was obtained by aerating the nutrient solution with aquarium pumps. The nutrient solution of hypoxia moderate and slight treatments also received sodium metabisulfite application in the same concentration used in severe hypoxia treatment two days before its use.

According to LOPES *et al*. 2020, this procedure is required for that the effects of severe hypoxia are not confused with this reducing agent's residual effects; hence all treatments contained identical residues. So, sodium metabisulfite acted on the dissolved oxygen only in the severe hypoxia treatment. The oxygenation of the nutrient solution was monitored daily with the aid of an oximeter (HI 9146-10; Hanna instruments). Dissolved oxygen measurements were taken in the center of the plastic pot. The nutrient solutions were renewed every two days, and the pH was monitored daily and corrected to 5.8 with KOH 1.0 M.

The collection of plant material for all the determinations described below was carried out on the 37th day after the sowing (tillering stage), which corresponds to plants under hypoxia treatments by ten days.

4.2.2 Growth and development analysis

The shoot and root lengths were measured with a tape measure aid. The longest root of the plant was considered to measure the root length. After collecting leaves, stems, and roots, the dry mass determination was made. The vegetable parts were left in an oven with forced air circulation at 65 ºC for 72 h and then weighed.

4.2.3 Relative water content and relative humidity

For determining the relative water content (RWC), the plant material was collected at sunrise, which corresponds to the daytime period of greatest cell turgidity. The RWC was analyzed according to the methodology of Barr and Weatherley (1962). The leaf samples consisted of ten leaf discs of 1 cm in diameter, taken from the first fully expanded leaf of the central tiller of the plant at the time of collection, while the roots samples were ten fragments of 1 cm from the median root part. The samples were weighed to obtain the fresh mass (FM), and immediately afterward, they were hydrated for three hours in distilled water under ambient light and temperature to get the turgid mass (TM) (ARNDT *et al*., 2015). The samples were then dried in an oven at 80 ° C for 48 h to determine the dry mass (DM). To calculate the RWC, the formula was used: RWC (%) = [(FM-DM)/(TM-DM)] x 100. And to determine relative humidity the formula used was: Relative humidity (%) = 100 - [(DM/FM) x 100].

4.2.4 Photosynthetic pigments contents

The levels of chlorophylls and carotenoids were determined using the method described by Wellburn (1994). At the time of collection, three leaf discs 1 cm in diameter were removed from the first fully expanded leaf of the rice plants and immersed in 2 ml of dimethyl sulfoxide solution saturated with $CaCO_3$ in test tubes protected from light for 48 h. Then, the tubes were incubated in a water bath at 65 °C for 30 min (BARNES *et al*., 1992). The concentrations of chlorophylls *a* (Chl *a*), *b* (Chl *b*) e *total* (Chl *total*) and carotenoids (CAR) were estimated using the following formulas: Chl *a* = $12.19A_{665} – 3.45A_{649}$, Chl *b* = $21.99A_{649} – 5.32A_{665}$, Chl *total* = $6.87A_{665} + 18.54A_{649}$; Car = $(1000A_{480} – 2.14$Clf *a* – 70.16Clf *b*)/220, whereby A_i corresponded to the absorbance at wavelength i (665, 649 and 480 nm). After determining the pigment concentrations, their levels were expressed based on the dry mass. The dry mass was determined by drying the three leaf discs in a forced circulation oven at 65 °C for 72 h.

4.2.5 Gas exchange and chlorophyll a fluorescence

Gas exchange and chlorophyll *a* fluorescence measurements were performed in fully expanded leaves under constant CO_2 concentration and photosynthetic photon flux density (PPFD) of 400 µmol mol^{-1} CO_2 and 1,400 µmol photons m^{-2} s^{-1}, respectively. At harvesting, CO_2 assimilation (*A*), stomatal conductance (g_s), transpiration (*E*), and intercellular CO_2 concentration (*Ci*) were determined on the middle of the first fully expanded leaf from the apex using an infrared gas analyzer (IRGA, LI-6400XT, LI-COR, USA) coupled with artificial light. The instantaneous carboxylation efficiency (ICE) of ribulose-1,5-bisphosphate carboxylase/oxygenase (Rubisco) and instantaneous water use efficiency (WUEi) were estimated by the *A/Ci* and *A/E* ratios, respectively. Some chlorophyll *a* fluorescence parameters were also evaluated using a fluorometer (6400-40, LI-COR, USA) coupled to IRGA, as maximum (Fm') and variable (Fv') fluorescence in light-adapted leaves, steady-state fluorescence (F') in equilibrium state in the presence of light, and basal fluorescence (Fo') after excitation state of photosystem I. From these parameters were determined effective quantum yield of PSII [ΦPSII = (Fm' − F')/Fm'], photochemical quenching [qP = (Fm' − F')/(Fm' − Fo')], electron transport rate [ETR = (ΦPSII × PPFD absorbed × 0.5)], and PSII maximum efficiency (Fv'/Fm').

4.2.6 Inorganic ions contents

To determine inorganic ions (Na^+, K^+, and Cl^-) contents, 20 mg of dry material from leaves, stems, and roots were homogenized separately with 2 mL of deionized water. The homogenates were kept in a water bath at 75 °C for one hour, shaking every 20 min. After that time, the samples were centrifuged at 3,000 x g for 10 min at room temperature (SARRUGE; HAAG, 1974). The Na^+ and K^+ contents were determined according to Malavolta, Vitti, and Oliveira (1989), with the aid of a flame photometer [Micronal, model B462 (São Paulo / SP, Brazil)] properly calibrated with 1 M NaCl and 1 M KCl solutions. The Cl^- content was determined according to a spectrophotometric mercury thiocyanate-iron method developed by Gaines, Parker e Gascho (1984), reading absorbance at 460 nm and NaCl as standard.

4.2.7 Metabolomic analysis

The extraction and derivatization of the metabolites were performed according to Lisec et al. (2006). The extraction was carried out from fresh samples of leaves and roots soaked and macerated in liquid nitrogen. For this, 50 mg of the pulverized plant material were homogenized in 700 µL of an extracting solution (water: methanol: chloroform in the proportion 1: 2.5: 1, respectively), at -20 °C, for 30 min, in an environment with a temperature at 4 °C. In each sample, 30 µL of ribitol at 0.2 mg mL^{-1} was added as an internal standard. The samples were incubated in a dry bath (Thermomixer, Bioer) for 15 min at 70 °C with 350 rpm shaking. Then, the homogenate was centrifuged for 5 min at 12,000 x g. The collected supernatant was subjected to a split in 375 µL of pure chloroform and 750 µL of Milli-Q water. On that occasion, the mixture was homogenized in a vortex and centrifuged for 15 min at 2,200 x g, with the upper (polar) portion being collected. Subsequently, the polar phase of the partition was dried in SpeedVac overnight and stored at -80 ºC.

The metabolites in the dry polar fraction in SpeedVac were derivatized by adding 20 µL of methoxyamine hydrochloride solution (20 mg ml^{-1} of pyridine). The mixture was shaken in a dry bath adjusted to 37 °C for 2 h at 550 rpm before adding 35 µL of N-methyl-N-trimethylsilyl-trifluoroacetamide (MSTFA). After MSTFA addition, the mixture was again stirred in a dry bath adjusted to 37 °C, for 30 min at 550 rpm. The detection and relative quantification of the metabolites were done using a gas chromatograph-mass spectrometer (GCMS, model QP2010, Shimadzu, Tokyo, Japan). Then, 1 µL of the derivatized sample was injected into the capillary column RTX-5MS (30 m x 0.25 mm x 0.25 µm, ResteK, Bellefonte,

USA), at a helium gas flow of 6,2 mL min^{-1}, injection in split mode, temperature, and interface of 230 °C, and ion source temperature of 250 °C. The chromatographic run was adjusted from a temperature of 80 °C for 2 min, followed by a heating ramp of 10 °C min^{-1} to 315 °C, with temperature maintenance for 8 min.

Each chromatography and mass spectrum were evaluated using Xcalibur™ 2.1 program (Thermo Fisher Scientific, Waltham, MA, USA) according to Roessner e*t al.* (2001). The compounds' identification was based on their retention times and mass spectrum fragmentation compared to standard mass spectra in the internal metabolite library and Golm metabolome database. Some unidentified metabolites were named as "unknown" and enumerated in order of output in the chromatogram. The relative value of each metabolite was determined by the division of their respective peak areas by internal standard peak area (ribitol, Sigma–Aldrich) and, after, divided by the dry mass of the sample.

4.2.8 Experimental design and statistical analysis

The experiment was conducted in a completely randomized design under a 2 x 3 factorial scheme (two rice cultivars x three hypoxia levels) with five repetitions with two plants each. The ES and SF were the two rice cultivars, and the three hypoxia levels (severe, moderate, and slight hypoxia). The physiological and biochemical data were submitted to a normality test (Shapiro-Wilk test) before the bidirectional analysis of variance (ANOVA). The Tukey test was applied to compare the means of the variables for a significant F-test at 5%. The software used for statistical analysis was GraphPad Prism 8.0 (www.graphpad.com). These data also were log-transformed and divided by the standard deviation of each variable (Autoscaling) for chemometrics analysis [PCA (Principal Component Analysis)] and correlation analysis [Pearson correlation ($p < 0.05$)] by MetabolAnalyst 5.0 (https://www.metaboanalyst.ca).

The relative abundance values of the metabolites were processed in MetabolAnalyst 5.0. The data were subjected to were cube root transformed and mean-centered and divided by the standard deviation of each variable (Autoscaling) before being subjected to one-way ANOVA and the Tukey test ($p < 0.05$). Besides, the transformed metabolomic data were submitted to the following multivariate analyzes: chemometric analysis [PLS-DA (Discriminant Analysis of Partial Least Squares)] and cluster analysis (hierarchical grouping). Hierarchical clustering was as a heatmap (Euclidean distance, Ward clustering algorithm).

4.3 Results

4.3.1 Growth and development

Rice plants growth was affected by hypoxia levels in both cultivars, however, SF plants exhibited bigger sizes than ES plants (Figures 14, 15). Anatomical changes were observed in the shoots and roots due to the alterations of oxygenation under hypoxia conditions (Figure 14b-d). The highest dry mass values found in all organs were in the SF cultivar regardless of the hypoxia level (Figure 15a-c). On average, the dry masses of leaves, stems, and roots were 25%, 48%, and 30% higher in SF than in the ES cultivar, respectively. In leaves, rice plants under slight and severe hypoxia had a similar dry mass to the control condition (moderate hypoxia) in both cultivars. However, dry mass was 20% higher under slight hypoxia than severe hypoxia (Figure 15a). In the other organs, the slight hypoxia resulted in a more considerable dry mass accumulation dry mass than moderate hypoxia, with no significant difference in dry mass accumulation between moderate and severe hypoxia. The dry mass gains obtained by cultivation under slight hypoxia were, on average, 26% in stem and 29% in roots in both cultivars (Figure 15b, c).

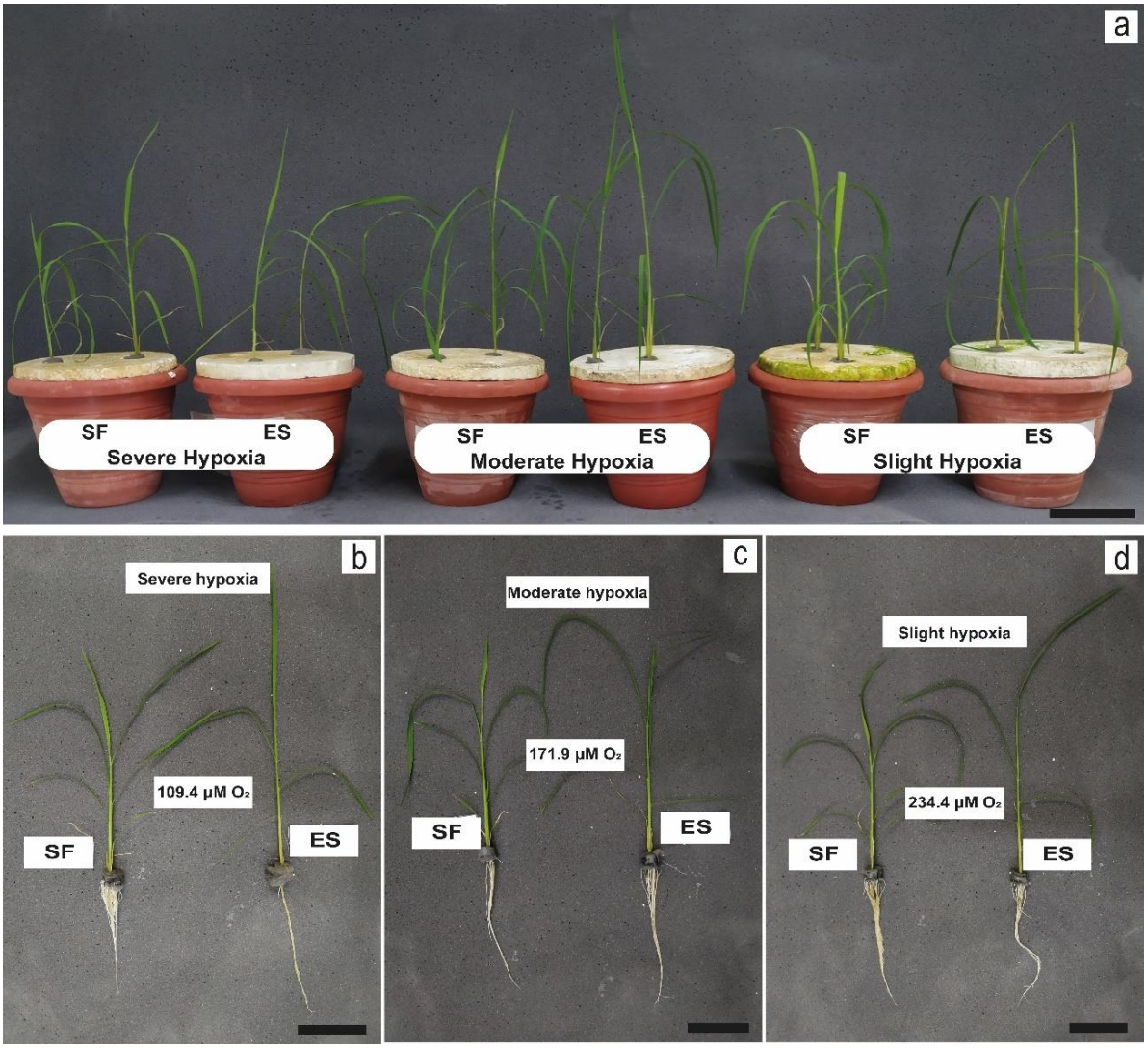

Figure 14 - Rice plants of the São Francisco (SF) and BRS Esmeralda (ES) cultivars under severe hypoxia (**a**, **b**; 109.4 µM O_2), moderate hypoxia (**a**, **c**; 171.9 µM O_2; control) or slight hypoxia (**a**, **d**; 234.4 µM O_2) for ten days. *Scale bars* **a-d**, 10 cm.

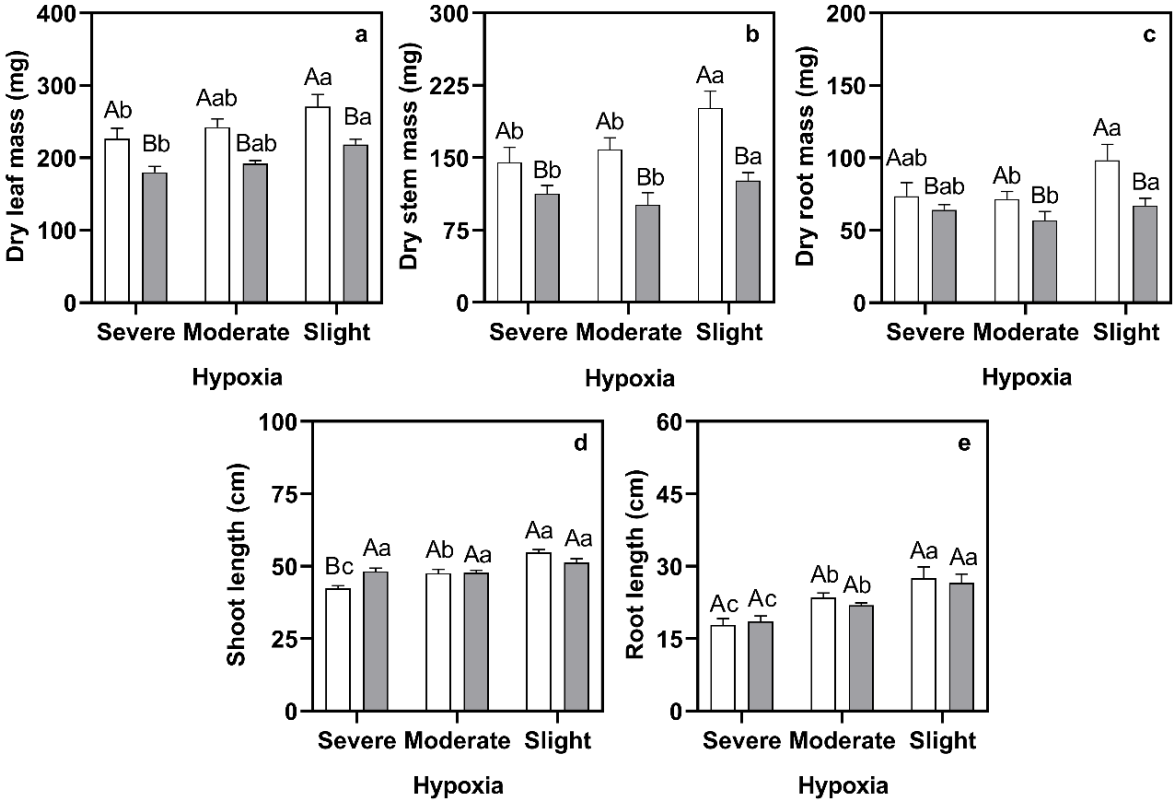

Figure 15 - Growth analysis of rice plants cv. São Francisco (SF, *white bars*) and BRS Esmeralda (ES, *grey bars*) under severe, moderate (control), or slight hypoxia conditions for ten days. Dry masses of leaves (**a**), stems (**b**), roots (**c**), and shoot (**d**), and root (**e**) length. For each variable, the capital letters and lowercase letters compare the cultivars and hypoxia treatments, respectively. According to F-test ($p < 0.05$), neither subfigure exhibit a significant interaction between treatments, except **d**. Bars represent means (n=5) + standard error.

In relation for length, a significant interaction of the factors evaluated in shoot length was observed so that there was no change in the growth of the ES shoots by the hypoxia levels (Figure 15d). In contrast, a higher oxygen restriction under hypoxic conditions promotes a reduction in shoot length of SF plants. Thus, SF shoots were 14% shorter than ES shoots under severe hypoxia. The root lengths were similar between cultivars under all hypoxic conditions despite the ES cultivar presenting lower root dry mass than the SF cultivar (Figure 15e). Also, there was an increase of 19% in slight hypoxia and a reduction of 20% in severe concerning moderate hypoxia. In addition, the relative humidity and RWC of leaves and roots were similar in cultivars and were not affected by hypoxia levels (Figure 16).

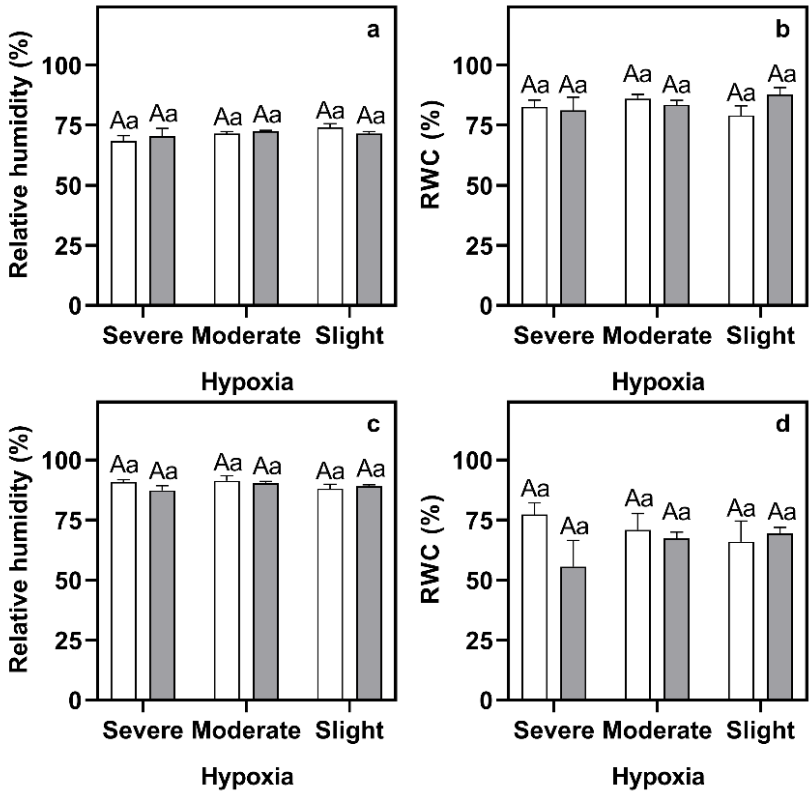

Figure 16 - Relative humidity and relative water content (RWC) of rice plants cv. São Francisco (SF, white bars) and BRS Esmeralda (ES, grey bars) under severe, moderate (control), or slight hypoxia conditions for ten days. Relative humidity of leaves (**a**) and roots (**c**), and RWC of leaves (**b**) and roots (**d**). For each variable, the capital letters and lowercase letters compare the cultivars and hypoxia treatments, respectively. According to F-test ($p < 0.05$), neither subfigure exhibit a significant interaction between treatments. Bars represent means (n=5) + standard error.

4.3.2 Photosynthetic pigments, gas exchange, and chlorophyll a fluorescence

The pigment contents were significantly affected only by the hypoxia level (Figure 17). The pigment contents in plants under slight and severe hypoxia were similar to plants under moderate hypoxia, except for Chl *b*. However, pigment contents in plants both cultivars under the slight and severe levels were significantly different from each other. The severe hypoxia induced reductions of 12% in Chl *a*, 14% in Chl *total*, and 19% in CAR compared to slight hypoxia (Figure 17a, c, d). In Chl *b*, severe hypoxia differed from moderate and slight levels, decreasing 21% of the values achieved (Figure 17b).

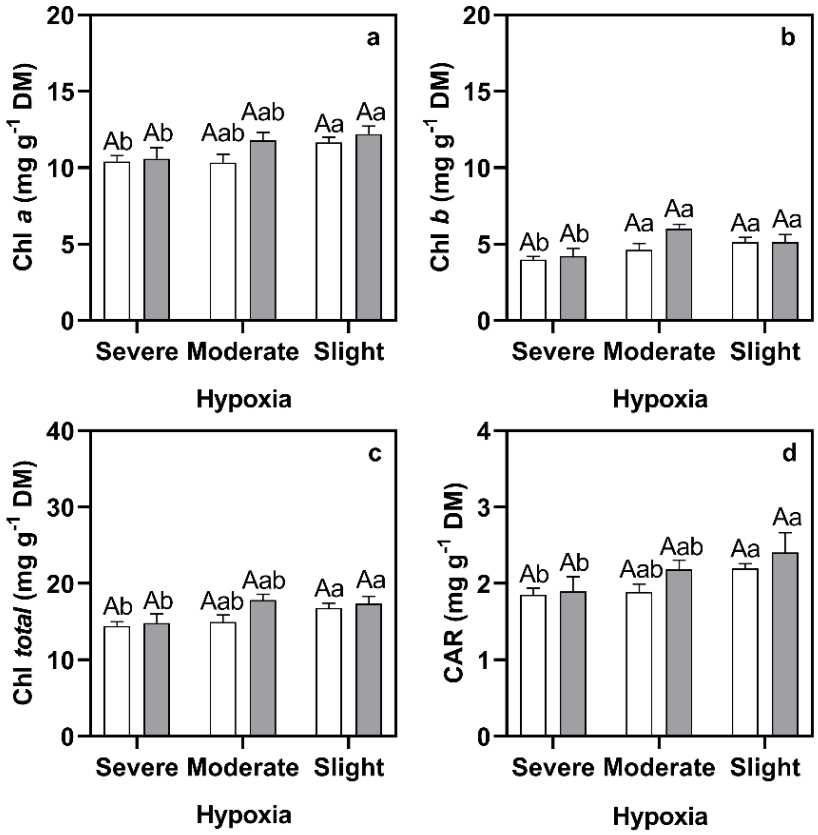

Figure 17 - Photosynthetic pigments contents of rice plants cv. São Francisco (SF, white bars) and BRS Esmeralda (ES, grey bars) under severe, moderate (control), or slight hypoxia conditions for ten days. Chlorophyll *a* (**a**, Chl *a*), *b* (**b**, Chl *b*), total (**c**, Chl *total*), and carotenoids (**d**, CAR). For each variable, the capital letters and lowercase letters compare the cultivars and hypoxia treatments, respectively. According to F-test ($p < 0.05$), neither subfigure exhibit a significant interaction between treatments. Bars represent means (n=5) + standard error.

The sources of cultivar variation and hypoxia level independently influenced the *A*, g_s, and ICE (Figure 18a, b, e). In SF cultivar, these variables were higher at 20%, 29%, and 18% than ES, respectively. The severe hypoxia significantly reduced *A*, g_s, and ICE by 28%, 48%, and 24%, respectively, about moderate hypoxia in both cultivars. Already E was influenced only by the hypoxia level so that both cultivars showed a reduction of 30% under severe conditions (Figure 18c). The results of *Ci* and *WUEi* were influenced by the interaction of cultivars and hypoxia levels (Figure 18d, f). The varieties differed in Ci only under moderate hypoxia, with SF 9% higher than ES (Figure 18d). Furthermore, concerning moderate hypoxia, the SF cultivar presented a 7% reduction in Ci under severe hypoxia, while the ES showed an increase of 12% under slight hypoxia. On the other hand, the severe and slight hypoxia reduced WUEi in ES cultivar by 21%. Although hypoxia levels did not influence the WUEi in SF, this cultivar exhibited values 24% and 25% higher than ES under slight and severe hypoxia conditions, respectively (Figure 18f).

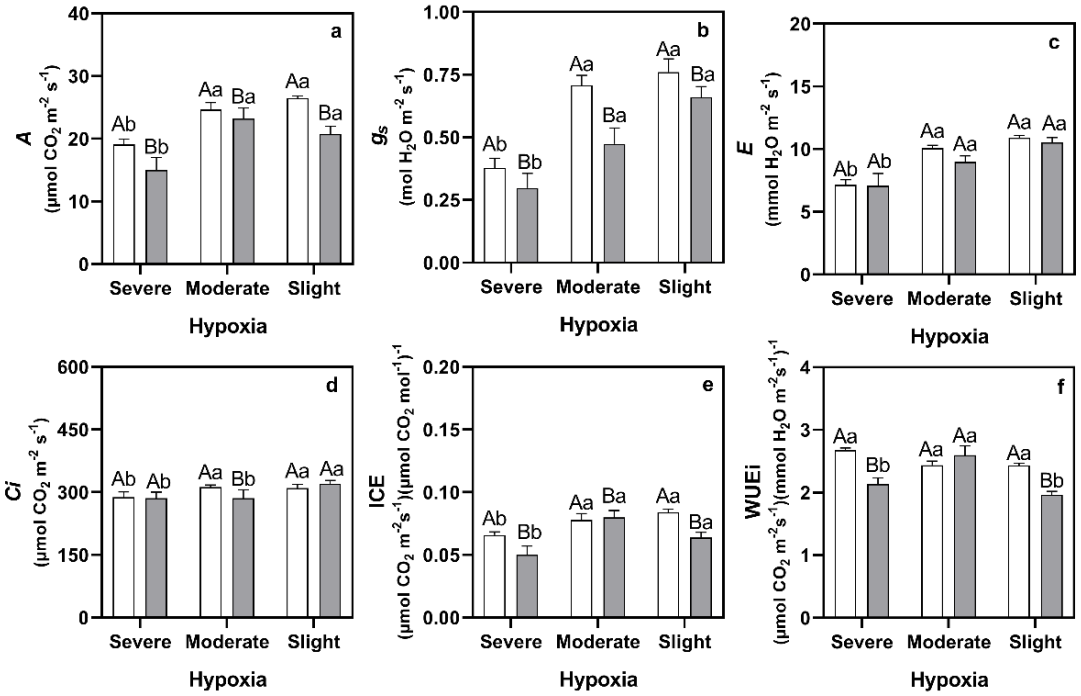

Figure 18 - Gas exchange of rice plants cv. São Francisco (SF, white bars) and BRS Esmeralda (ES, grey bars) under severe, moderate (control), or slight hypoxia conditions for ten days. CO_2 assimilation (**a**; *A*), stomatal conductance (**b**; g_s), transpiration (**c**; *E*), internal carbon concentration (**d**; *Ci*), instantaneous carboxylation efficiency (**e**; ICE) and instant water use efficiency (**f**; WUEi). For each variable, the capital letters and lowercase letters compare the cultivars and hypoxia treatments, respectively. According to F-test ($p < 0.05$), neither subfigure exhibit a significant interaction between treatments, except **d** and **f**. Bars represent means (n=5) + standard error.

Among the chlorophyll fluorescence parameters evaluated, only ΦPSII showed a significant interaction between cultivar and hypoxia (Figure 19). There was no significant difference in ΦPSII in SF plants under slight and severe hypoxia in relation the moderate hypoxia (Figure 19a). However, SF plants had ΦPSII 25% higher under slight hypoxia than severe hypoxia. In the ES plants, severe and slight hypoxia reduced ΦPSII by 23% concerning moderate hypoxia, which led to ES cultivar having ΦPSII 29% lower than SF under slight hypoxia. There was no change in qP promoted by hypoxia in both cultivars, but the SF cultivar had qP 13% higher than ES, regardless of the hypoxia level (Figure 19b). On the other hand, ETR was influenced by hypoxia levels, so the ETR of rice plants under severe hypoxia decreased by 17%, on average, in both cultivars concerning moderate hypoxia (Figure 19c). Also, the SF cultivar displayed ETR 15% higher than ES regardless of the hypoxia level. There was no significant difference in Fv'/Fm' between cultivars (Figure 19d). Also, the Fv'/Fm' of plants under slight and severe hypoxia did not differ from moderate hypoxia, but the Fv'/Fm' of plants under slight hypoxia was 9.0% higher than those under severe hypoxia.

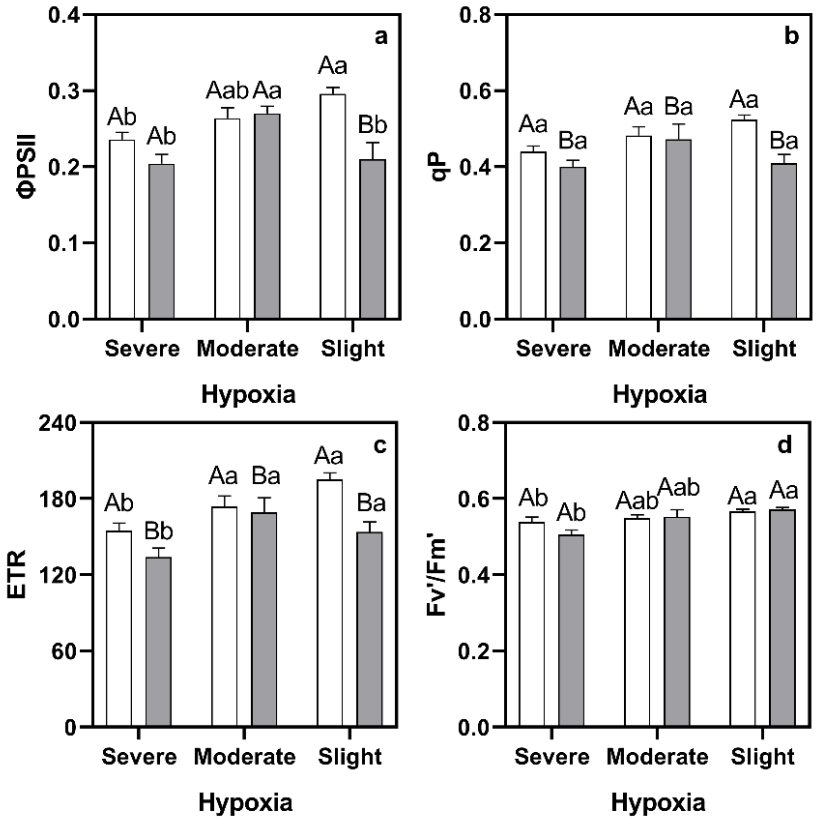

Figure 19 - Chlorophyll *a* fluorescence of rice plants cv. São Francisco (SF, white bars) or BRS Esmeralda (ES, grey bars) under severe, moderate, or slight hypoxia conditions for ten days. Effective quantum yield of PSII (**a**; ΦPSII), photochemical quenching (**b**; qP), electron transport rate (**c**; ETR), and PSII maximum efficiency (**d**; Fv'/Fm'). For each variable, the capital letters and lowercase letters compare the cultivars and hypoxia treatments, respectively. According to F-test ($p < 0.05$), neither subfigure exhibit a significant interaction between treatments, except **a**. Bars represent means (n=5) + standard error.

4.3.3 Inorganic ions contents

There was a significant interaction between cultivars and hypoxia levels in the Na^+ and Cl^- contents into the plant organs, except in the stem (Figure 20a-f). The Na^+ contents did not vary with hypoxia levels in SF leaves, as also occurred in the ES roots (Figure 20a, c). Nevertheless, slight hypoxia reduced 28% of the Na^+ content in ES leaves concerning moderate hypoxia (Figure 20a). Although there was no difference in Na^+ content in leaves between cultivars under moderate hypoxia, the ES leaves accumulated 31% and 37% less sodium than SF under slight and severe hypoxia. In stems, cultivar ES accumulated 14% more Na^+ than SF in any hypoxic condition (Figure 20b). Although the Na^+ contents under slight and severe hypoxia did not differ from the moderate hypoxia condition in the stems, there was a 22% increase in its content under severe hypoxia compared to slight hypoxia. Already in SF roots, there were a 15% reduction and a 13% increase in Na^+ content under slight and severe hypoxia, respectively in relation to moderate hypoxia (Figure 20c). Also, the SF roots accumulated 23% more Na^+ than ES roots only under severe hypoxia.

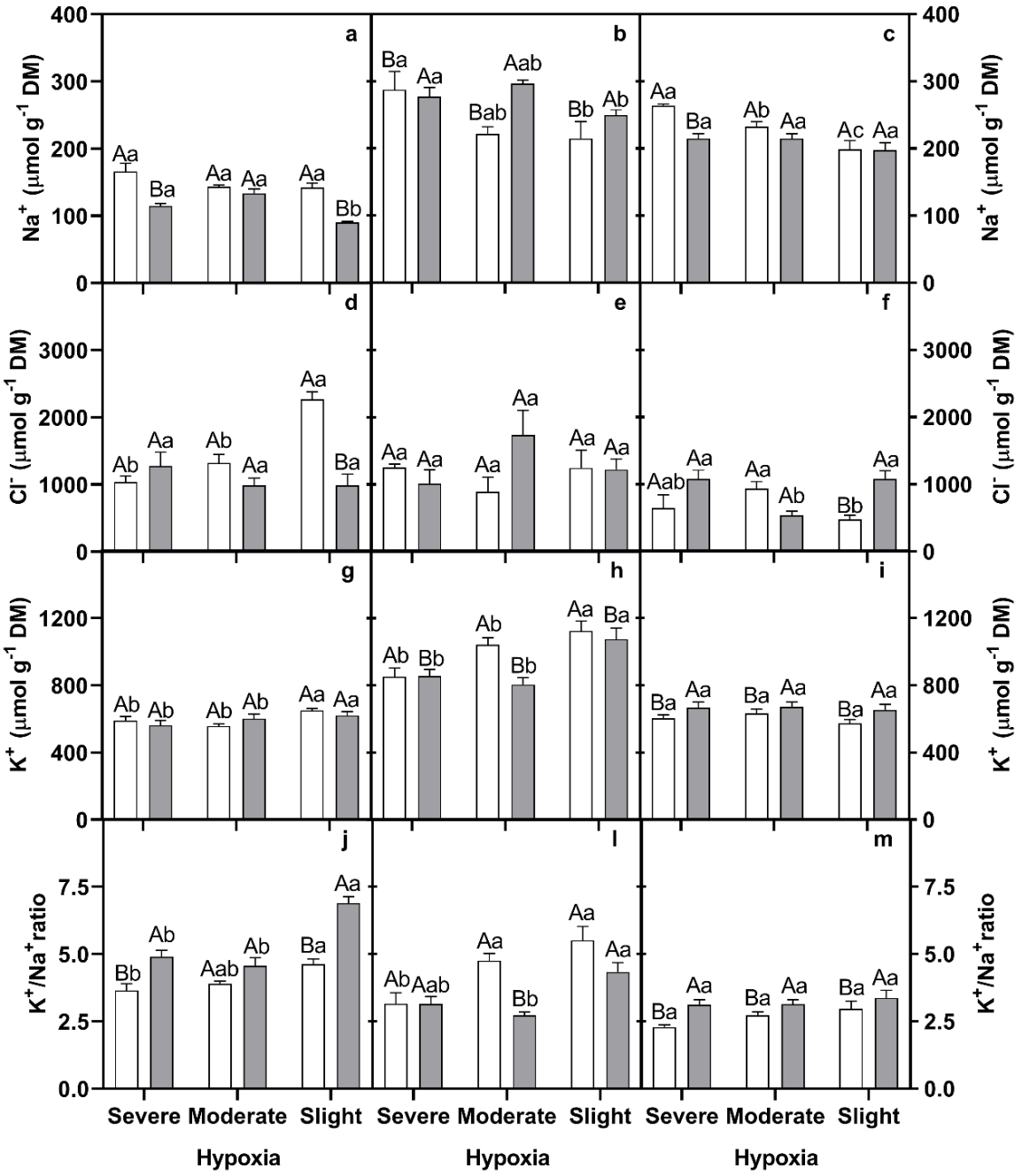

Figure 20 - Inorganic ions of rice plants cv. São Francisco (SF, white bars) and BRS Esmeralda (ES, grey bars) under severe, moderate, or slight hypoxia conditions for ten days. Na^+ content in leaves (**a**), stems (**b**), and roots (**c**); Cl^- content in leaves (**d**), stems (**e**), and roots (**f**); K^+ content in leaves (**g**), stems (**h**), and roots (**i**); and K^+/ Na^+ ratio in leaves (**j**), stems (**l**), and roots (**m**). For each variable, the capital letters and lowercase letters compare the cultivars and hypoxia treatments, respectively. According to *F*-test ($p < 0.05$), the subfigures **a**, **c**, **d**, **j**, and **l** exhibit a significant interaction between treatments. Bars represent means (n=5) + standard error.

The hypoxia levels did not affect the Cl^- content in the ES leaves, but the slight hypoxia raised 92% Cl^- content in the SF leaves compared to moderate hypoxia (Figure 20d). So, the Cl^- content in SF leaves was 130% higher than ES leaves under slight hypoxia. The hypoxia levels and the cultivars do not significantly alter the Cl^- content in the stem, which presented an average value of 1,229 µmol g^{-1} MS (Figure 20e). On the other hand, the slight and severe hypoxia increased the Cl^- content by 99% in the ES roots concerning moderate

hypoxia (Figure 20f). In contrast, the slight hypoxia reduced it by 49% in SF roots. Furthermore, there was a significant difference in Cl^- content between cultivars only under slight hypoxia, with Cl^- content being higher 125% in ES roots than SF.

There was no significant interaction between cultivars and hypoxia levels in relation to K^+ content (Figure 20g-i). In leaves and stems of both cultivars, the slight hypoxia elevated K^+ content, on average, by 10% and 24%, respectively (Figure 20g, h). The cultivar that most accumulated the K^+ in the stem was SF, 10% more than ES, while in the roots was ES, also 10% more than SF (Figure 20h, i). It is noteworthy that the K^+ content in the roots did not respond to changes in the hypoxia levels (Figure 20i).

There was a significant interaction between cultivars and hypoxia levels in the K^+/Na^+ ratio into the plant organs, except in the roots (Figure 20j-m). The K^+/Na^+ ratio in ES leaves was 34% e 49% higher than in SF leaves under severe and slight hypoxia, respectively (Figure 20j). Also, the slight hypoxia showed a higher K^+/Na^+ ratio in leaves than severe hypoxia in both cultivars. In stems, the K^+/Na^+ ratio in SF cultivar was higher than in ES cultivar only under moderate hypoxia (Figure 20l). In the SF cultivar, the K^+/Na^+ ratio was reduced 34% by severe hypoxia than moderate hypoxia. Already in ES cultivar, the K^+/Na^+ ratio was increased 59% by slight hypoxia concerning moderate hypoxia. On the other hand, the K^+/Na^+ ratio in ES roots was higher 21% than in SF roots at any hypoxia level. So the hypoxia level did not change the K^+/Na^+ ratio in rice roots (Figure 20m).

4.3.4 PCA of physiological and biochemical data

The first two principal components explained 43% of the total variation (70% - data not shown) considering all the physiological and biochemical data obtained (Figure 21a). With them, it was possible to clearly distinguish the groups of SF cultivar plants under slight and severe hypoxia. However, it was not possible to differentiate the hypoxia conditions so well in the ES cultivar, which were different from the SF cultivar under slight hypoxia. With the loading plot and biplot (data not shown), it was possible to observe the disposition of the total variation existing between physiological and biochemical parameters (Figure 21b). The first principal component (PC1) was positively influenced by 25 of 32 parameters evaluated, while it was indifferent to two parameters and negatively influenced by five parameters (Figure 21b). The second principal component (PC2) was positively influenced by 17 parameters and negatively influenced by 15 parameters. PC1 was the main component explaining the separation between the hypoxia levels (Figure 21a). Furthermore, the *A*, g_s, and *E* were the most favored parameters

with slight hypoxia, while the Na^+ content in the stems and roots were the parameters that increased the most under severe hypoxia (Figure 21b). According to the loading plot, these variables mentioned above were responsive to the separation between severe and slight hypoxia conditions in the SF cultivar, while PC2 contributed more to a separation between the ES and SF groups (Figure 21b). In this case, according to the loading plot, the contents of photosynthetic pigments and Na^+ in the roots were mainly responsible for this separation.

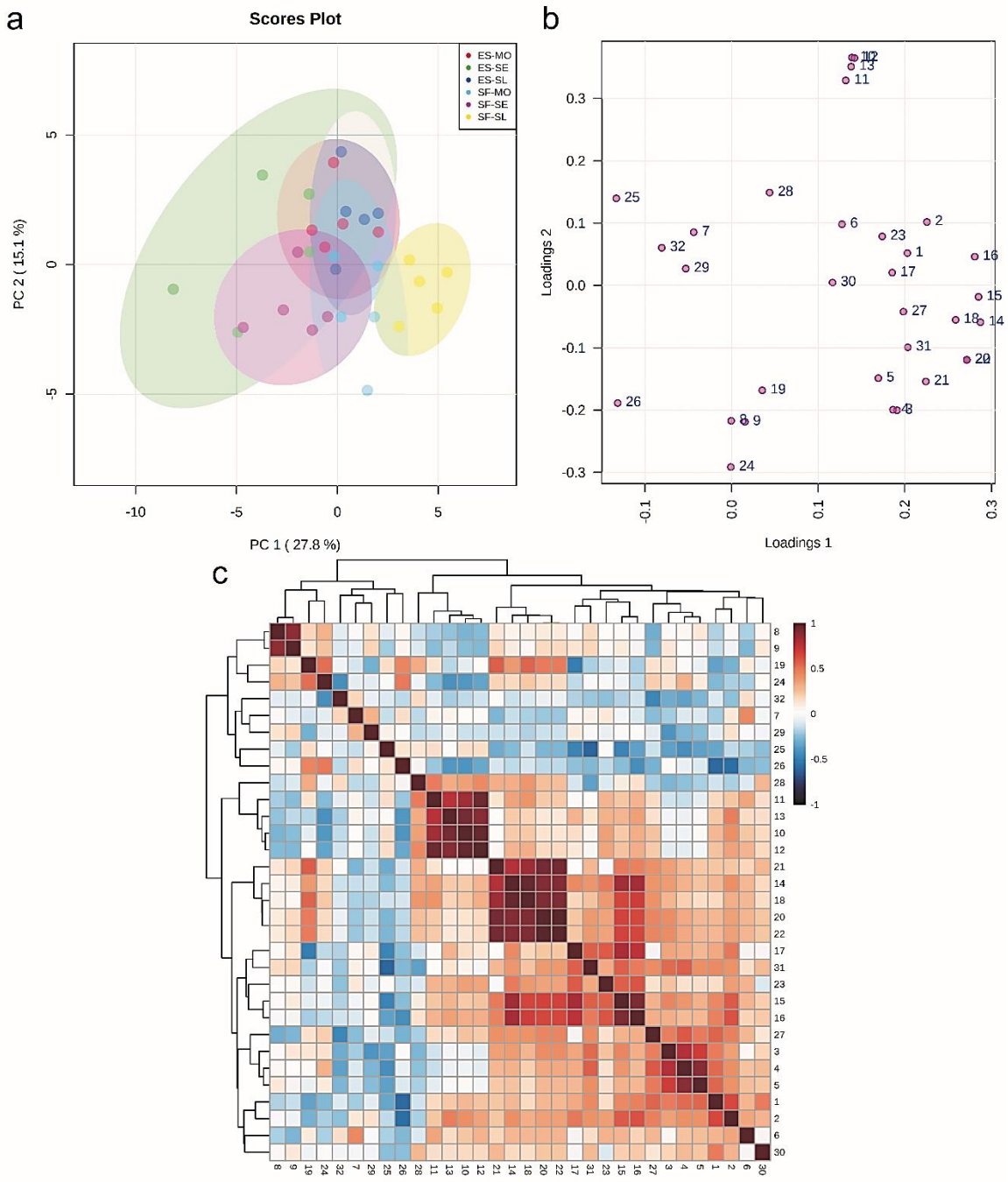

Figure 21 - Principal component analysis (PCA) of physiological and biochemical parameters of rice cv. BRS Esmeralda under severe (ES-SE), moderate (ES-MO), and slight (ES-SL) hypoxia and cv. São Francisco under severe (SF-SE), moderate (SF-MO), and slight (SF-SL) hypoxia conditions for ten days. Scores plot (a) and loading plot (b) of the first and second components (PC 1 and PC 2), indicating the clustering of samples into six groups. The heatmaps (c) shows the Pearson correlation level of the analyzed parameters. For more details, see Apêndice D. Paraments list: **1** - Shoot length, **2** - Root length, **3** - Leaf dry mass, **4** - Stem dry mass, **5** - Root dry mass, **6** - Leaf relative humidity, **7** - Relative water content of leaf, **8** - Root relative humidity, **9** - Relative water content of root, **10** - Chlorophyll *a*, **11** - Chlorophyll *b*, **12** - Chlorophyll *total*, **13** - Carotenoids, **14** - CO_2 assimilation, **15** - Stomatal conductance, **16** - Transpiration, **17** - Intercellular CO_2 concentration, **18** - Carboxylation efficiency of Rubisco, **19** - Instantaneous water use efficiency, **20** - Effective quantum yield of PSII, **21** - Photochemical quenching, **22** - Electron transport rate, **23** - PSII maximum efficiency, **24** - Na^+ leaf, **25** - Na^+ stem, **26** - Na^+ root, **27** - Cl^- leaf, **28** - Cl^- stem, **29** - Cl^- root, **30** - K^+ leaf, **31** - K^+ stem, **32** - K^+ root. All data were divided by the standard deviation of each variable (Autoscaling) for chemometrics analysis (PCA) and Pearson r-test by MetabolAnalyst 5.0.

As for the correlation of parameters, the group of variables *A*, ICE, ΦPSII, qP, ETR showed a strong positive correlation ($r > 0.7$, $p < 0.05$) among themselves, as well as the group formed by the parameters Chl *a*, Chl *b*, Chl *total*, CAR (Figure 21c; Apêndice D). It should be

noted that there were no strong negative correlations ($r < -0.7$) and significant ($p < 0.05$) between physiological and biochemical parameters.

4.3.5 Leaf metabolomic profiling

The scores plot showed that the first two components accounted for 47% of the total variability (64% - data not shown) in the leaves (Figure 22a). Loading plots generated show the variation of individual metabolites (Figure 22b). Furthermore, a cross-validation and permutation test ($p < 0.05$) allowed using PLS-DA instead of PCA (Figure 22c), being this more efficient to discriminate the groups. In rice leaves, 95 metabolic compounds were detected (Apêndice E). Among these, 65 were identified, being: 23 sugars and their derivatives, 20 amino acids, 15 organic acids, two phenolic precursors, one inorganic acid, one nucleotide, one polyamine, one nitrogen compound and one flavonoid. Considering the totality of metabolites found, the glutamic acid, unknown 8, quinic acid, and sucrose were the ones with the highest relative abundance, while the unknown 13, glucose, mannitol, unknown 14, unknown 15, unknown 19, cystine, unknown 21, unknown 25, cellobiose, and adenosine-5-monophosphate were the least abundant. Based on the metabolic profile pattern of the leaves of the two rice cultivars under three levels of hypoxia (six plant groups) and PLS-DA, it was not possible to distinguish the groups of hypoxia levels in each cultivar (Figure 22a). However, the groupings of each cultivar were distinct from each other for all hypoxia levels. The PC1 was positively affected by two metabolites and negatively affected by 93 metabolites. PC2 was positively affected by 71 metabolites and negatively affected by 24 metabolites.

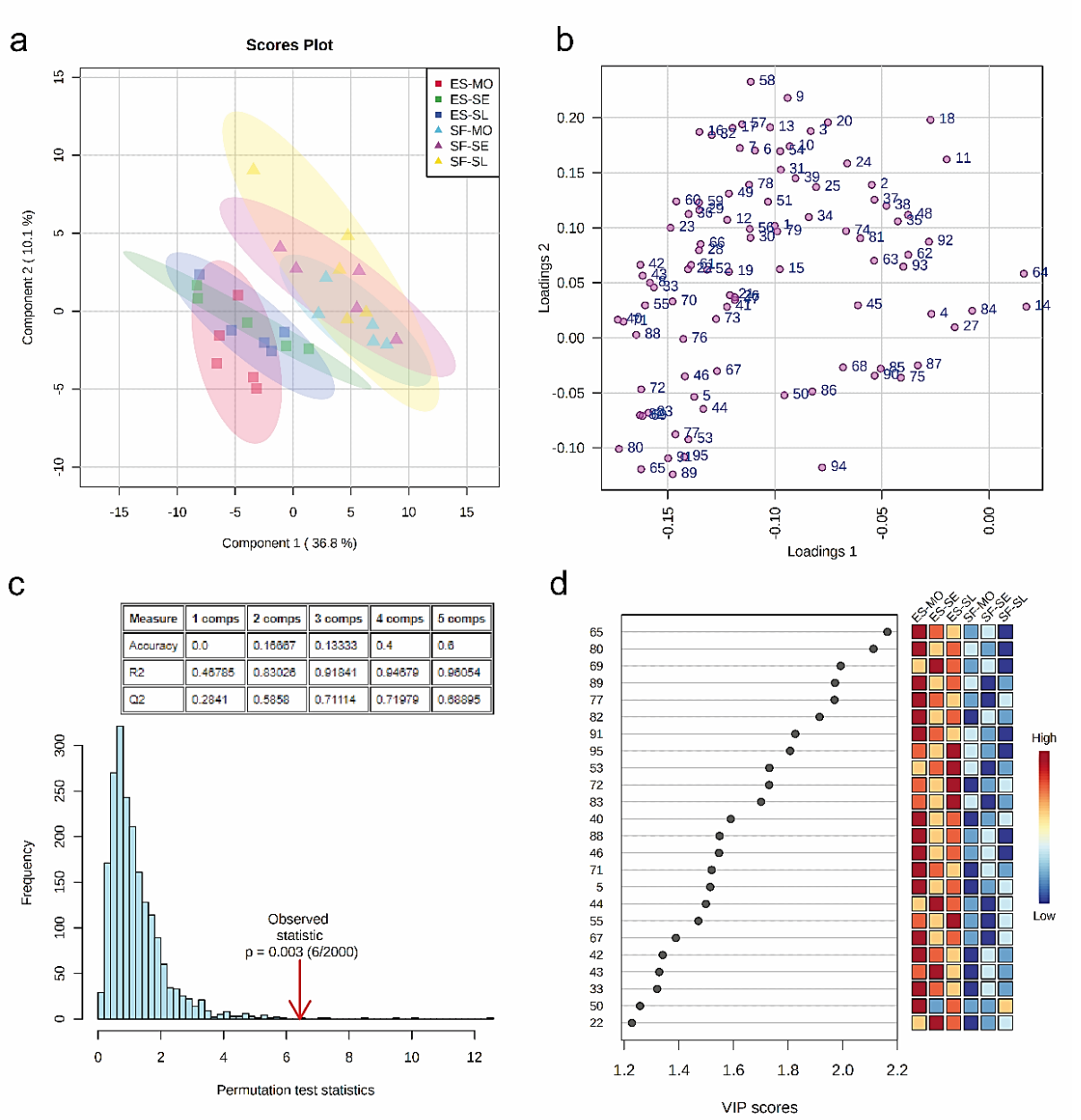

Figure 22 - Partial least squares - discriminant analysis (PLS-DA) of metabolic profiles in leaves of rice cv. BRS Esmeralda under severe (ES-SE), moderate (ES-MO), and slight (ES-SL) hypoxia and cv. São Francisco under severe (SF-SE), moderate (SF-MO), and slight (SF-SL) hypoxia conditions for ten days. Scores plot (**a**), loading plot (**b**), and PLS-DA cross-validation and permutation test (**c**) of the first and second components indicating the clustering of samples into four groups. VIP scores plot of metabolites (**d**) shows metabolites for displaying a VIP score of greater than 1.2. Red or blue squares on the right indicate the high and low abundance of the corresponding metabolite in each treatment, respectively. VIP score was based on the first component of the PLS-DA model. Metabolites class: **Amino acid** – Alanine (3), Valine (9), Serine (11), Leucine (13), Isoleucine (16), Proline (17), Glycine (18), Threonine (22), Aspartic acid (26), Hydroxyproline (27), Cysteine (334), Glutamic acid (35), Phenylalanine (36), Asparagine (38), Glutamine (45), Lysine (57), Ornithine (58), Tyrosine (60), Cystine (73); **Flavonoid** – Quercetin (95); **Inorganic acid** - Phosphoric acid (14); **Nitrogenous compounds** – Guanidine (6), Urea (10); **Nucleotide** - Adenosine-5-monophosphate (94); **Organic acid** - Pyruvic acid (1), Lactic acid (2), Oxalic acid (4), 2-aminoisobutyric acid (7), Malonic acid (8), Succinic acid (19), Glyceric acid (20), Fumaric acid (21), Malic acid (24), Erythronic acid (30), Lyxose (34), 2-Oxoglutaric acid (31), Citric acid (48), Glucaric acid (62), Gulonic acid (66), Glucuronic acid (71); **Phenolic precursor** - Shikimic acid (47), Quinic acid (52); **Polyamine** – Putrescine (32); **Sugar** – Lyxose (25), Xylulose (28), Erythrose (33), Ribose (40), Allose (51), Sorbose (53), Fructose (54), Mannose (55), Glucose (56), Galactose (59), Cellobiose (84), Sucrose (86), Trehalose (88), Raffinose (90), Fructose-1,6-diphosphate (91), Maltotriose (93); **Sugar alcohol** – Arabitol (43), Glycerol-2-phosphate (44), Mannitol (61), Galactinol (92), **Sugar derived** – Mannopyranoside (39), Glucopyranoside (68); **Unidentified Metabolites** - Unknown 2 (5), Unknown 3 (12), Unknown 4 (15), Unknown 5 (23), Unknown 7 (29), Unknown 8 (37), Unknown 9 (41), Unknown 10 (42), Unknown 11 (46), Unknown 12 (49), Unknown 13 (50), Unknown 14 (63), Unknown 15 (64), Unknown 16 (65), Unknown 17 (67), Unknown 18 (70), Unknown 19 (72), Unknown 20 (74), Unknown 21 (75), Unknown 22 (76), Unknown 23 (77), Unknown 24 (78), Unknown 25 (79), Unknown 26 (80), Unknown 27 (81), Unknown 28 (82), Unknown 30 (83), Unknown 32 (85), Unknown 33 (87), Unknown 34 (89). All data were cube root transformed and divided by the standard deviation of each variable (Autoscaling) for chemometrics analysis (PLS-DA) by MetabolAnalyst 5.0.

The variable importance in projection (VIP) scores graph displayed the most important metabolites for differentiating the treatments by the abundance of metabolites in each treatment (Figure 22d). VIP plot showed 24 metabolites of more than 1.2 scores, in descending order of VIP score they are: unknown 16, unknown 26, inositol, unknown 34, unknown 23, unknown 28, fructose-1,6-diphosphate, quercetin, sorbose, unknown 19, unknown 30, ribose, trehalose, unknown metabolite 11, glucuronic acid, unknown metabolite 2, glycerol-2-phosphate, mannose, unknown 17, unknown 10, arabitol, erythrose, unknown 13 and threonine.

Thirty-nine metabolites were differentially expressed in rice leaves considering the six analyzed groups (Figure 23; Apêndice E). Severe hypoxia upregulated glucopyranoside and slight hypoxia downregulated the metabolite unknown 21 in both cultivars about moderate hypoxia. In SF plants, the severe hypoxia upregulated five metabolites (glycine, erythronic acid, cysteine, unknown 22 and unknown 25) and the downregulated four metabolites (unknown 2, phosphoric acid, glycerol-2-phosphate, and unknown 23), while the slight hypoxia upregulated two metabolites (unknown 14 and unknown 17). Already ES plants, the severe hypoxia upregulated one metabolite (succinic acid) and downregulated four metabolites (unknown 13, cellobiose, unknown 34, and adenosine-5-monophosphate), while slight hypoxia upregulated (phosphoric acid and unknown 4) and downregulated a single metabolite (glucopyranoside).

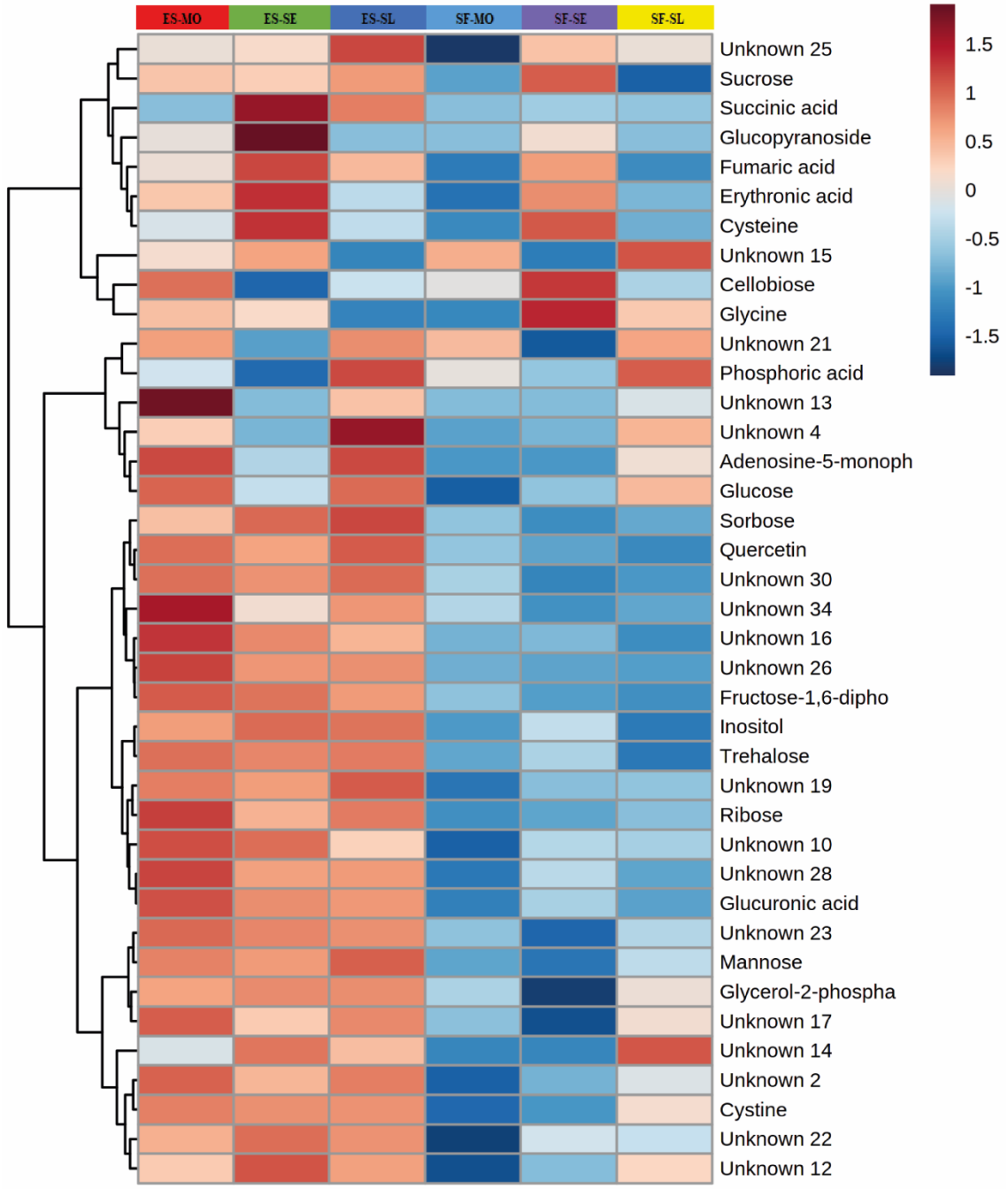

Figure 23 - Heatmap of normalized values of metabolites in leaves of rice cv. BRS Esmeralda under severe (ES-SE), moderate (ES-MO), and slight (ES-SL) hypoxia and cv. São Francisco under severe (SF-SE), moderate (SF-MO), and slight (SF-SL) hypoxia conditions for ten days. The heat map shows a high (red scale) or low (blue scale) relative amount of each metabolite. Metabolites class: **Amino acid** – Alanine (3), Valine (9), Serine (11), Leucine (13), Isoleucine (16), Proline (17), Glycine (18), Threonine (22), Aspartic acid (26), Hydroxyproline (27), Cysteine (334), Glutamic acid (35), Phenylalanine (36), Asparagine (38), Glutamine (45), Lysine (57), Ornithine (58), Tyrosine (60), Cystine (73); **Flavonoid** – Quercetin (95); **Inorganic acid** - Phosphoric acid (14); **Nitrogenous compounds** – Guanidine (6), Urea (10); **Nucleotide** - Adenosine-5-monophosphate (94); **Organic acid** - Pyruvic acid (1), Lactic acid (2), Oxalic acid (4), 2-aminoisobutyric acid (7), Malonic acid (8), Succinic acid (19), Glyceric acid (20), Fumaric acid (21), Malic acid (24), Erythronic acid (30), Lyxose (34), 2-Oxoglutaric acid (31), Citric acid (48), Glucaric acid (62), Gulonic acid (66), Glucuronic acid (71); **Phenolic precursor** - Shikimic acid (47), Quinic acid (52); **Polyamine** – Putrescine (32); **Sugar** – Lyxose (25), Xylulose (28), Erythrose (33), Ribose (40), Allose (51), Sorbose (53), Fructose (54), Mannose (55), Glucose (56), Galactose (59), Cellobiose (84), Sucrose (86), Trehalose (88), Raffinose (90), Fructose-1,6-diphosphate (91), Maltotriose (93); **Sugar alcohol** – Arabitol (43), Glycerol-2-phosphate (44), Mannitol (61), Galactinol (92), **Sugar derived** – Mannopyranoside (39), Glucopyranoside (68); **Unidentified Metabolites** - Unknown 2 (5), Unknown 3 (12), Unknown 4 (15), Unknown 5 (23), Unknown 7 (29), Unknown 8 (37), Unknown 9 (41), Unknown 10 (42), Unknown 11 (46), Unknown 12 (49), Unknown 13 (50), Unknown 14 (63), Unknown 15 (64), Unknown 16 (65), Unknown 17 (67), Unknown 18 (70), Unknown 19 (72), Unknown 20 (74), Unknown 21 (75), Unknown 22 (76), Unknown 23 (77), Unknown 24 (78), Unknown 25 (79), Unknown 26 (80), Unknown 27 (81), Unknown 28 (82), Unknown 30 (83), Unknown 32 (85), Unknown 33 (87), Unknown 34 (89). Each square represents the mean of five biological replicates, and the statistical difference was obtained according to *F*-test ($p < 0.05$) and Tukey test ($p < 0.05$). For more details, see Apêndice E.

Under severe hypoxia, one metabolite (cellobiose) showed higher relative abundance in SF cultivar than ES, and 17 metabolites showed fewer relative abundance in SF cultivar than ES, being these: unknown 2, succinic acid, glycerol-2-phosphate, sorbose, mannose, unknown 14, unknown 16, unknown 17, glucopyranoside, inositol, unknown 19, unknown 23, unknown 26, unknown 28, trehalose, fructose-1,6-diphosphate, and quercetin. Moreover, under moderate hypoxia, one metabolite (phosphoric acid) showed higher relative abundance in SF cultivar than ES, and 24 metabolites showed fewer relative abundance in SF cultivar than ES, being these: unknown 2, ribose, unknown 10, glycerol-2-phosphate, unknown 13, sorbose, mannose, glucose, unknown 16, unknown 17, glucopyranoside, inositol, glucuronic acid, unknown 19, cystine, unknown 22, unknown 23, unknown 25, unknown 26, unknown 28, trehalose, unknown 34, adenosine-5-monophosphate, and quercetin.

Finally, under slight hypoxia, two metabolites (phosphoric acid and unknown 15) showed higher relative abundance in SF cultivar than ES, and 12 metabolites showed fewer relative abundance in SF cultivar than ES, being these: unknown 2, sorbose, unknown 16, inositol, unknown 19, unknown 23, unknown 26, unknown 28, sucrose, trehalose, unknown 34 and quercetin.

4.3.6 Root metabolomic profiling

The scores plot showed that the first two components accounted for 48% of the total variability (72% - data not shown) in the roots (Figure 24a). Loading plots generated show the variation of individual metabolites (Figure 24b). Moreover, the cross-validation and permutation test ($p < 0.01$) allowed using PLS-DA instead of PCA (Figure 24c). In rice roots, 70 metabolic compounds were detected (Apêndice F). Among these, 57 were identified, being: 22 sugars and their derivatives, 18 amino acids, 12 organic acids, two phenolic precursors, one inorganic acid, one polyamine, and one nitrogenous compound. Of all metabolites found, cellobiose, glycerol-2-phosphte, sucrose, fructose, sorbose and phosphoric acid were the most abundant, while the unknown 2, erythrose, arabitol, unknown 33, glyceric acid, fructose-1,6-diphosphate, unknown 34, unknown 25, xylitol, unknown 23 and putrescine were the lowest abundances. Based on the root metabolic profile pattern of the six plant groups of both cultivars under three different hypoxic conditions and PLS-DA, it was not possible to distinguish the groups of hypoxia levels in ES cultivar (Figure 24a). However, there was a separation of the SF cultivar under severe hypoxia (SF-SE) from other groups of this same cultivar, mainly under moderate hypoxia (SF-MO). Also, as with the leaf metabolic profile, groupings of each cultivar

were distinct from each other for all hypoxia levels. The PC1 was positively affected by 13 metabolites and negatively affected by 57 metabolites, while PC2 was positively affected by 62 metabolites and negatively affected by eight metabolites (Figure 24c). The VIP plot showed 18 metabolites with scores greater than 1.0 (Figure 24d) In descending order of VIP score, they are: arabitol, sorbose, fructose, phosphoric acid, glucaric acid, unknown 13, galactose, gulonic acid, raffinose, inositol, 2-oxoglutaric acid, ornithine, glyceric acid, unknown 2, erythrose, glucose, unknown 34, and lysine.

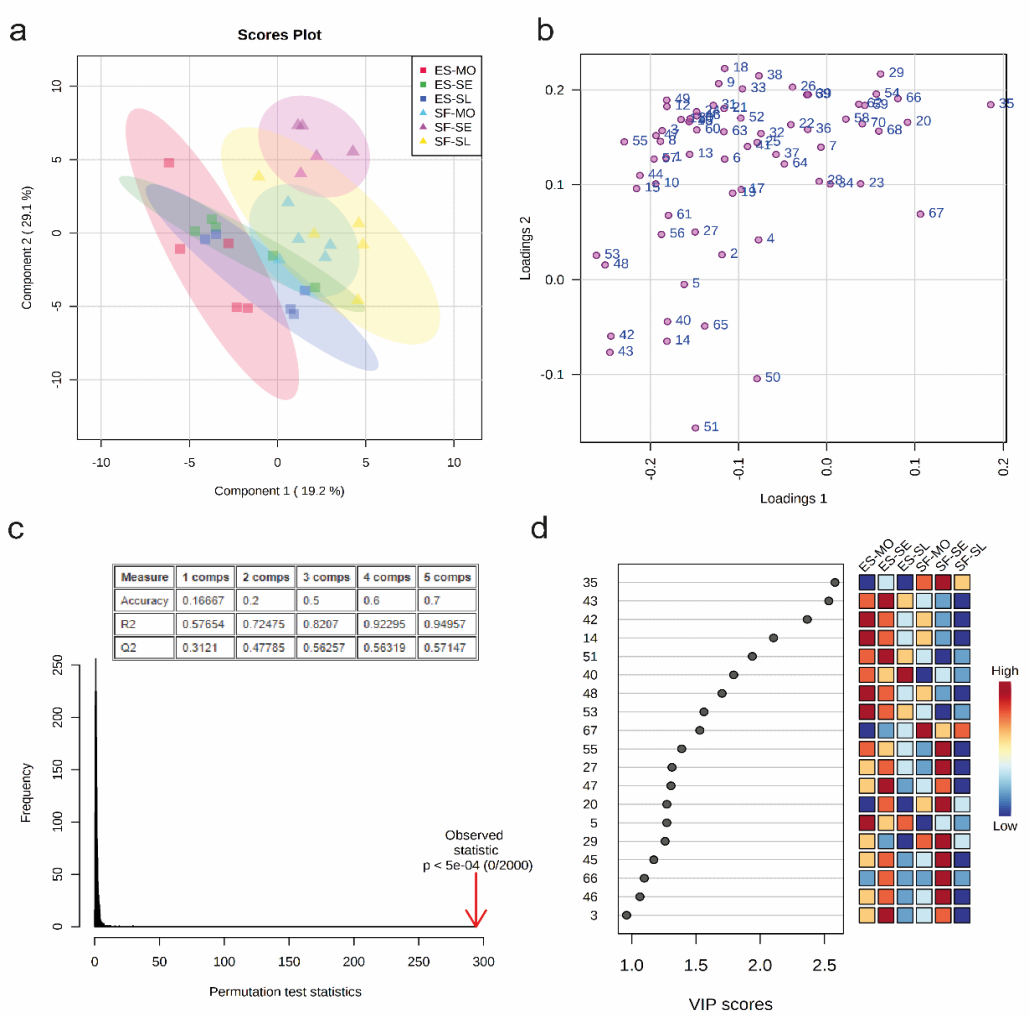

Figure 24 - Partial least squares - discriminant analysis (PLS-DA) of metabolic profiles in roots of rice cv. BRS Esmeralda under severe (ES-SE), moderate (ES-MO), and slight (ES-SL) hypoxia and cv. São Francisco under severe (SF-SE), moderate (SF-MO), and slight (SF-SL) hypoxia conditions for ten days. Scores plot (**a**), loading plot (**b**), and PLS-DA cross-validation and permutation test (**c**) of the first and second components indicating the clustering of samples into four groups. VIP scores plot of metabolites (**d**) shows metabolites for displaying a VIP score of greater than 1.0. Red or blue squares on the right indicate the high and low abundance of the corresponding metabolite in each treatment, respectively. VIP score was based on the first component of the PLS-DA model. Metabolites class: **Amino acid** – Alanine (3), Valine (9), Serine (11), Leucine (13), Isoleucine (16), Proline (17), Glycine (18), Threonine (21), Aspartic acid (24), Hydroxyproline (25), Glutamic acid (30), Phenylalanine (31), Asparagine (32), Glutamine (37), Lysine (46), Ornithine (47), Tyrosine (49); **Inorganic acid** - Phosphoric acid (14); **Nitrogenous compounds** – Guanidine (6), Urea (10); **Nucleotide** - Adenosine-5-monophosphate (94); **Organic acid** - Pyruvic acid (1), Lactic acid (2), Oxalic acid (4), 2-aminoisobutyric acid (7), Malonic acid (8), Succinic acid (19), Glyceric acid (20), Malic acid (22), 2-Oxoglutaric acid (27), Citric acid (39), Glucaric acid (51), Gulonic acid (53); **Phenolic precursor** - Shikimic acid (38), Quinic acid (41); **Polyamine** – Putrescine (28); **Sugar** – Lyxose (23), Xylulose (26), Erythrose (29), Ribose (33), Fructose (42), Sorbose (43), Mannose (44), Glucose (45), Galactose (48), Cellobiose (62), Sucrose (63), Trehalose (65), Raffinose (67), Fructose-1,6-diphosphate (68), Maltotriose (70); **Sugar alcohol** – Xylitol (34), Arabitol (35), Glycerol-2-phosphate (36), Mannitol (50), Inositol (55), Galactinol (69); **Sugar derived** – Glucopyranoside (54); **Unidentified Metabolites** - Unknown 2 (5), Unknown 3 (12), Unknown 4 (15), Unknown 13 (40), Unknown 16 (52), Unknown 20 (56), Unknown 21 (57), Unknown 23 (58), Unknown 25 (59), Unknown 26 (60), Unknown 27 (61), Unknown 33 (64), Unknown 34 (66). All data were cube root transformed and divided by the standard deviation of each variable (Autoscaling) for chemometrics analysis (PLS-DA) by MetabolAnalyst 5.0.

Forty metabolites were differentially expressed in rice roots considering the six groups analyzed (Figure 25; Apêndice F). Severe hypoxia downregulated mannitol and upregulated 12 metabolites (glyceric acid, malic acid, putrescine, xylitol, glycerol-2-phosphate, glucopyranoside, unknown 23, unknown 25, cellobiose, fructose-1,6-diphosphate, galactinol, and maltotriose), in both cultivars in relation to moderate hypoxia (control). Also, slight hypoxia downregulated malic acid, erythrose, citric acid, and mannitol in both cultivars. In SF plants, the severe hypoxia upregulated 13 metabolites (guanidine, isoleucine, glycine, lyxose, arabitol, citric acid, glucose, lysine, ornithine, unknown 16, inositol, unknown 26 and unknown 34) and downregulated two metabolites (2-oxobutyric acid and fructose), while the slight hypoxia upregulated one metabolite (arabitol) and downregulated four metabolites (glycine, shikimic acid, unknown 16, and unknown 26) concerning moderate hypoxia. Already ES plants, the severe hypoxia upregulated one metabolite (2-oxobutyric acid) and downregulated two metabolites (lyxose and trehalose), while slight hypoxia downregulated six metabolites (lyxose, glucose, lysine, ornithine, unknown 16, and trehalose).

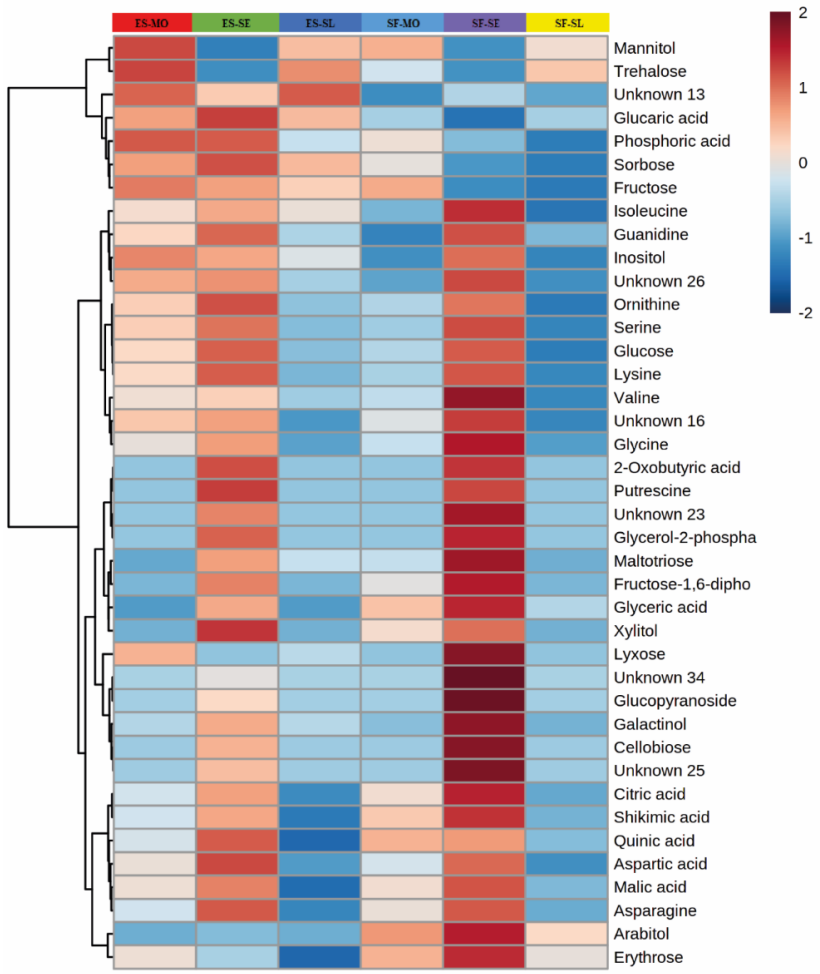

Figure 25 - Heatmap of normalized values of metabolites in roots rice cv. BRS Esmeralda under severe (ES-SE), moderate (ES-MO), and slight (ES-SL) hypoxia and cv. São Francisco under severe (SF-SE), moderate (SF-MO), and slight (SF-SL) hypoxia conditions for ten days. The heat map shows a high (red scale) or low (blue scale) relative amount of each metabolite. Significant metabolites list ($p < 0.05$) grouped according to metabolites class: **Amino acid** – Alanine (3), Valine (9), Serine (11), Leucine (13), Isoleucine (16), Proline (17), Glycine (18), Threonine (22), Aspartic acid (26), Hydroxyproline (27), Cysteine (34), Glutamic acid (35), Phenylalanine (36), Asparagine (38), Glutamine (45), Lysine (57), Ornithine (58), Tyrosine (60), Cystine (73); **Flavonoid** – Quercetin (95); **Inorganic acid** - Phosphoric acid (14); **Nitrogenous compounds** – Guanidine (6), Urea (10); **Nucleotide** - Adenosine-5-monophosphate (94); **Organic acid** - Pyruvic acid (1), Lactic acid (2), Oxalic acid (4), 2-aminoisobutyric acid (7), Malonic acid (8), Succinic acid (19), Glyceric acid (20), Fumaric acid (21), Malic acid (24), Erythronic acid (30), Lyxose (34), 2-Oxoglutaric acid (31), Citric acid (48), Glucaric acid (62), Gulonic acid (66), Glucuronic acid (71); **Phenolic precursor** - Shikimic acid (47), Quinic acid (52); **Polyamine** – Putrescine (32); **Sugar** – Lyxose (25), Xylulose (28), Erythrose (33), Ribose (40), Allose (51), Sorbose (53), Fructose (54), Mannose (55), Glucose (56), Galactose (59), Cellobiose (84), Sucrose (86), Trehalose (88), Raffinose (90), Fructose-1,6-diphosphate (91), Maltotriose (93); **Sugar alcohol** – Arabitol (43), Glycerol-2-phosphate (44), Mannitol (61), Galactinol (92); **Sugar derived** – Mannopyranoside (39), Glucopyranoside (68); **Unidentified Metabolites** - Unknown 2 (5), Unknown 3 (12), Unknown 4 (15), Unknown 5 (23), Unknown 7 (29), Unknown 8 (37), Unknown 9 (41), Unknown 10 (42), Unknown 11 (46), Unknown 12 (49), Unknown 13 (50), Unknown 14 (63), Unknown 15 (64), Unknown 16 (65), Unknown 17 (67), Unknown 18 (70), Unknown 19 (72), Unknown 20 (74), Unknown 21 (75), Unknown 22 (76), Unknown 23 (77), Unknown 24 (78), Unknown 25 (79), Unknown 26 (80), Unknown 27 (81), Unknown 28 (82), Unknown 30 (83), Unknown 32 (85), Unknown 33 (87), Unknown 34 (89). Each square represents the mean of five biological replicates, and the statistical difference was obtained according to *F*-test ($p < 0.05$) and Tukey test ($p < 0.05$). For more details, see Apêndice F.

Under severe hypoxia, 11 metabolites (glyceric acid, lyxose, arabitol, citric acid, unknown 16, glucopyranoside, unknown 23, unknown 25, unknown 34, galactinol, and maltotriose) showed higher relative abundance in SF cultivar than ES, and seven metabolites (2-oxobutyric acid, unknown 13, fructose, sorbose, glucose, glucaric acid e cellobiose) showed fewer relative abundance in SF cultivar than ES. Moreover, under moderate hypoxia, five metabolites (2-oxobutyric acid, glyceric acid, lyxose, erythrose, and arabitol) showed higher relative abundance in SF cultivar than ES, and five metabolites (unknown 13, lysine, ornithine,

mannitol, and inositol) showed fewer relative abundance in SF cultivar than ES. Finally, under slight hypoxia, three metabolites (lyxose, erythrose, and arabitol) showed higher relative abundance in SF cultivar than ES, and six metabolites (isoleucine, unknown 13, sorbose, glucose, mannitol, and unknown 26) showed lower relative abundance in SF cultivar than ES.

4.4 Discussion

4.4.1 Physiological performance of São Francisco and BRS Esmeralda cultivars under hypoxia

Plants, in general, show high growth reduction under hypoxic conditions, which can lead to death (LORETI; PERATA, 2020). On the other hand, some species, such as rice, survive to low O_2 concentrations in the rhizosphere (PEDERSEN; PERATA; VOESENEK, 2017). Despite this, the additional oxygen limitation (severe hypoxia) promoted alteration in growth, limiting rice plant elongation (Figure 15d-e). Besides, the oxygen supply (slight hypoxia) favored an more significant accumulation of dry mass and shoot and root length mainly in plants of the SF cultivar (Figure 15a-c), which is adequate and very productive on flooded cultivation (EMBRAPA, 2013). The PCA also showed that the performance of plants at severe and slight hypoxia showed a contrast in the totality of their physiological and biochemical data (Figure 22). Although oxygen is not generally a limiting factor, lack of it can restrict the generation of ATP from breathing, which is necessary for a series of metabolic reactions vital to normal growth and development (LORETI; PERATA, 2020).

The rice plants of both cultivars survived in environments with severe hypoxia, which confirms that they are plant species relatively more tolerant to hypoxia (ENGELAAR *et al*., 2000). However, this does not entirely relieve the adverse effects found in hypoxic environments, mainly with the aggravation of hypoxia by lowering the dissolved oxygen concentration in the culture medium (YAMAUCHI *et al*., 2018; LOPES *et al*., 2020). The photosynthetic pigment contents in both cultivars were reduced in plants under severe hypoxia compared to slight hypoxia conditions (Figure 17). This may be related to the oxidative stress generated by the severe hypoxia environment (CAO *et al*., 2020), which leads to significant damage to pigments so like under other abiotic stresses (SHAREEF; ABDI; FAHAD, 2020; ARAÚJO *et al*., 2021). However, compared to other agricultural species such as *Phaseolus vulgaris* L., these reductions were smaller in rice plants (VELASCO *et al*., 2019).

The severely limited oxygenation of the root environment promotes losses in carbon

assimilation in plants, including rice plants, due to promoting stomatal closure (LORETI; PERATA, 2020; CAO *et al*., 2020; LOPES *et al*., 2020). The severe hypoxia conditions also limited the gas exchanges in both rice cultivars so that significant reductions in *A*, g_s, *E*, and ICE were observed (Figure 18a-c, e). Therefore, rice plants under severe hypoxia had the lowest photosynthetic efficiency. However, under slight hypoxia conditions, *A*, g_s, and *E* were significantly favored in SF plants considering moderate hypoxia (Figure 21a, b). This represented significant gains in plant development and growth (Figure 15b-e), since such parameters imply carbon effectively incorporated and converted into usable substrates in the most diverse essential metabolic processes (SANTOS et al., 2017). The WUEi of the SF cultivar was indifferent to the hypoxia levels (Figure 18f), ensuring that the SF plants have better water use in a stressful environment, unlike plants of the ES cultivar that showed WUEi reduces by a higher restriction in *A* than SF under severe hypoxia. Although a significant decrease in *Ci* could lead to a drop in *A*, due to reducing the concentration of CO_2 for rubisco activity (MACHADO *et al*., 2005), ES plants reduced the *A* but kept the *Ci*, which is a strong indication of photorespiration, common in C3 plants, which leads Rubisco to perform the oxygenation of the ribulose-1,5-bisphosphate sugar instead of the carboxylation (IGAMBERDIEV; ROUSSEL, 2012; HUMA *et al*., 2018; VON CAEMMERER, 2020). As a result, there is low production efficiency of carbon skeletons. Besides, the chlorophyll *a* fluorescence parameters, except for qP, were also influenced by hypoxia levels in both cultivars with ΦPSII being higher in SF plants than in ES plants under slight hypoxia and reduced in ES plants under slight and severe hypoxia compared to moderate hypoxia (Figure 19). This can reflect a low efficiency of CO_2 assimilation combined with a reduced ETR (PORCEL *et al*., 2015), as occurs in ES plants.

In plants under environmental stress, the accumulation of toxic ions, such as Na^+ and Cl^-, impairs cell metabolism, causing a reduction in photosynthesis (SHABALA; POTTOSIN, 2014; ARAÚJO *et al*., 2021). Thus, effective control of the accumulation of toxic ions contributes to adequate plant growth; however, the hypoxia levels can change the content and distribution of these ions (LOPES *et al*., 2020), as occurred in this study. In addition, there was an interaction of this response to hypoxia levels with the rice cultivars studied for Na^+ and Cl^- in roots and leaves (Figure 20). Plants under severe hypoxia tend to accumulate more Na+ in the aerial part (FALAKBOLAND *et al*., 2017; PEDERSON *et al*., 2017), but not necessarily in the leaves (LOPES *et al*., 2020), as is the case with SF and ES cultivars, that accumulated more Na^+ in the stem when subjected to severe hypoxia compared to slight hypoxia (Figure 20b). So, Na^+ stem content was an essential parameter for distinguishing plants under severe and slight hypoxia as well as Cl^- content in roots and gas exchange parameters, mainly in SF

cultivar (Figure 21a, b). Besides, there was a significant increase in Na^+ content under severe hypoxia in the SF roots (Figure 20c). It is important to point out that Na^+, followed by Cl^-, when accumulated at toxic levels, can induce harmful and significant effects on plant growth and development; this is because Na^+ mainly triggers the overproduction of reactive oxygen species, leading to oxidative stress in plant cells (KUMAR; KHARE, 2014, 2016). In addition, the Cl^-, on the other hand, although at toxic levels it can induce deleterious effects on plant growth and development, it is essential in water photolysis, an introductory process to photosynthesis that indirectly stimulates the functioning of ATPase pumps located in the tonoplast (SILVA, 2018). It should be noted yet that even having observed high levels of Cl^- in the SF leaves, with relief from hypoxia (slight hypoxia), and a small increase in Cl^- in the roots of cultivar ES under severe and slight hypoxia (Figure 20d-f). These significant increments, in the Cl^- contents, did not have harmful effects on the growth and development of these cultivars.

Potassium, another essential ion, is a macronutrient that regulates the cellular osmotic potential and indirectly participates in photosynthesis and respiration, acting in the activation of many enzymes involved in such processes (DECHEN; NACHTIGALL, 2018). In barley varieties, severe hypoxia reduced the K^+ content in the aerial part (FALAKBOLAND *et al*., 2017). Still, this condition did not reduce the K^+ content in the aerial part in both rice cultivars (Figure 20g, h), as noted in another rice cultivar (LOPES *et al*., 2020). On the other hand, slight hypoxia promoted the K^+ contents in leaves and stems (Figure 20g, h). This can result, in addition to the benefits of promoting typical physiological responses dependent on potassium, in a better response to stressful conditions such as drought and salinity (WU *et al*., 2014; AHMAD; MIAN; MAATHUIS, 2016).

In addition to an increase in K^+ content over slight hypoxia, a reduction in Na^+ content was observed in SF roots and ES leaves (Figure 20a, c). This is important because in some environments such as salinity, for example, the excessive accumulation of ions such as Na^+, leads vegetables to rupture essential organelles, such as chloroplasts, leading to reduced photosynthesis, the emergence of oxidative stress, and resulting in a reduction in the pattern of growth and development (ALVES *et al*., 2020; LEMOS NETO *et al*., 2020; ALENCAR *et al*., 2021; ARAÚJO *et al*., 2021). Thus, the decrease in Na^+ content under slight hypoxia may contribute to better mitigation of the potential toxic effects generated by this chemical element when accumulated. And in the case of ES leaves, the substantial increase in the K^+/Na^+ ratio (Figure 20j) indicates an improvement in the osmotic condition of these plants under slight hypoxia. Thus, oxygenation can improve the control mechanisms for excessive Na^+ content differently in these cultivars.

4.4.2 The adjustment in the metabolic profile to hypoxia level occurs mainly in the roots

The present study characterizes the modulation induced by hypoxia levels in leaves and roots of two rice cultivars to understand the necessary adjustments to tolerate the most severe oxygen limitations, typical in flooded rice fields. This additional O_2 limitation in flooded soils may arise, for example, from the excessive chemical oxidation of iron and heterotrophic and methanotrophic respiration (VAN BODEGOM *et al*., 2001). Although there is no clear separation of the leaf metabolic profile induced by hypoxia levels within each of the cultivars as occurred with the root metabolic profile (Figures 22a, 24a), there were particularities in the modulations of the leaf metabolic profile since there was no total overlap of the groups formed by the levels of hypoxia in each cultivar. Also, considering the differentially modulated metabolites in leaves, the separation between SF and ES cultivars at all levels of hypoxia was mainly due to the relative abundances higher in ES cultivar than SF for most of the metabolites detected (Figure 23; Apêndice E).

In the modulations of organic acids found in leaves, succinic acid increased only in ES under severe hypoxia concerning to moderate hypoxia (Figure 23, Apêndice E). Succinic acid is one of the key metabolites of the tricarboxylic acid (TCA) cycle, and its increase is associated with the anaplerotic effect of the GABA shunt pathway, which in turn is an essential inducer of tolerance to environmental stresses (LÜ *et al*., 2019). However, based on the results found here, it is not possible to confirm that the GABA shunt mechanism is used in the ES leaves under severe hypoxia. In contrast, erythronic acid, a compound derived from erythrose indicated as a biomarker of salt stress in Lotus species, increased only in cultivar SF under severe hypoxia (SANCHEZ *et al*., 2011). Besides, oxygen restriction promoted phosphoric acid reduction so that it was downregulated by severe hypoxia in SF cultivar and upregulated by slight hypoxia in ES cultivar. Phosphoric acid, as a metabolite, is a vital component in the supply of compounds that can be used in ATP production or essential constituents for life, such as DNA (MALHOTRA *et al*., 2018). Thus, a high oxygen limitation can generate a greater demand in the leaves for this raw material for ATP synthesis, mainly in the SF cultivar.

Interestingly, amino acids did not undergo significant changes in their relative intensities under different hypoxia conditions, except for cysteine and glycine amino acids, accumulated in leaves of SF plants subjected to severe hypoxia (Figure 23; Apêndice E). It should be noted that cysteine is an essential amino acid for plant metabolism, acting directly and indirectly in the photosystems protection, protein autophagy inhibition, and mitigating

damages resulting from the attack of pathogens (ROMERO et al., 2014). Therefore, it can help defend against hypoxia stress imposed by severe hypoxia on the development and growth of rice plants. On the other hand, glycine is crucial because it is one of the main precursors of glycine betaine (KRASENSKY; JONAK, 2012). The glycine betaine is a secondary metabolite that interacts with stress-responsive hormones (abscisic acid and salicylic acid), growth-related hormones (gibberellins, auxins, and cytokinins) well as reactive oxygen species (WUTIPRADITKUL; WONGWEAN; BUABOOCHA, 2015; KUREPIN *et al*., 2017; HASANUZZAMAN *et al*., 2019). The increases in glycine betaine in organelles such as chloroplasts have been associated with greater tolerance to abiotic stresses, such as those arising from hypoxic conditions (CASTRO-DUQUE; CHÁVEZ-ARIAS; RESTREPO-DÍAZ, 2020; LI *et al*., 2021).

Among the 95 metabolites detected in the leaves, 23 are sugars and derivatives, and 11 of these metabolites were significantly modulated by treatments (Figure 23; Apêndice E). Sugars such as fructose-1,6-diphosphate had lower relative abundance in SF leaves than ES only under severe hypoxia; conversely, the cellobiose decreased in ES leaves under severe hypoxia, being lower than SF leaves same conditions (Apêndice E). Already, the cellobiose is one of the essential growth regulators, providing carbon skeletons for such, being one of the main constituent components of the plant cell wall (HISAJIMA; THORPE, 1985; LÓPEZ *et al*., 2018). Thus, possibly, the SF cultivar used fructose-1,6-diphosphate to maintain a continuous supply of sucrose due to impaired photosynthesis with severe hypoxia (Figure 18). On the other hand, the lower cellobiose in ES certainly contributed to the plants having lower dry mass contents than SF plants (Figure 15a-c). Not only sugars but also their derivatives were affected by the hypoxia level. Glucopyranoside increased in both cultivars under severe hypoxia, but in ES leaves, it reduced under slight hypoxia. Glucopyranoside is one of the fundamental constituents of trehalose, an important regulator of carbohydrate metabolism (LUNN *et al*., 2014). Furthermore, the nucleotide adenosine-5-monophosphate decreased immensely due to severe hypoxia in ES leaves. This metabolite is the main structural supplier for the production of ATP, whose depletion can lead to cell death, since it is necessary for numerous intracellular biochemical reactions, and a signaling factor in the regulation of numerous physiological processes that occur in the extracellular environment (FENG et al., 2015).

Most differential modulations occurred in the roots, the plant organ in direct contact with hypoxia conditions. The most meaningful modulations occurred in SF roots under severe hypoxia, with the sugars and their derivatives being the metabolites that were most affected by

the imposed hypoxia conditions (Figure 25; Apêndice F). The glycolysis was stimulated since some of the intermediates and products of the glycolytic pathway were upregulated. Furthermore, the plants under severe hypoxia showed a similar accumulation of root dry mass to plants under moderate and slight hypoxia conditions, even with significant reductions in gas exchange parameters under severe hypoxia (Figures 15c; 18). The roots have been shortened under severe hypoxia, but new adventitious roots emerged (Figures 14a-c, 15e). This anatomical alteration is well documented and appears to be a typical adaptive response of plants under severe oxygen restriction (TEAKLE *et al*., 2013; KOTULA *et al*., 2015; LOPES *et al*., 2020). Thus, it is possible to assume that, under conditions of limited photosynthesis, the necessary supply of substrate for root development was provided by the glycolytic pathway. The results suggest that starch was the primary source used in the supply of glucose for SF roots, as the observed increase in glucose was accompanied by the rise in maltotriose (Figure 25; Apêndice F), an intermediary in converting starch to glucose. In this case, SF plants would start to use the starch stored in the plastids to compensate for the *A* reduction observed in the cultivar under severe hypoxia. The glucose must have contributed to the observed increase in fructose-1,6-diphosphate in SF plants because the fructose, one of the fructose-1,6-diphosphate precursors, was reduced in the SF roots under severe hypoxia (KRASENSKY; JONAK, 2012; SILVA; FREITAS FILHO; FREITAS, 2018).

Although the stimulation of glycolysis and deceleration of the TCA cycle is the common effect in plants under low oxygen supply (ANTÓNIO *et al*., 2016), the TCA cycle seems not limited in the roots of both rice cultivars under severe hypoxia. On the contrary, the stimulation of the TCA cycle seems evident, considering that several intermediate metabolites of the TCA cycle were positively modulated, such as 2-oxoglutaric and malic acids (Figure 25; Apêndice F). The stimulus of the TCA cycle was even more evident in SF roots by the upregulation of citric acid and some by-products of the cycle, such as lysine and isoleucine (PATEL *et al*., 2020). Isoleucine can be one of the alternative substrates to improve respiratory processes under carbon deficit conditions through the supply of electrons from its catabolic pathway (HILDEBRANDT *et al*., 2015). On the other hand, lysine is a significant growth regulator in plants, whose regulation varies due to stressful conditions (STEPANSKY *et al*., 2006).

Many sugar alcohols lead to an adaptive response capable of overcoming many of the harmful effects of various environmental stresses, working as a carbon source, osmoprotectants, and signalers of stress in plant cells (STEINITZ, 1999; CONDE *et al*., 2014; BHATTACHARYA; KUNDU, 2020). Sugar alcohols were modulated distinctly by severe

hypoxia in roots but with a more remarkable uniqueness in the SF cultivar. Inositol, for example, was upregulated by severe hypoxia only in SF roots, being one of the precursors in the synthesis of glucaric acid, an essential component of antioxidant molecules such as leontopodic acid which acts to protect DNA and is found in *Leontopodium alpinum* Cass. (ISHERWOOD, 1953; SCHWAIGER *et al*., 2005). Furthermore, inositol is important in the synthesis of ascorbic acid, which is a non-enzymatic antioxidant that acts to mitigate the deleterious effects of reactive oxygen species (BAI *et al*., 2013; MEI *et al*., 2015; IQBAL *et al*., 2021). This can certainly be explored in SF plants to mitigate the action of oxidative stress in their roots under low O_2 supply. Another sugar alcohol modulated in roots of both cultivars with severe hypoxia stress was xylitol, which can be converted to xylulose and thus enter the pentose phosphate pathway (ZHAO *et al*. 2020). However, the indication is that xylitol was destined for the synthesis of other sugars, such as lyxose and arabitol, which were also positively regulated in SF roots (Figure 25; Apêndice F) (CHO *et al*., 2007; KOGANTI *et al.*, 2010). While in ES, lyxose was reduced in slight and severe hypoxia environments, and arabitol was not detected in this cultivar at any hypoxia level.

Ornithine, an amino acid participating in the biosynthetic pathways of glutamate and polyamines, was upregulated only in SF roots (HU *et al*., 2014). The ornithine accumulation has been pointed to as a strategy developed by plants to increase tolerance to abiotic stresses. The high content of this non-toxic metabolite can be easily converted into osmoprotective molecules after stress induction (KALAMAKI; MERKOUROPOULOS; KANELLIS, 2009). An example of this is putrescine (Figure 25, Apêndice F), a polyamine just detected under severe hypoxia in both cultivars (CHO et al., 2007). Putrescine has excellent value in relieving abiotic stresses, as it, in addition to being a compatible osmolyte, acts to stimulate the expression of specific genes that regulate the main enzymes involved in glycolysis and the TCA cycle, in addition to reducing loss of water and stimulates the synthesis of fatty acids and amino acids, but it does not always indicate better plant growth and development (KOTAKIS *et al*., 2014; PALMA *et al*., 2015; ZHONG *et al*., 2015; ELBAR; FARAG; SHEHATA, 2019; OLIVEIRA *et al*., 2020).

Glycine was also a modulated metabolite due to severe hypoxia conditions in SF roots, but with similar relative intensity values than ES (Figure 25, Apêndice F). When glycine is protein-associated, forming the proteins rich in glycine can play a regulatory role in plants to different abiotic stresses, especially those that cause osmotic and oxidative stress; however, how this happens has not yet been elucidated (CZOLPINSKA; RUREK, 2018). Another metabolite also regulated like glycine was guanidine, which the apparent effect on stress is unknown.

Nevertheless, it is a metabolite used in nitrogen (N) cycling (MARSDEN *et al*., 2015), being the N an essential macronutrient in the growth of rice plants (SCHMIDT, 2017). It is important to emphasize that some metabolites, such as proline and hydroxyproline, pointed out as possible biomarkers and alleviators of the negative impacts of several abiotic stresses, including hypoxia (KAUR; ASTHIR, 2015; KAVI KISHOR et al., 2015; CAO et al., 2020), did not undergo significant modulations in response to severe hypoxia in the roots of both rice cultivars. Nevertheless, this only denotes that both cultivars use other means and metabolic pathways to modulate response to different oxygenation levels in the environment.

4.5 Conclusion

According to physiological performance, the two cultivars studied could not be fully differentiated in terms of tolerance to severe hypoxia. However, severe hypoxia reduced the growth and development of rice plants, especially of the roots, which was partly due to reductions in photosynthetic pigment contents, gas exchanges (CO_2 assimilation, stomatal conductance, and transpiration rate), carboxylation efficiency, and electron transport rate. Otherwise, the metabolomic analysis showed differences regarding response to hypoxia levels between the two cultivars, but the metabolic adjustment occurred mainly in the roots. There was no clear separation of the metabolic profile between the two cultivars regarding hypoxia levels in leaves, but in roots this was possible. Seventy metabolites were detected in the roots, being 40 were responsive to O_2 changes in the growth medium. The SF cultivar, recommended for flooded cultivation due to its high yield under these conditions, modulates root metabolites linked to glycolysis and the TCA cycle to mitigate such effects. Also, the SF plants seem to convert the starch stored in plastids of root cells into glucose instead of using sucrose transported from the sprout as the initial substrate of the glycolytic pathway. This ensures the continuous supply of the biosynthetic pathway linked to glycolysis and the TCA cycle, and the growth and development maintenance under conditions of low photosynthesis induced by hypoxia severe. Among the severe hypoxia-adjusted metabolites in rice plants, the glucopyranoside, in leaves and roots, and also only roots, the glyceric acid, malic acid, putrescine, xylitol, glycerol-2-phosphate, glucopyranoside, fructose-1,6-diphosphate, cellobiose, galactinol, and maltotriose stand out for their high potential as a biomarker of severe hypoxia in rice plants.

5 CONSIDERAÇÕES FINAIS

Os resultados dos estudos fisiológicos e metabolômicos com as cultivares de arroz São Francisco (SF) e BRS Esmeralda (ES), submetidas a condições de estresse salino e a diferentes níveis de hipóxia, revelaram mecanismos importantes na aclimatação das plantas a essas condições. A salinidade causou consideráveis efeitos prejudiciais ao crescimento e desenvolvimento de ambas as cultivares de arroz. O efeito da salinidade deveu-se principalmente ao acúmulo dos íons Na^+ e Cl^- nas folhas, caules e raízes, afetando a maioria dos parâmetros fisiológicos analisados. A tolerância ao sal da cultivar SF na fase de pré-perfilhamento, observado por outros autores, não se manteve no estágio de perfilhamento, resultado que demonstra que a tolerância diferencial dessas cultivares é variável com o estádio de desenvolvimento das plantas. A análise do metaboloma revelou que, em resposta ao estresse salino, cada cultivar regula seu metabolismo de forma específica, porém ambas modulam positivamente, principalmente, metabólitos como os aminoácidos e derivados, e os ácidos orgânicos nas folhas, e os açúcares e derivados nas raízes. A principal diferença observada foi a evidência de um provável o uso do desvio GABA nas folhas da cultivar SF, como forma de garantir a continuidade do ciclo do ácido tricarboxílico e dos intermediários metabólicos dele derivados, necessários para os ajustes ao ambiente salino.

A hipóxia severa também limitou o crescimento e desenvolvimento de ambas as cultivares de arroz, porém de forma mais branda que sob condições de salinidade, e foi mais evidente nas raízes, o que demonstra a tolerância do arroz às condições de baixa disponibilidade de oxigênio. Em parte, isso deveu-se aos impactos negativos nos parâmetros de trocas gasosas, de fluorescência da clorofila *a* e nos teores de pigmentos fotossintéticos. O perfil metabólico de folhas e raízes foram modulados distintamente em resposta ao nível de hipóxia e/ou a cultivar, sendo que as modulações mais evidentes nos níveis dos metabólitos ocorreram nas raízes da cultivar SF, como resposta a hipóxia severa. Nestas condições, a cultivar SF estimula em suas raízes o ciclo do ácido tricarboxílico como forma de aclimatação às condições de baixa disponibilidade de oxigênio.

Portanto, os resultados deste trabalho apresentam informações importantes sobre os mecanismos de aclimatação das plantas às condições de salinidade e de hipóxia. Também aponta para alguns potenciais marcadores metabólicos à salinidade e hipóxia severa. Glucopiranosídeo, lisina, ornitina, 2-aminoisobutírico, glutamina, arabitol, ácido glicérico e ácido 2-oxoglutárico se destacam por apresentarem alto potencial como biomarcadores do estresse salino, enquanto ácido glicérico, ácido málico, putrescina, xilitol, glicerol-2-fosfato,

glucopiranosídeo, frutose-1,6-difosfato, celobiose, galactinol e maltotriose se destacam como metabólitos de elevado potencial para biomarcadores de hipóxia severa em plantas de arroz.

REFERÊNCIAS

ABDELGAWAD, H.; ZINTA, G.; HAMED, B. A.; SELIM, S.; BEEMSTER, G.; HOZZEIN, W. N.; WADAAN, M. A. M.; ASARD, H.; ABUELSOUD, W. Maize roots and shoots show distinct profiles of oxidative stress and antioxidant defense under heavy metal toxicity. **Environmental Pollution**, v. 258, p. 113705, 2020.

AHMAD, I.; MIAN, A.; MAATHUIS, F. J. M. Overexpression of the rice AKT1 potassium channel affects potassium nutrition and rice drought tolerance. **Journal of Experimental Botany**, v. 67, p. 2689-2698, 2016.

ALENCAR, N. L. M.; OLIVEIRA, A. B. de; ALVAREZ-PIZARRO, J. C.; MARQUES, E. C.; PRISCO, J. T.; GOMES-FILHO, E. Differential responses of dwarf cashew clones to salinity are associated to osmotic adjustment mechanisms and enzymatic antioxidative defense. **Anais da Academia Brasileira de Ciências**, v. 93, p. 1-20, 2021.

ALVAREZ-PIZARRO, J. C.; GOMES-FILHO, E.; DE LACERDA, C. F.; ALENCAR, N. L. M.; PRISCO, J. T. Salt-induced changes on H^+-ATPase activity, sterol and phospholipid content and lipid peroxidation of root plasma membrane from dwarf-cashew (*Anacardium occidentale* L.) seedlings. **Plant Growth Regulation**, v. 59, p. 125-135, 2009.

ALVES, F. A. L.; FERREIRA-SILVA, S. L.; MAIA, J. M.; FREITAS, J. B. S.; SILVEIRA, J. A. G. Regulação do acúmulo de Na+ e resistência à salinidade em (*Vigna unguiculata* (L.) Walp). **Pesquisa Agropecuária Pernambucana**, v. 20, p. 1-10, 2015.

ALVES, P. R.; LUCENA, E. M. P. de; BONILLA, O. H.; MARQUES, E. C.; GOMES-FILHO, E.; COSTA, C. S. B. Solutos orgânicos e inorgânicos em *Salicornia neei* Lag. sob lâminas de irrigação e adubação no semiárido cearense. **Revista Verde de Agroecologia e Desenvolvimento Sustentável**, v. 15, p. 360-367, 2020.

ANTÓNIO, C.; PÄPKE, C.; ROCHA, M; DIAB, H.; LIMAMI, A. M.; OBATA, T.; FERNIE, A. R.; VAN DONGEN, J. T. Regulation of primary metabolism in response to low oxygen availability as revealed by carbon and nitrogen isotope redistribution. **Plant Physiology**, v. 170, p. 43-56, 2015.

ARAÚJO, G. dos S.; PAULA-MARINHO, S. de O.; PINHEIRO, S. K. de P.; MIGUEL, E. de C.; LOPES, L. de S.; MARQUES, E. C.; CARVALHO, H. H. de; GOMES-FILHO, E. H2O2 priming promotes salt tolerance in maize by protecting chloroplasts ultrastructure and primary metabolites modulation. **Plant Science**, v. 303, p. 110774, 2021.

ARAÚJO, W. L.; MARTINS, A. O.; FERNIE, A. R.; TOHGE, T. 2-Oxoglutarate: linking TCA cycle function with amino acid, glucosinolate, flavonoid, alkaloid, and gibberellin biosynthesis. **Frontiers in Plant Science**, v. 5, p. 23-212, 2014.

ARIF, Y.; SINGH, P.; SIDDIQUI, H.; BAJGUZ, A.; HAYAT, S. Salinity induced physiological and biochemical changes in plants: an omic approach towards salt stress tolerance. **Plant Physiology and Biochemistry**, v. 156, p. 64-77, 2020.

ARNDT, S. K.; IRAWAN, A.; SANDERS, G. J. Apoplastic water fraction and rehydration

techniques introduce significant errors in measurements of relative water content and osmotic potential in plant leaves. **Physiology Plantarum**, v. 155, p. 355–368, 2015.

BACHA, R., MOREL, D. A., KNOBLAUCH, R. Competição regional de cultivares e linhagens de arroz irrigado em Santa Catarina, 2000/01. *In*: CONGRESSO BRASILEIRO DE ARROZ IRRIGADO, 2/REUNIÃO DA CULTURA DO ARROZ IRRIGADO, 24., 2001, Porto Alegre. **Anais...** Porto Alegre: Instituto Rio Grandense do Arroz. 2001. p. 29-31.

BAI, T.; MA, P.; LI, C.; YIN, R.; MA, F. Role of ascorbic acid in enhancing hypoxia tolerance in roots of sensitive and tolerant apple rootstocks. **Scientia Horticulturae**, v. 164, p. 372-379, 2013.

BANFALVI, G. Prebiotic pathway from ribose to RNA formation. International **Journal of Molecular Sciences**, v. 22, p. 3857, 2021.

BARBOSA, M. R.; SILVA, M. M. A.; WILLADINO, L.; ULISSES, C.; CAMARA, T. R. Geração e desintoxicação enzimática de espécies reativas de oxigênio em plantas. **Ciência Rural**, v. 44, p. 453-460, 2014.

BARKER, A. V.; PILBEAM, D. J. (Ed.). **Handbook of plant nutrition**. 2. ed. Boca Raton: CRC press, 2015.

BARNES, J. D.; BALAGUER, L.; MANRIQUE, E.; ELVIRA, S.; DAVISON, A. W. A reappraisal of the use of DMSO for the extraction and determination of chlorophylls a and b in lichens and higher plants. **Environmental and Experimental Botany**, v. 32, p. 85–100, 1992.

BARR, H. D.; WEATHERLEY, P. E. A Re-Examination of the Relative Turgidity Technique for Estimating Water Deficits in Leaves. **Australian Journal of Biological Sciences**, v. 15, p. 413, 1962.

BARRETT-LENNARD, E.G. The interaction between waterlogging and salinity in higher plants: causes, consequences and implications. **Plant and Soil**, v. 253, p. 35-54, 2003.

BARROS, L. C. G.; UCHÓA, B. F.; SANTOS, A. L. C. dos. **São Francisco, nova cultivar de arroz irrigado para o Sub-médio e Baixo São Francisco.** Aracajú: Embrapa Tabuleiros Costeiros, 2000. 12 p.

BATOOL, N.; SHAHZAD, A.; ILYAS, N. Responses of Spinach to Salinity and Nutrient Deficiency in Growth, Physiology, and Nutritional Value. **International Journal of Agriculture and Crop Sciences**, v. 7, p.1439-1446, 2014.

BHATTACHARYA, S.; KUNDU, A. Sugars and sugar polyols in overcoming environmental stresses. **Protective Chemical Agents in The Amelioration of Plant Abiotic Stress**, p. 71-101, 2020.

BRAGA, F. T. **Resposta do vegetal ao estresse**. 2015. Paulo Afonso – BA, 2012. Slides. Disponível em: https://pt.slideshare.net/mfdaiane/resposta-do-vegetal-ao-estresse. Acesso em: 24 fev. 2020.

BRAZILIAN RICE. **Perfil da Produção.** Disponível em: http://brazilianrice.com.br/br/sobre-o-brasil/. Acesso em: 25 mar. 2019.

BREDEMEIER, C.; MUNDSTOCK, C. M. Regulação da absorção e assimilação do nitrogênio nas plantas. **Ciência Rural**, v. 30, p. 365-372, 2000.

BUCHANAN, B. B.; GRUISSEM, W.; JONES, R. L. **Biochemistry and Molecular Biology of Plants.** 2. ed. Berkeley:Wiley, 2015.

CAMARGO, I. A. **Sistema antioxidante de cana-de-açúcar em resposta à seca**. 2013. 85f. Dissertação (Mestrado em ciências) - Centro de Energia Nuclear na Agricultura, Universidade de São Paulo, Piracicaba, 2013.

CAMPOSTRINI, E. **Fluorescência da clorofila a: considerações teóricas e aplicações práticas**. Disponível em: http://www.uenf.br/Uenf/Downloads/CENTRO_CCTA_1629_1112121492.pdf. Acesso em: 14 mai. 2020.

CANTRELL, R. The Rice genome - The cereal of the world's poor takes center stage. **Science**, v. 296, p. 53, 2002.

CAO, X.; WU, L.; WU, M.; ZHU, C.; JIN, Q.; ZHANG, J. Abscisic acid mediated proline biosynthesis and antioxidant ability in roots of two different rice genotypes under hypoxic stress. **BMC Plant Biology**, v. 20, p. 1-14, 2020.

CASTILLO-CAMPOHERMOSO, M. A.; BROETTO, F.; RODRÍGUEZ-HERNÁNDEZ, A. M.; SORIANO-MELGAR, L. de A. A.; MOUNZER, O.; SÁNCHEZ-BLANCO, M. J. Plant-available water, stem diameter variations, chlorophyll fluorescence, and ion content in Pistacia lentiscus under salinity stress. **Revista Terra Latinoamericana**, v. 38, p. 103, 2020.

CASTRO, A. P. de; MORAIS, O. P. de; BRESEGHELLO, F.; LOBO, V. L. da S.; GUIMARÃES, C. M.; BASSINELLO, P. Z.; COLOMBARI FILHO, J. M.; SANTIAGO, C. M.; FURTINI, I. V.; TORGA, P. P.; UTUMI, M. M.; PEREIRA, J. A.; CORDEIRO, A. C. C.; AZEVEDO, R. de; SOUSA, N. R. G.; SOARES, A. A.; RADMANN, V.; PETERS, V. J. **BRS Esmeralda: cultivar de arroz de terras altas com elevada produtividade e maior tolerância à seca.** Santo Antônio de Goiás: Embrapa Arroz e Feijão, 2014. 4 p.

CASTRO-DUQUE, N. E.; CHÁVEZ-ARIAS, C. C.; RESTREPO-DÍAZ, H. Foliar glycine betaine or hydrogen peroxide sprays ameliorate waterlogging stress in cape gooseberry. **Plants**, v. 9, p. 644, 2020.

CHANG, J.; CHEONG, B. E.; NATERA, S.; ROESSNER, U. Morphological and metabolic responses to salt stress of rice (*Oryza sativa* L.) cultivars which differ in salinity tolerance. **Plant Physiology and Biochemistry**, v. 144, p. 427-435, 2019.

CHEN, D.; SHAO, Q.; YIN, L.; YOUNIS, A.; ZHENG, B. Polyamine function in plants: metabolism, regulation on development, and roles in abiotic stress responses. **Frontiers in Plant Science**, v. 9, p. 1-13, 2019.

CHEN, Z.; POTTOSIN, I. I.; CUIN, T. A.; FUGLSANG, A. T.; TESTER, M.; JHA, D.;

ZEPEDA-JAZO, I.; ZHOU, M.; PALMGREN, M. G.; NEWMAN, I. A. Root plasma membrane transporters controlling K^+/Na^+ homeostasis in salt-stressed barley. **Plant Physiology**, v. 145, p. 1714-1725, 2007.

CHE-OTHMAN, M. H.; JACOBY, R. P.; MILLAR, A. H.; TAYLOR, N. L. Wheat mitochondrial respiration shifts from the tricarboxylic acid cycle to the GABA shunt under salt stress. **New Phytologist**, v. 225, p. 1166-1180, 2019.

CHO, E. A.; LEE, D. W.; CHA, Y. H.; LEE, S. J.; JUNG, H. C.; PAN, J. G.; PYUN, Y. R. Characterization of a novel D-lyxose isomerase from *Cohnella laevoribosii* RI-39 sp. nov. **Journal of Bacteriology**, v. 189, p. 1655-1663, 2007.

CLARK, R. B. Characterization of phosphatase of intact maize roots. **Journal of Agricultural and Food Chemistry**, v. 23, n. 3, p. 458-460, 1975.

COLLADO, M. B.; AULICINO, M. B.; ARTURI, M. J.; MOLINA, M. del C. Generational mean analysis of salt tolerance during osmotic phase in maize seedling. **American Journal of Plant Sciences**, v. 10, p. 555-571, 2019.

COLMER, T. D. Aerenchyma and an inducible barrier to radial oxygen loss facilitate root aeration in upland, paddy and deep-water rice (*Oryza sativa* L.). **Annals of Botany**, v. 91, p. 301-309, 2003.

COLMER, T. D.; GREENWAY, H. Ion transport in seminal and adventitious roots of cereals during O2 deficiency. **Journal of Experimental Botany**, v. 62, p. 39-57, 2011.

COLMER, T. D.; MUNNS, R.; FLOWERS, T. J. Improving salt tolerance of wheat and barley: future prospects. **Australian Journal of Experimental Agriculture**, v. 45, p. 1425, 2005.

CONAB - COMPANHIA NACIONAL DE ABASTECIMENTO. **Acompanhamento da Safra Brasileira de Grãos**, Brasília - DF, v. 8, safra 2020/21, n. 7, sétimo levantamento, abr. 2021.

CONDE, A.; REGALADO, A.; RODRIGUES, D.; COSTA, J. M.; BLUMWALD, E.; CHAVES, M. M.; GERÓS, H. Polyols in grape berry: transport and metabolic adjustments as a physiological strategy for water-deficit stress tolerance in grapevine. **Journal of Experimental Botany**, v. 66, p. 889-906, 2014.

COVA, A. M. W. **Respostas fisiológicas e bioquímicas do noni (*Morinda citrifolia* L.) ao estresse salino**. 2016. 104f. Tese (Doutorado em engenharia agrícola) - centro de Ciências Agrárias Ambientais e Biológicas, Universidade Federal do Recôncavo da Bahia, Cruz das Almas, 2016.

CZOLPINSKA, M.; RUREK, M. Plant glycine-rich proteins in stress response: an emerging, still prospective story. **Frontiers in Plant Science**, v. 9, p. 1-20, 2018.

DECHEN, A. R.; NACHTIGALL, G. R. Elementos essenciais e benéficos às plantas superiores. In: FERNANDES, M. S.; SOUZA, S. R. de; SANTOS, L. A. **Nutrição Mineral de Plantas**. 2. ed. Viçosa: SBCS, 2018. Cap. 1. p. 1-20.

DEPARTMENT OF PRIMARY INDUSTRIES AND REGIONAL DEVELOPMENT - DPIRD. **Dryland salinity in Western Australia.** Disponível em: https://www.agric.wa.gov.au/soil-salinity/dryland-salinity-western-australia-0. Acesso em: 08 ago. 2019.

DIAS, A. S.; LIMA, G. S.; GHEYI, H. R.; NOBRE, R. G.; FERNANDES, P. D.; SILVA F. A. Trocas gasosas e eficiência fotoquímica do gergelim sob estresse salino e adubação com nitrato-amônio. **Irriga**, v. 23, p. 220-234, 2018.

DUHAN, S.; KUMARI, A.; BALA, S.; SHARMA, N.; SHEOKAND, S. Effects of waterlogging, salinity and their combination on stress indices and yield attributes in pigeonpea (*Cajanus cajan* L. Mill sp.) genotypes. **Indian Journal of Plant Physiology**, v. 23, p. 65-76, 2018.

DUTRA, C. C.; PRADO, E. A. F. do; PAIM, L. R.; SCALON, S. de P. Q. Desenvolvimento de plantas de Desenvolvimento de plantas de girassol sob diferentes condições de fornecimento de água. **Semina**: **Ciências Agrárias**, v. 33, p.2657-2668, 2012.

EBEED, H. T.; HASSAN, N. M.; ALJARANI, A. M. Exogenous applications of polyamines modulate drought responses in wheat through osmolytes accumulation, increasing free polyamine levels and regulation of polyamine biosynthetic genes. **Plant Physiology and Biochemistry**, v. 118, p. 438-448, 2017.

ELBAR, O. H. A.; FARAG, R. E.; SHEHATA, S. A. Effect of putrescine application on some growth, biochemical and anatomical characteristics of *Thymus vulgaris* L. under drought stress. **Annals of Agricultural Sciences**, v. 64, p. 129-137, 2019.

EL-SHABRAWI, H.; KUMAR, B.; KAUL, T.; REDDY, M. K.; SILNGLA-PAREEK, S. L.; SOPORY, S. K. Redox homeostasis, antioxidant defense, and methylglyoxal detoxification as markers for salt tolerance in Pokkali rice. **Protoplasma**, v. 245, p.85-96, 2010.

EMBRAPA (Ed.). **São Francisco**: Cultivar de arroz irrigado de alta produtividade para o Médio e Baixo São Franciso. Aracajú: Embrapa, 1996. 1 Folder.

EMBRAPA ARROZ E FEIJÃO (ed.). **Catálogo de cultivares de arroz**. Santo Antônio de Goiás: Embrapa Arroz e Feijão, 2013. 11 p.

EMBRAPA. **Arroz - BRS Primavera.** [20--]. Disponível em: https://www.embrapa.br/busca-de-solucoes-tecnologicas/-/produto-servico/161/arroz---brs-primavera. Acesso em: 29 abr. 2019.

ENGELAAR, W. M. H. G.; MATSUMARU, T.; YONEYAMA, T. Combined effects of soil waterlogging and compaction on rice (*Oryza sativa* L.) growth, soil aeration, soil N transformations and ^{15}N discrimination. **Biology and Fertility of Soils**, v. 32, p. 484-493, 2000.

ERB, M.; KLIEBENSTEIN, D. J. Plant secondary metabolites as defenses, regulators, and primary metabolites: the blurred functional trichotomy. **Plant Physiology**, v. 184, p. 39-52, 2020.

ESTEVES, B. dos S.; SUZUKI, M. S. Efeito da salinidade sobre as plantas. **Oecologia Australis**, v. 12, p. 662-679, 2008.

EVERT, R. F. Anatomia das plantas de Esau: meristemas, células e tecidos do corpo da planta: sua estrutura, função e desenvolvimento. São Paulo: Blucher, 2013. p. 728.

FALAKBOLAND, Z.; ZHOU, M.; ZENG, F.; KIANI-POUYA, A.; SHABALA, L.; SHABALA, S. Plant ionic relation and whole-plant physiological responses to waterlogging, salinity and their combination in barley. **Functional Plant Biology**, v. 44, p. 941, 2017.

FAO. **Status of the World's Soil Resources**: main report. Rome: FAO, 2015. 650 p.

FAO. **The state of the world's land and water resources for food and agriculture (SOLAW) – Managing systems at risk**. London: Earthscan/fao, 2011. 308 p.

FENG, H.; GUAN, D.; BAI, J.; SUN, K.; JIA, L. Extracellular ATP: a potential regulator of plant cell death. **Molecular Plant Pathology**, v. 16, p. 633-639, 2015.

FERREIRA, I. Q.; RODRIGUES, M. Â.; MOUTINHO-PEREIRA, J. M.; CORREIA, C. M.; ARROBAS, M. Olive tree response to applied phosphorus in field and pot experiments. **Scientia Horticulturae**, v. 234, p. 236-244, 2018.

FONSECA, J. R. *et al.* **Descritores Botânicos, Agronômicos e Fenológicos do Arroz (*Oryza sativa* L.).** 1. ed. Santo Antônio de Goiás: Embrapa Arroz e Feijão, 2008.

FREITAS, P. A. F. de; CARVALHO, H. H. de; COSTA, J. H.; MIRANDA, R. de S.; SARAIVA, K. D. da C.; OLIVEIRA, F. D. B. de; COELHO, D. G.; PRISCO, J. T.; GOMES-FILHO, E. Salt acclimation in sorghum plants by exogenous proline: physiological and biochemical changes and regulation of proline metabolism. **Plant Cell Reports**, v. 38, p. 403-416, 2019.

GADELHA, C. G. **Bases bioquímicas e moleculares para tolerância ao estresse salino em cultivares de arroz**. 2020. 129f. Tese (Doutorado em Bioquímica) - Universidade Federal do Ceará, Fortaleza, 2020.

GAINES, T. P.; PARKER, M. B.; GASCHO, G. J. Automated determination of chlorides in soil and plant tissue by sodium nitrate extraction. **Agronomy Journal**, v. 76, p. 371-374, 1984.

GUO, R.; SHI, L.; YAN, C.; ZHONG, X.; GU, F.; LIU, Q.; XIA, X.; LI, H. Ionomic and metabolic responses to neutral salt or alkaline salt stresses in maize (*Zea mays* L.) seedlings. **BMC Plant Biology**, v. 17, p. 1-13, 2017.

HANAFIAH, N. M.; MISPAN, M. S.; LIM, P. E.; BAISAKH, N.; CHENG, A. The 21st century agriculture: when rice research draws attention to climate variability and how weedy rice and underutilized grains come in handy. **Plants**, v. 9, p. 365, 2020.

HARRIS, M. J.; DUGGER, W. M. The occurrence of abscisic acid and abscisyl-β-d-glucopyranoside in developing and mature citrus fruit as determined by enzyme

immunoassay. **Plant Physiology**, v. 82, p. 339-345, 1986.

HASANUZZAMAN, M.; BANERJEE, A.; BHUYAN, M. H. M. B.; ROYCHOUDHURY, A.; MAHMUD, J. Al.; FUJITA, M. Targeting glycinebetaine for abiotic stress tolerance in crop plants: physiological mechanism, molecular interaction and signaling. **Phyton**, v. 88, p. 185-221, 2019.

HEINEMANN, A. B.; PINHEIRO, B. S. **Características morfológicas.** Disponível em: http://www.agencia.cnptia.embrapa.br/gestor/arroz/arvore/CONT000fe75wint02wx5eo07qw4xeclygdut.html. Acesso em: 24 mar. 2019.

HENRIQUE, P. de C.; ALVES, J. D.; GOULART, P. de F. P.; DEUNER, S.; SILVEIRA, N. M.; ZANANDREA, I.; CASTRO, E. M. Características fisiológicas e anatômicas de plantas de sibipiruna submetidas à hipoxia. **Ciência Rural**, v. 40, p.70-76, 2009.

HILDEBRANDT, T. M.; NESI, A. N.; ARAÚJO, W. L.; BRAUN, H.-P. Amino acid catabolism in plants. **Molecular Plant**, v. 8, p. 1563-1579, 2015.

HISAJIMA, S.; THORPE, T. A. Carbohydrate utilization and activities of various glycosidases in cultured japanese morning-glory callus. **Plant tissue culture Letters**, v. 2, p. 14-21, 1985.

HOLZSCHUH, M. J.; BOHNEN, H.; ANGHINONI, I. Avaliação da porosidade e placa férrica de raízes de arroz cultivado em hipoxia. **Revista Brasileira de Ciência do Solo**, v. 34, p. 1763-1769, 2010.

HU, X.; KANG, J.; LU, K.; ZHOU, R.; MU, L.; ZHOU, Q. Graphene oxide amplifies the phytotoxicity of arsenic in wheat. **Scientific Reports**, v. 4, p. 1-10, 2014.

HUANG, J.; LEVINE, A.; WANG, Z. Plant Abiotic Stress. **The scientific world journal**, v. 2013, p.1-2, 2013.

HUMA, B.; KUNDU, S.; POOLMAN, M. G.; KRUGER, N. J.; FELL, D. A. Stoichiometric analysis of the energetics and metabolic impact of photorespiration in C3 plants. **The Plant Journal**, v. 96, p. 1228-1241, 2018.

IGAMBERDIEV, A. U.; HILL, R. D. Plant mitochondrial function during anaerobiosis. **Annals of Botany**, v. 103, p.259-268, 2008.

IGAMBERDIEV, A. U.; ROUSSEL, M. R. Feedforward non-Michaelis–Menten mechanism for CO_2 uptake by Rubisco: contribution of carbonic anhydrases and photorespiration to optimization of photosynthetic carbon assimilation. **Biosystems**, v. 107, p. 158-166, 2012.

IQBAL, Z.; SARKHOSH, A.; BALAL, R. M.; GÓMEZ, C.; ZUBAIR, M.; ILYAS, N.; KHAN, N.; SHAHID, M. A. Silicon alleviate hypoxia stress by improving enzymatic and non-enzymatic antioxidants and regulating nutrient uptake in muscadine grape (*Muscadinia rotundifolia* Michx.). **Frontiers in Plant Science**, v. 11, p. 2288, 2021.

ISAYENKOV, S. V.; MAATHUIS, F. J. M. Plant Salinity Stress: Many Unanswered Questions Remain. **Frontiers in Plant Science**, v. 10, p.1-11, 2019.

ISHERWOOD, F. A. Synthesis of L–ascorbic acid in plants and animals. **Proceedings of The Nutrition Society**, v. 12, p. 335-339, 1953.

JEONG, S. J.; LEE, H. B.; AN, S. K.; KIM, K. S. High temperature stress prior to induction phase delays flowering initiation and inflorescence development in Phalaenopsis queen beer 'Mantefon'. **Scientia Horticulturae**, v. 263, p. 109092, 2020.

JIMÉNEZ-ARIAS, D.; GARCÍA-MACHADO, F. J.; MORALES-SIERRA, S.; LUIS, J. C.; SUAREZ, E.; HERNÁNDEZ, M.; VALDÉS, F.; BORGES, A. A. Lettuce plants treated with L-pyroglutamic acid increase yield under water deficit stress. **Environmental and Experimental Botany**, v. 158, p. 215-222, 2019.

JORGE, T. F.; DURO, N.; COSTA, M. da; FLORIAN, A.; RAMALHO, J. C.; RIBEIRO-BARROS, A. I.; FERNIE, A. R.; ANTÓNIO, C. GC-TOF-MS analysis reveals salt stress-responsive primary metabolites in *Casuarina glauca* tissues. **Metabolomics**, v. 13, p. 1-13, 2017.

JOUYBAN, Z. The effects of salt stress on plant growth. **Technical Journal of Engineering and Applied Science**s, v. 2, p. 7-10, 2012.

KALAMAKI, M. S.; MERKOUROPOULOS, G.; KANELLIS, A. K. Can ornithine accumulation modulate abiotic stress tolerance in Arabidopsis? **Plant Signaling & Behavior**, v. 4, p. 1099-1101, 2009.

KARTIKA, K.; SAKAGAMI, J.; LAKITAN, B.; YABUTA, S.; WIJAYA, A.; KADIR, S.; WIDURI, L. I.; SIAGA, E.; NAKAO, Y. Morpho-physiological response of *Oryza glaberrima* to gradual soil drying. **Rice Science**, v. 27, p. 67-74, 2020.

KAUR, G.; ASTHIR, B. Proline: a key player in plant abiotic stress tolerance. **Biologia Plantarum**, v. 59, p. 609-619, 2015.

KAVI KISHOR, P. B.; HIMA KUMARI, P.; SUNITA, M. S. L.; SREENIVASULU, N. Role of proline in cell wall synthesis and plant development and its implications in plant ontogeny. **Frontiers in Plant Science**, v. 6, p. 1-2, 2015.

KEUNEN, E.; PESHEV, D.; VANGRONSVELD, J.; ENDE, W. V. D.; CUYPERS, A. Plant sugars are crucial players in the oxidative challenge during abiotic stress: extending the traditional concept. **Plant, Cell & Environment**, v. 36, p. 1242-1255, 2013.

KHAN, M. S.; KANWAL, B.; NAZIR, S. Metabolic engineering of the chloroplast genome reveals that the yeast ArDH gene confers enhanced tolerance to salinity and drought in plants. **Frontiers in Plant Science**, v. 6, p. 725, 2015.

KHUNPON, B.; CHA-UM, S.; FAIYUE, B.; UTHAIBUTRA, J.; SAENGNIL, K. Influence of paclobutrazol on growth performance, photosynthetic pigments, and antioxidant efficiency of Pathumthani 1 rice seedlings grown under salt stress. **Science Asia**, v. 43, p. 70, 2017.

KINNERSLEY, A. M.; TURANO, F. J. Gamma Aminobutyric Acid (GABA) and plant responses to stress. **Critical Reviews in Plant Sciences**, v. 19, p. 479-509, 2010.

KOGANTI, S.; KUO, T. M.; KURTZMAN, C. P.; SMITH, N.; JU, L.-K. Production of arabitol from glycerol: strain screening and study of factors affecting production yield. **Applied Microbiology and Biotechnology**, v. 90, p. 257-267, 2010.

KOTAKIS, C.; THEODOROPOULOU, E.; TASSIS, K.; OUSTAMANOLAKIS, C.; IOANNIDIS, N. E.; KOTZABASIS, K. Putrescine, a fast-acting switch for tolerance against osmotic stress. **Journal of Plant Physiology**, v. 171, p. 48-51, 2014.

KOTULA, L.; CLODE, P. L.; STRIKER, G. G.; PEDERSEN, O.; LÄUCHLI, A.; SHABALA, S.; COLMER, T. D. Oxygen deficiency and salinity affect cell-specific ion concentrations in adventitious roots of barley (*Hordeum vulgare*). **New Phytologist**, v. 208, p. 1114-1125, 2015.

KOTULA, L.; RANATHUNGE, K.; SCHREIBER, L.; STEUDLE, E. Functional and chemical comparison of apoplastic barriers to radial oxygen loss in roots of rice (*Oryza sativa* L.) grown in aerated or deoxygenated solution. **Journal of Experimental Botany**, v. 60, p. 2155-2167, 2009.

KRASENSKY, J.; JONAK, C. Drought, salt, and temperature stress-induced metabolic rearrangements and regulatory networks. **Journal of Experimental Botany**, v. 63, p. 1593-1608, 2012.

KUMAR, V.; KHARE, T. Differential growth and yield responses of salt-tolerant and susceptible rice cultivars to individual (Na^+ and Cl^-) and additive stress effects of NaCl. **Acta Physiologiae Plantarum**, v. 38, p. 86-94, 2016.

KUMAR, V.; KHARE, T. Individual and additive effects of Na^+ and Cl^- ions on rice under salinity stress. **Archives of Agronomy and Soil Science**, v. 61, p. 381-395, 2014.

KUREPIN, L. V.; IVANOV, A. G.; ZAMAN, M.; PHARIS, R. P.; HURRY, V.; HÜNER, N. P. A. Interaction of glycine betaine and plant hormones: protection of the photosynthetic apparatus during abiotic stress. **Photosynthesis**: structures, mechanisms, and applications, p. 185-202, 2017.

KUSVURAN, S.; KIRAN, S.; ELLIALTIOGLU, S. S. Antioxidant enzyme activities and abiotic stress tolerance relationship in vegetable crops. In: INTECH (ed.). **Antioxidant enzyme activities and abiotic stress tolerance relationship in vegetable crops.** Croatia: Intech, 2016. p. 481-503.

LAMBERS, H.; CHAPIN III, F. S.; PONS, T. L. **Plant Physiological Ecology**. 2 ed. New York: Springer, 2008.

LAMERS, J.; MEER, T. van D.; TESTERINK, C. How plants sense and respond to stressful environments. **Plant Physiology**, v. 182, p. 1624-1635, 2020.

LÄUCHLI, A.; GRATTAN, S. R. Plant Abiotic Stress: Salt. **Encyclopedia of Agriculture and Food Systems**, v. 4, p. 313–329, 2014.

LEMES, E. S.; OLIVEIRA, S. de; NEVES, E. H. das; RITTER, R.; MENDONÇA, A. O. de;

MENEGHELLO, G. E. Crescimento inicial e acúmulo de sódio em plantas de arroz submetidas à salinidade. **Revista de Ciências Agrárias - Amazonian Journal of Agricultural and Environmental Sciences**, v. 61, p. 1-9, 2018.

LEMOS NETO, H. de S.; GUIMARÃES, M. de A.; MESQUITA, R. O.; FREITAS, W. E. S.; OLIVEIRA, A. B. de; DIAS, N. da S.; GOMES-FILHO, E. Silicon supplementation induces physiological and biochemical changes that assist lettuce salinity tolerance. **Silicon**, p. 1-15, 2020.

LI, D.; WANG, M.; ZHANG, T.; CHEN, X.; LI, C.; LIU, Y.; BRESTIC, M.; CHEN, Tony H. H.; YANG, X. Glycinebetaine mitigated the photoinhibition of photosystem II at high temperature in transgenic tomato plants. **Photosynthesis Research**, v. 147, p. 301-315, 2021.

LI, P.-C.; YANG, X.-Y.; WANG, H.-M.; PAN, T.; YANG, J.-Y.; WANG, Y.-Y.; XU, Y.; YANG, Z.-F.; XU, C.-W. Metabolic responses to combined water deficit and salt stress in maize primary roots. **Journal of Integrative Agriculture**, v. 20, p. 109-119, 2021.

LI, Y.; WANG, X.; ZENG, Y.; LIU, P. Metabolic profiling reveals local and systemic responses of kiwifruit to *Pseudomonas syringae* pv. actinidiae. **Plant Direct**, v. 4, p. e00297, 2020.

LISEC, J.; SCHAUER, N.; KOPKA, J.; WILLMITZER, L.; FERNIE, A. R. Gas chromatography mass spectrometry-based metabolite profiling in plants. **Nature Protocols**, v. 1, p. 387-396, 2006.

LLANES, A.; ANDRADE, A.; ALEMANO, S.; LUNA, V. Metabolomic approach to understand plant adaptations to water and salt stress. **Plant Metabolites and Regulation Under Environmental Stress**, p. 133-144, 2018.

LOBO, M. G.; HOUNSOME, N.; HOUNSOME, B. Biochemistry of Vegetables. **Handbook of Vegetables and Vegetable Processing**, p. 47-82, 2018.

LOPES, L. de S.; CARVALHO, H. H. de; MIRANDA, R. de S.; GALLÃO, M. I.; GOMES-FILHO, E. The influence of dissolved oxygen around rice roots on salt tolerance during pre-tillering and tillering phases. **Environmental and Experimental Botany**, v. 178, p. 104169, 2020.

LÓPEZ, S. C.; PENG, M.; ISSAK, T. Y.; DALY, P.; VRIES, R. P. de; MÄKELÄ, M. R. Induction of genes encoding plant cell wall-degrading carbohydrate-active enzymes by lignocellulose-derived monosaccharides and cellobiose in the white-rot fungus *Dichomitus squalens*. **Applied and Environmental Microbiology**, v. 84, p. 1-26, 2018.

LORETI, E.; PERATA, P. The Many Facets of Hypoxia in Plants. **Plants**, v. 9, p. 745, 2020.

LOUREIRO, R. R.; REIS, R. P.; MARROIG, R. G. Effect of the commercial extract of the brown alga *Ascophyllum nodosum* Mont. on *Kappaphycus alvarezii* (Doty) Doty ex P.C. Silva in situ submitted to lethal temperatures. **Journal of Applied Phycology**, v. 26, p. 629-634, 2013.

LÜ, G.; LIANG, Y.; WU, X.; LI, J.; MA, W.; ZHANG, Y.; GAO, H. Molecular cloning and functional characterization of mitochondrial malate dehydrogenase (mMDH) is involved in exogenous GABA increasing root hypoxia tolerance in muskmelon plants. **Scientia Horticulturae**, v. 258, p. 108741, 2019.

LUNN, J. E.; DELORGE, I.; FIGUEROA, C. M.; VAN DIJCK, P.; STITT, M. Trehalose metabolism in plants. **The Plant Journal**, v. 79, p. 544-567, 2014.

MACHADO, E. C.; SCHMIDT, P. T.; MEDINA, C. L.; RIBEIRO, R. V. Respostas da fotossíntese de três espécies de citros a fatores ambientais. **Pesquisa Agropecuária Brasileira**, v. 40, p. 1161-1170, 2005.

MAGALHAES JUNIOR, ARIANO MARTINS DE; GOMES, ALGENOR DA SILVA; SANTOS, ALBERTO BAÊTA DOS (ed.). **Sistema de Cultivo de Arroz Irrigado no Brasil**. Pelotas: Embrapa Clima Temperado, 2004. 270 p.

MALAVOLTA, E.; VITTI, G. C.; OLIVEIRA, S. A. **Avaliação do estado nutricional de plantas**. Piracicaba: POTAFOS, 1989.

MALHOTRA, H.; VANDANA; SHARMA, S.; PANDEY, R. Phosphorus nutrition: plant growth in response to deficiency and excess. **Plant Nutrients and Abiotic Stress Tolerance**, p. 171-190, 2018.

MARIANI, L.; FERRANTE, A. Agronomic management for enhancing plant tolerance to abiotic stresses - drought, salinity, hypoxia, and lodging. **Horticulturae**, v. 3, p. 52, 2017.

MARSDEN, K. A.; SCOWEN, M.; HILL, P. W.; JONES, D. L.; CHADWICK, D. R. Plant acquisition and metabolism of the synthetic nitrification inhibitor dicyandiamide and naturally-occurring guanidine from agricultural soils. **Plant and Soil**, v. 395, p. 201-214, 2015.

MEI, L.; DAUD, M. K.; ULLAH, N.; ALI, S.; KHAN, M.; MALIK, Z.; ZHU, S. J. Pretreatment with salicylic acid and ascorbic acid significantly mitigate oxidative stress induced by copper in cotton genotypes. **Environmental Science and Pollution Research**, v. 22, p. 9922-9931, 2015.

MELLO, M. O. de. **Utilização das fontes de carbono sacarose, galactose, sorbitol e glicerol por células in vitro de plantas**. 1998. 126f. Dissertação (Mestrado em Fisiologia e Bioquímica de Plantas) - Escola Superior de Agricultura Luiz de Queiroz, Universidade de São Paulo, Piracicaba, 1998.

MIRANDA, R. S.; GOMES-FILHO, E.; PRISCO, J. T.; ALVAREZ-PIZARRO, J. C. Ammonium improves tolerance to salinity stress in *Sorghum bicolor* plants. **Plant Growth Regulation**, v. 78, p. 121-131, 2015.

MIRANDA, R.S.; ALVAREZ-PIZARRO, J. C.; COSTA, J. H.; PAULA, S.O.; PRISCO, J. T.; GOMES-FILHO, E. Putative role of glutamine in the activation of CBL/CIPK signalling pathways during salt stress in sorghum. **Plant Signaling & Behavior**, v. 12, p. e1361075, 2017.

MITTLER, R. Oxidative stress, antioxidants and stress tolerance. **Trends in Plant Science**, v. 7, p. 405-410, 2002.

MORAES, J. F. Efeitos da inundação do solo. I. Influência sobre o pH, o potencial de óxido-redução e a disponibilidade do fósforo no solo. **Pesquisa Agropecuária Brasileira,** v.8, p. 53-101, 1973.

MUNNS, R.; GILLIHAM, M. Salinity tolerance of crops – what is the cost? **New Phytologist**, v. 208, p. 668-673, 2015.

MUNNS, R.; TESTER, M. Mechanisms of salinity tolerance. **Annual Review of Plant Biology**, v. 59, p.651-681, 2008.

NAM, M.; BANG, E.; KWON, T.; KIM, Y.; KIM, E.; CHO, K.; PARK, W.; KIM, B.-G.; YOON, I. Metabolite profiling of diverse rice germplasm and identification of conserved metabolic markers of rice roots in response to long-term mild salinity stress. **International Journal of Molecular Sciences**, v. 16, p. 21959-21974, 2015.

NEGRÃO, S.; SCHMÖCKEL, S. M.; TESTER, M. Evaluating physiological responses of plants to salinity stress. **Annals of Botany**, v. 119, p. 1-11, 2016.

NEILL, S.; BARROS, R.; BRIGHT, J.; DESIKAN, R.; HANCOCK, J.; HARRISON, J.; MORRIS, P.; RIBEIEO, D.; WILSON, I. Nitric oxide, stomatal closure, and abiotic stress. **Journal of Experimental Botany**, v. 59, p.165-176, 2008.

NIELSEN, T; RUNG, J; VILLADSEN, D. Fructose-2,6-bisphosphate: a traffic signal in plant metabolism. **Trends in Plant Science**, v. 9, p. 556-563, 2004.

NISHIZAWA, A.; YABUTA, Y.; SHIGEOKA, S. Galactinol and raffinose constitute a novel function to protect plants from oxidative damage. **Plant Physiology**, v. 147, p.1251-1263, 2008.

NUNES JUNIOR, F. H.; GONDIM, F. A.; FREITAS, V. S.; BRAGA, B. B.; BRITO, P. O. B.; MARTINS, K. Crescimento foliar e atividades das enzimas antioxidativas em plântulas de girassol suplementadas com percolado de aterro sanitário e submetidas a estresse hídrico. **Ambiente e Água - An Interdisciplinary Journal of Applied Science**, v. 12, p.71-86, 2017.

NUNES, J. L. S. **Histórico.** 2016. Disponível em: https://www.agrolink.com.br/culturas/arroz/informacoes/historico_361591.html. Acesso em: 25 mar. 2019.

NXELE, X.; KLEIN, A.; NDIMBA, B. K. Drought and salinity stress alters ROS accumulation, water retention, and osmolyte content in sorghum plants. **South African Journal of Botany**, v. 108, p. 261-266, 2017.

OBATA, T.; FERNIE, A. R. The use of metabolomics to dissect plant responses to abiotic stresses. **Cellular and Molecular Life Sciences**, v. 69p.3225-3243, 2012.

OLIVEIRA, D. F.; LOPES, L. S.; GOMES-FILHO, E. Metabolic changes associated with

differential salt tolerance in sorghum genotypes. **Planta**, v. 252, n. 3, p. 1-18, 2020.

OLIVEIRA, L. E. M. de. **Metabolismo anaeróbico.** Disponível em: http://www.ledson.ufla.br/respiracao_plantas/respiracao-anaerobica/. Acesso em: 23 fev. 2020.

OLIVEIRA, W. J. de; SOUZA, E. R. de; SANTOS, H. R. B.; SILVA, Ê. F. de F. e; DUARTE, H. H. F.; MELO, D. V. M. de. Fluorescência da clorofila como indicador de estresse salino em feijão caupi. **Revista Brasileira de Agricultura Irrigada**, v. 12, p. 2592-2603, 2018.

PALMA, F.; CARVAJAL, F.; RAMOS, J. M.; JAMILENA, M.; GARRIDO, D. Effect of putrescine application on maintenance of zucchini fruit quality during cold storage: contribution of GABA shunt and other related nitrogen metabolites. **Postharvest Biology and Technology**, v. 99, p. 131-140, 2015.

PAN, Y. Q.; GUO, H.; WANG, S.-M.; ZHAO, B.; ZHANG, J.-L.; MA, Q., YIN, H.-J.; BAO A.-K. The photosynthesis, Na^+/K^+ homeostasis and osmotic adjustment of *Atriplex canescen*s in response to salinity. **Frontiers in Plant Science**, v. 7, p.1-14, 2016.

PANDEY, G. K.; MAHIWAL, S. Potassium homeostasis. **Role of Potassium in Plants**, p. 11-18, 2020.

PANDEY, P.; IRULAPPAN, V.; BAGAVATHIANNAN, M.V.; SENTHIL-KUMAR, M. Impact of combined abiotic and biotic stresses on plant growth and avenues for crop improvement by exploiting physio-morphological traits. **Frontiers in Plant Science**, v. 8, p.1-15, 2017.

PARIHAR, P.; SINGH, S.; SINGH, R.; SINGH, V. P.; PRASAD, S. M. Effect of salinity stress on plants and its tolerance strategies: a review. **Environmental Science and Pollution Research International**, v. 22, p. 4056-4075, 2014.

PASSAMANI, L. Z.; BARBOSA, R. R.; REIS, R. S.; HERINGER, A. S.; RANGEL, P. L.; SANTA-CATARINA, C.; GRATIVOL, C.; VEIGA, C. F. M.; SOUZA-FILHO, G.A.; SILVEIRA, V. Salt stress induces changes in the proteomic profile of micropropagated sugarcane shoots. **Plos One**, v. 12, p. 0176076-125255, 2017.

PASSRICHA, N.; SAIFI, S. K.; KHARB, P.; TUTEJA, N. Rice lectin receptor-like kinase provides salinity tolerance by ion homeostasis. **Biotechnology and Bioengineering**, v. 117, n. 2, p. 498-510, 2020.

PATEL, M. K.; KUMAR, M.; LI, W.; LUO, Y.; BURRITT, D. J.; ALKAN, N.; TRAN, L.-S. P. Enhancing salt tolerance of plants: from metabolic reprogramming to exogenous chemical treatments and molecular approaches. **Cells**, v. 9, p. 2492, 2020.

PEDERSEN, O.; PERATA, P.; VOESENEK, L. A. C. J. Flooding and low oxygen responses in plants. **Functional Plant Biology**, v. 44, p. iii-vi, 2017.

PEREIRA, J. A. **Cultura do arroz no Brasil**: subsídios para a sua história. Teresina: Embrapa Meio-Norte, 2002.

PEREIRA, T. S.; LOBATO, A. K. S.; ALVES, G. A. R.; FERREIRA, R. N.; SILVA, O. N.; MARTINS FILHO, A. P.; PEREIRA, E. S.; SAMPAIO, L. S. Tolerance to waterlogging in young *Euterpe oleracea* plants. **Photosynthetica**, v. 52, p. 186-192, 2014.

PERES, A. R.; RODRIGUES, R. A. F.; PORTUGAL, J. R.; ARF, O.; GONZAGA, A. R.; MEIRELLES, F. C.; GARCIA, N. F. S.; CORSINI, D. C. D. C.; TAKASU, A. T. Effect of irrigatation, rainfed conditions and nitrogen sources on newly released upland rice cultivar (BRS Esmeralda) with greater tolerance to drought stress. **Australian Journal of Crop Science**, v. 12, p. 1072-1081, 2018.

PESSARAKLI, M. (Ed.). **Handbook of photosynthesis**. Boca Raton: CRC press, 2016.

PIRES, J. L. F.; SOPRANO, E.; CASSOL, B. Adaptações morfofisiológicas da soja em solo inundado. **Pesquisa Agropecuária Brasileira**, v. 37, p.41-50, 2002.

PORCEL, R.; REDONDO-GÓMEZ, S.; MATEOS-NARANJO, E.; AROCA, R.; GARCIA, R.; RUIZ-LOZANO, J. M. Arbuscular mycorrhizal symbiosis ameliorates the optimum quantum yield of photosystem II and reduces non-photochemical quenching in rice plants subjected to salt stress. **Journal of Plant Physiology**, v. 185, p. 75-83, 2015.

PRISCO, J. T.; GOMES-FILHO, E. Fisiologia e bioquímica do estresse salino em plantas. In: GHERY, H. R.; DIAS, N. S.; LACERDA, C. F. **Manejo da salinidade na agricultura**: **estudos básicos e aplicados**. Fortaleza: INCTSal, 2010. Cap. 10, p. 143-149.

QIU, J.; HENDERSON, S.W.; TESTER, M.; ROY, S. J.; GILLIHAM, M. SLAH1, a homologue of the slow type anion channel SLAC1, modulates shoot Cl^- accumulation and salt tolerance in *Arabidopsis thaliana*. **Journal of Experimental Botany**, v. 67, p. 4495-4505, 2016.

RADY, M. M.; KUŞVURAN, A.; ALHARBY, H. F.; ALZAHRANI, Y.; KUŞVURAN, S. Pretreatment with proline or an organic bio-stimulant induces salt tolerance in wheat plants by improving antioxidant redox state and enzymatic activities and reducing the oxidative stress. **Journal of Plant Growth Regulation**, v. 38p. 449-462, 2018.

RAJHI, I.; YAMAUCHI, T.; TAKAHASHI, H.; NISHIUCHI, S.; SHIONO, K.; WATANABE, R.; MLIKI, A.; NAGAMURA, Y.; TSUTSUMI, N.; NISHIZAWA, N. K.; NAKAZONO, M. Identification of genes expressed in maize root cortical cells during lysigenous aerenchyma formation using laser microdissection and microarray analyses. **New Phytologist**, v. 190, p.351-368, 2010.

RAO, M. P. N.; DONG, Z.-Y.; XIAO, M.; LI, W.-J. Effect of salt stress on plants and role of microbes in promoting plant growth under salt stress. **Soil Biology**, p. 423-435, 2019.

RHODES, D.; NADOLSKA-ORCZYK, A. Plant Stress Physiology. **Encyclopedia of life sciences**, p.1-7, 2001.

RIBEIRO, M. R.; RIBEIRO FILHO, R.; JACOMINE, P. K. T. Origem e classificação dos solos afetados por sais. In: GHEYI, R. H.; DIAS, N. S.; LACERDA, C. F.; GOMES-FILHO, E. **Manejo da salinidade na agricultura**: Estudos básicos e aplicados. Fortaleza: INCTSal, 2016. cap.2, p. 9-15.

ROESSNER, U.; LUEDEMANN, A.; BRUST, D.; FIEHN, O.; LINKE, T.; WILLMITZER, L.; FERNIE, A. R. Metabolic profiling allows comprehensive phenotyping of genetically or environmentally modified plant systems. **The Plant Cell**, v. 13, p. 11-29, 2001.

ROMERO, L. C.; AROCA, M. Á.; LAUREANO-MARÍN, A. M.; MORENO, I.; GARCÍA, I.; GOTOR, C. Cysteine and cysteine-related signaling pathways in *Arabidopsis thaliana*. **Molecular Plant**, v. 7, p. 264-276, 2014.

RYBUS-ZAJĄC, M.; KUBIŚ, J. Nitrogen metabolism in cucumber cotyleons and leaves exposed to the drought stress and excessive UV-B radiation. **Acta Scientiarum Polonorum Hortorum Cultus**, v. 17, p. 23-36, 2018.

RYU, H.; CHO, Y. G. Plant hormones in salt stress tolerance. **Journal of Plant Biology**, v. 58, p. 147-155, 2015.

SÁ, F. V. S.; BRITO, M. E. B.; MELO, A. S.; ANTÔNIO NETO, P.; FERNANDES, P. D.; FERREIRA, I. B. Produção de mudas de mamoeiro irrigadas com água salina. **Revista Brasileira de Engenharia Agrícola e Ambiental,** v. 17, p. 1047-1054, 2013.

SAFDAR, H.; AMIN, A.; SHAFIQ, Y.; ALI, A.; YASIN, R.; SHOUKAT, A.; HUSSAN, M. U.; SARWAR, M. I. A review: Impact of salinity on plant growth. **Nature and Science**, v. 17, p. 34-40, 2019.

SANCHEZ, D. H.; PIECKENSTAIN, F. L.; ESCARAY, F.; ERBAN, A.; KRAEMER, U.; UDVARDI, M. K.; KOPKA, J. Comparative ionomics and metabolomics in extremophile and glycophytic Lotus species under salt stress challenge the metabolic pre-adaptation hypothesis. **Plant, Cell & Environment**, v. 34, p. 605-617, 2011.

SANTIAGO, C. M.; BRESEGHELLO, H. C. P.; FERREIRA, C. M. (Ed.). **Arroz:** o produtor pergunta, a Embrapa responde. 2. ed. rev. ampl. Brasília, DF: Embrapa, 2013. 245 p.

SANTOS, A. B.; RABELO, R. R. (Ed.). **Informações técnicas para a cultura do arroz irrigado no Estado do Tocantins.** Santo Antônio de Goiás: Embrapa Arroz e Feijão, 2008.

SANTOS, A. L. F.; MECHI, I. A.; RIBEIRO, L. M.; CECCON, G. Photosynthetic and productive efficiency of off-season corn in the function of sowing dates and plant populations. **Revista de Agricultura Neotropical**, v. 5, p. 52-60, 2018.

SANTOS, S. T. dos; OLIVEIRA, F. de A. de; OLIVEIRA, G. B. S.; SÁ, F. V. da S.; COSTA, J. P. B. de M.; FERNANDES, P. D. Photochemical efficiency of basil cultivars fertigated with salinized nutrient solutions. **Revista Brasileira de Engenharia Agrícola e Ambiental**, v.24, p.319-324, 2020.

SANTOS, V. S. dos. **Homeostase.** Brasil Escola. Disponível em: https://brasilescola.uol.com.br/biologia/homeostase.htm. Acesso em: 13 jan. 2020.

SANTOS-SÁNCHEZ, N. F.; SALAS-CORONADO, R.; HERNÁNDEZ-CARLOS, B.; VILLANUEVA-CAÑONGO, C. Shikimic acid pathway in biosynthesis of phenolic compounds. **Plant physiological aspects of phenolic compounds**, v. 1, p. 1-15, 2019.

SARKAR, R. K.; CHAKRABORTY, K.; CHATTOPADHYAY, K.; RAY, S.; PANDA, D.; ISMAIL, A.M. Responses of rice to individual and combined stresses of flooding and salinity. **Advances in Rice Research for Abiotic Stress Tolerance**, p. 281-297, 2019.

SARRUGE, J. R. & HAAG, H. P. **Análises químicas em plantas**. Piracicaba (SP): ESALQ, 1974. 56 p.

SCHMIDT, F. Crescimento e produção de arroz irrigado de pericarpo colorido em função da aplicação de nitrogênio e potássio. **Scientia Agraria**, v. 18, p. 34, 2017.

SCHOSSLER, T. R.; MACHADO, D. M.; ZUFFO, A. M.; ANDRADE, F. R.; PIAUILINO, A. C. Salinidade: efeitos na fisiologia e na nutrição mineral de plantas. **Enciclopédia Biosfera, Centro Científico Conhecer,** v.8, p. 1563-1578**,** 2012.

SCHWAIGER, S.; CERVELLATI, R.; SEGER, C.; ELLMERER, E. P.; ABOUT, N.; RENIMEL, I.; GODENIR, C.; ANDRÉ, P.; GAFNER, F.; STUPPNER, H. Leontopodic acid—a novel highly substituted glucaric acid derivative from Edelweiss (*Leontopodium alpinum* Cass.) and its antioxidative and DNA protecting properties. **Tetrahedron**, v. 61, p. 4621-4630, 2005.

SHABALA, S. Signalling by potassium: another second messenger to add to the list? **Journal of Experimental Botany**, v. 68, p. 4003-4007, 2017.

SHABALA, S.; POTTOSIN, I. Regulation of potassium transport in plants under hostile conditions: implications for abiotic and biotic stress tolerance. **Physiologia Plantarum**, v. 151, p. 257-279, 2014.

SHABALA, S.; SHABALA, L.; BARCELO, J.; POSCHENRIEDER, C. Membrane transporters mediating root signalling and adaptive responses to oxygen deprivation and soil flooding. **Plant, Cell & Environment**, v. 37, p. 2216-2233, 2014.

SHAHID, M. A.; SARKHOSH, A.; KHAN, N.; BALAL, R. M.; ALI, S.; ROSSI, L.; GÓMEZ, C.; MATTSON, N.; NASIM, W.; GARCIA-SANCHEZ, F. Insights into the physiological and biochemical impacts of salt stress on plant growth and development. **Agronomy**, v. 10, p. 938, 2020.

SHAHID, S. A.; ZAMAN, M.; HENG, L. Soil salinity: historical perspectives and a world overview of the problem. **Guideline for Salinity Assessment, Mitigation and Adaptation Using Nuclear and Related Techniques**, p. 43-53, 2018.

SHAREEF, H. J.; ABDI, G.; FAHAD, S. Change in photosynthetic pigments of date palm offshoots under abiotic stress factors. **Folia Oecologica**, v. 47, p. 45-51, 2020.

SHAVRUKOV, Y. Salt stress or salt shock: which genes are we studying? **Journal of Experimental Botany**, v. 64, p. 119-127, 2012.

SHRIVASTAVA, P.; KUMAR, R. Soil salinity: A serious environmental issue and plant growth promoting bacteria as one of the tools for its alleviation. **Saudi Journal of Biological Sciences**, v. 22, p.123-131, 2015.

SHU, S.; YUAN, Y.; CHEN, J.; SUN, J.; ZHANG, W.; TANG, Y.; ZHONG, M.; GUO, S. The role of putrescine in the regulation of proteins and fatty acids of thylakoid membranes under salt stress. **Scientific Reports**, v. 5, p. 1-16, 2015.

SIDDIQUI, M. F.; BANO, B. Insight into the functional and structural transition of garlic phytocystatin induced by urea and guanidine hydrochloride: a comparative biophysical study. **International Journal of Biological Macromolecules**, v. 106, p. 20-29, 2018.

SILVA, D. J. Nutrição mineral. In: MOTOIKE, S.; BORÉM, A. (Ed.). **Uva**: do plantio à colheita. Viçosa: Editora UFV, 2018. p. 84-103.

SILVA, E. N.; SILVEIRA, A. G.; RODRIGUES, C. R. F.; VIÉGAS, R. A. Physiological adjustment to salt stress in *Jatropha curcasis* associated with accumulation of salt ions, transport and selectivity of K^+, osmotic adjustment and K^+/Na^+ homeostasis. **Plant Biology**, v. 17, p.1023-1029, 2015.

SILVA, R. O.; FREITAS FILHO, J. R. de; FREITAS, J. C. R. D-Glucose, a fascinating biomolecule: history, properties, production and application. **Revista Virtual de Química**, v. 10, p. 875-891, 2018.

SIMOVA-STOILOVA, L.; DEMIREVSKA, K.; PETROVA, T.; TSENOV, N.; FELLER, U. Antioxidative protection and proteolytic activity in tolerant and sensitive wheat (*Triticum aestivum* L.) varieties subjected to long-term field drought. **Plant Growth Regulation**, v. 58, p. 107-117, 2009.

SINGH, M.; KUMAR, J.; SINGH, S.; SINGH, V. P.; PRASAD, S. M. Roles of osmoprotectants in improving salinity and drought tolerance in plants: a review. **Reviews in Environmental Science and Bio/Technology**, v. 14, p. 407-426, 2015.

SMEETS, K.; OPDENAKKER, K.; REMANS, T.; VAN SANDER, S.; VAN BELLEGHEM, F.; SEMANE, B.; HOREMANS, N.; GUISEZ, Y. VANGRONSVELD, J.; CUYPERS, A. Oxidative stress-related responses at transcriptional and enzymatic levels after exposure to Cd or Cu in a multipollution context. **Journal of Plant Physiology**, v. 166, p. 1982-1992, 2009.

SOCIEDADE SUL-BRASILEIRA DE ARROZ IRRIGADO. **Arroz irrigado**: recomendações técnicas da pesquisa para o Sul do Brasil. Pelotas: SOSBAI, 2007. p. 161.

SOUSA, J. R. M.; GHEYI, H. R.; BRITO, M. E. B.; SILVA, F. A. F. D.; LIMA, G. S. Dano na membrana celular e pigmentos clorofilianos de citros sob águas salinas e adubação nitrogenada. **Irriga**, v. 22, p. 353-368, 2017.

STEINITZ, B. Sugar alcohols display nonosmotic roles in regulating morphogenesis and metabolism in plants that do not produce polyols as primary photosynthetic products. **Journal of Plant Physiology**, v. 155, p. 1-8, 1999.

STEPANSKY, A.; LESS, H.; ANGELOVICI, R.; AHARON, R.; ZHU, X.; GALILI, G. Lysine catabolism, an effective versatile regulator of lysine level in plants. **Amino Acids**, v. 30, p. 121-125, 2006.

STINCONE, A.; PRIGIONE, A.; CRAMER, T.; WAMELINK, M. M. C.; CAMPBELL, K.; CHEUNG, E.; OLIN-SANDOVAL, V.; GRÜNING, N.-M.; KRÜGER, A.; ALAM, M. T. The return of metabolism: biochemistry and physiology of the pentose phosphate pathway. **Biological Reviews**, v. 90, p. 927-963, 2014.

STONE, LUÍS FERNANDO; SILVEIRA, PEDRO MARQUES DA; MOREIRA, JOSÉ ALOÍSIO ALVES. **Métodos de irrigação**. Disponível em: https://www.agencia.cnptia.embrapa.br/gestor/arroz/arvore/CONT000foh49q3602wyiv8065610d5y5f5im.html. Acesso em: 19 maio 2020.

STREIT, N. M.; CANTERLE, L. P.; CANTO, M. W. do; HECKTHEUER, L. H. H. As clorofilas. **Ciência Rural**, v. 35, p. 748-755, 2005.

SUN, Y.-L.; HONG, S.-K. Effects of citric acid as an important component of the responses to saline and alkaline stress in the halophyte *Leymus chinensis* (Trin.). **Plant Growth Regulation**, v. 64, p. 129-139, 2010.

TAIZ, L.; ZEIGER, E. **Plant Physiology and Development**. 6 ed. Sinauer Associates: Sunderland, 2017.

TAVARES, A. C.; DUARTE, S. N.; DIAS, N. D. S.; DE MIRANDA, J. H.; ARRAES, F. D.; SOUSA NETO, O. N. de; FERNANDES, C. D. S. Efeito da inundação do solo nos índices fisiológicos da cana-de-açúcar. **Revista de Ciências Agrárias**, v. 41, n. 1, p. 229-235, 2018.

TEAKLE, N. L.; BAZIHIZINA, N.; SHABALA, S.; COLMER, T. D.; BARRETT-LENNARD, E.G.; RODRIGO-MORENO, A.; LÄUCHLI, A. E. Differential tolerance to combined salinity and O2 deficiency in the halophytic grasses *Puccinellia ciliata* and *Thinopyrum ponticum*: the importance of K^+ retention in roots. **Environmental and Experimental Botany**, v. 87, p. 69-78, 2013.

TRIPATHI K. K.; WARRIER, R.; GOVILA, O. P.; AHUJA, V. **Biology of *oryza sativa* L. (Rice)**. **India**: Series of Crop Specifc Biology Documents. Ministry of Science and Technology, India. 2011.

TURK, H.; ERDAL, S.; DUMLUPINAR, R. Carnitine-induced physio-biochemical and molecular alterations in maize seedlings in response to cold stress. **Archives of Agronomy and Soil Science**, v. 66, p. 925-941, 2019.

VAN BODEGOM, P.; STAMS, F.; MOLLEMA, L.; BOEKE, S.; LEFFELAAR, P. Methane oxidation and the competition for oxygen in the rice rhizosphere. **Applied and Environmental Microbiology**, v. 67, p. 3586-3597, 2001.

VAN ZELM, E.; ZHANG, Y.; TESTERINK, C. Salt tolerance mechanisms of plants. **Annual Review of Plant Biology**, v. 71, p. 24.1–24.31, 2020.

VANDESOMPELE, J.; DE PRETER, K.; PATTYN, F.; POPPE, B.; VAN ROY, N.; DE PAEPE, A.; SPELEMAN, F. Accurate normalization of real-time quantitative RT-PCR data by geometric averaging of multiple internal control genes. **Genome Biology**, v.3, p.532-538, 2002.

VELASCO, N. F.; LIGARRETO, G. A.; DÍAZ, H. R.; FONSECA, L. P. M. Photosynthetic responses and tolerance to root-zone hypoxia stress of five bean cultivars (*Phaseolus vulgaris* L.). **South African Journal of Botany**, v. 123, p. 200-207, 2019.

VON CAEMMERER, S. Rubisco carboxylase/oxygenase: from the enzyme to the globe. **Journal of Plant Physiology**, v. 252, p. 153240, 2020.

WANG, F.; CHEN, Z-H.; LIU, X.; COLMER, T.D.; SHABALA, L.; SALIH, A.; ZHOU, M.; SHABALA, S. Revealing the roles of GORK channels and NADPH oxidase in acclimation to hypoxia in Arabidopsis. **Journal of Experimental Botany**, v.68, p. 3191–3204, 2017.

WELLBURN, A. R. The spectral determination of chlorophylls a and b, as well as total carotenoids, using various solvents with spectrophotometers of different resolution. **Journal of Plant Physiology**, v. 144, p. 307-313, 1994.

WILLADINO, L.; CAMARA, T. R. Tolerância das plantas à salinidade: aspectos fisiológicos e bioquímicos. **Enciclopédia Biosfera**, v. 6, p.1-23, 2010.

WU, H.; ZHANG, X.; GIRALDO, J. P.; SHABALA, S. It is not all about sodium: revealing tissue specificity and signalling roles of potassium in plant responses to salt stress. **Plant and Soil**, v. 431, p. 1-17, 2018.

WU, H.; ZHU, M.; SHABALA, L.; ZHOU, M.; SHABALA, S. K^+ retention in leaf mesophyll, an overlooked component of salinity tolerance mechanism: a case study for barley**. Journal of Integrative Plant Biology**, v. 57, p. 171-185, 2014.

WUTIPRADITKUL, N.; WONGWEAN, P.; BUABOOCHA, T. Alleviation of salt-induced oxidative stress in rice seedlings by proline and/or glycinebetaine. **Biologia Plantarum**, v. 59, p. 547-553, 2015.

XU, C.; MOU, B. Responses of spinach to salinity and nutrient deficiency in growth, physiology, and nutritional value. **Journal of the American Society for Horticultural Science**, v. 141, p.12-21, 2016.

XU, L.; PAN, R.; ZHOU, M.; XU, Y.; ZHANG, W. Lipid remodelling plays an important role in wheat (*Triticum aestivum*) hypoxia stress. **Functional Plant Biology**, v. 47, p. 58-66, 2020.

YAMAUCHI, T.; COLMER, T. D.; PEDERSEN, O.; NAKAZONO, M. Regulation of root traits for internal aeration and tolerance to soil waterlogging-flooding stress. **Plant Physiology**, v. 176, p. 1118-1130, 2017.

YANG, Y.; GUO, Y. Elucidating the molecular mechanisms mediating plant salt-stress responses. **New Phytologist**, v. 217, p. 523-539, 2017.

YIN, F.; ZHANG, S.; CAO, B.; XU, K. Low pH alleviated salinity stress of ginger seedlings by enhancing photosynthesis, fluorescence, and mineral element contents. **PeerJ**, v. 9, p. e10832, 2021.

ZAMAN, M.; SHAHID, S. A.; HENG, L. **Guideline for salinity assessment, mitigation and adaptation using nuclear and related techniques**. [*S.l.*]: Springer, Cham, 2018. Disponível

em: https://doi.org/10.1007/978-3-319-96190-3_2. Acesso em: 7 ago. 2019.

ZANDALINAS, S. I.; MITTLER, R.; BALFAGÓN, D.; ARBONA, V.; GÓMEZ-CADENAS, A. Plant adaptations to the combination of drought and high temperatures. **Physiologia Plantarum**, v. 162, p. 2-12, 2017.

ZHANG, H.; ZHANG, J.; YAN, J.; GOU, F.; MAO, Y.; TANG, G.; BOTELLA, J. R.; ZHU, J.-K. Short tandem target mimic rice lines uncover functions of miRNAs in regulating important agronomic traits. **Proceedings of The National Academy Of Sciences**, v. 114, p. 5277-5282, 2017.

ZHANG, L.; BECKER, D. F. Connecting proline metabolism and signaling pathways in plant senescence. **Frontiers in Plant Science**, v. 6, p. 552, 2015.

ZHAO, Z.; XIAN, M.; LIU, M.; ZHAO, G. Biochemical routes for uptake and conversion of xylose by microorganisms. **Biotechnology for Biofuels**, v. 13, p. 1-12, 2020.

ZHONG, M.; YUAN, Y.; SHU, S.; SUN, J.; GUO, S.; YUAN, R.; TANG, Y. Effects of exogenous putrescine on glycolysis and Krebs cycle metabolism in cucumber leaves subjected to salt stress. **Plant Growth Regulation**, v. 79, p. 319-330, 2015.

ZHU, J. - K. Abiotic stress signaling and responses in plants. **Cell**, v. 167, p.313-324, 2016.

APÊNDICE A - PEARSON CORRELATION COEFFICIENT FOR PHYSIOLOGICAL AND BIOCHEMICAL PARAMETERS RICE CV. BRS ESMERALDA AND SÃO FRANCISCO UNDER SALT STRESS.

Table S1 - Pearson correlation coefficient for physiological and biochemical parameters rice cv. BRS Esmeralda (ES) and São Francisco (SF) under non-salt conditions (C) and salt stress conditions (S) for ten days.

Parameters	Cl^- leaf	Cl^- stem	Cl^- root	Na^+ leaf	Na^+ stem	Na^+ root	Instantaneous water use efficiency	Photochemical quenching	Effective quantum yield of PSII	Electron transport rate	CO_2 assimilation
Cl^- leaf	1.000	0.348	0.700	0.683	0.571	0.641	0.176	0.162	0.028	0.027	-0.136
Cl^- stem	0.348	1.000	0.609	0.698	0.781	0.760	-0.213	-0.142	-0.376	-0.375	-0.571
Cl^- root	0.700	0.609	1.000	0.884	0.837	0.879	-0.397	-0.234	-0.376	-0.377	-0.575
Na^+ leaf	0.683	0.698	0.884	1.000	0.946	0.972	-0.313	-0.265	-0.422	-0.422	-0.616
Na^+ stem	0.571	0.781	0.837	0.946	1.000	0.973	-0.364	-0.273	-0.470	-0.469	-0.675
Na^+ root	0.641	0.760	0.879	0.972	0.973	1.000	-0.335	-0.268	-0.473	-0.473	-0.681
Instantaneous water use efficiency	0.176	-0.213	-0.397	-0.313	-0.364	-0.335	1.000	0.811	0.820	0.820	0.808
Photochemical quenching	0.162	-0.142	-0.234	-0.265	-0.273	-0.268	0.811	1.000	0.926	0.926	0.736
Effective quantum yield of PSII	0.028	-0.376	-0.376	-0.422	-0.470	-0.473	0.820	0.926	1.000	1.000	0.909
Electron transport rate	0.027	-0.375	-0.377	-0.422	-0.469	-0.473	0.820	0.926	1.000	1.000	0.909
CO_2 assimilation	-0.136	-0.571	-0.575	-0.616	-0.675	-0.681	0.808	0.736	0.909	0.909	1.000
Carboxylation efficiency of Rubisco	-0.098	-0.485	-0.569	-0.589	-0.630	-0.642	0.879	0.788	0.923	0.922	0.984
PSII maximum efficiency	-0.251	-0.663	-0.498	-0.524	-0.621	-0.639	0.373	0.200	0.549	0.548	0.730
Stomatal conductance	-0.228	-0.722	-0.531	-0.643	-0.728	-0.708	0.541	0.524	0.752	0.751	0.900
Transpiration	-0.246	-0.676	-0.610	-0.677	-0.740	-0.750	0.643	0.595	0.826	0.825	0.961
Chlorophyll *b*	-0.211	-0.334	-0.540	-0.605	-0.622	-0.663	0.349	0.124	0.292	0.291	0.461

Table S1 *continue*.

Parameters	Cl^- leaf	Cl^- stem	Cl^- root	Na^+ leaf	Na^+ stem	Na^+ root	Instantaneous water use efficiency	Photochemical quenching	Effective quantum yield of PSII	Electron transport rate	CO_2 assimilation
Relative water content of leaf	-0.343	-0.296	-0.457	-0.658	-0.511	-0.539	0.225	0.236	0.291	0.290	0.374
Stem dry mass	-0.544	-0.666	-0.569	-0.770	-0.748	-0.746	0.030	0.030	0.211	0.210	0.461
Root dry mass	-0.633	-0.683	-0.686	-0.865	-0.835	-0.844	0.102	0.100	0.282	0.282	0.523
K^+ stem	-0.566	-0.782	-0.667	-0.887	-0.891	-0.882	0.180	0.173	0.361	0.361	0.565
Shoot length	-0.649	-0.579	-0.818	-0.930	-0.868	-0.900	0.176	0.127	0.260	0.260	0.463
K^+ leaf	-0.481	-0.601	-0.674	-0.869	-0.891	-0.881	0.347	0.336	0.485	0.484	0.622
Leaf dry mass	-0.562	-0.805	-0.794	-0.938	-0.949	-0.947	0.308	0.277	0.464	0.464	0.670
K^+ root	-0.618	-0.625	-0.883	-0.963	-0.947	-0.960	0.416	0.331	0.490	0.489	0.681
Carotenoids	0.282	0.035	0.084	0.018	-0.100	-0.061	-0.007	-0.087	-0.013	-0.014	-0.008
Chlorophyll *a*	0.014	0.029	-0.125	-0.228	-0.201	-0.258	0.055	-0.115	0.010	0.009	0.105
Chlorophyll *total*	-0.085	-0.130	-0.315	-0.406	-0.398	-0.450	0.188	-0.015	0.135	0.134	0.268
Root length	-0.575	-0.301	-0.377	-0.440	-0.348	-0.427	-0.313	-0.042	0.024	0.024	0.049
Intercellular CO_2 concentration	-0.203	-0.473	-0.026	-0.161	-0.253	-0.259	-0.460	-0.338	-0.097	-0.098	0.069
Leaf relative humidity	-0.178	0.140	0.124	-0.101	-0.072	-0.008	-0.348	-0.208	-0.325	-0.325	-0.370
Root relative humidity	0.042	-0.230	0.120	0.045	0.010	0.029	-0.017	0.078	0.088	0.088	0.031
Relative water content of root	-0.121	-0.359	-0.015	-0.032	-0.076	-0.037	0.047	0.009	0.032	0.032	0.035

Table S1 continue.

Parameters	Carboxylation efficiency of Rubisco	PSII maximum efficiency	Stomatal conductance	Transpiration	Chlorophyll *b*	Relative water content of leaf	Stem dry mass	Root dry mass	K^+ stem	Shoot length
Cl^- leaf	-0.098	-0.251	-0.228	-0.246	-0.211	-0.343	-0.544	-0.633	-0.566	-0.649
Cl^- stem	-0.485	-0.663	-0.722	-0.676	-0.334	-0.296	-0.666	-0.683	-0.782	-0.579
Cl^- root	-0.569	-0.498	-0.531	-0.610	-0.540	-0.457	-0.569	-0.686	-0.667	-0.818
Na^+ leaf	-0.589	-0.524	-0.643	-0.677	-0.605	-0.658	-0.770	-0.865	-0.887	-0.930
Na^+ stem	-0.630	-0.621	-0.728	-0.740	-0.622	-0.511	-0.748	-0.835	-0.891	-0.868
Na^+ root	-0.642	-0.639	-0.708	-0.750	-0.663	-0.539	-0.746	-0.844	-0.882	-0.900
Instantaneous water use efficiency	0.879	0.373	0.541	0.643	0.349	0.225	0.030	0.102	0.180	0.176
Photochemical quenching	0.788	0.200	0.524	0.595	0.124	0.236	0.030	0.100	0.173	0.127
Effective quantum yield of PSII	0.923	0.549	0.752	0.826	0.292	0.291	0.211	0.282	0.361	0.260
Electron transport rate	0.922	0.548	0.751	0.825	0.291	0.290	0.210	0.282	0.361	0.260
CO_2 assimilation	0.984	0.730	0.900	0.961	0.461	0.374	0.461	0.523	0.565	0.463
Carboxylation efficiency of Rubisco	1.000	0.658	0.812	0.908	0.497	0.361	0.358	0.441	0.493	0.440
PSII maximum efficiency	0.658	1.000	0.761	0.825	0.504	0.274	0.473	0.507	0.535	0.433
Stomatal conductance	0.812	0.761	1.000	0.946	0.312	0.399	0.681	0.668	0.713	0.514
Transpiration	0.908	0.825	0.946	1.000	0.447	0.389	0.603	0.647	0.652	0.544
Chlorophyll *b*	0.497	0.504	0.312	0.447	1.000	0.258	0.243	0.373	0.459	0.586

Table S1 *continue*.

Parameters	Carboxylation efficiency of Rubisco	PSII maximum efficiency	Stomatal conductance	Transpiration	Chlorophyll *b*	Relative water content of leaf	Stem dry mass	Root dry mass	K^+ stem	Shoot length
Relative water content of leaf	0.361	0.274	0.399	0.389	0.258	1.000	0.598	0.609	0.633	0.589
Stem dry mass	0.358	0.473	0.681	0.603	0.243	0.598	1.000	0.960	0.846	0.767
Root dry mass	0.441	0.507	0.668	0.647	0.373	0.609	0.960	1.000	0.891	0.831
K^+ stem	0.493	0.535	0.713	0.652	0.459	0.633	0.846	0.891	1.000	0.833
Shoot length	0.440	0.433	0.514	0.544	0.586	0.589	0.767	0.831	0.833	1.000
K^+ leaf	0.611	0.522	0.596	0.639	0.662	0.536	0.613	0.743	0.838	0.834
Leaf dry mass	0.610	0.597	0.780	0.754	0.507	0.563	0.843	0.875	0.922	0.908
K^+ root	0.662	0.544	0.674	0.715	0.662	0.567	0.683	0.777	0.797	0.889
Carotenoids	-0.001	0.167	-0.029	-0.002	0.608	-0.240	-0.133	-0.122	-0.081	0.033
Chlorophyll *a*	0.139	0.293	0.023	0.095	0.807	0.144	0.022	0.058	0.136	0.302
Chlorophyll *total*	0.305	0.401	0.152	0.255	0.933	0.202	0.121	0.200	0.286	0.443
Root length	-0.032	0.117	0.257	0.192	-0.037	0.258	0.535	0.494	0.431	0.482
Intercellular CO_2 concentration	-0.102	0.421	0.434	0.263	-0.008	0.009	0.501	0.406	0.386	0.154
Leaf relative humidity	-0.355	-0.393	-0.286	-0.396	-0.118	0.238	0.075	0.112	0.211	0.213
Root relative humidity	0.014	0.034	0.037	0.028	-0.160	-0.086	0.141	0.210	0.146	-0.140
Relative water content of root	0.033	0.024	0.033	0.014	-0.149	-0.120	0.124	0.173	0.168	-0.138

Table S1 *continue*.

Parameters	K^+ leaf	Leaf dry mass	K^+ root	Carotenoids	Chlorophyll *a*	Chlorophyll *total*	Root length	Intercellular CO_2 concentration	Leaf relative humidity	Root relative humidity	Relative water content of root
Cl^- leaf	-0.481	-0.562	-0.618	0.282	0.014	-0.085	-0.575	-0.203	-0.178	0.042	-0.121
Cl^- stem	-0.601	-0.805	-0.625	0.035	0.029	-0.130	-0.301	-0.473	0.140	-0.230	-0.359
Cl^- root	-0.674	-0.794	-0.883	0.084	-0.125	-0.315	-0.377	-0.026	0.124	0.120	-0.015
Na^+ leaf	-0.869	-0.938	-0.963	0.018	-0.228	-0.406	-0.440	-0.161	-0.101	0.045	-0.032
Na^+ stem	-0.891	-0.949	-0.947	-0.100	-0.201	-0.398	-0.348	-0.253	-0.072	0.010	-0.076
Na^+ root	-0.881	-0.947	-0.960	-0.061	-0.258	-0.450	-0.427	-0.259	-0.008	0.029	-0.037
Instantaneous water use efficiency	0.347	0.308	0.416	-0.007	0.055	0.188	-0.313	-0.460	-0.348	-0.017	0.047
Photochemical quenching	0.336	0.277	0.331	-0.087	-0.115	-0.015	-0.042	-0.338	-0.208	0.078	0.009
Effective quantum yield of PSII	0.485	0.464	0.490	-0.013	0.010	0.135	0.024	-0.097	-0.325	0.088	0.032
Electron transport rate	0.484	0.464	0.489	-0.014	0.009	0.134	0.024	-0.098	-0.325	0.088	0.032
CO_2 assimilation	0.622	0.670	0.681	-0.008	0.105	0.268	0.049	0.069	-0.370	0.031	0.035
Carboxylation efficiency of Rubisco	0.611	0.610	0.662	-0.001	0.139	0.305	-0.032	-0.102	-0.355	0.014	0.033
PSII maximum efficiency	0.522	0.597	0.544	0.167	0.293	0.401	0.117	0.421	-0.393	0.034	0.024
Stomatal conductance	0.596	0.780	0.674	-0.029	0.023	0.152	0.257	0.434	-0.286	0.037	0.033
Transpiration	0.639	0.754	0.715	-0.002	0.095	0.255	0.192	0.263	-0.396	0.028	0.014
Chlorophyll *b*	0.662	0.507	0.662	0.608	0.807	0.933	-0.037	-0.008	-0.118	-0.160	-0.149

Table S1 *continue.*

Parameters	K^+ leaf	Leaf dry mass	K^+ root	Carotenoids	Chlorophyll *a*	Chlorophyll *total*	Root length	Intercellular CO_2 concentration	Leaf relative humidity	Root relative humidity	Relative water content of root
Relative water content of leaf	0.536	0.563	0.567	-0.240	0.144	0.202	0.258	0.009	0.238	-0.086	-0.120
Stem dry mass	0.613	0.843	0.683	-0.133	0.022	0.121	0.535	0.501	0.075	0.141	0.124
Root dry mass	0.743	0.875	0.777	-0.122	0.058	0.200	0.494	0.406	0.112	0.210	0.173
K^+ stem	0.838	0.922	0.797	-0.081	0.136	0.286	0.431	0.386	0.211	0.146	0.168
Shoot length	0.834	0.908	0.889	0.033	0.302	0.443	0.482	0.154	0.213	-0.140	-0.138
K^+ leaf	1.000	0.830	0.864	0.078	0.266	0.454	0.232	0.109	0.321	0.013	0.005
Leaf dry mass	0.830	1.000	0.908	0.004	0.168	0.327	0.445	0.330	0.058	-0.038	0.022
K^+ root	0.864	0.908	1.000	0.086	0.280	0.463	0.387	0.128	0.047	-0.194	-0.101
Carotenoids	0.078	0.004	0.086	1.000	0.785	0.746	-0.171	0.145	-0.151	-0.123	-0.221
Chlorophyll *a*	0.266	0.168	0.280	0.785	1.000	0.965	-0.085	0.042	-0.077	-0.241	-0.323
Chlorophyll *total*	0.454	0.327	0.463	0.746	0.965	1.000	-0.068	0.022	-0.099	-0.217	-0.262
Root length	0.232	0.445	0.387	-0.171	-0.085	-0.068	1.000	0.448	0.057	-0.009	-0.092
Intercellular CO_2 concentration	0.109	0.330	0.128	0.145	0.042	0.022	0.448	1.000	-0.087	0.055	-0.048
Leaf relative humidity	0.321	0.058	0.047	-0.151	-0.077	-0.099	0.057	-0.087	1.000	0.063	-0.015
Root relative humidity	0.013	-0.038	-0.194	-0.123	-0.241	-0.217	-0.009	0.055	0.063	1.000	0.840
Relative water content of root	0.005	0.022	-0.101	-0.221	-0.323	-0.262	-0.092	-0.048	-0.015	0.840	1.000

APÊNDICE B - RELATIVE INTENSITY VALUES OF METABOLITES IN LEAVES OF RICE CVS. BRS ESMERALDA AND SÃO FRANCISCO GROWING UNDER SALT STRESS.

Table S2 - Relative intensity values of metabolites in leaves of rice cv. BRS Esmeralda growing under non-salt conditions (ES-C) and salt stress conditions (ES-S) and cv. São Francisco growing under non-salt conditions (SF-C) and salt stress conditions (SF-S) for ten days. Values represent the means of five repetitions ± standard error

ID[a]	RT[b]	Metabolites	Relative intensity [c]							
			ES-C		ES-S		SF-C		SF-S	
Amino acid										
4	8.42	Alanine *	32.55 ± 2.28	B	73.21 ± 24.75	B	27.23 ± 5.35	B	215.61 ± 32.35	A
11	11.01	Valine *	8.20 ± 1.54	B	191.64 ± 27.98	A	4.89 ± 0.97	B	164.99 ± 33.70	A
13	11.82	Serine	40.70 ± 5.54	A	87.76 ± 30.97	A	62.89 ± 3.83	A	125.55 ± 20.46	A
15	12.16	Leucine *	1.79 ± 0.44	B	66.79 ± 30.56	A	1.03 ± 0.22	B	101.93 ± 26.56	A
18	12.58	Isoleucine *	2.21 ± 0.44	B	71.41 ± 33.57	A	1.18 ± 0.22	B	119.22 ± 34.18	A
19	12.63	Proline *	2.77 ± 0.57	C	83.33 ± 37.38	B	1.38 ± 0.24	C	399.00 ± 105.28	A
20	12.78	Glycine *	38.10 ± 8.09	AB	72.36 ± 19.41	AB	17.56 ± 3.58	B	116.98 ± 39.43	A
24	14.33	Threonine *	2.23 ± 0.34	B	14.12 ± 4.59	A	1.20 ± 0.16	B	24.82 ± 4.61	A
28	16.53	Aspartic acid *	39.81 ± 4.63	AB	36.84 ± 10.35	B	28.56 ± 5.94	B	78.18 ± 11.46	A
29	16.59	Hydroxyproline *	12.59 ± 1.65	AB	8.31 ± 2.24	B	23.72 ± 4.65	A	18.54 ± 4.06	AB
37	17.73	Cysteine *	6.98 ± 1.25	B	18.08 ± 6.54	B	4.75 ± 1.20	B	74.92 ± 13.17	A
38	17.98	Glutamic acid *	110.33 ± 26.19	B	102.64 ± 31.45	B	111.78 ± 28.03	B	280.27 ± 30.93	A
39	18.11	Phenylalanine *	1.58 ± 0.25	B	26.04 ± 12.24	A	0.59 ± 0.11	B	51.84 ± 15.41	A
41	18.77	Asparagine *	0.80 ± 0.22	C	8.09 ± 2.97	B	0.90 ± 0.25	C	20.45 ± 4.52	A

Identification number [a]; Retention time (min) [b]; Ratio of metabolite peak area to the ribitol peak area [c]. The capital letters compare the four group treatments, according to Tukey's test ($p < 0.05$); Metabolite shows significant difference according to F-test ($p < 0.05$) *

Table S2 *continue*.

ID[a]	RT[b]	Metabolites	Relative intensity [c]							
			ES-C		ES-S		SF-C		SF-S	
Amino acid										
50	20.16	Glutamine *	9.16 ± 2.45	C	25.09 ± 6.94	B	5.99 ± 1.96	C	105.71 ± 17.84	A
62	22.05	Lysine *	2.09 ± 0.07	B	18.08 ± 8.74	B	1.88 ± 0.25	B	92.02 ± 23.74	A
63	22.05	Ornithine *	1.26 ± 0.13	B	11.65 ± 5.13	B	1.03 ± 0.14	B	69.89 ± 19.89	A
65	22.30	Tyrosine *	2.76 ± 0.12	C	15.38 ± 6.27	B	1.99 ± 0.16	C	35.07 ± 7.23	A
78	25.28	Cystine *	0.61 ± 0.11	B	2.79 ± 1.21	A	0.12 ± 0.08	B	4.08 ± 0.93	A
Amino acid derived										
30	16.75	Pyroglutamic acid *	0.07 ± 0.05	B	2.93 ± 1.74	A	0.00 ± 0.00	B	1.59 ± 0.62	A
Flavonoid										
102	33.58	Quercetin	9.32 ± 0.90	A	3.35 ± 2.06	A	2.90 ± 0.32	A	3.60 ± 1.67	A
Inorganic acid										
16	12.22	Phosphoric acid *	108.84 ± 20.33	B	447.70 ± 35.04	A	116.47 ± 6.17	B	217.15 ± 40.99	B
Nitrogenous compounds										
7	9.62	Guanidine *	1.54 ± 0.27	B	21.82 ± 12.40	A	1.67 ± 0.27	B	26.83 ± 7.18	A
12	11.42	Urea *	2.11 ± 0.35	B	2.18 ± 0.93	B	1.21 ± 0.28	B	5.50 ± 1.19	A
Nucleotide										
101	33.57	Adenosine-5-monophosphate *	0.52 ± 0.10	A	0.64 ± 0.09	A	0.00 ± 0.00	B	0.49 ± 0.23	A
Organic acid										
1	7.10	Pyruvic acid	3.11 ± 0.13	A	1.82 ± 0.68	A	1.89 ± 0.51	A	3.23 ± 1.24	A

Table S2 *continue*.

ID[a]	RT[b]	Metabolites	Relative intensity [c]							
			ES-C		ES-S		SF-C		SF-S	
Organic acid										
2	7.37	Lactic acid	18.24 ± 5.22	A	14.51 ± 3.35	A	16.37 ± 3.26	A	20.84 ± 3.16	A
5	9.18	Oxalic acid	6.67 ± 1.75	A	18.11 ± 10.29	A	3.51 ± 0.52	A	7.42 ± 4.55	A
8	10.03	2-Aminoisobutyric acid *	0.00 ± 0.00	B	3.07 ± 1.77	B	0.00 ± 0.00	B	19.56 ± 6.70	A
9	10.08	2-Oxobutyric acid *	1.36 ± 0.24	B	23.74 ± 13.98	A	1.19 ± 0.22	B	32.55 ± 9.80	A
10	10.13	Malonic acid *	21.88 ± 1.62	A	7.91 ± 1.93	B	13.19 ± 2.02	AB	15.15 ± 2.46	AB
21	12.89	Succinic acid	17.76 ± 2.22	A	19.73 ± 7.22	A	17.67 ± 2.02	A	35.55 ± 4.46	A
22	13.32	Glyceric acid	43.70 ± 4.74	A	24.14 ± 6.15	A	32.06 ± 5.56	A	50.35 ± 12.92	A
23	14.08	Fumaric acid *	3.38 ± 0.21	AB	2.36 ± 0.65	B	2.45 ± 0.38	B	6.32 ± 0.89	A
26	16.02	Malic acid *	41.79 ± 4.66	A	13.89 ± 3.19	B	37.88 ± 6.16	AB	26.39 ± 8.13	AB
33	17.23	Erythronic acid *	4.95 ± 0.57	AB	5.23 ± 2.30	AB	2.72 ± 0.55	B	11.25 ± 2.85	A
34	17.35	2-Oxoglutaric acid	3.83 ± 1.15	A	12.89 ± 5.29	A	2.33 ± 0.15	A	11.22 ± 3.76	A
46	19.36	2-aminoadipic acid *	0.00 ± 0.00	B	4.27 ± 2.61	A	0.00 ± 0.00	B	1.93 ± 0.97	A
71	23.57	Gulonic acid *	2.10 ± 0.12	B	7.28 ± 2.88	B	0.93 ± 0.11	B	23.08 ± 7.91	A
76	24.74	Glucuronic acid*	2.26 ± 0.19	AB	1.54 ± 0.39	B	1.31 ± 0.19	B	3.47 ± 0.33	A
53	20.84	Citric acid *	31.49 ± 7.74	A	8.33 ± 2.22	B	33.63 ± 4.99	A	16.12 ± 4.30	AB
67	22.43	Glucaric acid	3.89 ± 0.58	A	2.91 ± 0.79	A	5.95 ± 1.40	A	5.53 ± 0.66	A
Phenolic precursor										
52	20.64	Shikimic acid	111.21 ± 9.67	A	64.08 ± 18.09	A	79.79 ± 14.16	A	96.52 ± 33.23	A
57	21.47	Quinic acid	113.61 ± 6.14	A	56.40 ± 15.02	A	80.11 ± 11.98	A	81.32 ± 30.77	A

Table S2 *continue*.

ID[a]	RT[b]	Metabolites	Relative intensity [c]							
			ES-C		ES-S		SF-C		SF-S	
Polyamine										
35	17.42	Putrescine *	1.03 ± 0.29	B	20.78 ± 12.20	A	0.40 ± 0.03	B	43.00 ± 15.47	A
Sugar										
27	16.43	Lyxose	7.57 ± 3.91	A	4.97 ± 1.60	A	3.89 ± 0.83	A	13.85 ± 6.15	A
31	16.83	Xylulose *	1.57 ± 0.31	B	18.73 ± 10.77	A	1.01 ± 0.22	B	15.95 ± 3.97	A
36	17.56	Erythrose *	5.79 ± 0.83	AB	4.29 ± 1.01	AB	2.86 ± 0.39	B	7.11 ± 0.88	A
43	19.00	Ribose *	1.30 ± 0.03	B	1.48 ± 0.42	B	0.60 ± 0.09	B	6.52 ± 1.69	A
56	21.30	Allose	63.66 ± 13.15	A	38.30 ± 11.42	A	31.69 ± 3.44	A	59.78 ± 26.25	A
58	21.73	Sorbose	6.73 ± 1.15	A	3.72 ± 0.95	A	2.89 ± 0.55	A	3.17 ± 0.47	A
59	21.77	Fructose *	23.82 ± 1.63	C	191.50 ± 52.46	B	13.26 ± 3.47	C	360.31 ± 39.20	A
60	21.88	Mannose *	1.10 ± 0.04	B	3.45 ± 1.67	AB	0.37 ± 0.08	B	19.50 ± 8.97	A
61	21.97	Glucose *	0.37 ± 0.07	B	1.20 ± 0.25	A	0.00 ± 0.00	B	2.10 ± 0.91	A
64	22.20	Galactose *	9.31 ± 0.67	B	41.77 ± 17.58	A	4.22 ± 0.92	B	129.70 ± 43.04	A
91	29.05	Cellobiose *	5.82 ± 2.99	A	0.91 ± 0.31	B	2.20 ± 0.60	AB	3.72 ± 0.74	AB
93	30.04	Sucrose *	495.05 ± 47.09	AB	413.85 ± 44.62	B	371.77 ± 30.47	B	658.46 ± 50.30	A
95	30.98	Trehalose *	8.74 ± 1.04	A	4.54 ± 1.18	B	4.88 ± 0.70	B	8.84 ± 1.17	A
97	32.18	Raffinose	6.28 ± 2.27	A	18.98 ± 10.35	A	2.60 ± 0.52	A	28.93 ± 7.02	A
98	32.43	Fructose-1.6-diphosphate *	2.72 ± 0.51	AB	2.70 ± 0.64	AB	1.24 ± 0.19	B	3.20 ± 0.19	A
100	33.13	Maltotriose *	0.83 ± 0.17	B	2.17 ± 0.74	AB	0.80 ± 0.24	B	4.13 ± 1.09	A

Table S2 *continue*.

ID[a]	RT[b]	Metabolites	Relative intensity [c]							
			ES-C		ES-S		SF-C		SF-S	
Sugar alcohol										
44	19.15	Xylitol *	0.00 ± 0.00	B	0.64 ± 0.23	A	0.00 ± 0.00	B	1.32 ± 0.41	A
48	19.90	Arabitol *	13.71 ± 1.60	AB	11.99 ± 2.86	AB	7.36 ± 0.79	B	19.05 ± 1.96	A
49	20.11	Glycerol-2-phosphate *	0.84 ± 0.09	AB	2.30 ± 0.85	A	0.29 ± 0.05	B	2.27 ± 0.36	A
66	22.36	Mannitol *	1.01 ± 0.07	B	0.85 ± 0.22	B	0.61 ± 0.08	B	2.02 ± 0.26	A
74	24.28	Inositol *	99.68 ± 6.66	A	99.39 ± 23.33	A	41.99 ± 6.08	B	112.23 ± 8.49	A
99	33.13	Galactinol *	2.40 ± 0.44	B	6.79 ± 2.02	AB	2.44 ± 0.56	B	12.44 ± 3.08	A
Sugar derived										
42	18.95	Methyl α-D-mannopyranoside *	0.19 ± 0.12	B	1.23 ± 0.21	A	0.00 ± 0.00	B	1.10 ± 0.46	A
73	23.95	Glucopyranoside *	0.24 ± 0.03	B	0.45 ± 0.06	A	0.00 ± 0.00	C	0.00 ± 0.00	C
Unidentified Metabolites										
3	7.98	Unknown 1 *	0.00 ± 0.00	B	1.67 ± 0.89	A	0.00 ± 0.00	B	1.96 ± 0.36	A
6	9.41	Unknown 2 *	4.40 ± 0.66	A	3.74 ± 1.06	AB	0.47 ± 0.20	B	3.67 ± 1.81	AB
14	12.03	Unknown 3 *	17.06 ± 4.43	B	29.10 ± 7.74	A	4.55 ± 0.97	B	54.51 ± 7.32	A
17	12.23	Unknown 4 *	42.86 ± 4.50	B	78.35 ± 26.64	AB	29.08 ± 2.22	B	130.79 ± 26.56	A
25	15.78	Unknown 5 *	1.37 ± 0.14	AB	2.03 ± 0.73	AB	0.71 ± 0.17	B	2.94 ± 0.48	A
32	16.98	Unknown 7	4.16 ± 0.37	A	3.86 ± 1.02	A	3.06 ± 0.42	A	6.14 ± 0.80	A
40	18.22	Unknown 8 *	92.40 ± 19.83	AB	45.56 ± 16.47	B	83.78 ± 25.74	AB	193.55 ± 39.34	A
45	19.25	Unknown 9 *	5.38 ± 0.69	B	6.78 ± 1.83	B	4.01 ± 0.41	B	13.31 ± 1.58	A
47	19.89	Unknown 10 *	1.61 ± 0.16	AB	1.47 ± 0.35	AB	0.76 ± 0.09	B	2.29 ± 0.25	A

Table S2 *continue*.

ID[a]	RT[b]	Metabolites	Relative intensity [c]							
			ES-C		ES-S		SF-C		SF-S	
51	20.16	Unknown 11	6.70 ± 0.34	A	3.42 ± 1.09	A	3.36 ± 0.48	A	6.43 ± 1.43	A
54	20.92	Unknown 12	1.84 ± 0.50	A	4.02 ± 1.32	A	0.75 ± 0.07	A	4.98 ± 2.09	A
55	20.97	Unknown 13 *	0.79 ± 0.15	A	0.41 ± 0.15	A	0.00 ± 0.00	B	0.33 ± 0.15	AB
68	22.53	Unknown 14 *	0.21 ± 0.14	B	1.74 ± 0.84	A	0.00 ± 0.00	B	1.29 ± 0.27	A
69	22.70	Unknown 15	0.23 ± 0.04	A	0.22 ± 0.02	A	0.31 ± 0.08	A	0.84 ± 0.35	A
70	23.44	Unknown 16 *	3.59 ± 0.46	A	2.25 ± 0.66	AB	1.20 ± 0.14	B	2.60 ± 0.38	AB
72	23.82	Unknown 17 *	3.97 ± 0.73	AB	8.04 ± 1.89	A	1.79 ± 0.18	B	4.68 ± 1.55	AB
75	24.61	Unknown 18 *	3.51 ± 0.30	AB	2.48 ± 0.64	B	2.37 ± 0.33	B	6.21 ± 0.48	A
77	24.88	Unknown 19 *	0.76 ± 0.07	A	0.80 ± 0.26	A	0.21 ± 0.03	B	1.29 ± 0.21	A
79	25.36	Unknown 20	13.83 ± 5.28	A	15.44 ± 4.33	A	8.24 ± 1.71	A	18.94 ± 4.68	A
80	25.38	Unknown 21 *	0.30 ± 0.05	B	1.67 ± 0.51	A	0.26 ± 0.04	B	1.21 ± 0.22	A
81	25.59	Unknown 22 *	1.06 ± 0.09	B	13.31 ± 4.63	A	0.15 ± 0.10	B	15.60 ± 3.74	A
82	26.52	Unknown 23 *	1.92 ± 0.14	A	1.92 ± 0.48	B	0.53 ± 0.05	B	2.03 ± 0.34	A
83	26.53	Unknown 24 *	2.08 ± 0.22	B	1.92 ± 0.50	B	1.84 ± 0.34	B	5.54 ± 0.60	A
84	26.72	Unknown 25 *	0.94 ± 0.34	B	3.39 ± 1.80	AB	0.16 ± 0.08	B	9.29 ± 2.83	A
85	27.32	Unknown 26 *	4.49 ± 0.72	A	2.57 ± 0.90	AB	1.36 ± 0.14	B	3.47 ± 0.40	AB
86	27.99	Unknown 27	3.84 ± 1.61	A	4.56 ± 1.37	A	2.28 ± 0.60	A	5.26 ± 1.51	A
87	28.27	Unknown 28 *	2.09 ± 0.75	A	1.75 ± 0.68	A	0.00 ± 0.00	B	1.10 ± 0.17	A
88	28.44	Unknown 29 *	0.12 ± 0.05	AB	0.47 ± 0.27	AB	0.00 ± 0.00	B	0.51 ± 0.08	A

Table S2 *continue*.

ID[a]	RT[b]	Metabolites	Relative intensity [c]							
			ES-C		ES-S		SF-C		SF-S	
89	28.52	Unknown 30 *	2.77 ± 0.25	AB	1.81 ± 0.52	B	1.79 ± 0.24	B	3.99 ± 0.25	A
90	28.69	Unknown 31 *	0.00 ± 0.00	B	1.10 ± 0.52	A	0.00 ± 0.00	B	0.75 ± 0.33	AB
92	29.33	Unknown 32	9.61 ± 1.44	A	4.90 ± 1.94	A	6.39 ± 1.40	A	9.57 ± 1.81	A
94	30.92	Unknown 33	1.50 ± 0.35	A	1.22 ± 0.33	A	1.13 ± 0.26	A	2.32 ± 0.26	A
96	31.49	Unknown 34 *	7.89 ± 1.24	A	2.57 ± 0.93	B	3.22 ± 0.48	AB	4.76 ± 0.92	AB

APÊNDICE C - RELATIVE INTENSITY VALUES OF METABOLITES IN ROOTS OF RICE CVS. BRS ESMERALDA AND SÃO FRANCISCO GROWING UNDER UNDER SALT STRESS.

Table S3 - Relative intensity values of metabolites in roots of rice cv. BRS Esmeralda growing under non-salt conditions (ES-C) and salt stress conditions (ES-S) and cv. São Francisco growing under non-salt conditions (SF-C) and salt stress conditions (SF-S) for ten days. Values represent the means of five repetitions ± standard error.

ID[a]	RT[b]	Metabolites	Relative intensity [c]							
			ES-C		ES-S		SF-C		SF-S	
Amino acid										
3	8.42	Alanine	43.28 ± 13.37	A	43.33 ± 20.30	A	30.72 ± 5.49	A	33.65 ± 9.91	A
8	11.01	Valine	14.46 ± 3.88	A	16.50 ± 7.69	A	11.23 ± 2.79	A	10.94 ± 3.05	A
10	11.82	Serine	23.79 ± 7.14	A	41.91 ± 11.99	A	14.95 ± 1.95	A	23.16 ± 9.19	A
12	12.16	Leucine	3.52 ± 0.64	A	7.46 ± 2.49	A	1.56 ± 0.48	A	2.69 ± 0.86	A
15	12.58	Isoleucine	3.44 ± 0.63	A	6.40 ± 1.85	A	1.79 ± 0.43	A	2.77 ± 0.76	A
16	12.63	Proline *	2.23 ± 0.54	B	7.90 ± 2.02	A	1.57 ± 0.39	B	3.65 ± 0.33	AB
17	12.78	Glycine	13.67 ± 5.21	A	24.61 ± 16.33	A	9.77 ± 1.40	A	10.14 ± 3.34	A
20	14.33	Threonine	0.89 ± 0.23	A	1.89 ± 0.82	A	0.69 ± 0.33	A	1.21 ± 0.39	A
23	16.53	Aspartic acid	9.73 ± 4.82	A	9.96 ± 3.68	A	5.77 ± 0.80	A	12.18 ± 4.96	A
24	16.59	Hydroxyproline	4.35 ± 1.25	A	6.83 ± 1.83	A	3.12 ± 0.31	A	8.21 ± 3.41	A
29	17.98	Glutamic acid	38.21 ± 17.43	A	26.13 ± 14.71	A	23.26 ± 2.87	A	63.73 ± 30.54	A
30	18.11	Phenylalanine	1.10 ± 0.54	A	0.93 ± 0.36	A	0.70 ± 0.09	A	1.22 ± 0.54	A
31	18.77	Asparagine	7.03 ± 4.95	A	1.08 ± 0.48	A	4.71 ± 0.69	A	5.60 ± 3.08	A
35	20.16	Glutamine	20.25 ± 14.42	A	5.27 ± 2.55	A	14.80 ± 2.00	A	12.38 ± 6.02	A
44	22.05	Lysine	2.15 ± 0.54	A	3.05 ± 1.17	A	1.16 ± 0.07	A	1.23 ± 0.59	A
45	22.05	Ornithine	2.15 ± 0.54	A	3.05 ± 1.17	A	1.16 ± 0.07	A	1.38 ± 0.57	A

Table S3 *continue*.

ID[a]	RT[b]	Metabolites	Relative intensity [c]							
			ES-C		ES-S		SF-C		SF-S	
Amino acid										
47	22.30	Tyrosine	4.95 ± 1.50	A	5.06 ± 1.66	A	2.58 ± 0.23	A	4.26 ± 1.35	A
Inorganic acid										
13	12.22	Phosphoric acid	193.40 ± 45.62	A	247.35 ± 49.75	A	95.47 ± 17.70	A	151.74 ± 33.43	A
Nitrogenous compound										
6	9.62	Guanidine	2.86 ± 0.57	A	4.12 ± 0.68	A	1.23 ± 0.20	A	4.79 ± 2.42	A
9	11.42	Urea	26.40 ± 7.85	A	24.94 ± 13.99	A	12.25 ± 2.79	A	19.63 ± 5.50	A
Organic acid										
1	7.10	Pyruvic acid	2.04 ± 0.61	A	3.47 ± 1.39	A	1.24 ± 0.16	A	1.81 ± 0.70	A
2	7.37	Lactic acid	80.54 ± 26.65	A	69.86 ± 12.20	A	26.52 ± 6.63	A	138.30 ± 60.03	A
4	9.18	Oxalic acid	0.58 ± 0.31	A	0.00 ± 0.00	A	0.35 ± 0.08	A	0.81 ± 0.44	A
7	10.13	Malonic acid	14.39 ± 4.30	A	10.66 ± 2.77	A	8.59 ± 1.13	A	11.95 ± 3.37	A
18	12.89	Succinic acid	15.09 ± 5.95	A	2.92 ± 0.89	A	3.84 ± 0.90	A	12.80 ± 3.78	A
19	13.32	Glyceric acid *	0.00 ± 0.00	B	0.14 ± 0.05	AB	0.46 ± 0.08	A	0.49 ± 0.23	A
21	16.02	Malic acid *	20.00 ± 9.82	A	3.08 ± 0.94	B	16.72 ± 2.15	A	7.62 ± 2.54	B
26	17.35	2-Oxoglutaric acid *	2.21 ± 0.64	B	5.66 ± 0.76	A	0.82 ± 0.28	B	0.60 ± 0.22	C
37	20.84	Citric acid	3.69 ± 3.12	A	0.95 ± 0.34	A	2.88 ± 0.39	A	2.22 ± 0.91	A
49	22.43	Glucaric acid	1.61 ± 0.49	A	0.78 ± 0.17	A	0.77 ± 0.19	A	1.89 ± 1.36	A
51	23.57	Gulonic acid	2.70 ± 0.43	A	1.84 ± 0.44	A	1.67 ± 0.28	A	2.59 ± 0.94	A

Table S3 *continue*.

ID[a]	RT[b]	Metabolites	Relative intensity [c]							
			ES-C		ES-S		SF-C		SF-S	
Phenolic precursor										
36	20.64	Shikimic acid *	21.65 ± 9.14	A	4.26 ± 1.20	B	25.77 ± 3.39	A	11.27 ± 3.35	AB
39	21.47	Quinic acid *	35.88 ± 15.81	A	6.85 ± 1.80	B	45.97 ± 6.93	A	15.51 ± 4.53	B
Polyamine										
27	17.42	Putrescine *	0.00 ± 0.00	B	1.18 ± 0.26	A	0.00 ± 0.00	B	0.12 ± 0.07	B
Sugar										
22	16.43	Lyxose	6.06 ± 3.97	A	11.39 ± 5.89	A	0.00 ± 0.00	A	0.00 ± 0.00	A
25	16.83	Xylulose	1.00 ± 0.28	A	1.94 ± 0.28	A	0.80 ± 0.07	A	0.91 ± 0.34	A
28	17.56	Erythrose	2.35 ± 1.40	A	0.71 ± 0.25	A	2.57 ± 0.24	A	3.33 ± 1.02	A
32	19.00	Ribose	2.84 ± 0.85	A	1.48 ± 0.35	A	2.16 ± 0.31	A	5.49 ± 2.49	A
40	21.65	Fructose *	318.48 ± 66.04	A	53.40 ± 15.33	B	330.98 ± 19.10	A	70.76 ± 28.26	B
41	21.73	Sorbose *	225.54 ± 47.49	A	45.95 ± 11.14	B	196.64 ± 31.83	A	47.37 ± 18.54	B
42	21.88	Mannose	2.22 ± 0.26	A	1.47 ± 0.19	A	1.09 ± 0.13	A	1.71 ± 0.67	A
43	21.97	Glucose	11.11 ± 1.82	A	7.04 ± 1.59	A	6.93 ± 1.32	A	9.22 ± 3.34	A
46	22.20	Galactose	2.13 ± 0.50	A	3.56 ± 1.00	A	1.07 ± 0.05	A	1.09 ± 0.48	A
58	30.04	Sucrose	310.01 ± 88.05	A	295.34 ± 65.80	A	266.15 ± 49.84	A	358.64 ± 60.74	A
60	30.98	Trehalose	39.23 ± 7.76	A	39.91 ± 7.95	A	18.70 ± 1.94	A	59.48 ± 19.27	A
61	32.18	Raffinose	0.00 ± 0.00	A	4.86 ± 1.41	A	3.54 ± 1.21	A	2.94 ± 1.31	A
62	32.43	Fructose-1.6-diphosphate	0.00 ± 0.00	A	0.00 ± 0.00	A	0.25 ± 0.12	A	0.10 ± 0.06	A
64	33.13	Maltotriose *	0.09 ± 0.06	B	1.40 ± 0.33	A	0.36 ± 0.01	B	0.16 ± 0.08	B

Table S3 *continue*.

ID[a]	RT[b]	Metabolites	Relative intensity [c]							
			ES-C		ES-S		SF-C		SF-S	
Sugar alcohol										
33	19.90	Arabitol *	0.00 ± 0.00	C	0.25 ± 0.04	B	1.86 ± 0.11	A	3.19 ± 1.03	A
34	20.11	Glycerol-2-phosphate *	0.00 ± 0.00	B	258590.95 ± 25587.92	A	0.00 ± 0.00	B	330192.12 ± 33458.55	A
48	22.36	Mannitol	48.46 ± 15.40	A	39.89 ± 5.65	A	24.03 ± 4.45	A	68.24 ± 33.41	A
53	24.28	Inositol	9.15 ± 1.20	A	10.71 ± 2.05	A	4.06 ± 0.29	A	7.71 ± 2.40	A
63	33.13	Galactinol *	1.54 0.34	AB	3.81 0.67	A	1.05 0.14	B	0.92 0.31	B
Sugar derived										
52	23.95	Glucopyranoside *	0.00 ± 0.00	B	0.00 ± 0.00	B	0.00 ± 0.00	B	0.39 ± 0.18	A
Unidentified Metabolites										
5	9.41	Unknown 2 *	8.56 ± 2.27	AB	15.47 ± 3.08	A	2.85 ± 1.13	B	10.47 ± 2.03	A
11	12.03	Unknown 3	93.78 ± 28.74	A	47.19 ± 15.43	A	57.64 ± 14.16	A	49.16 ± 15.84	A
14	12.23	Unknown 4	152.28 ± 23.83	A	125.80 ± 24.04	A	77.26 ± 8.10	A	150.81 ± 47.27	A
38	20.97	Unknown 13	0.67 ± 0.13	A	0.66 ± 0.19	A	0.26 ± 0.07	A	0.41 ± 0.17	A
50	23.44	Unknown 32	1.46 ± 0.36	A	1.41 ± 0.39	A	0.93 ± 0.15	A	0.52 ± 0.14	A
54	25.36	Unknown 20	84.85 ± 14.61	A	66.27 ± 12.41	A	46.08 ± 7.71	A	91.13 ± 33.41	A
55	25.38	Unknown 21	1.91 ± 0.34	A	1.67 ± 0.18	A	0.98 ± 0.15	A	2.15 ± 0.76	A
56	27.32	Unknown 26	2.64 ± 0.61	A	3.14 ± 0.76	A	1.27 ± 0.15	A	3.10 ± 0.95	A
57	27.99	Unknown 27	20.55 ± 3.81	A	16.46 ± 2.64	A	10.98 ± 1.92	A	20.71 ± 6.81	A
59	30.92	Unknown 33	0.89 ± 0.40	A	0.68 ± 0.14	A	0.28 ± 0.08	A	1.23 ± 0.38	A

APÊNDICE D - PEARSON CORRELATION COEFFICIENT FOR PHYSIOLOGICAL AND BIOCHEMICAL PARAMETERS RICE CV. BRS ESMERALDA (ES) AND SÃO FRANCISCO UNDER DIFFERENT LEVELS OF HYPOXIA.

Table S4 - Pearson correlation coefficient for physiological and biochemical parameters rice cv. BRS Esmeralda (ES) and São Francisco (SF) under severe (SE), moderate (MO), and slight (SL) hypoxia for ten days.

Parameters	Root relative humidity	Relative water content of root	Instantaneous water use efficiency	Na^+ leaf	K^+ root	Relative water content of leaf	Cl^- root	Na^+ stem	Na^+ root	Cl^- stem
Root relative humidity	1.000	0.876	0.180	0.303	-0.086	0.002	0.137	-0.092	0.078	-0.142
Relative water content of root	0.876	1.000	0.140	0.236	-0.103	-0.076	0.200	-0.209	0.083	-0.108
Instantaneous water use efficiency	0.180	0.140	1.000	0.524	-0.035	-0.116	-0.293	0.158	0.445	0.325
Na^+ leaf	0.303	0.236	0.524	1.000	-0.432	-0.088	-0.084	0.005	0.499	-0.047
K^+ root	-0.086	-0.103	-0.035	-0.432	1.000	0.183	-0.066	-0.100	-0.161	0.171
Relative water content of leaf	0.002	-0.076	-0.116	-0.088	0.183	1.000	0.302	-0.145	0.151	-0.160
Cl^- root	0.137	0.200	-0.293	-0.084	-0.066	0.302	1.000	0.090	0.045	-0.151
Na^+ stem	-0.092	-0.209	0.158	0.005	-0.100	-0.145	0.090	1.000	0.134	0.129
Na^+ root	0.078	0.083	0.445	0.499	-0.161	0.151	0.045	0.134	1.000	0.050
Cl^- stem	-0.142	-0.108	0.325	-0.047	0.171	-0.160	-0.151	0.129	0.050	1.000
Chlorophyll *b*	-0.200	-0.249	0.135	-0.257	-0.081	0.083	-0.120	0.153	-0.213	0.487
Carotenoids	-0.225	-0.158	-0.166	-0.410	-0.200	0.081	-0.045	0.024	-0.384	0.328
Chlorophyll *a*	-0.276	-0.249	-0.090	-0.384	-0.154	0.008	-0.136	0.149	-0.395	0.358
Chlorophyll *total*	-0.253	-0.261	0.011	-0.342	-0.127	0.043	-0.135	0.157	-0.328	0.434
Photochemical quenching	0.120	0.185	0.575	0.193	0.024	-0.270	-0.138	-0.305	-0.115	0.315
CO_2 assimilation	0.085	0.097	0.375	0.174	-0.136	-0.148	-0.121	-0.257	-0.154	0.315
Carboxylation efficiency of Rubisco	0.086	0.076	0.551	0.220	-0.097	-0.183	-0.177	-0.129	-0.116	0.389

Table S4 *continue*.

Parameters	Root relative humidity	Relative water content of root	Instantaneous water use efficiency	Na^+ leaf	K^+ root	Relative water content of leaf	Cl^- root	Na^+ stem	Na^+ root	Cl^- stem
Effective quantum yield of PSII	0.102	0.179	0.489	0.171	-0.061	-0.214	-0.134	-0.267	-0.156	0.252
Electron transport rate	0.102	0.179	0.489	0.171	-0.061	-0.215	-0.136	-0.267	-0.157	0.252
Intercellular CO_2 concentration	0.034	0.137	-0.492	-0.151	-0.180	0.077	0.105	-0.470	-0.227	-0.111
K^+ stem	0.165	0.184	-0.181	0.003	-0.212	0.093	-0.007	-0.607	-0.259	-0.357
PSII maximum efficiency	0.018	0.075	-0.122	-0.006	-0.231	0.113	-0.065	0.043	-0.153	-0.097
Stomatal conductance	0.040	0.108	-0.071	-0.041	-0.177	-0.023	0.032	-0.472	-0.250	0.102
Transpiration	-0.005	0.053	-0.201	-0.150	-0.129	-0.106	0.031	-0.356	-0.432	0.147
Cl^- leaf	-0.302	-0.268	0.144	0.206	-0.462	-0.250	-0.084	-0.138	-0.283	-0.190
Leaf dry mass	0.038	0.119	0.132	0.141	-0.306	-0.205	-0.393	-0.356	0.040	-0.267
Stem dry mass	0.078	0.019	0.042	0.299	-0.358	-0.105	-0.271	-0.427	-0.064	-0.229
Root dry mass	0.117	0.066	-0.056	0.108	-0.268	-0.108	-0.247	-0.353	-0.108	-0.194
Shoot length	-0.173	-0.148	-0.349	-0.264	-0.094	-0.208	-0.078	-0.335	-0.600	-0.129
Root length	-0.003	-0.035	-0.289	-0.188	-0.233	0.114	0.144	-0.151	-0.571	-0.181
Leaf relative humidity	-0.185	-0.267	0.103	-0.184	0.152	0.434	0.003	-0.187	-0.264	-0.096
K^+ leaf	0.077	0.113	-0.040	0.043	-0.023	-0.027	-0.019	-0.241	-0.239	0.275

Table S4 *continue*.

Parameters	Chlorophyll *b*	Carotenoids	Chlorophyll *a*	Chlorophyll *total*	Photochemical quenching	CO_2 assimilation	Carboxylation efficiency of Rubisco	Effective quantum yield of PSII
Root relative humidity	-0.200	-0.225	-0.276	-0.253	0.120	0.085	0.086	0.102
Relative water content of root	-0.249	-0.158	-0.249	-0.261	0.185	0.097	0.076	0.179
Instantaneous water use efficiency	0.135	-0.166	-0.090	0.011	0.575	0.375	0.551	0.489
Na^+ leaf	-0.257	-0.410	-0.384	-0.342	0.193	0.174	0.220	0.171
K^+ root	-0.081	-0.200	-0.154	-0.127	0.024	-0.136	-0.097	-0.061
Relative water content of leaf	0.083	0.081	0.008	0.043	-0.270	-0.148	-0.183	-0.214
Cl^- root	-0.120	-0.045	-0.136	-0.135	-0.138	-0.121	-0.177	-0.134
Na^+ stem	0.153	0.024	0.149	0.157	-0.305	-0.257	-0.129	-0.267
Na^+ root	-0.213	-0.384	-0.395	-0.328	-0.115	-0.154	-0.116	-0.156
Cl^- stem	0.487	0.328	0.358	0.434	0.315	0.315	0.389	0.252
Chlorophyll *b*	1.000	0.765	0.830	0.946	0.140	0.347	0.398	0.217
Carotenoids	0.765	1.000	0.927	0.893	0.017	0.212	0.188	0.112
Chlorophyll *a*	0.830	0.927	1.000	0.966	0.020	0.215	0.223	0.133
Chlorophyll *total*	0.946	0.893	0.966	1.000	0.077	0.286	0.315	0.178
Photochemical quenching	0.140	0.017	0.020	0.077	1.000	0.780	0.840	0.936
CO_2 assimilation	0.347	0.212	0.215	0.286	0.780	1.000	0.962	0.902
Carboxylation efficiency of Rubisco	0.398	0.188	0.223	0.315	0.840	0.962	1.000	0.913

Table S4 *continue* .

Parameters	Chlorophyll *b*	Carotenoids	Chlorophyll *a*	Chlorophyll *total*	Photochemical quenching	CO_2 assimilation	Carboxylation efficiency of Rubisco	Effective quantum yield of PSII
Effective quantum yield of PSII	0.217	0.112	0.133	0.178	0.936	0.902	0.913	1.000
Electron transport rate	0.216	0.112	0.132	0.177	0.937	0.901	0.912	1.000
Intercellular CO_2 concentration	0.036	0.291	0.163	0.111	0.016	0.436	0.183	0.228
K^+ stem	0.015	0.133	0.084	0.056	0.268	0.383	0.237	0.381
PSII maximum efficiency	0.284	0.303	0.353	0.336	0.003	0.498	0.381	0.348
Stomatal conductance	0.234	0.288	0.221	0.237	0.497	0.834	0.662	0.671
Transpiration	0.292	0.352	0.315	0.318	0.469	0.826	0.686	0.650
Cl^- leaf	0.164	0.143	0.235	0.213	0.410	0.394	0.402	0.449
Leaf dry mass	-0.128	-0.022	-0.033	-0.079	0.357	0.367	0.286	0.425
Stem dry mass	-0.144	-0.050	-0.044	-0.093	0.280	0.300	0.205	0.329
Root dry mass	-0.091	-0.004	0.032	-0.024	0.220	0.240	0.161	0.271
Shoot length	0.176	0.220	0.270	0.239	0.232	0.267	0.177	0.277
Root length	0.234	0.481	0.418	0.351	0.234	0.421	0.316	0.352
Leaf relative humidity	0.340	0.165	0.229	0.291	0.186	0.277	0.269	0.285
K^+ leaf	0.151	0.153	0.179	0.174	0.279	0.177	0.161	0.232

Table S4 *continue*.

Parameters	Electron transport rate	Intercellular CO_2 concentration	K^+ stem	PSII maximum efficiency	Stomatal conductance	Transpiration	Cl^- leaf	Leaf dry mass	Stem dry mass	Root dry mass	Shoot length
Root relative humidity	0.102	0.034	0.165	0.018	0.040	-0.005	-0.302	0.038	0.078	0.117	-0.173
Relative water content of root	0.179	0.137	0.184	0.075	0.108	0.053	-0.268	0.119	0.019	0.066	-0.148
Instantaneous water use efficiency	0.489	-0.492	-0.181	-0.122	-0.071	-0.201	0.144	0.132	0.042	-0.056	-0.349
Na^+ leaf	0.171	-0.151	0.003	-0.006	-0.041	-0.150	0.206	0.141	0.299	0.108	-0.264
K^+ root	-0.061	-0.180	-0.212	-0.231	-0.177	-0.129	-0.462	-0.306	-0.358	-0.268	-0.094
Relative water content of leaf	-0.215	0.077	0.093	0.113	-0.023	-0.106	-0.250	-0.205	-0.105	-0.108	-0.208
Cl^- root	-0.136	0.105	-0.007	-0.065	0.032	0.031	-0.084	-0.393	-0.271	-0.247	-0.078
Na^+ stem	-0.267	-0.470	-0.607	0.043	-0.472	-0.356	-0.138	-0.356	-0.427	-0.353	-0.335
Na^+ root	-0.157	-0.227	-0.259	-0.153	-0.250	-0.432	-0.283	0.040	-0.064	-0.108	-0.600
Cl^- stem	0.252	-0.111	-0.357	-0.097	0.102	0.147	-0.190	-0.267	-0.229	-0.194	-0.129
Chlorophyll *b*	0.216	0.036	0.015	0.284	0.234	0.292	0.164	-0.128	-0.144	-0.091	0.176
Carotenoids	0.112	0.291	0.133	0.303	0.288	0.352	0.143	-0.022	-0.050	-0.004	0.220
Chlorophyll *a*	0.132	0.163	0.084	0.353	0.221	0.315	0.235	-0.033	-0.044	0.032	0.270
Chlorophyll *total*	0.177	0.111	0.056	0.336	0.237	0.318	0.213	-0.079	-0.093	-0.024	0.239
Photochemical quenching	0.937	0.016	0.268	0.003	0.497	0.469	0.410	0.357	0.280	0.220	0.232
CO_2 assimilation	0.901	0.436	0.383	0.498	0.834	0.826	0.394	0.367	0.300	0.240	0.267
Carboxylation efficiency of Rubisco	0.912	0.183	0.237	0.381	0.662	0.686	0.402	0.286	0.205	0.161	0.177

Table S4 *continue*.

Parameters	Electron transport rate	Intercellular CO_2 concentration	K^+ stem	PSII maximum efficiency	Stomatal conductance	Transpiration	Cl^- leaf	Leaf dry mass	Stem dry mass	Root dry mass	Shoot length
Effective quantum yield of PSII	1.000	0.228	0.381	0.348	0.671	0.650	0.449	0.425	0.329	0.271	0.277
Electron transport rate	1.000	0.227	0.381	0.347	0.670	0.649	0.449	0.426	0.330	0.271	0.279
Intercellular CO_2 concentration	0.227	1.000	0.578	0.592	0.819	0.754	0.052	0.342	0.322	0.273	0.335
K^+ stem	0.381	0.578	1.000	0.332	0.578	0.496	0.422	0.534	0.571	0.419	0.437
PSII maximum efficiency	0.347	0.592	0.332	1.000	0.575	0.608	0.146	0.239	0.148	0.153	0.157
Stomatal conductance	0.670	0.819	0.578	0.575	1.000	0.918	0.303	0.449	0.388	0.310	0.439
Transpiration	0.649	0.754	0.496	0.608	0.918	1.000	0.316	0.316	0.266	0.277	0.476
Cl^- leaf	0.449	0.052	0.422	0.146	0.303	0.316	1.000	0.481	0.594	0.496	0.552
Leaf dry mass	0.426	0.342	0.534	0.239	0.449	0.316	0.481	1.000	0.785	0.694	0.492
Stem dry mass	0.330	0.322	0.571	0.148	0.388	0.266	0.594	0.785	1.000	0.898	0.536
Root dry mass	0.271	0.273	0.419	0.153	0.310	0.277	0.496	0.694	0.898	1.000	0.546
Shoot length	0.279	0.335	0.437	0.157	0.439	0.476	0.552	0.492	0.536	0.546	1.000
Root length	0.352	0.505	0.405	0.362	0.586	0.613	0.476	0.359	0.422	0.399	0.647
Leaf relative humidity	0.285	0.049	0.162	0.294	0.282	0.190	0.266	0.075	0.239	0.256	0.282
K^+ leaf	0.232	0.070	0.262	-0.097	0.208	0.213	0.132	0.202	0.262	0.233	0.486

Table S4 *continue*.

Parameters	Root length	Leaf relative humidity	K^+ leaf
Root relative humidity	-0.003	-0.185	0.077
Relative water content of root	-0.035	-0.267	0.113
Instantaneous water use efficiency	-0.289	0.103	-0.040
Na^+ leaf	-0.188	-0.184	0.043
K^+ root	-0.233	0.152	-0.023
Relative water content of leaf	0.114	0.434	-0.027
Cl^- root	0.144	0.003	-0.019
Na^+ stem	-0.151	-0.187	-0.241
Na^+ root	-0.571	-0.264	-0.239
Cl^- stem	-0.181	-0.096	0.275
Chlorophyll *b*	0.234	0.340	0.151
Carotenoids	0.481	0.165	0.153
Chlorophyll *a*	0.418	0.229	0.179
Chlorophyll *total*	0.351	0.291	0.174
Photochemical quenching	0.234	0.186	0.279
CO_2 assimilation	0.421	0.277	0.177
Carboxylation efficiency of Rubisco	0.316	0.269	0.161
Effective quantum yield of PSII	0.352	0.285	0.232
Electron transport rate	0.352	0.285	0.232
Intercellular CO_2 concentration	0.505	0.049	0.070
K^+ stem	0.405	0.162	0.262
PSII maximum efficiency	0.362	0.294	-0.097
Stomatal conductance	0.586	0.282	0.208
Transpiration	0.613	0.190	0.213
Cl^- leaf	0.476	0.266	0.132
Leaf dry mass	0.359	0.075	0.202
Stem dry mass	0.422	0.239	0.262
Root dry mass	0.399	0.256	0.233
Shoot length	0.647	0.282	0.486
Root length	1.000	0.341	0.290
Leaf relative humidity	0.341	1.000	0.069
K^+ leaf	0.290	0.069	1.000

APÊNDICE E - RELATIVE INTENSITY VALUES OF METABOLITES IN LEAVES OF RICE CVS. BRS ESMERALDA AND SÃO FRANCISCO GROWING UNDER DIFFERENT LEVELS OF HYPOXIA.

Table S5 - Relative intensity values of metabolites in leaves of rice cv. BRS Esmeralda under severe (ES-SE), moderate (ES-MO), and slight (ES-SL) hypoxia and cv. São Francisco under severe (SF-SE), moderate (SF-MO), and slight (SF-SL) hypoxia conditions for ten days. Values represent the means of five repetitions ± standard error.

ID[a]	RT[b]	Metabolites	Relative intensity [c]											
			ES-SE		ES-MO		ES-SL		SF-SE		SF-MO		SF-SL	
Amino acid														
3	8.42	Alanine	66.50 ± 12.5	A	32.55 ± 2.3	A	31.21 ± 5.6	A	47.81 ± 9.5	A	27.23 ± 5.4	A	43.77 ± 10.7	A
9	11.01	Valine	11.45 ± 2.4	A	8.20 ± 1.5	A	6.79 ± 2.3	A	8.88 ± 2.7	A	4.89 ± 1.0	A	9.66 ± 2.6	A
11	11.82	Serine	54.27 ± 7.6	A	40.70 ± 5.5	A	39.99 ± 2.4	A	45.84 ± 8.2	A	62.89 ± 3.8	A	66.90 ± 26.3	A
13	12.16	Leucine	2.81 ± 0.8	A	1.79 ± 0.4	A	1.72 ± 0.6	A	1.73 ± 0.5	A	1.03 ± 0.2	A	2.14 ± 0.8	A
16	12.58	Isoleucine	3.04 ± 0.7	A	2.21 ± 0.4	A	2.63 ± 1.1	A	1.64 ± 0.5	A	1.18 ± 0.2	A	2.33 ± 0.9	A
17	12.63	Proline	3.75 ± 1.2	A	2.77 ± 0.6	A	2.79 ± 0.8	A	2.65 ± 0.9	A	1.38 ± 0.2	A	3.41 ± 1.5	A
18	12.78	Glycine *	33.03 ± 4.1	AB	38.10 ± 8.1	AB	16.77 ± 2.9	B	57.29 ± 13.5	A	17.56 ± 3.6	B	39.37 ± 13.7	AB
22	14.33	Threonine	2.69 ± 0.5	A	2.23 ± 0.3	A	2.43 ± 0.5	A	1.49 ± 0.3	A	1.20 ± 0.2	A	1.59 ± 0.2	A
26	16.53	Aspartic acid	57.72 ± 18.8	A	39.81 ± 4.6	A	48.86 ± 6.7	A	28.07 ± 5.4	A	28.56 ± 5.9	A	38.51 ± 6.3	A
27	16.59	Hydroxyproline	20.48 ± 2.7	A	12.59 ± 1.7	A	13.41 ± 1.0	A	17.51 ± 4.7	A	23.72 ± 4.7	A	13.05 ± 3.1	A
34	17.73	Cysteine *	11.69 ± 2.3	A	6.98 ± 1.3	AB	6.36 ± 0.7	AB	11.14 ± 2.1	A	4.75 ± 1.2	B	5.37 ± 0.9	AB
35	17.98	Glutamic acid	152.53 ± 35.4	A	110.33 ± 26.2	A	88.24 ± 12.0	A	127.87 ± 21.9	A	111.78 ± 28.0	A	115.48 ± 25.5	A
36	18.11	Phenylalanine	1.79 ± 0.4	A	1.58 ± 0.3	A	1.87 ± 0.9	A	0.73 ± 0.2	A	0.59 ± 0.1	A	1.30 ± 0.4	A
38	18.77	Asparagine	2.31 ± 0.7	A	0.80 ± 0.2	A	0.69 ± 0.4	A	1.33 ± 0.4	A	0.90 ± 0.2	A	0.82 ± 0.1	A

Table S5 *continue*.

ID[a]	RT[b]	Metabolites	Relative intensity [c]											
			ES-SE		ES-MO		ES-SL		SF-SE		SF-MO		SF-SL	
Amino acid														
45	20.16	Glutamine	11.29 ± 1.8	A	9.16 ± 2.5	A	5.04 ± 1.6	A	10.26 ± 2.2	A	5.99 ± 2.0	A	4.95 ± 1.7	A
57	22.05	Lysine	3.16 ± 0.4	A	2.09 ± 0.1	A	2.52 ± 0.7	A	2.66 ± 0.7	A	1.88 ± 0.2	A	2.51 ± 0.8	A
58	22.05	Ornithine	1.74 ± 0.3	A	1.26 ± 0.1	A	1.52 ± 0.3	A	1.45 ± 0.4	A	1.03 ± 0.1	A	1.63 ± 0.4	A
60	22.3	Tyrosine	3.57 ± 0.7	A	2.76 ± 0.1	A	3.15 ± 0.5	A	1.67 ± 0.3	A	1.99 ± 0.2	A	2.85 ± 0.6	A
73	25.28	Cystine *	0.59 ± 0.1	A	0.61 ± 0.1	A	0.56 ± 0.1	A	0.26 ± 0.2	AB	0.12 ± 0.1	B	0.39 ± 0.1	AB
Flavonoid														
95	33.58	Quercetin *	8.22 ± 2.1	A	9.32 ± 0.9	A	10.37 ± 1.8	A	2.50 ± 0.6	B	2.90 ± 0.3	B	3.10 ± 1.4	B
Inorganic acid														
14	12.22	Phosphoric acid *	48.94 ± 14.6	B	108.84 ± 20.3	B	237.08 ± 54.8	A	80.60 ± 10.1	B	116.47 ± 6.2	A	215.14 ± 25.7	A
Nitrogenous compound														
6	9.62	Guanidine	2.71 ± 0.6	A	1.54 ± 0.3	A	2.19 ± 0.6	A	1.17 ± 0.2	A	1.67 ± 0.3	A	2.18 ± 0.7	A
10	11.42	Urea	2.24 ± 0.4	A	2.11 ± 0.3	A	2.02 ± 0.1	A	1.92 ± 0.5	A	1.21 ± 0.3	A	2.54 ± 0.7	A
Nucleotide														
94	33.57	Adenosine-5-monophosphate *	0.10 ± 0.1	B	0.52 ± 0.1	A	0.53 ± 0.1	A	0.00 ± 0.0	B	0.00 ± 0.0	B	0.19 ± 0.1	AB
Organic acid														
1	7.1	Pyruvic acid	1.79 ± 0.2	A	3.11 ± 0.1	A	2.59 ± 0.2	A	1.60 ± 0.1	A	1.89 ± 0.5	A	2.72 ± 0.7	A
2	7.37	Lactic acid	22.94 ± 2.9	A	18.24 ± 5.2	A	20.56 ± 3.6	A	21.61 ± 4.0	A	16.37 ± 3.3	A	22.13 ± 3.9	A
4	9.18	Oxalic acid	6.65 ± 0.6	A	6.67 ± 1.7	A	8.42 ± 1.6	A	6.69 ± 1.3	A	3.51 ± 0.5	A	9.70 ± 4.0	A

Table S5 *continue*.

ID[a]	RT[b]	Metabolites	Relative intensity [c]											
			ES-SE		ES-MO		ES-SL		SF-SE		SF-MO		SF-SL	
Organic acid														
7	10.08	2-Oxobutyric acid	2.33 ± 0.5	A	1.36 ± 0.2	A	2.16 ± 1.0	A	1.02 ± 0.2	A	1.19 ± 0.2	A	1.89 ± 0.7	A
8	10.13	Malonic acid	17.11 ± 2.7	A	21.88 ± 1.6	A	20.52 ± 1.2	A	15.35 ± 2.3	A	13.19 ± 2.0	A	14.87 ± 2.3	A
19	12.89	Succinic acid *	35.74 ± 6.3	A	17.76 ± 2.2	B	28.07 ± 2.1	AB	18.58 ± 2.1	B	17.67 ± 2.0	B	17.92 ± 1.7	B
20	13.32	Glyceric acid	40.33 ± 5.5	A	43.70 ± 4.7	A	41.34 ± 7.3	A	43.83 ± 6.2	A	32.06 ± 5.6	A	52.81 ± 17.5	A
21	14.08	Fumaric acid *	4.56 ± 0.7	A	3.38 ± 0.2	AB	3.71 ± 0.1	AB	4.04 ± 0.6	AB	2.45 ± 0.4	B	2.51 ± 0.2	B
24	16.02	Malic acid	33.94 ± 2.7	A	41.79 ± 4.7	A	35.05 ± 2.6	A	39.75 ± 5.3	A	37.88 ± 6.2	A	41.92 ± 12.4	A
30	17.23	Erythronic acid *	6.83 ± 1.2	A	4.95 ± 0.6	AB	3.83 ± 0.2	AB	5.77 ± 1.0	A	2.72 ± 0.5	B	3.43 ± 0.5	B
31	17.35	2-Oxoglutaric acid	3.69 ± 0.5	A	3.83 ± 1.1	A	4.19 ± 0.6	A	1.73 ± 0.2	A	2.33 ± 0.1	A	5.61 ± 2.2	A
48	20.84	Citric acid	32.72 ± 13.6	A	31.49 ± 7.7	A	15.87 ± 3.7	A	18.15 ± 3.2	A	33.63 ± 5.0	A	31.60 ± 13.5	A
62	22.43	Glucaric acid	7.28 ± 1.1	A	3.89 ± 0.6	A	5.83 ± 1.5	A	3.64 ± 0.6	A	5.95 ± 1.4	A	5.68 ± 1.1	A
66	23.57	Gulonic acid	1.60 ± 0.3	A	2.10 ± 0.1	A	1.89 ± 0.3	A	1.39 ± 0.2	A	0.93 ± 0.1	A	1.57 ± 0.3	A
71	24.74	Glucuronic acid *	2.13 ± 0.3	AB	2.26 ± 0.2	A	2.05 ± 0.1	AB	1.59 ± 0.2	AB	1.31 ± 0.2	B	1.40 ± 0.2	AB
Phenolic precursor														
47	20.64	Shikimic acid	122.99 ± 11.3	A	111.21 ± 9.7	A	113.11 ± 13.3	A	100.12 ± 16.7	A	79.79 ± 14.2	A	84.08 ± 20.4	A
52	21.47	Quinic acid	108.47 ± 7.0	A	113.61 ± 6.1	A	126.07 ± 16.1	A	79.03 ± 13.2	A	80.11 ± 12.0	A	99.47 ± 19.3	A
Polyamine														
32	17.42	Putrescine	1.37 ± 0.3	A	1.03 ± 0.3	A	1.28 ± 0.5	A	0.72 ± 0.2	A	0.40 ± 0.0	A	1.54 ± 0.9	A

Table S5 *continue*.

ID[a]	RT[b]	Metabolites	Relative intensity [c]											
			ES-SE		ES-MO		ES-SL		SF-SE		SF-MO		SF-SL	
Sugar														
25	16.43	Lyxose	5.52 ± 1.9	A	7.57 ± 3.9	A	2.94 ± 0.4	A	2.13 ± 0.6	A	3.89 ± 0.8	A	7.96 ± 4.4	A
28	16.83	Xylulose	1.84 ± 0.4	A	1.57 ± 0.3	A	2.05 ± 0.9	A	0.67 ± 0.2	A	1.01 ± 0.2	A	1.28 ± 0.5	A
33	17.56	Erythrose	5.49 ± 1.0	A	5.79 ± 0.8	A	4.48 ± 0.2	A	4.39 ± 0.8	A	2.86 ± 0.4	A	3.37 ± 0.9	A
40	19	Ribose *	1.05 ± 0.1	AB	1.30 ± 0.0	A	1.18 ± 0.2	AB	0.67 ± 0.2	B	0.60 ± 0.1	B	0.75 ± 0.2	AB
51	21.3	Allose	57.79 ± 7.4	A	63.66 ± 13.2	A	67.03 ± 6.7	A	34.82 ± 9.8	A	31.69 ± 3.4	A	67.73 ± 17.0	A
53	21.73	Sorbose *	9.59 ± 1.2	A	6.73 ± 1.2	A	10.88 ± 1.5	A	1.95 ± 0.6	B	2.89 ± 0.5	B	3.01 ± 1.4	B
54	21.77	Fructose	15.87 ± 4.8	A	23.82 ± 1.6	A	24.07 ± 7.0	A	17.00 ± 4.3	A	13.26 ± 3.5	A	27.03 ± 7.2	A
55	21.88	Mannose *	1.05 ± 0.2	A	1.10 ± 0.0	A	1.29 ± 0.3	A	0.36 ± 0.1	B	0.37 ± 0.1	B	0.59 ± 0.2	AB
56	21.97	Glucose *	0.16 ± 0.1	AB	0.37 ± 0.1	A	0.37 ± 0.1	A	0.11 ± 0.1	AB	0.00 ± 0.0	B	0.33 ± 0.1	AB
59	22.2	Galactose	6.55 ± 1.4	A	9.31 ± 0.7	A	9.04 ± 2.1	A	5.21 ± 1.0	A	4.22 ± 0.9	A	7.88 ± 1.8	A
69	24.28	Inositol *	116.59 ± 18.0	A	99.68 ± 6.7	A	111.62 ± 5.8	A	62.95 ± 10.3	B	41.99 ± 6.1	B	34.32 ± 2.6	B
84	29.05	Cellobiose *	0.50 ± 0.3	B	5.82 ± 3.0	A	1.73 ± 0.2	AB	7.68 ± 4.0	A	2.20 ± 0.6	AB	1.53 ± 0.4	AB
86	30.04	Sucrose *	482.80 ± 11.3	AB	495.05 ± 47.1	AB	530.18 ± 57.1	A	568.24 ± 55.9	A	371.77 ± 30.5	AB	332.56 ± 46.3	B
88	30.98	Trehalose *	8.53 ± 1.3	A	8.74 ± 1.0	A	8.67 ± 1.3	A	5.87 ± 1.1	B	4.88 ± 0.7	B	4.53 ± 1.3	B
90	32.18	Raffinose	14.70 ± 8.5	A	6.28 ± 2.3	A	7.07 ± 1.9	A	4.33 ± 1.2	A	2.60 ± 0.5	A	4.87 ± 2.2	A
91	32.43	Fructose-1.6-diphosphate *	2.51 ± 0.5	A	2.72 ± 0.5	A	2.20 ± 0.2	AB	1.17 ± 0.3	B	1.24 ± 0.2	AB	1.02 ± 0.2	B
93	33.13	Maltotriose	1.09 ± 0.2	A	0.83 ± 0.2	A	0.72 ± 0.0	A	1.64 ± 0.4	A	0.80 ± 0.2	A	0.67 ± 0.1	A

Table S5 *continue*.

ID[a]	RT[b]	Metabolites	Relative intensity [c]											
			ES-SE		ES-MO		ES-SL		SF-SE		SF-MO		SF-SL	
Sugar alcohol														
43	19.9	Arabitol	14.43 ± 2.5	A	13.71 ± 1.6	A	11.57 ± 0.5	A	10.38 ± 1.6	A	7.36 ± 0.8	A	9.02 ± 2.3	A
44	20.11	Glycerol-2-phosphate *	1.15 ± 0.4	A	0.84 ± 0.1	A	0.94 ± 0.1	A	0.00 ± 0.0	C	0.29 ± 0.0	B	0.50 ± 0.1	AB
61	22.36	Mannitol	0.79 ± 0.1	A	1.01 ± 0.1	A	1.25 ± 0.4	A	0.80 ± 0.2	A	0.61 ± 0.1	A	0.67 ± 0.1	A
92	33.13	Galactinol	3.14 ± 0.4	A	2.40 ± 0.4	A	2.30 ± 0.2	A	4.67 ± 1.0	A	2.44 ± 0.6	A	2.30 ± 0.3	A
Sugar derived														
39	18.95	Methyl α-D-mannopyranoside	0.14 ± 0.1	A	0.19 ± 0.1	A	0.21 ± 0.0	A	0.00 ± 0.0	A	0.00 ± 0.0	A	0.30 ± 0.2	A
68	23.95	Glucopyranoside *	3.35 ± 0.7	A	0.24 ± 0.0	B	0.00 ± 0.0	C	0.45 ± 0.2	B	0.00 ± 0.0	C	0.00 ± 0.0	C
Unidentified Metabolites														
5	9.41	Unknown 2 *	2.98 ± 0.3	A	4.40 ± 0.7	A	3.89 ± 0.4	A	1.00 ± 0.2	B	0.47 ± 0.2	C	1.92 ± 0.4	B
12	12.03	Unknown 3	12.16 ± 2.6	A	17.06 ± 4.4	A	17.37 ± 4.8	A	7.20 ± 1.6	A	4.55 ± 1.0	A	14.51 ± 4.7	A
15	12.23	Unknown 4 *	31.70 ± 5.3	B	42.86 ± 4.5	AB	60.67 ± 2.9	A	31.20 ± 4.1	B	29.08 ± 2.2	B	44.85 ± 2.0	AB
23	15.78	Unknown 5	1.35 ± 0.2	A	1.37 ± 0.1	A	1.30 ± 0.1	A	1.04 ± 0.1	A	0.71 ± 0.2	A	1.04 ± 0.2	A
29	16.98	Unknown 7	3.79 ± 0.4	A	4.16 ± 0.4	A	3.92 ± 0.3	A	3.70 ± 0.6	A	3.06 ± 0.4	A	3.45 ± 0.3	A
37	18.22	Unknown 8	107.83 ± 21.0	A	92.40 ± 19.8	A	80.52 ± 11.8	A	128.87 ± 25.0	A	83.78 ± 25.7	A	83.23 ± 18.1	A
41	19.25	Unknown 9	6.36 ± 0.9	A	5.38 ± 0.7	A	5.77 ± 0.8	A	4.03 ± 0.8	A	4.01 ± 0.4	A	4.45 ± 1.2	A
42	19.89	Unknown 10 *	1.58 ± 0.3	A	1.61 ± 0.2	A	1.28 ± 0.1	AB	1.08 ± 0.2	AB	0.76 ± 0.1	B	1.08 ± 0.2	AB
46	20.16	Unknown 11	4.88 ± 0.8	A	6.70 ± 0.3	A	5.50 ± 1.0	A	3.86 ± 0.9	A	3.36 ± 0.5	A	2.95 ± 1.0	A
49	20.92	Unknown 12 *	2.20 ± 0.3	A	1.84 ± 0.5	AB	1.90 ± 0.3	AB	1.18 ± 0.3	AB	0.75 ± 0.1	B	1.74 ± 0.4	AB

Table S5 *continue*.

ID[a]	RT[b]	Metabolites	Relative intensity [c]													
			ES-SE		ES-MO		ES-SL		SF-SE		SF-MO		SF-SL	
50	20.97	Unknown 13 *	0.00 ± 0.0	B	0.79 ± 0.2	A	0.35 ± 0.2	AB	0.00 ± 0.0	B	0.00 ± 0.0	B	0.12 ± 0.1	B
63	22.53	Unknown 14 *	0.36 ± 0.1	A	0.21 ± 0.1	AB	0.34 ± 0.2	AB	0.00 ± 0.0	B	0.00 ± 0.0	B	0.43 ± 0.1	A
64	22.7	Unknown 15 *	0.32 ± 0.1	AB	0.23 ± 0.0	AB	0.09 ± 0.0	B	0.10 ± 0.1	B	0.31 ± 0.1	AB	0.41 ± 0.1	A
65	23.44	Unknown 16 *	2.88 ± 0.5	A	3.59 ± 0.5	A	2.44 ± 0.2	A	1.31 ± 0.3	B	1.20 ± 0.1	B	0.97 ± 0.2	B
67	23.82	Unknown 17 *	2.91 ± 0.5	A	3.97 ± 0.7	A	3.46 ± 0.4	A	1.07 ± 0.1	B	1.79 ± 0.2	B	2.63 ± 0.4	A
70	24.61	Unknown 18	3.67 ± 0.7	A	3.51 ± 0.3	A	3.06 ± 0.2	A	3.01 ± 0.5	A	2.37 ± 0.3	A	2.32 ± 0.3	A
72	24.88	Unknown 19 *	0.71 ± 0.1	A	0.76 ± 0.1	A	0.84 ± 0.1	A	0.34 ± 0.1	B	0.21 ± 0.0	B	0.35 ± 0.1	B
74	25.36	Unknown 20	15.32 ± 3.5	A	13.83 ± 5.3	A	15.82 ± 4.2	A	10.20 ± 1.9	A	8.24 ± 1.7	A	10.44 ± 1.4	A
75	25.38	Unknown 21 *	0.07 ± 0.0	B	0.30 ± 0.1	A	0.32 ± 0.0	A	0.00 ± 0.0	B	0.26 ± 0.0	A	0.30 ± 0.1	A
76	25.59	Unknown 22 *	1.55 ± 0.5	A	1.06 ± 0.1	A	1.31 ± 0.4	A	0.66 ± 0.1	A	0.15 ± 0.1	B	0.60 ± 0.1	AB
77	26.52	Unknown 23 *	1.75 ± 0.2	A	1.92 ± 0.1	A	1.64 ± 0.1	A	0.26 ± 0.2	C	0.53 ± 0.1	B	0.68 ± 0.1	B
78	26.53	Unknown 24	2.06 ± 0.3	A	2.08 ± 0.2	A	2.08 ± 0.2	A	2.12 ± 0.4	A	1.84 ± 0.3	A	1.93 ± 0.3	A
79	26.72	Unknown 25 *	0.85 ± 0.2	A	0.94 ± 0.3	A	1.54 ± 0.3	A	0.91 ± 0.1	A	0.16 ± 0.1	B	0.75 ± 0.2	AB
80	27.32	Unknown 26 *	3.51 ± 0.6	A	4.49 ± 0.7	A	3.45 ± 0.2	A	1.34 ± 0.3	B	1.36 ± 0.1	B	1.27 ± 0.3	B
81	27.99	Unknown 27	4.24 ± 1.2	A	3.84 ± 1.6	A	4.42 ± 1.3	A	2.45 ± 0.5	A	2.28 ± 0.6	A	2.88 ± 0.5	A
82	28.27	Unknown 28 *	1.09 ± 0.1	A	2.09 ± 0.7	A	1.15 ± 0.1	A	0.55 ± 0.4	B	0.00 ± 0.0	B	0.13 ± 0.1	B
83	28.52	Unknown 30 *	2.66 ± 0.4	AB	2.77 ± 0.3	A	2.77 ± 0.2	A	1.49 ± 0.3	B	1.79 ± 0.2	AB	1.50 ± 0.2	AB
85	29.33	Unknown 32	5.02 ± 0.9	A	9.61 ± 1.4	A	3.72 ± 0.6	A	5.79 ± 1.6	A	6.39 ± 1.4	A	4.34 ± 0.7	A
87	30.92	Unknown 33	1.30 ± 0.2	A	1.50 ± 0.4	A	0.79 ± 0.2	A	1.76 ± 0.4	A	1.13 ± 0.3	A	0.70 ± 0.1	A
89	31.49	Unknown 34 *	4.13 ± 0.5	B	7.89 ± 1.2	A	5.45 ± 0.5	A	2.35 ± 0.6	B	3.22 ± 0.5	B	2.47 ± 0.3	B

APÊNDICE F - RELATIVE INTENSITY VALUES OF METABOLITES IN ROOTS OF RICE CVS. BRS ESMERALDA AND SÃO FRANCISCO GROWING UNDER DIFFERENT LEVELS OF HYPOXIA.

Table S6 - Relative intensity values of metabolites in roots of rice cv. BRS Esmeralda under severe (ES-SE), moderate (ES-MO), and slight (ES-SL) hypoxia and cv. São Francisco under severe (SF-SE), moderate (SF-MO), and slight (SF-SL) hypoxia conditions for ten days. Values represent the means of five repetitions ± standard error.

ID[a]	RT[b]	Metabolites	Relative intensity [c]											
			ES-SE		ES-MO		ES-SL		SF-SE		SF-MO		SF-SL	
Amino acid														
3	8.42	Alanine	64.76 ± 23.06	A	43.28 ± 13.37	A	38.34 ± 16.89	A	54.86 ± 7.41	A	30.72 ± 5.49	A	15.90 ± 5.37	A
9	11.01	Valine *	17.53 ± 5.37	AB	14.46 ± 3.88	AB	11.68 ± 4.52	AB	31.07 ± 4.92	A	11.23 ± 2.79	AB	7.63 ± 3.92	B
11	11.82	Serine *	29.96 ± 7.53	AB	23.79 ± 7.14	AB	15.02 ± 3.81	AB	30.51 ± 3.27	A	14.95 ± 1.95	AB	10.94 ± 1.79	B
13	12.16	Leucine	5.27 ± 1.99	A	3.52 ± 0.64	A	3.86 ± 1.37	A	6.45 ± 1.64	A	1.56 ± 0.48	A	1.35 ± 0.72	A
16	12.58	Isoleucine *	5.30 ± 1.62	A	3.44 ± 0.63	AB	3.61 ± 1.15	AB	7.33 ± 1.41	A	1.79 ± 0.43	B	1.31 ± 0.70	B
17	12.63	Proline	3.84 ± 1.09	A	2.23 ± 0.54	A	3.96 ± 0.95	A	4.07 ± 0.90	A	1.57 ± 0.39	A	1.77 ± 0.37	A
18	12.78	Glycine *	19.47 ± 4.22	A	13.67 ± 5.21	AB	6.99 ± 2.35	B	28.43 ± 2.93	A	9.77 ± 1.40	B	5.96 ± 1.63	C
21	14.33	Threonine	1.59 ± 0.42	A	0.89 ± 0.23	A	1.05 ± 0.47	A	2.35 ± 0.50	A	0.69 ± 0.33	A	0.45 ± 0.25	A
24	16.53	Aspartic acid *	26.45 ± 7.72	A	9.73 ± 4.82	AB	2.97 ± 1.70	B	20.79 ± 5.27	A	5.77 ± 0.80	AB	1.44 ± 0.46	B
25	16.59	Hydroxyproline	2.95 ± 0.33	A	4.35 ± 1.25	A	3.89 ± 0.89	A	5.70 ± 1.01	A	3.12 ± 0.31	A	2.52 ± 0.52	A
30	17.98	Glutamic acid	33.87 ± 13.44	A	38.21 ± 17.43	A	21.45 ± 13.00	A	34.14 ± 8.67	A	23.26 ± 2.87	A	14.20 ± 6.13	A
31	18.11	Phenylalanine	1.58 ± 0.15	A	1.10 ± 0.54	A	0.70 ± 0.34	A	1.25 ± 0.21	A	0.70 ± 0.09	A	0.77 ± 0.33	A
32	18.77	Asparagine*	22.43 ± 13.72	A	7.03 ± 4.95	AB	0.95 ± 0.48	B	19.15 ± 8.42	A	4.71 ± 0.69	AB	1.76 ± 1.01	AB
37	20.16	Glutamine	19.21 ± 10.30	A	20.25 ± 14.42	A	5.69 ± 2.87	A	21.14 ± 9.17	A	14.80 ± 2.00	A	8.41 ± 4.04	A
46	22.05	Lysine *	3.68 ± 0.60	A	2.15 ± 0.54	A	1.02 ± 0.29	B	3.70 ± 0.54	A	1.16 ± 0.07	B	0.64 ± 0.17	B

Table S6 *continue*.

ID[a]	RT[b]	Metabolites	Relative intensity [c]											
			ES-SE		ES-MO		ES-SL		SF-SE		SF-MO		SF-SL	
Amino acid														
47	22.05	Ornithine *	3.83 ± 0.89	A	2.13 ± 0.50	A	1.05 ± 0.34	B	3.03 ± 0.29	A	1.07 ± 0.05	B	0.57 ± 0.29	B
49	22.3	Tyrosine	6.08 ± 1.11	A	4.95 ± 1.50	A	3.69 ± 1.15	A	5.78 ± 0.74	A	2.58 ± 0.23	A	3.60 ± 1.25	A
Inorganic acid														
14	12.22	Phosphoric acid *	167.12 ± 39.29	A	160.82 ± 31.94	A	96.04 ± 33.36	AB	58.03 ± 1.20	AB	95.47 ± 17.70	AB	50.70 ± 23.55	B
Nitrogenous compound														
6	9.62	Guanidine *	4.02 ± 0.59	A	2.86 ± 0.57	AB	1.94 ± 0.28	B	4.26 ± 0.65	A	1.23 ± 0.20	B	1.70 ± 0.41	B
10	11.42	Urea	12.00 ± 2.56	A	26.40 ± 7.85	A	16.87 ± 5.81	A	10.84 ± 1.90	A	12.25 ± 2.79	A	14.12 ± 5.32	A
Organic acid														
1	7.1	Pyruvic acid	1.58 ± 0.22	A	2.04 ± 0.61	A	1.26 ± 0.16	A	1.71 ± 0.38	A	1.24 ± 0.16	A	1.25 ± 0.24	A
2	7.37	Lactic acid	64.88 ± 16.47	A	80.54 ± 26.65	A	68.19 ± 11.96	A	50.68 ± 21.73	A	26.52 ± 6.63	A	54.37 ± 16.06	A
4	9.18	Oxalic acid	0.50 ± 0.10	A	0.58 ± 0.31	A	0.42 ± 0.17	A	0.24 ± 0.10	A	0.35 ± 0.08	A	0.43 ± 0.06	A
7	10.08	2-Oxobutyric acid *	4.43 ± 1.15	A	0.00 ± 0.00	B	0.00 ± 0.00	B	4.90 ± 1.23	A	0.00 ± 0.00	B	0.00 ± 0.00	B
8	10.13	Malonic acid	9.89 ± 1.54	A	14.39 ± 4.30	A	9.75 ± 2.77	A	9.64 ± 0.78	A	8.59 ± 1.13	A	11.36 ± 2.43	A
19	12.89	Succinic acid	9.45 ± 1.69	A	15.09 ± 5.95	A	8.62 ± 3.20	A	9.47 ± 2.97	A	3.84 ± 0.90	A	13.76 ± 3.53	A
20	13.32	Glyceric acid *	0.58 ± 0.09	B	0.00 ± 0.00	D	0.00 ± 0.00	D	1.40 ± 0.19	A	0.46 ± 0.08	B	0.13 ± 0.04	C
22	16.02	Malic acid *	45.19 ± 12.88	A	20.00 ± 9.82	B	0.85 ± 0.62	C	52.71 ± 2.02	A	16.72 ± 2.15	B	3.45 ± 0.30	C
27	17.35	2-Oxoglutaric acid	4.05 ± 2.06	A	2.21 ± 0.64	A	1.55 ± 0.42	A	3.00 ± 1.22	A	0.82 ± 0.28	A	0.29 ± 0.10	A
39	20.84	Citric acid *	6.97 ± 1.36	B	3.69 ± 3.12	B	0.00 ± 0.00	C	17.33 ± 2.72	A	2.88 ± 0.39	B	0.26 ± 0.16	C
51	22.43	Glucaric acid *	1.98 ± 0.29	A	1.61 ± 0.49	AB	1.33 ± 0.27	AB	0.53 ± 0.25	B	0.77 ± 0.19	AB	0.78 ± 0.21	AB
53	23.57	Gulonic acid	2.36 ± 0.54	A	2.70 ± 0.43	A	1.84 ± 0.43	A	1.37 ± 0.38	A	1.67 ± 0.28	A	1.57 ± 0.51	A

Table S6 *continue*.

ID[a]	RT[b]	Metabolites	Relative intensity [c]											
			ES-SE		ES-MO		ES-SL		SF-SE		SF-MO		SF-SL	
Phenolic precursor														
38	20.64	Shikimic acid *	30.19 ± 4.90	A	21.65 ± 9.14	AB	8.56 ± 2.03	B	43.30 ± 5.61	A	25.77 ± 3.39	A	12.95 ± 3.17	B
41	21.47	Quinic acid *	63.40 ± 11.28	A	35.88 ± 15.81	AB	11.98 ± 3.45	B	61.76 ± 17.22	AB	45.97 ± 6.93	AB	22.33 ± 5.94	AB
Polyamine														
28	17.42	Putrescine *	0.67 ± 0.30	A	0.00 ± 0.00	B	0.00 ± 0.00	B	0.60 ± 0.31	A	0.00 ± 0.00	B	0.00 ± 0.00	B
Sugar														
23	16.43	Lyxose *	0.00 ± 0.00	C	6.06 ± 3.97	B	0.44 ± 0.34	C	18.51 ± 5.04	A	0.00 ± 0.00	C	0.00 ± 0.00	C
26	16.83	Xylulose	1.10 ± 0.30	A	1.00 ± 0.28	A	0.71 ± 0.12	A	1.88 ± 0.29	A	0.80 ± 0.07	A	1.03 ± 0.19	A
29	17.56	Erythrose *	0.59 ± 0.06	BC	2.35 ± 1.40	B	0.00 ± 0.00	C	5.89 ± 0.59	A	2.57 ± 0.24	AB	1.53 ± 0.52	B
33	19	Ribose	1.61 ± 0.32	A	2.84 ± 0.85	A	1.55 ± 0.47	A	3.12 ± 0.38	A	2.16 ± 0.31	A	2.51 ± 0.66	A
42	21.65	Fructose *	353.80 ± 59.42	A	380.39 ± 22.98	A	317.69 ± 85.35	AB	145.58 ± 37.62	B	330.98 ± 19.10	A	132.25 ± 34.79	B
43	21.73	Sorbose *	351.45 ± 60.52	A	268.65 ± 19.92	A	256.65 ± 51.15	AB	107.87 ± 24.82	B	196.64 ± 31.83	AB	93.97 ± 27.01	C
44	21.88	Mannose	1.15 ± 0.26	A	2.22 ± 0.26	A	1.33 ± 0.29	A	1.74 ± 0.32	A	1.09 ± 0.13	A	1.09 ± 0.29	A
45	21.97	Glucose *	3.68 ± 0.60	A	2.15 ± 0.54	A	1.02 ± 0.29	B	3.70 ± 0.54	A	1.16 ± 0.07	B	0.54 ± 0.19	B
48	22.2	Galactose	10.17 ± 2.49	A	11.11 ± 1.82	A	6.65 ± 1.39	A	5.76 ± 1.94	A	6.93 ± 1.32	A	5.32 ± 1.76	A
62	29.05	Cellobiose *	509605.62 ± 153926.70	A	0.00 ± 0.00	C	0.00 ± 0.00	C	2146982.02 ± 97671.35	B	0.00 ± 0.00	C	0.00 ± 0.00	C
63	30.04	Sucrose	247.22 ± 51.17	A	310.01 ± 88.05	A	259.16 ± 60.62	A	368.49 ± 8.44	A	266.15 ± 49.84	A	236.77 ± 54.91	A
65	30.98	Trehalose *	11.00 ± 1.57	B	39.23 ± 7.76	A	31.17 ± 4.20	A	11.65 ± 2.56	B	18.70 ± 1.94	AB	27.34 ± 6.97	AB
67	32.18	Raffinose	1.57 ± 0.99	A	0.00 ± 0.00	A	1.51 ± 0.42	A	2.11 ± 1.15	A	3.54 ± 1.21	A	1.79 ± 0.78	A

Table S6 *continue*.

ID[a]	RT[b]	Metabolites	Relative intensity [c]																			
			ES-SE				ES-MO				ES-SL				SF-SE				SF-MO				SF-SL			
Sugar																										
68	32.43	Fructose-1.6-diphosphate *	0.65	±	0.03	A	0.00	±	0.00	B	0.00	±	0.00	B	1.58	±	0.72	A	0.25	±	0.12	B	0.00	±	0.00	B
70	33.13	Maltotriose *	1.59	±	0.18	B	0.09	±	0.06	C	0.39	±	0.09	C	4.29	±	0.76	A	0.36	±	0.01	C	0.13	±	0.08	C
Sugar alcohol																										
34	19.15	Xylitol *	0.64	±	0.15	A	0.00	±	0.00	B	0.00	±	0.00	B	0.47	±	0.13	A	0.22	±	0.10	B	0.00	±	0.00	B
35	19.9	Arabitol *	0.03	±	0.03	D	0.00	±	0.00	D	0.00	±	0.00	D	5.25	±	0.35	A	1.86	±	0.11	C	0.76	±	0.15	B
36	20.11	Glycerol-2-phosphate *	463607.89	±	174724.76	A	0.00	±	0.00	B	0.00	±	0.00	B	556211.56	±	87519.71	A	0.00	±	0.00	B	0.00	±	0.00	B
50	22.36	Mannitol *	1.37	±	0.65	D	48.46	±	15.40	A	21.62	±	4.44	B	1.69	±	0.29	D	24.03	±	4.45	B	14.83	±	3.96	C
55	24.28	Inositol *	8.65	±	1.47	AB	9.15	±	1.20	A	6.63	±	1.40	AB	9.67	±	1.42	A	4.06	±	0.29	B	4.12	±	1.06	B
69	33.13	Galactinol *	4.06	±	0.43	B	1.54	±	0.34	C	1.55	±	0.26	C	9.79	±	1.88	A	1.05	±	0.14	C	1.00	±	0.36	C
Sugar derived																										
54	23.95	Glucopyranoside *	4.65	±	1.36	B	0.00	±	0.00	C	0.00	±	0.00	C	46.47	±	11.00	A	0.00	±	0.00	C	0.00	±	0.00	C
Unidentified Metabolites																										
5	9.41	Unknown 2	8.20	±	4.09	A	8.56	±	2.27	A	8.49	±	2.11	A	6.19	±	4.21	A	2.85	±	1.13	A	2.85	±	0.81	A
12	12.03	Unknown 3	62.78	±	16.58	A	93.78	±	28.74	A	42.14	±	16.87	A	79.74	±	17.88	A	57.64	±	14.16	A	47.19	±	18.35	A
15	12.23	Unknown 4	80.08	±	15.99	A	152.28	±	23.83	A	97.93	±	17.56	A	94.93	±	16.89	A	77.26	±	8.10	A	93.07	±	18.40	A
40	20.97	Unknown 13 *	0.50	±	0.10	A	0.67	±	0.13	A	0.73	±	0.22	A	0.34	±	0.04	B	0.26	±	0.07	B	0.27	±	0.04	B
52	23.44	Unknown 16 *	1.76	±	0.30	B	1.46	±	0.36	B	0.38	±	0.13	C	2.81	±	0.61	A	0.93	±	0.15	B	0.28	±	0.10	C
56	25.36	Unknown 20	33.60	±	7.60	A	84.85	±	14.61	A	66.81	±	7.28	A	51.44	±	14.67	A	46.08	±	7.71	A	47.74	±	11.25	A

Table S6 *continue*.

ID[a]	RT[b]	Metabolites	Relative intensity [c]											
			ES-SE		ES-MO		ES-SL		SF-SE		SF-MO		SF-SL	
Unidentified Metabolites														
57	25.38	Unknown 21	0.88 ± 0.12	A	1.91 ± 0.34	A	1.33 ± 0.25	A	1.40 ± 0.17	A	0.98 ± 0.15	A	1.06 ± 0.28	A
58	26.53	Unknown 23 *	0.44 ± 0.07	B	0.00 ± 0.00	C	0.00 ± 0.00	C	0.88 ± 0.09	A	0.00 ± 0.00	C	0.00 ± 0.00	C
59	26.72	Unknown 25 *	0.21 ± 0.03	B	0.00 ± 0.00	C	0.00 ± 0.00	C	1.13 ± 0.25	A	0.00 ± 0.00	C	0.00 ± 0.00	C
60	27.32	Unknown 26 *	2.67 ± 0.40	AB	2.64 ± 0.61	AB	1.59 ± 0.24	AB	3.30 ± 0.79	A	1.27 ± 0.15	B	1.34 ± 0.52	B
61	27.99	Unknown 27	7.98 ± 1.88	A	20.55 ± 3.81	A	16.92 ± 1.76	A	13.50 ± 3.64	A	10.98 ± 1.92	A	11.60 ± 2.88	A
64	30.92	Unknown 33	0.41 ± 0.06	A	0.89 ± 0.40	A	0.73 ± 0.20	A	0.93 ± 0.32	A	0.28 ± 0.08	A	0.58 ± 0.11	A
66	31.49	Unknown 34 *	0.11 ± 0.05	B	0.00 ± 0.00	B	0.00 ± 0.00	B	1.65 ± 0.38	A	0.00 ± 0.00	B	0.00 ± 0.00	B